Syntheses and Antimicrobial Activities of the Naphthalenyl-ethenylpyridinium Benzenesulfonate Derivatives

Kullapa Chanawanno

A Thesis Submitted in Partial Fulfillment of the Requirements
for the Degree of Master of Science in Inorganic Chemistry
Prince of Songkla University
2010

Copyright of Prince of Songkla University

Thesis Title Syntheses and Antimicrobial Activities of the Naphthalenylethenylpyridinium Benzenesulfonate Derivatives
Author Miss Kullapa Chanawanno
Major Program Inorganic Chemistry

Major Advisor:	**Examining Committee:**
………………………………………	………………………………Chairperson
(Assoc. Prof. Dr. Suchada Chantrapromma)	(Prof. Dr. Supot Hannongbua)
	………………………………………
Co-Advisor:	(Assoc. Prof. Dr. Suchada Chantrapromma)
……………………………....................	……………………………....................
(Assoc. Prof. Dr. Chatchanok Karalai)	(Assoc. Prof. Dr. Chatchanok Karalai)
	……………………………....................
	(Assoc. Prof. Dr. Adisorn Ratanaphan)

The Graduate School, Prince of Songkla University, has approved this thesis as partial fulfillment of the requirements for the Master of Science Degree in Inorganic Chemistry

…………………………………………….
(Assoc. Prof. Dr. Krerkchai Thongnoo)
Dean of Graduate School

ชื่อวิทยานิพนธ์	การสังเคราะห์และสมบัติทางชีวภาพของสารอนุพันธ์ Naphthalenyl-ethenylpyridinium Benzenesulfonate
ผู้เขียน	นางสาวกุลภา ชนะวรรโณ
สาขาวิชา	เคมีอินทรีย์
ปีการศึกษา	2552

บทคัดย่อ

ทำการสังเคราะห์และหาโครงสร้างสารอนุพันธ์ pyridinium 24 ชนิด (**PNAP1-PNAP4** และ **PNAP1M-PNAP4N**) โดยเทคนิคทางสเปกโทรสโกปีได้แก่ FT-IR, UV-vis และ ^{1}H-NMR และศึกษาฤทธิ์ทางชีวภาพของสารสังเคราะห์โดยทดสอบกับเชื้อแบคทีเรียแกรมบวก 5 ชนิด คือ *S. aureus* *B. subtilis* *E. faecalis* Methicillin-Resistant *S. aureus* และ Vancomycin-Resistant *E. faecalis* แบคทีเรียแกรมลบ 3 ชนิดคือ *P. aeruginosa* *S. typhi* และ *S. sonnei* และเชื้อรา 1 ชนิด คือ *C. albicans* นอกจากนี้ทำการยืนยันโครงสร้างโดยเทคนิคการเลี้ยวเบนของรังสีเอ็กซ์บนผลึกเดี่ยวของสาร **PNAP2B**, **PNAP2C** และ **PNAP4** พบว่า สารประกอบ **PNAP2B** และ **PNAP2C** ตกผลึกในหมู่ปริภูมิ $Pna2_1$ สารประกอบ **PNAP4** ตกผลึกในหมู่ปริภูมิ $P2_1/c$ จากการทดสอบฤทธิ์ทางชีวภาพกับเชื้อจุลชีพข้างต้นพบว่า สารกลุ่ม **PNAP1** และ **PNAP2** ออกฤทธิ์ต้านแบคทีเรียได้ปานกลางถึงต่ำ ส่วนสารกลุ่ม **PNAP3** และ **PNAP4** ออกฤทธิ์ต้านแบคทีเรียได้ต่ำมากถึงไม่แสดงฤทธิ์ และสารอนุพันธ์ pyridinium ทั้ง 24 ชนิดไม่แสดงฤทธิ์ต้านเชื้อรา *C. albicans*

Thesis Title	Syntheses and Antimicrobial Activities of the Naphthalenyl-ethenylpyridinium Benzenesulfonate Derivatives
Author	Miss Kullapa Chanawanno
Major Program	Inorganic Chemistry
Academic Year	2552

Abstract

The twenty-four derivatives of naphthalenyl-ethenylpyridinium benzenesulfonate (**PNAP1**-**PNAP4** and **PNAP1M**-**PNAP4N**) were synthesized and characterized by FT-IR, UV-vis and ^{1}H-NMR spectroscopic methods. In addition, compounds **PNAP2B**, **PNAP2C** and **PNAP4** were also determined by the single crystal X-ray diffraction. Compounds **PNAP2B** and **PNAP2C** crystallized out in the $Pna2_1$ space group whereas compound **PNAP4** crystallized out in the $P2_1/c$ space group. All compounds were evaluated for antimicrobial activities against some pathogenic Gram-positive bacteria i.e. *S. aureus, B. subtilis, E. faecalis,* Methicillin-Resistant *S. aureus*, Vancomycin-Resistant *E. faecalis*, Gram-negative bacteria i.e. *P. aeruginosa, S. typhi*, *S. sonnei* and one fungus which was *C. albicans*. It was found that all of the twelve compounds in both **PNAP1** and **PNAP2** series exhibited the moderate to low activity against the tested bacteria whereas the compounds in **PNAP3** and **PNAP4** series showed either very low activity or inactive. In addition, all the synthesized naphthalenyl-ethenylpyridinium benzenesulfonates were inactive against the *C. albicans*.

ACKNOWLEDGEMENT

In the first place, I would like to record my gratitude to Associate Professor Dr. Suchada Chantrapromma for her supervision, advice, kindness and guidance from the very early stage of this research as well as giving me extraordinary experiences through out the work. Above all, she provided me unflinching encouragement and support in various ways. She was always there to meet and talk about my ideas, to proofread and mark up my papers and chapters, and to ask me good questions to help me think through my problems.

My special thanks go to my co-advisor, Associate Professor Dr. Chatchanok Karalai, for his valuable advice in science discussion. Special thanks are addressed to Professor Dr. Hoong-Kun Fun, X-ray Crystallography Unit, School of Physics, Universiti Sains Malaysia, Malaysia for X-ray data collections. I also benefited by the bioactivity assays performed by Assistant Professor Dr. Akkharawit Kanjana-Opas and his Ph.D. student, Mr. Theerasak Anantapong, Department of Industrial Biotechnology, Faculty of Argo-Industry, Prince of Songkla University. My precious crystals and antimicrobial activities data would not have been existed without them.

I would like to thank the thesis committees, Professor Dr. Supot Hannongbua, Department of Chemistry, Faculty of Science, Chulalongkorn University, who gave insightful comments and reviewed my work. I also thank Associate Professor Dr. Adisorn Ratanaphan, Department of Pharmaceutical Chemistry, Faculty of Pharmaceutical Sciences, Prince of Songkla University for the valuable suggestions.

Appreciative thanks were expressed to the Development and Promotion of Science and Technology Talents Project (DPST) for a fellowship, the Center of Excellence for Innovation in Chemistry (PERCH-CIC), Commission on Higher Education, Ministry of Education for financial support. I also thank the Graduate

School (PSU) and Prince of Songkla University for financial support through the Crystal Materials Research Unit.

I also would like to thank Department of Chemistry, Faculty of Science, Prince of Songkla University for making available the facilities used in this research. I am also greatly indebted to many staffs here especially Dr. Yaowapa Sukpondma for recording ^{1}H-NMR spectral data.

Collective and individual acknowledgments are also owed to my colleagues at Crystal Materials Research Unit (CMRU) whose present somehow perpetually refreshed, helpful, and memorable. It was such a pleasant time when working together with them. Many thanks go in particular to Mr. Nawong Boonnak for giving me advices and willingness to share his bright thoughts. Words fail me to express my appreciation to Mr. Khamphe Phoungthong, whose dedication, love and persistent confidence in me, has taken the load off my shoulder.

Last, but not least, I thank my family. None of this would have been possible without love and encouragement from them. My grandparents deserve special mention for their inseparable support and prayers. They sincerely raised me with their caring and gently love.

Finally, I would like to thank everybody who was important to the successful realization of my thesis, as well as expressing my apology that I could not mention personally one by one.

Kullapa Chanawanno

THE RELEVANCE OF THE RESEARCH WORK TO THAILAND

The relevancies of this research are listed below:-

1) Twenty-four naphthalenyl-ethenylpyridinium derivatives were designed and synthesized based on the combination of advantages from some well-known antibacterial agents. These synthesized compounds exhibited moderate to low antimicrobial activities against Gram-positive bacteria i.e. *S. aureus, B. subtilis, E. faecalis,* Methicillin-Resistant *S. aureus*, and Vancomycin-Resistant *E. faecalis*. The **PNAP1** series showed the specific activity against *S. aureus* and Methicillin-Resistant *S. aureus* which is the resistant-type pathogenic bacteria spreading all over the world. However, these compounds showed no activity against Gram-negative bacteria.

2) The synthesized silver (I) 4-substitutedbenzenesulfonate salts exhibited high antibacterial activity especially against Gram-positive bacteria. The compounds containing electron donating *para*-substituents (**ANM**, **ANOM** and **ANNH**) showed potent activity against all tested Gram-positive bacteria and one Gram-negative bacteria; *S. sonnei*.

3) The pyridinium stilbene derivatives exhibited the low-level antibacterial activity. By introducing the 4-substitutedbenzenesulfonate anion, the antibacterial activity of the pyridinium benzenesulfonate salts was enhanced to be moderate level.

4) The synthesized naphthalenyl-ethenylpyridinium derivatives can be potential disinfectants candidatures.

CONTENTS

Page

บทคัดย่อ **(iii)**

ABSTRACT **(v)**
ACKNOWNLEDGEMENT **(vii)**
THE RELEVANCE OF THE RESEARCH WORK TO THAILAND **(ix)**
CONTENTS **(x)**
LIST OF TABLES **(xvi)**
LIST OF ILLUSTRATIONS **(xviii)**
ABBREVIATIONS AND SYMBOLS **(xxii)**
1. INTRODUCTION **1**
  1.1 Motivation of research 1
  1.2 Disinfectants 2
    1.2.1 Types of disinfectants 3
  1.3 Pathogenic microbes 8
  1.4 Sulfonamide Drugs 18
  1.5 Review of Literatures 20
  1.6 Objective and outline of this study 39
2. EXPERIMENT **41**
  2.1 Instruments and chemicals 41
    2.1.1 Instruments 41
    2.1.2 Chemicals 42
  2.2 Synthesis of the starting materials 43
    2.2.1 1,2-dimethylpyridinium iodide (**PO-ST**) 43
    2.2.2 1,4-dimethylpyridinium iodide (**PP-ST**) 44
  2.3 Synthesis of cation parts 45
    2.3.1 (*E*)-1-methyl-2-(2-(naphthalen-1-yl)vinyl)pyridinium iodide (**PNAP1**) 45
    2.3.2 (*E*)-1-methyl-4-(2-(naphthalen-1-yl)vinyl)pyridinium iodide (**PNAP2**) 46
    2.3.3 (*E*)-1-methyl-2-(2-(naphthalen-2-yl)vinyl)pyridinium iodide (**PNAP3**) 47
    2.3.4 (*E*)-1-methyl-4-(2-(naphthalen-2-yl)vinyl)pyridinium iodide (**PNAP4**) 48

CONTENTS (Continued)

Page

2.4 Synthesis of anions counter parts 49

2.4.1 Silver (I) 4-methylbenzenesulfonate (**ANM**) 49

2.4.2 Silver (I) 4-methoxybenzenesulfonate (**ANOM**) 49

2.4.3 Silver (I) 4-chlorobenzenesulfonate (**ANCL**) 50

2.4.4 Silver (I) 4-bromobenzenesulfonate (**ANBR**) 51

2.4.5 Silver (I) 4-aminobenzenesulfonate (**ANNH**) 52

2.5 Salt formations 53

2.5.1 (*E*)-1-methyl-2-(2-(naphthalen-1-yl)vinyl)pyridinium 4-methylbenzenesulfonate (**PNAP1M**) 53

2.5.2 (*E*)-1-methyl-2-(2-(naphthalen-1-yl)vinyl)pyridinium 4-methoxybenzenesulfonate (**PNAP1O**) 54

2.5.3 (*E*)-1-methyl-2-(2-(naphthalen-1-yl)vinyl)pyridinium 4-chlorobenzenesulfonate (**PNAP1C**) 55

2.5.4 (*E*)-1-methyl-2-(2-(naphthalen-1-yl)vinyl)pyridinium 4-bromobenzenesulfonate (**PNAP1B**) 56

2.5.5 (*E*)-1-methyl-2-(2-(naphthalen-1-yl)vinyl)pyridinium 4-aminobenzenesulfonate (**PNAP1N**) 57

2.5.6 (*E*)-1-methyl-4-(2-(naphthalen-1-yl)vinyl)pyridinium 4-methylbenzenesulfonate (**PNAP2M**) 58

2.5.7 (*E*)-1-methyl-4-(2-(naphthalen-1-yl)vinyl)pyridinium 4-methoxybenzenesulfonate (**PNAP2O**) 59

2.5.8 (*E*)-1-methyl-4-(2-(naphthalen-1-yl)vinyl)pyridinium 4-chlorobenzenesulfonate (**PNAP2C**) 60

2.5.9 (*E*)-1-methyl-4-(2-(naphthalen-1-yl)vinyl)pyridinium 4-bromobenzenesulfonate (**PNAP2B**) 61

2.5.10 (*E*)-1-methyl-4-(2-(naphthalen-1-yl)vinyl)pyridinium 4-aminobenzenesulfonate (**PNAP2N**) 62

CONTENTS (Continued)

Page

2.5.11 (*E*)-1-methyl-2-(2-(naphthalen-2-yl)vinyl)pyridinium 4-methylbenzenesulfonate (**PNAP3M**) 63

2.5.12 (*E*)-1-methyl-2-(2-(naphthalen-2-yl)vinyl)pyridinium 4-methoxybenzenesulfonate (**PNAP3O**) 64

2.5.13 (*E*)-1-methyl-2-(2-(naphthalen-2-yl)vinyl)pyridinium 4-chlorobenzenesulfonate (**PNAP3C**) 65

2.5.14 (*E*)-1-methyl-2-(2-(naphthalen-2-yl)vinyl)pyridinium 4-bromobenzenesulfonate (**PNAP3B**) 66

2.5.15 (*E*)-1-methyl-2-(2-(naphthalen-2-yl)vinyl)pyridinium 4-aminobenzenesulfonate (**PNAP3N**) 67

2.5.16 (*E*)-1-methyl-4-(2-(naphthalen-2-yl)vinyl)pyridinium 4-methylbenzenesulfonate (**PNAP4M**) 68

2.5.17 (*E*)-1-methyl-4-(2-(naphthalen-2-yl)vinyl)pyridinium 4-methoxybenzenesulfonate (**PNAP4O**) 69

2.5.18 (*E*)-1-methyl-4-(2-(naphthalen-2-yl)vinyl)pyridinium 4-chlorobenzenesulfonate (**PNAP4C**) 70

2.5.19 (*E*)-1-methyl-4-(2-(naphthalen-2-yl)vinyl)pyridinium 4-bromobenzenesulfonate (**PNAP4B**) 71

2.5.20 (*E*)-1-methyl-4-(2-(naphthalen-2-yl)vinyl)pyridinium 4-aminobenzenesulfonate (**PNAP4N**) 72

2.5 Antimicrobial assay 73

3. RESULTS AND DISCUSSION **74**

3.1 Structural elucidation of starting materials 74

3.1.1 1,2-dimethylpyridinium iodide (**PO-ST**) 74

3.1.2 1,4-dimethylpyridinium iodide (**PP-ST**) 75

3.2 Structural elucidation of cation parts 76

3.2.1 (*E*)-1-methyl-2-(2-(naphthalen-1-yl)vinyl)pyridinium iodide (**PNAP1**) 76

CONTENTS (Continued)

Page

3.2.2 (*E*)-1-methyl-4-(2-(naphthalen-1-yl)vinyl)pyridinium iodide (**PNAP2**) 78

3.2.3 (*E*)-1-methyl-2-(2-(naphthalen-2-yl)vinyl)pyridinium iodide (**PNAP3**) 80

3.2.4 (*E*)-1-methyl-4-(2-(naphthalen-2-yl)vinyl)pyridinium iodide (**PNAP4**) 82

3.3 Structural elucidation of anions counter parts 92

3.3.1 Silver (I) 4-methylbenzenesulfonate (**ANM**) 92

3.3.2 Silver (I) 4-methoxybenzenesulfonate (**ANOM**) 92

3.3.3 Silver (I) 4-chlorobenzenesulfonate (**ANCL**) 93

3.3.4 Silver (I) 4-bromobenzenesulfonate (**ANBR**) 93

3.3.5 Silver (I) 4-aminobenzenesulfonate (**ANNH**) 94

3.4 Structural elucidation of salt formations 95

3.4.1 (*E*)-1-methyl-2-(2-(naphthalen-1-yl)vinyl)pyridinium 4-methylbenzenesulfonate (**PNAP1M**) 95

3.4.2 (*E*)-1-methyl-2-(2-(naphthalen-1-yl)vinyl)pyridinium 4-methoxybenzenesulfonate (**PNAP1O**) 97

3.4.3 (*E*)-1-methyl-2-(2-(naphthalen-1-yl)vinyl)pyridinium 4-chlorobenzenesulfonate (**PNAP1C**) 99

3.4.4 (*E*)-1-methyl-2-(2-(naphthalen-1-yl)vinyl)pyridinium 4-bromobenzenesulfonate (**PNAP1B**) 101

3.4.5 (*E*)-1-methyl-2-(2-(naphthalen-1-yl)vinyl)pyridinium 4-aminobenzenesulfonate (**PNAP1N**) 103

3.4.6 (*E*)-1-methyl-4-(2-(naphthalen-1-yl)vinyl)pyridinium 4-methylbenzenesulfonate (**PNAP2M**) 105

3.4.7 (*E*)-1-methyl-4-(2-(naphthalen-1-yl)vinyl)pyridinium 4-methoxybenzenesulfonate (**PNAP2O**) 107

CONTENTS (Continued)

Page

3.4.8 (*E*)-1-methyl-4-(2-(naphthalen-1-yl)vinyl)pyridinium 4-chlorobenzenesulfonate (**PNAP2C**) 109

3.4.9 (*E*)-1-methyl-4-(2-(naphthalen-1-yl)vinyl)pyridinium 4-bromobenzenesulfonate (**PNAP2B**) 118

3.4.10 (*E*)-1-methyl-4-(2-(naphthalen-1-yl)vinyl)pyridinium 4-aminobenzenesulfonate (**PNAP2N**) 127

3.4.11 (*E*)-1-methyl-2-(2-(naphthalen-2-yl)vinyl)pyridinium 4-methylbenzenesulfonate (**PNAP3M**) 129

3.4.12 (*E*)-1-methyl-2-(2-(naphthalen-2-yl)vinyl)pyridinium 4-methoxybenzenesulfonate (**PNAP3O**) 131

3.4.13 (*E*)-1-methyl-2-(2-(naphthalen-2-yl)vinyl)pyridinium 4-chlorobenzenesulfonate (**PNAP3C**) 133

3.4.14 (*E*)-1-methyl-2-(2-(naphthalen-2-yl)vinyl)pyridinium 4-bromobenzenesulfonate (**PNAP3B**) 135

3.4.15 (*E*)-1-methyl-2-(2-(naphthalen-2-yl)vinyl)pyridinium 4-aminobenzenesulfonate (**PNAP3N**) 137

3.4.16 (*E*)-1-methyl-4-(2-(naphthalen-2-yl)vinyl)pyridinium 4-methylbenzenesulfonate (**PNAP4M**) 139

3.4.17 (*E*)-1-methyl-4-(2-(naphthalen-2-yl)vinyl)pyridinium 4-methoxybenzenesulfonate (**PNAP4O**) 141

3.4.18 (*E*)-1-methyl-4-(2-(naphthalen-2-yl)vinyl)pyridinium 4-chlorobenzenesulfonate (**PNAP4C**) 143

3.4.19 (*E*)-1-methyl-4-(2-(naphthalen-2-yl)vinyl)pyridinium 4-bromobenzenesulfonate (**PNAP4B**) 145

3.4.20 (*E*)-1-methyl-4-(2-(naphthalen-2-yl)vinyl)pyridinium 4-aminobenzenesulfonate (**PNAP4N**) 147

3.4 The antimicrobial activity 149

CONTENTS (Continued)

Page

4. CONCLUSION 153

REFERENCES 156

APPENDIX 160

VITAE 218

LIST OF TABLES

Table **Page**

1 Antibacterial activities (µg/ml) of bis-*iso*quinolinium salts **1-4** 20

2 MIC (µg/ml) of bis-*iso*quinolinium salts **5** and **6** 21

3 Zones of inhibition of *β*-picoline derivatives 22

4 The MIC values (µM) of pyridinium and benzimidazolium chlorides 23

5 The MIC values (µM) of pyridinium salts **4a, 4b, 4d, 5e, 5f** and **5g** 24

6 MIC values (µM) for all tested biocides 25

7 MIC values (µM) and the LD$_{50}$ (µM) of bis-quaternary ammonium compounds 26

8 The MIC (µg/ml) of quaternary imidazolium and pyrrolidinonium salts 27

9 MIC (mg/l) of 1-alkyl-2-(4-pyridyl)pyridinium bromides series 28

10 The MIC values (µg/ml) for the compounds **1**–**5** 29

11 MIC (mg/l) of natural and synthetic 3-alkylpyridinium salts against bacteria *in vitro* 30

12 MIC (µM) of bis(pyridinium)alkanes 31

13 MIC (µM) of bis(pyridinium)alkanes 33

14 MIC (µg/ml) of pyridinium functionalized polynorbornenes against *B.subtilis* 33

15 The MIC (µg/ml) values of PPh-n-QAB 34

16 MIC values (µg/ml) of three compounds 35

17 MIC values (µM) for the synthesized compounds 37

18 Antibacterial activity of **51-66** against *Pseudomonas aeruginosa* according to minimal inhibitory concentrations (MICs) expressed in µM 38

19 ^{1}H NMR of compound **PNAP1** 77

20 ^{1}H NMR of compound **PNAP2** 79

21 ^{1}H NMR of compound **PNAP3** 81

22 ^{1}H NMR of compound **PNAP4** 83

23 Crystal data of **PNAP4** 86

24 Bond lengths [Å] and angles [°] for **PNAP4** 87

25 Hydrogen-bond geometry [Å, °] of **PNAP4** 91

26 ^{1}H NMR of compound **PNAP1M** 96

27 ^{1}H NMR of compound **PNAP1O** 98

LIST OF TABLES (Continued)

Table **Page**

28 ^{1}H NMR of compound **PNAP1C** 100

29 ^{1}H NMR of compound **PNAP1B** 102

30 ^{1}H NMR of compound **PNAP1N** 104

31 ^{1}H NMR of compound **PNAP2M** 106

32 ^{1}H NMR of compound **PNAP2O** 108

33 ^{1}H NMR of compound **PNAP2C** 110

34 Crystal data of **PNAP2C** 113

35 Bond lengths [Å] and angles [°] for **PNAP2C** 114

36 Hydrogen-bond geometry [Å, °] of **PNAP2C** 117

37 ^{1}H NMR of compound **PNAP2B** 119

38 Crystal data of **PNAP2B** 122

39 Bond lengths [Å] and angles [°] for **PNAP2B** 123

40 Hydrogen-bond geometry [Å, °] of **PNAP2B** 126

41 ^{1}H NMR of compound **PNAP2N** 128

42 ^{1}H NMR of compound **PNAP3M** 130

43 ^{1}H NMR of compound **PNAP3O** 132

44 ^{1}H NMR of compound **PNAP3C** 134

45 ^{1}H NMR of compound **PNAP3B** 136

46 ^{1}H NMR of compound **PNAP3N** 138

47 ^{1}H NMR of compound **PNAP4M** 140

48 ^{1}H NMR of compound **PNAP4O** 142

49 ^{1}H NMR of compound **PNAP4C** 144

50 ^{1}H NMR of compound **PNAP4B** 146

51 ^{1}H NMR of compound **PNAP4N** 148

52 Antibacterial activity of silver (I) salts of anionic parts 149

53 Antibacterial activity of naphthalenyl-ethenylpyridinium benzenesulfonate derivatives 150

54 Antifungal activity (*C. albicans*) of Silver (I) 4-substitutedbenzenesulfonate parts 152

LIST OF TABLES (Continued)

Table Page

55 Antifungal activity (*C. albicans*) of naphthalenyl-ethenylpyridinium benzenesulfonate derivatives 152

LIST OF ILLUSTRATIONS

Figure Page

1 The comparison of sulfa drugs and PABA structures 19

2 The tetrahydrofolate synthesis pathway of bacteria interrupted by sulfonamide drugs 19

3 Sulfonamides act as competitive inhibitors in the tetrahydrofolate synthesis pathway of bacteria 19

4 The naphthalenyl-ethenylpyridinium benzenesulfonate derivatives 40

5 X-ray ORTEP diagram of the compound **PNAP4** 85

6 Packing diagram of **PNAP4** viewed down the *a* axis with H-bonds shown as dashed lines. 85

7 X-ray ORTEP diagram of the compound **PNAP2C** 112

8 The crystal packing of the compound **PNAP2C** viewed down the *b* axis. Weak C—H···O interactions are shown as dashed lines. 112

9 X-ray ORTEP diagram of the compound **PNAP2B** 121

10 Packing diagram of **PNAP2B** viewed down the *a* axis with weak C—H···O interactions shown as dashed lines. 121

11 UV-Vis (CH_3OH) spectrum of compound **PO-ST** 161

12 FT-IR (KBr) spectrum of compound **PO-ST** 161

13 ^{1}H NMR (300 MHz, $CDCl_3$ + DMSO-d_6) spectrum of compound **PO-ST** 162

14 UV-Vis (CH_3OH) spectrum of compound **PP-ST** 163

15 FT-IR (KBr) spectrum of compound **PP-ST** 163

16 ^{1}H NMR (300 MHz, $CDCl_3$ + DMSO-d_6) spectrum of compound **PP-ST** 164

17 UV-Vis (CH_3OH) spectrum of compound **PNAP1** 165

18 FT-IR (KBr) spectrum of compound **PNAP1** 165

LIST OF ILLUSTRATIONS (Continued)

Figure **Page**

19 ^{1}H NMR (300 MHz, $CDCl_3$ + DMSO-d_6) spectrum of compound **PNAP1** 166

20 UV-Vis (CH_3OH) spectrum of compound **PNAP2** 167

21 FT-IR (KBr) spectrum of compound **PNAP2** 167

22 ^{1}H NMR (300 MHz, $CDCl_3$ + DMSO-d_6) spectrum of compound **PNAP2** 168

23 UV-Vis (CH_3OH) spectrum of compound **PNAP3** 169

24 FT-IR (KBr) spectrum of compound **PNAP3** 169

25 ^{1}H NMR (300 MHz, $CDCl_3$ + DMSO-d_6) spectrum of compound **PNAP3** 170

26 UV-Vis (CH_3OH) spectrum of compound **PNAP4** 171

27 FT-IR (KBr) spectrum of compound **PNAP4** 171

28 ^{1}H NMR (300 MHz, $CDCl_3$ + DMSO-d_6) spectrum of compound **PNAP4** 172

29 ^{1}H NMR (300 MHz, $CDCl_3$ + DMSO-d_6) spectrum of compound **ANM** 173

30 ^{1}H NMR (300 MHz, $CDCl_3$ + DMSO-d_6) spectrum of compound **ANOM** 174

31 ^{1}H NMR (300 MHz, $CDCl_3$ + DMSO-d_6) spectrum of compound **ANCL** 175

32 ^{1}H NMR (300 MHz, $CDCl_3$ + DMSO-d_6) spectrum of compound **ANBR** 176

33 ^{1}H NMR (300 MHz, $CDCl_3$ + DMSO-d_6) spectrum of compound **ANNH** 177

34 UV-Vis (CH_3OH) spectrum of compound **PNAP1M** 178

35 FT-IR (KBr) spectrum of compound **PNAP1M** 178

36 ^{1}H NMR (300 MHz, $CDCl_3$ + DMSO-d_6) spectrum of compound **PNAP1M** 179

37 UV-Vis (CH_3OH) spectrum of compound **PNAP1O** 180

38 FT-IR (KBr) spectrum of compound **PNAP1O** 180

39 ^{1}H NMR (300 MHz, $CDCl_3$ + DMSO-d_6) spectrum of compound **PNAP1O** 181

40 UV-Vis (CH_3OH) spectrum of compound **PNAP1C** 182

41 FT-IR (KBr) spectrum of compound **PNAP1C** 182

42 ^{1}H NMR (300 MHz, $CDCl_3$ + DMSO-d_6) spectrum of compound **PNAP1C** 183

43 UV-Vis (CH_3OH) spectrum of compound **PNAP1B** 184

44 FT-IR (KBr) spectrum of compound **PNAP1B** 184

45 ^{1}H NMR (300 MHz, $CDCl_3$ + DMSO-d_6) spectrum of compound **PNAP1B** 185

46 UV-Vis (CH_3OH) spectrum of compound **PNAP1N** 186

47 FT-IR (KBr) spectrum of compound **PNAP1N** 186

LIST OF ILLUSTRATIONS (Continued)

Figure **Page**

48 ^{1}H NMR (300 MHz, $CDCl_3$ + DMSO-d_6) spectrum of compound **PNAP1N** 187

49 UV-Vis (CH_3OH) spectrum of compound **PNAP2M** 188

50 FT-IR (KBr) spectrum of compound **PNAP2M** 188

51 ^{1}H NMR (300 MHz, $CDCl_3$ + DMSO-d_6) spectrum of compound **PNAP2M** 189

52 UV-Vis (CH_3OH) spectrum of compound **PNAP2O** 190

53 FT-IR (KBr) spectrum of compound **PNAP2O** 190

54 ^{1}H NMR (300 MHz, $CDCl_3$ + DMSO-d_6) spectrum of compound **PNAP2O** 191

55 UV-Vis (CH_3OH) spectrum of compound **PNAP2C** 192

56 FT-IR (KBr) spectrum of compound **PNAP2C** 192

57 ^{1}H NMR (300 MHz, $CDCl_3$ + DMSO-d_6) spectrum of compound **PNAP2C** 193

58 UV-Vis (CH_3OH) spectrum of compound **PNAP2B** 194

59 FT-IR (KBr) spectrum of compound **PNAP2B** 194

60 ^{1}H NMR (300 MHz, $CDCl_3$ + DMSO-d_6) spectrum of compound **PNAP2B** 195

61 UV-Vis (CH_3OH) spectrum of compound **PNAP2N** 196

62 FT-IR (KBr) spectrum of compound **PNAP2N** 196

63 ^{1}H NMR (300 MHz, $CDCl_3$ + DMSO-d_6) spectrum of compound **PNAP2N** 197

64 UV-Vis (CH_3OH) spectrum of compound **PNAP3M** 198

65 FT-IR (KBr) spectrum of compound **PNAP3M** 198

66 ^{1}H NMR (300 MHz, $CDCl_3$ + DMSO-d_6) spectrum of compound **PNAP3M** 199

67 UV-Vis (CH_3OH) spectrum of compound **PNAP3O** 200

68 FT-IR (KBr) spectrum of compound **PNAP3O** 200

69 ^{1}H NMR (300 MHz, $CDCl_3$ + DMSO-d_6) spectrum of compound **PNAP3O** 201

70 UV-Vis (CH_3OH) spectrum of compound **PNAP3C** 202

71 FT-IR (KBr) spectrum of compound **PNAP3C** 202

72 ^{1}H NMR (300 MHz, $CDCl_3$ + DMSO-d_6) spectrum of compound **PNAP3C** 203

73 UV-Vis (CH_3OH) spectrum of compound **PNAP3B** 204

74 FT-IR (KBr) spectrum of compound **PNAP3B** 204

75 ^{1}H NMR (300 MHz, $CDCl_3$ + DMSO-d_6) spectrum of compound **PNAP3B** 205

76 UV-Vis (CH_3OH) spectrum of compound **PNAP3N** 206

LIST OF ILLUSTRATIONS (Continued)

Figure		**Page**
77	FT-IR (KBr) spectrum of compound **PNAP3N**	206
78	^{1}H NMR (300 MHz, $CDCl_3$ + DMSO-d_6) spectrum of compound **PNAP3N**	207
79	UV-Vis (CH_3OH) spectrum of compound **PNAP4M**	208
80	FT-IR (KBr) spectrum of compound **PNAP4M**	208
81	^{1}H NMR (300 MHz, $CDCl_3$ + DMSO-d_6) spectrum of compound **PNAP4M**	209
82	UV-Vis (CH_3OH) spectrum of compound **PNAP4O**	210
83	FT-IR (KBr) spectrum of compound **PNAP4O**	210
84	^{1}H NMR (300 MHz, $CDCl_3$ + DMSO-d_6) spectrum of compound **PNAP4O**	211
85	UV-Vis (CH_3OH) spectrum of compound **PNAP4C**	212
86	FT-IR (KBr) spectrum of compound **PNAP4C**	212
87	^{1}H NMR (300 MHz, $CDCl_3$ + DMSO-d_6) spectrum of compound **PNAP4C**	213
88	UV-Vis (CH_3OH) spectrum of compound **PNAP4B**	214
89	FT-IR (KBr) spectrum of compound **PNAP4B**	214
90	^{1}H NMR (300 MHz, $CDCl_3$ + DMSO-d_6) spectrum of compound **PNAP4B**	215
91	UV-Vis (CH_3OH) spectrum of compound **PNAP4N**	216
92	FT-IR (KBr) spectrum of compound **PNAP4N**	216
93	^{1}H NMR (300 MHz, $CDCl_3$ + DMSO-d_6) spectrum of compound **PNAP4N**	217

ABBREVIATIONS AND SYMBOLS

s = singlet
d = doublet
t = triplet
q = quartet
m = multiplet
br s = broad singlet
g = gram
μg = microgram
nm = nanometer
ml = milliliter
mp. = melting point
cm^{-1} = reciprocal centimeter (wave number)
δ = chemical shift relative to TMS
J = coupling constant
λ_{max} = maximum wavelength
ν = absorption frequencies
ε = molar extinction frequencies
°C = degree celcius
MHz = Megahertz
Hz = Hertz
ppm = part per million
Å = Angstrom
hr = hour
Fig. = Figure
IR = Infrared
UV-Vis = Ultraviolet-Visible
NMR = Nuclear magnetic resonance

ABBREVIATIONS AND SYMBOLS (Continued)

TMS = tetramethylsilane

$CDCl_3$ = deuterochloroform

DMSO-d_6 = hexadeutero-dimethyl sulphoxide

CHAPTER 1
INTRODUCTION

1.1 Motivation of Research

Since the dawn of time, mankind has suffered from diseases caused by bacteria. The only defense humans had against bacterial infections was their immune system. Humans were susceptible to simple bacterial infections such as those caused by *Staphylococcus aureus*. However, in the 20th century, antibacterial discoveries were made which provided alternative approaches to defend against bacterial attack. However, almost as quickly as these agents were developed, resistance to them was also observed. As we enter the 21th century, the prospect of "superbugs" which are resistant to all known clinical antimicrobial agents is becoming more of a reality. There is a pressing need to develop new and innovative antimicrobial agents to regain the ascendancy over pathogenic bacteria.

With the increasing resistance of bacteria to antibiotics, the need to prevent bacterial infections in hospitals and in everyday life is growing at an alarming rate (McGowan & Tenover, 2004). Specifically, preventing infection in hospital and medical devices is becoming increasingly important as it is estimated that 45% of hospital infections are associated with medical devices (Arciola *et al.*, 1993). Disinfection is one of the most effective method to prevent the pathogenic bacterial growth which can cause some fatal diseases. Commercial disinfectants are used extensively in hospitals and other health care settings. They are an essential part of infection control practices and aid in the prevention of nosocomial infections (Rutala *et al.*, 1995). Mounting concerns over the potential for microbial contamination and infection risks in the food and general consumer markets have also led to increased use of disinfectants by the general public. The widespread use of disinfectants has prompted some speculation on the development of microbial resistance.

Quaternary ammonium compounds (Quats) are usually used as low level disinfectants. They are effective against bacteria, but not against some species of *Pseudomonas* bacteria or bacterial spores. Quats are biocides which also kill algae and are used as an additive in large-scale industrial water systems to minimize undesired biological growth (Gamage, 2003). Due to these interesting features, quats-type disinfectant is the good choice to be studied and developed.

In this work, the twenty four novel naphthalenyl-ethenylpyridinium benzenesulfonate derivatives were synthesized and characterized with the hope that the antimicrobial properties of pyridinium-type quats can be improved. Our goal is to preliminarily produce the potential compounds which can inhibit the growth of both susceptible bacteria which were *S. aureus, B. subtilis, E. faecalis* (gram positive), *S. sonei, P. aeruginosa* and *S. typhi* (gram negative), fungi which was *C. albicans* and resistant bacteria (Methicillin-Resistant *S. aureus* and Vancomycin-Resistant *E. faecalis*) which can resist the common disinfectants such as benzalkonium chloride.

1.2 Disinfectants

Disinfectants are antimicrobial agents that are applied to non-living objects to destroy microorganisms, the process of which is known as disinfection. Disinfection may be defined as cleaning an article of some or all of the pathogenic organisms which may cause infection to a safe level.

Disinfectants should generally be distinguished from antibiotics that destroy microorganisms within the body, and from antiseptics, which destroy microorganisms on living tissue. A perfect disinfectant would also offer complete and full sterilisation, without harming other forms of life, be inexpensive, and non-corrosive. Unfortunately ideal disinfectants do not exist. Most disinfectants are also, by their very nature, potentially harmful (even toxic) to humans or animals. They should be treated with appropriate care.

Disinfectants are frequently used in hospitals, dental surgeries, kitchens and bathrooms to kill infectious organisms. The choice of the disinfectant to be used depends on the particular situation. Some disinfectants have a wide spectrum (kill nearly all microorganisms), while others kill a smaller range of disease-causing organisms but are preferred for other properties (they may be non-corrosive, non-toxic, or inexpensive).

1.2.1 Types of disinfectants

Low level disinfectants

- ***Phenolic Compounds***

Phenol is commonly found in mouthwashes, scrub soaps and surface disinfectants, and is the active ingredient found in household disinfectants (e.g. Lysol, Pine Sol). Phenolic disinfectants are effective against bacteria (especially gram positive bacteria) and enveloped viruses. They are not effective against nonenveloped viruses and spores. These disinfectants maintain their activity in the presence of organic material. This class of compounds is used for decontamination of the hospital environment, including laboratory surfaces, and noncritical medical items. Phenolics are not recommended for semicritical items because of the lack of validated efficacy data for many of the available formulations and because the residual disinfectant on porous materials may cause tissue irritation even when thoroughly rinsed. Phenolic disinfectants are generally safe, but prolonged exposure to the skin may cause irritation. The use of phenolics in nurseries is questioned because of toxicity to infants.

- ***Quaternary Ammonium Compounds***

The quaternary ammonium compounds are widely used as disinfectants. The quaternaries are good cleaning agents but high water hardness and materials such as cotton and gauze pads may make them less microbiocidal because these materials absorb the active ingredients. As with several other disinfectants (e.g., phenolics, iodophors), gram-negative bacteria have been found to survive or grow in these preparations.

Quaternary ammonium compounds (Quats) disinfectants contain NH_4^+. The labels often list a form of ammonium chloride (AC) such as alkyl aryl, benzyl, didecyl, dimethyl, ethylbenzyl, octyl or a combination thereof. Benzalkonium chloride (BAC) is a more tissue friendly quats than AC. Quats disinfectants are effective against gram positive and gram negative bacteria, and enveloped viruses. They are not effective against non-enveloped viruses, fungi and bacterial spores. Quats disinfectants carry a very strong positive charge that makes good contact with negatively charged surfaces. This characteristic makes most very good cleaning agents. Quats compounds are generally low in toxicity, but prolonged contact can be irritating. The quaternaries are commonly used in ordinary environmental sanitation of noncritical surfaces such as floors, furniture, and walls.

Intermediate level disinfectants

- *Alcohols*

Alcohols are sometimes used as a disinfectant, but more often as an antiseptic (the distinction being that alcohol tends to be used on living tissue rather than nonliving surfaces). They have wide microbicidal activity, are non corrosive, but can be a fire hazard. They also have limited residual activity due to evaporation, which results in brief contact times, and have a limited activity in the presence of organic material. Alcohols are more effective combined with purified water. A 70% isopropyl alcohol or 70% ethyl alcohol is more effective than 90% alcohol because the higher water content allows for greater diffusion through the cell membrane. Alcohol is, however, not effective against resistant fungal and bacterial spores.

These alcohols are rapidly bactericidal rather than bacteriostatic against vegetative forms of bacteria (gram positive and gram negative). Alcohols are not effective against bacterial spores and have limited effectiveness against nonenveloped viruses. The antimicrobial activity of alcohols can be attributed to their ability to denature proteins. Higher concentrations are less effective as the action of denaturing proteins is inhibited without the presence of water.

- *Chlorine and Chlorine Compounds*

It was not until the first half of the nineteenth century that the disinfecting and deodorizing properties of chloride of lime were first recognized. Chlorinated lime was applied in the treatment of sewage in London as early as 1854 and also used for disinfection and deodorization in hospital wards. Chloride of lime was first introduced to the North American continent in 1908 for purification of water.

Today, it is rare to find municipal water that is not treated by chlorination. The use of chlorine as a disinfectant gained wide acceptance later in other industries.

Hypochlorites are the most widely used of the chlorine disinfectants and are available in a liquid (e.g. sodium hypochlorite) or solid (e.g. calcium hypochlorite, sodium dichloroisocyanurate) form. The most common chlorine products are aqueous solutions of 4 to 6% sodium hypochlorite, which are readily available as “household bleach”. They have a broad spectrum of antimicrobial activity, are unaffected by water hardness, are inexpensive and fast acting, and have a low incidence of serious toxicity. The exact method by which free chlorine destroys microorganisms has not been elucidated. Sodium hypochlorite at the concentration used in household bleach (4-6%) may produce skin and ocular irritation or oropharygeal, esophageal, and gastric burns. Other disadvantages of hypochlorites include corrosiveness to metals in high concentrations (>500 ppm), inactivation by organic matter, discoloring or “bleaching” of fabrics, and release of toxic chlorine gas when mixed with ammonia or acid.

- ***Iodine and Iodine Compounds***

So far as is known, the first use of iodine in medical practice was as a remedy for bronchocele (Halliday, 1821) Iodine was officially recognized by the Phamacopedia of the United States in 1830, specifically as tincture of iodine. Iodine disinfectant kills most food spoilage microorganisms, odor causing bacteria and bacteria that may cause disease or economic losses to the livestock and food industries. The adverse side effects of iodine are an unpleasant odor and painfulness on open wounds led to a production of many iodine compounds with the aim of avoiding these incompatibilities without a significant loss of germicidal efficiency.

Iodine and iodophors are well established chemical disinfectants. These compounds have been incorporated in time release formulations and in soaps (surgical scrubs). Simple iodine tinctures (dissolved in alcohol) have limited cleaning ability. These compounds are bactericidal, sporicidal, virucidal and fungicidal but require a prolonged contact time. The disinfective ability of iodine, like chlorine, is neutralized in the presence of organic material and hence frequent applications are needed for thorough disinfection. Iodine tinctures can be very irritating to tissues, can stain fabric and be corrosive. "Tamed" iodines such as surgical scrubs and surgical antiseptics generally do not irritate tissues. Besides their use as an antiseptic, iodophors have been used for the disinfection of blood culture bottles and medical equipment such as hydrotherapy tanks, thermometers, and endoscopes. Antiseptic iodophor preparations are not suitable for use as hard-surface disinfectants because of concentration differences. Iodophors formulated as antiseptics contain less free iodine than those formulated as disinfectants. Iodine or iodine-based antiseptics should not be used on silicone catheters as the silicone tubing may be adversely affected.

High level disinfectants

- *Hydrogen peroxide*

Hydrogen peroxide is used in hospitals to disinfect surfaces and it is used in solution alone or in combination with other chemicals as a high level disinfectant. Hydrogen peroxide vapor is used as a medical sterilant and as room disinfectant. Hydrogen peroxide has the advantage that it decomposes to form oxygen and water thus leaving no long term residues, but hydrogen peroxide as with most other strong oxidants is hazardous, and solutions are a primary irritant. The vapor is hazardous to the respiratory system and eyes. Therefore, engineering controls, personal protective equipment, gas monitoring etc. should be employed where high concentrations of hydrogen peroxide are used in the workplace. Hydrogen peroxide is sometimes mixed with colloidal silver. It is often preferred because it causes far fewer allergic reactions than alternative disinfectants. However, recent studies have shown hydrogen peroxide to be toxic to growing cells as well as bacteria; its use as an antiseptic is no longer recommended.

- *Aldehyde*

Gluteraldehyde

Aldehydes have a wide germicidal spectrum. Gluteraldehydes are bactericidal, virucidal, fungicidal, sporicidal and parasiticidal. They are used as a disinfectant or sterilant in both liquid and gaseous forms. They have moderate residual activity and are effective in the presence of limited amounts of organic material. Gluteraldehydes are very potent disinfectants, which can be highly toxic. Use them only as a last resort and then under trained supervision in a well-ventilated setting and with appropriate personal protective equipment.

Formaldehyde

Formaldehyde is used as a disinfectant and sterilant both in the liquid and gaseous states. Formaldehyde is sold and used principally as a water-based solution called formalin, which is 37% formaldehyde by weight. The aqueous solution is bactericidal, tuberculocidal, fungicidal, virucidal and sporicidal. Formaldehyde should be handled in the workplace as a potential carcinogen with an employee exposure standard that limits an 8 hour time-weighted average exposure to a concentration of 0.75 ppm. For this reason, employees should have limited direct contact with formaldehyde and these considerations limit its role in sterilization and disinfection processes. A wide range of microorganisms is destroyed by varying concentrations of aqueous formaldehyde solutions. Although formaldehyde-alcohol is a chemical sterilant and formaldehyde is a high-level disinfectant, the hospital uses of formaldehyde are limited by its irritating fumes and the pungent odor that is apparent at very low levels (<1 ppm).

Ortho-phthalaldehyde

Ortho-phthalaldehyde (OPA) is a chemical sterilant similar to gluteraldehyde with similar antimicrobial activity. OPA has several potential advantages compared to gluteraldehyde. It has excellent stability over a wide pH range (pH 3-9), is not a known irritant to the eyes and nasal passages, does not require exposure monitoring, has a barely perceptible odor, and requires no activation. OPA, like gluteraldehyde, has excellent material compatibility. A potential disadvantage of OPA is that it stains proteins gray (including unprotected skin) and thus must be handled with caution. However, skin staining would indicate improper handling that requires additional training and/or personal protective equipment (gloves, eye and mouth protection, fluid-resistant gowns) and good ventilation should be provided. In addition, equipment must be thoroughly rinsed to prevent discoloration of a patient's skin or mucous membrane.

1.3 Pathogenic microbes

Pathogenic microbes are microbes that are pathogens and thus cause infectious diseases. The organisms involved include pathogenic bacteria, causing diseases such as plague, tuberculosis and anthrax; protozoa, causing diseases such as malaria, sleeping sickness and toxoplasmosis; and also fungi causing diseases such as ringworm, candidiasis or histoplasmosis. However, other diseases such as influenza, yellow fever or AIDS are caused by pathogenic viruses, which are not living organisms and are not therefore microorganisms.

In this work, all of the tested microbe's infections were described here.

Staphylococcus aureus

It is the best example of an opportunistic microorganism. The most common diseases are on the skin due to it is normal flora of the skin (Archer, 1998).

1. Boils (furuncle)

It is an abscess just beneath the skin. It eventually opens to the surface and heals quickly in a healthy person. It is cause when *S. aureus* enters the skin through pores or hair follicles and causes infection.

2. Impetigo

It is a skin disease with blisters that rupture and form yellowish sores. It is especially common in children and can lead to death in infants. Usually, it is no problem if treated. The treatment consists of careful cleaning with alcohol. Anti-microbial drugs are indicated only if it is a serious case. It is extremely contagious and caregivers must make sure clothing, linen, towels, etc. are kept away from others.

3. Scalded Skin Syndrome

It is an infection of the skin usually in infants. The skin cells are killed and it peels off. Exfoliative toxin separates epidermal layer from the dermis and causes the skin to peel away. The skin looks burned. 90 % of infants become carriers in the first 10 days of life.

4. Deeper infections

Internal infections are rare, but they are more serious. They occur usually in compromised hosts and almost any organ can be affected.

a. Blood

When bacteria are actively growing in the circulating blood, the condition is called septicemia. *S. aureus* produce many toxins such as:

- Leukocidin: targets white blood cells
- Hemolysins: targets or lyses red blood cells.
- Pyemia (pus in blood or dead inflammation cell) is produced as a result.
- Abscesses can be produced throughout the body. Once the bacteria is in the circulating blood, they can spread throughout the body to cause Endocarditis (inflammation of the Endocardium inner lining of the heart and valves) or Meningitis, an inflammation of the meninges, the membrane covering the brain and the Central Nervous System.

b. Broncho-pneumonia

Results from the nose and nasopharynx normal flora. It can infect the lungs and form abscesses in them.

5. Toxic Shock Syndrome

Correlated with the use of super-absorbent Tampons. They may provide with a favorable environment (marked decrease of Magnesium ions) which favor the production of toxins. The patient shows fever, vomiting, diarrhea, rash, etc. and death can follow.

6. Staphylococcal Food Poisoning

There are two kinds of food conditions:

- Food intoxications:

It is due to the ingestion of preformed exotoxins by the bacteria contaminating the food. The exotoxins accumulate in the food where the microorganism is growing. The microorganism per se is not harmful. The toxin affects the digestive tract directly Therefore, it is classified as an Enterotoxin. Examples of this type of poisoning or intoxication are Staphylococcal food poisoning and Botulism.

- Food Infections

Refers to the infectious microorganism actively growing and producing toxins in the intestinal tract. This condition involves the ingestion of contaminated food with the infectious organism and its duplication and production of toxins. This condition takes longer (2 to 3 days) in producing signs and symptoms than food intoxications (2 to 8 hours).

Methicillin resistant *Staphylococcus aureus* (MRSA)

This type of bacteria causes "staph" infections (like *S. aureus*) that are resistant to treatment with usual antibiotics. Most MRSA infections are skin infections that produce the following signs and symptoms:

1. Cellulitis

Cellulitis usually begins as a small area of tenderness, swelling, and redness. As this red area begins to enlarge, the person may develop a fever—sometimes with chills and sweats—and swollen lymph nodes ("swollen glands") near the area of infected skin.

2. Boils

A boil is a localized infection deep in the skin. A boil generally starts as a reddened, tender area. Over time, the area becomes firm and hard and tender. Eventually, the center of the abscess softens and becomes filled with infection-fighting white blood cells that the body sends from the bloodstream to eradicate the infection. This collection of white blood cells, bacteria, and proteins is known as pus. Finally, the pus "forms a head," which can be surgically opened or spontaneously drain out through the surface of the skin. A boil is also referred to as a skin abscess.

3. Abscesses

A local accumulation of pus anywhere in the body.

4. Sty

A sty (sometimes spelled stye) is a tender, painful red bump located at the base of an eyelash or under or inside the eyelid. The medical term for a sty is hordeolum (plural, hordeola).

5. Carbuncles

A carbuncle is a skin abscess, a collection of pus that forms inside the body. Antibiotics are often not very helpful in treating abscesses. The main treatments include hot packs and draining ("lancing") the abscess, but only when it is soft and ready to drain. If you have a fever or long-term illness, such as cancer or diabetes, or are taking medications that suppress the immune system, you should contact your healthcare practitioner if you develop an abscess.

6. Impetigo

An impetigo is a skin infection with pus-filled blisters.

Bacillus subtilis

In general, *B. subtilis* is considered an opportunistic microorganism with no pathogenic potential to humans. However, *B. subtilis* is virtually ubiquitous and it is therefore inevitable that it sometimes may be found in association with other microorganisms in infected humans, but only patients treated with immunosuppressive drugs appear to be susceptible to infection with this otherwise harmless microorganism (Doyle *et al.*, 1985).

Enterococcus faecalis

E. faecalis can cause lower urinary tract infections (UTI), such as cystisis, prostatitis, and epididymitis (Michael, 2002). *E. faecalis* are also found in intra-abdominal, pelvic, and soft tissue infections. The *E. faecalis* can cause nosocomial bacteremia. The source of bacteremia is most often the urinary tract, occurring from an infected intravenous catheter. Endocarditis is the most serious enterococcal infection, as it causes inflammation of the heart valves. In many cases of endocarditis, antibiotic treatment fails and surgery to remove the infected valve is necessary.

1. Infective endocarditis

The valves of the heart do not receive any dedicated blood supply, defensive immune mechanisms (such as white blood cells) cannot directly reach the valves via the bloodstream. If an organism (such as bacteria) attaches to a valve surface and forms a vegetation, the host immune response is blunted. The lack of blood supply to the valves also has implications on treatment, since drugs also have difficulty reaching the infected valve.

2. Urinary tract infection (UTI)

UTI is a bacterial infection that affects any part of the urinary tract. Although urine contains a variety of fluids, salts, and waste products, it usually does not have bacteria in it. When bacteria get into the bladder or kidney and multiply in the urine, they cause a UTI. The most common type of UTI is a bladder infection which is also often called cystitis.

3. Cystitis

Cystitis is the medical term for inflammation of the bladder by a bacterial infection. A bladder infection can be painful and annoying, and can become a serious health problem if the infection spreads to your kidneys.

4. Prostatitis

Prostatitis, a disease of the prostate gland, can cause pain in the groin, painful urination, difficulty urinating and related symptoms. The prostate gland produces components of semen, the fluid that helps support and transport sperm. The gland, about the size and shape of a walnut, sits directly below the bladder and surrounds the urethra, the tube that transports both semen and urine to the penis.

5. Epididymitis

Epididymitis is a medical condition in which there is inflammation of the epididymis (a curved structure at the back of the testicle in which sperm matures is stored). This condition may be mildly to very painful, and the scrotum (sac containing the testicles) may become red, warm and swollen. It may be acute (of sudden onset) or rarely chronic.

Vancomycin-Resistant *Enterococcal Infections* (VRE)

Vancomycin is an antibiotic that is often used to treat infections caused by enterococci. In some cases, enterococci have become resistant to vancomycin and are called vancomycin-resistant enterococci or VRE. Most VRE infections occur in people in hospitals. The acquisition of VRE has seriously affected the treatment and infection control of these organisms. VRE are frequently resistant to all antibiotics that are effective treatment for vancomycin-susceptible enterococci, which leaves clinicians treating VRE infections with limited therapeutic options.

VRE can live in the human intestines and female genital tract without causing disease (often called colonization). However, sometimes, it can be the cause infections of the urinary tract, the bloodstream or of wounds. The symptoms of a VRE infection often depend on where the infection is. If VRE is causing a wound infection, that area of your skin may be red or tender. If one has a urinary tract infection, you may have back pain, a burning sensation when you urinate, or a need to urinate more often than usual. Other symptoms include diarrhea, weakness, fever, and chills.

Shigella sonnei

After being ingested, Shigella species cause disease in humans by establishing infection in the intestinal lumen and in the colonie mucosa. Responses may range in severity from asymptomatic to febrile dysentery. Infected persons most commonly present with watery diarrhea, often with fecal leukocytosis, and less than half develop bloody stools and systemic symptoms such as fever and malaise.

Shigellosis

Shigellosis is endemic throughout the world where it is held responsible for some 120 million cases of severe dysentery with blood and mucus in the stools, the overwhelming majority of which occur in developing countries and involve children less than five years of age. The disease is characterized by a short period of watery diarrhoea with intestinal cramps and general malaise, soon followed by permanent emission of bloody, mucoid, often mucopurulent stools.

Salmonella typhi

Typhoid/ Enteric Fever

Infection of *S. typhi* leads to the development of typhoid, or enteric fever. This disease is characterized by the sudden onset of a sustained and systemic fever, severe headache, nausea, and loss of appetite. Other symptoms include constipation or diarrhea, enlargement of the spleen, possible development of meningitis, and/or general malaise. Untreated typhoid fever cases result in mortality rates ranging from 12-30% while treated cases allow for 99% survival.

Pseudomonas aeruginosa

P. aeruginosa is a common bacterium which can cause disease in animals and humans. It is found in soil, water, skin flora and most man-made environments throughout the world. It thrives not only in normal atmospheres, but also with little oxygen, and has thus colonised many natural and artificial environments.

P. aeruginosa is an opportunistic pathogen. It rarely causes disease in healthy persons. In most cases of infection, the integrity of a physical barrier to infection (e.g., skin, mucous membrane) is lost or an underlying immune deficiency (e.g., neutropenia, immunosuppression) is present. Adding to its pathogenicity, this bacterium has minimal nutritional requirements and can tolerate a wide variety of physical conditions. Diseases caused by *P. aeruginosa* were;

1. Endocarditis

P. aeruginosa infects heart valves of intravenous (IV) drug users and prosthetic heart valves. The organism establishes itself on the endocardium by direct invasion from the blood stream.

2. Respiratory infections

Respiratory infections occur almost exclusively in individuals with a compromised lower respiratory tract or a compromised systemic defense mechanism. Primary pneumonia occurs in patients with chronic lung disease and congestive heart failure. Bacteremic pneumonia commonly occurs in neutropenic cancer patients undergoing chemotherapy. Lower respiratory tract colonization of cystic fibrosis patients by mucoid strains of *P. aeruginosa* is common and difficult to eradicate.

3. Bacteremia and septicemia

P. aeruginosa causes bacteremia primarily in immunocompromised patients. Predisposing conditions include hematologic malignancies, immunodeficiency relating to AIDS, neutropenia, diabetes mellitus, and severe burns. Most *Pseudomonas* bacteremia is acquired in hospitals and nursing homes. *P. aeruginosa* accounts for about 25 percent of all hospital acquired gram negative bacteremias.

4. Central nervous system (CNS) infections

P. aeruginosa causes meningitis and brain abscesses. The organism invades the CNS from a contiguous structure such as the inner ear or paranasal sinus, or is inoculated directly by means of head trauma, surgery or invasive diagnostic procedures, or spreads from a distant site of infection such as the urinary tract.

5. Ear infections including external otitis

P. aeruginosa is the predominant bacterial pathogen in some cases of external otitis, including "swimmer's ear". The bacterium is infrequently found in the normal ear, but often inhabits the external auditory canal in association with injury, maceration, inflammation, or simply wet and humid conditions.

6. Eye infections

P. aeruginosa can cause devastating infections in the human eye. It is one of the most common causes of bacterial keratitis. *P. aeruginosa* can colonize the ocular epithelium by means of a fimbrial attachment to sialic acid receptors. If the defenses of the environment are compromised in any way, the bacterium can proliferate rapidly through the production of enzymes such as elastase, alkaline protease and exotoxin A, and cause a rapidly destructive infection that can lead to loss of the entire eye.

7. Bone and joint infections

P. aeruginosa infections of bones and joints result from direct inoculation of the bacteria or the hematogenous spread of the bacteria from other primary sites of infection. Blood-borne infections are most often seen in IV drug users and in conjunction with urinary tract or pelvic infections. *P. aeruginosa* has a particular tropism for fibrocartilagenous joints of the axial skeleton. *P. aeruginosa* causes chronic contiguous osteomyelitis, usually resulting from direct inoculation of bone and is the most common pathogen implicated in osteochondritis after puncture wounds of the foot.

8. Urinary tract infections

Urinary tract infections (UTI) caused by *P. aeruginosa* are usually hospital-acquired and related to urinary tract catheterization, instrumentation or surgery. *P. aeruginosa* is the third leading cause of hospital-acquired UTIs, accounting for about 12 percent of all infections of this type.

9. Gastrointestinal infections

P. aeruginosa can produce disease in any part of the gastrointestinal tract from the oropharynx to the rectum. As in other forms of *Pseudomonas* disease, those involving the GI tract occur primarily in immunocompromised individuals. The organism has been implicated in perirectal infections, pediatric diarrhea, typical gastroenteritis, and necrotizing enterocolitis.

10. Skin and soft tissue infections, including wound infections, pyoderma and dermatitis

P. aeruginosa can cause a variety of skin infections, both localized and diffuse. The common predisposing factors are breakdown of the integument which may result from burns, trauma or dermatitis; high moisture conditions such as those found in the ear of swimmers and the toe webs of athletes, hikers and combat troops, in the perineal region and under diapers of infants, and on the skin of whirlpool and hot tub users. Individuals with AIDS are easily infected.

Candida albicans

C. albicans is a fungus that is normally present on the skin and in mucous membranes such as the vagina, mouth, or rectum. The fungus also can travel through the blood stream and affect the throat, intestines, and heart valves. *C. albicans* becomes an infectious agent when there is some change in the body environment that allows it to grow out of control.

Most of the time, *C. albicans* infections of the mouth, skin, or vagina occur for no apparent reason. A common cause of infection may be the use of antibiotics that destroy beneficial, as well as harmful, microorganisms in the body, permitting *C. albicans* to multiply in their place. The resulting condition is known as *candidiasis moniliasis*, or a "yeast" infection.

C. albicans infection of the penis is more common among uncircumcised than circumcised men and may result from sexual intercourse with an infected partner.

Symptoms of C. albicans

1. Thrush

Thrush appears as creamy-white or bluish-white patches on the tongue - which is inflamed and sometimes beefy red - and on the lining of the mouth, or in the throat.

2. Diaper rash

Diaper rash was caused by *C. albicans* is an inflammation of the skin, usually red and sometimes scaly.

3. Vaginitis

Vaginitis is characterized by a white or yellow discharge. Inflammation of the walls of the vagina and of the vulva (external genital area) causes burning and itching.

4. Infections of the fingernails and toenails appear as red, painful swelling around the nail. Later, pus may develop.

5. Infection of the penis often results in balanitis (inflammation of the head of the penis).

6. An infection in the bloodstream can affect the kidneys, heart, lungs, eyes, or other organs causing high fever, chills, anemia, and sometimes a rash or shock. *C. albicans* can cause the following problems depending upon the organ infected:

- in the kidneys can cause blood in the urine
- in the heart can cause murmurs and valve damage
- in the lungs can cause bloody sputum (mucus discharge)
- in the eyes can cause pain and blurred vision
- in the brain can cause seizures and acute changes in mental function or behavior

1.4 Sulfonamide Drugs

Sulfonamide drugs were the first antimicrobial drugs, and paved the way for the antibiotic revolution in medicine. Sulfonamide is an organic sulfur compounds containing the -SO_2NH_2 (the amides of sulfonic acids). Its molecular structure is similar to *para*-aminobenzoic acid (PABA) which is needed in bacteria organisms as a substrate of the enzyme dihydropteroate synthetase for the synthesis of tetrahydrofolic acid (THF). Sulfonamides, derived from chiefly sulfanilamide, are capable of interfering with the metabolic processes in bacteria that require PABA. They act as antimicrobial agents by inhibiting bacterial growth and activity and called sulfa drugs. They are used in the prevention and treatment of bacterial infections.

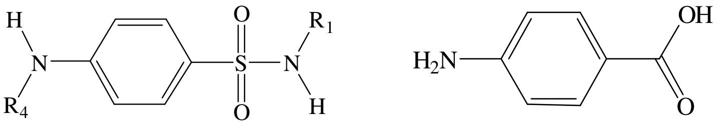
H
N
R4
O
S
O
R1
N
H
H2N
OH
O

Sulfonamide base structure *para*-**aminobenzoic acid**

Figure 1 The comparison of sulfa drugs and PABA structures

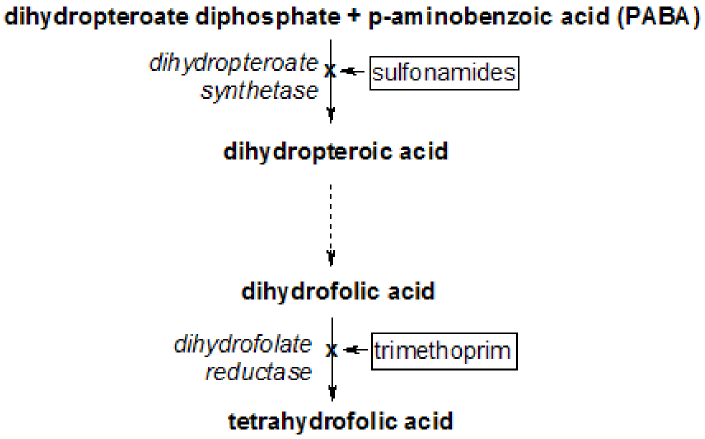
dihydropteroate diphosphate + p-aminobenzoic acid (PABA)
dihydropteroate synthetase
x
sulfonamides
dihydropteroic acid
dihydrofolic acid
dihydrofolate reductase
x
trimethoprim
tetrahydrofolic acid

Figure 2 The tetrahydrofolate synthesis pathway of bacteria interrupted by sulfonamide drugs (adapted from http://en.wikipedia.org/wiki/Tetrahydrofolic_acid)

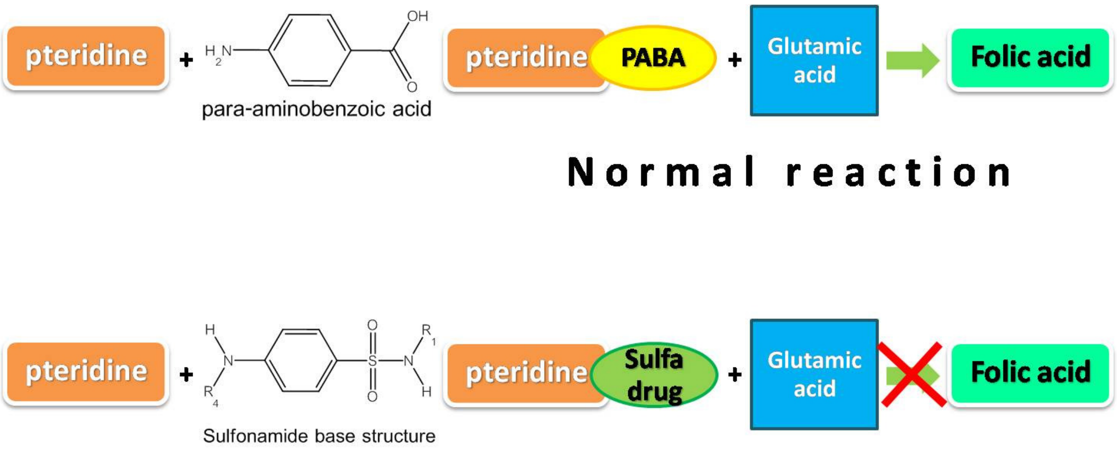
pteridine
+
H2N
OH
O
para-aminobenzoic acid
pteridine
PABA
+
Glutamic acid
Folic acid
Normal reaction
pteridine
+
H
N
R4
O
S
O
R1
N
H
Sulfonamide base structure
pteridine
Sulfa drug
+
Glutamic acid
Folic acid

Figure 3 Sulfonamides act as competitive inhibitors in the tetrahydrofolate synthesis pathway of bacteria (adapted from http://www.elmhurst.edu/~chm/vchembook/ 653sulfa.html)

1.5 Review of Literatures

Collier *et al.* (1953) inquired how far the antibacterial activities of bis*iso*quinilinium salts were influenced by alterations in chemical structure. The *in vitro* activities of four decamethylene compounds against a variety of bacteria are expressed in **Table 1**.

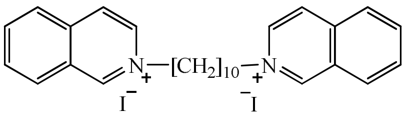

1

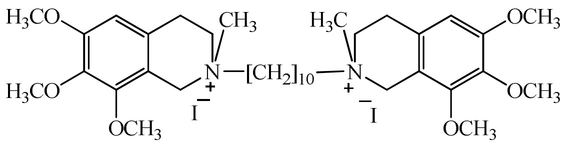

3

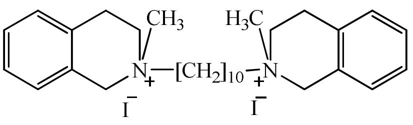

2

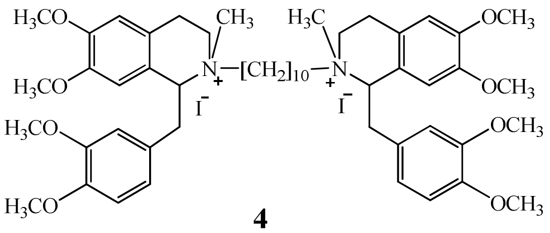

4

Table 1 Antibacterial activities (µg/ml) of bis*iso*quinolinium salts **1-4**

Strains	**Compounds**			
	1	**2**	**3**	**4**
E. faecalis	160	80	125	50
S. aureus	1.26	2.5	0.78	1.56
S. typhi	40	40	250	312

They found that in some species, inhibitory activity increased with increase in methoxy groups.

Collier *et al.* (1955) explored the antifungal properties of bis*iso*quinolinium series and some corresponding bisquinolinium salts by varying the methylene member (n). The minimal inhibitory concentration (MIC) values determined for prepared compounds were shown in **Table 2**.

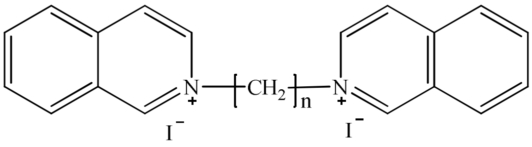

5 ; n = 14

6 ; n = 16

Table 2 MIC (µg/ml) of bis*iso*quinolinium salts **5** and **6**

Strain	**Compounds**	
	5	**6**
C. albicans	5.0	1.25

Activity was increased with increase in chain-length up to the tetradecamethylene member. The tetradeca- and hexadecamethylene members were found to efficiently inhibit the fungi.

Hameed *et al.* (1994) synthesized six different phenacyl halide derivative of *β*-picoline and studied for their antibacterial activity against some gram negative and gram positive bacteria. The measured zones of inhibition were enlisted in **Table 3**.

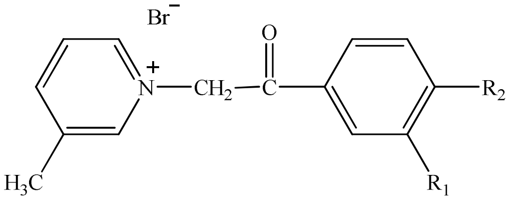

Compound	**R_1**	**R_2**
7	OH	OH
8	OCH_3	H
9	H	Br
10	H	Cl

11	H	OCH_3
12	H	CH_3

Table 3 Zones of inhibition of *β*-picoline derivatives

Bacteria	**Zones of inhibition of compounds (in mm.)**					
	7	**8**	**9**	**10**	**11**	**12**
Gram-positive						
E. faecalis	20	6	28	14	0	12
S. aureus	14	6	30	24	6	10
B. subtilis	22	8	10	16	10	0
Gram-negative						
S. typhi	16	12	20	26	6	0
S. sonei	10	16	10	10	0	6
P. aeruginosa	18	12	14	30	8	0

Among all the tested compounds only three derivatives (**7**, **9** and **10**) showed promising antibacterial activity against both gram positive and gram negative bacteria.

Pernak *et al.* (2001) reported on the synthesis and antimicrobial activities of new pyridinium, bispyridinium and benzimidazolium chlorides as potential novel antimicrobial agents. The minimal inhibitory concentration (MIC) values determined for prepared compounds were shown in **Table 4**.

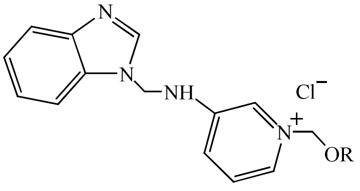

13

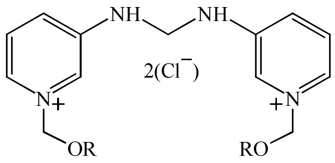

14

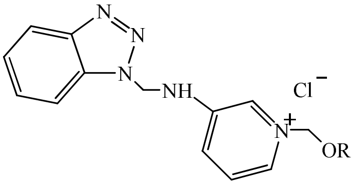

15

13a; R = $C_{11}H_{23}$ **14a**; R = C_9H_{19} **14b**; R = $C_{10}H_{21}$
14c; R = $C_{11}H_{23}$ **14d**; R = $C_{12}H_{25}$ **15a**; R = $C_{12}H_{25}$

Table 4 The MIC values (μM) of pyridinium and benzimidazolium chlorides

Strains	**Compounds**					
	13a	**14a**	**14b**	**14c**	**14d**	**15a**
P. aeruginosa	140	27	51	97	93	135
S. aureus	18	14	13	12	24	34.8
B. subtilis	32	14	13	25	46	17.4
C. albicans	70	13.5	13	195	93	69.6

Their activities are greatly affected by an alkyl chain length in the alkoxymethyl substituent and a kind of quaternary ammonium moieties in a molecule.

Pernak *et al.* (2001) investigated to see if there is any correlation between 1-alkoxymethylcarbamoylpyridinium chlorides and their anti-microbial activity. The minimal inhibitory concentration (MIC) values determined for prepared compounds were shown in **Table 5**.

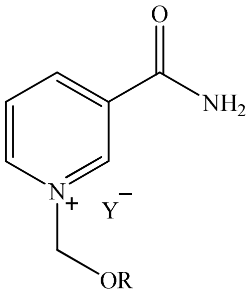

16

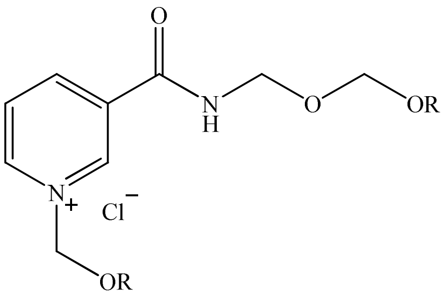

17

16a; R = $C_{10}H_{21}$, Y = $CoCl_4^{2-}$

16b; R = $C_{10}H_{21}$, Y = $CuCl_4^{2-}$

16c; R = $C_{10}H_{21}$, Y = $MgCl_4^{2-}$

17a; R = C_7H_{15}

17b; R = C_8H_{17}

17c; R = C_9H_{19}

Table 5 The MIC values (μM) of some pyridinium salts

Strains	**Compounds**					
	16a	**16b**	**16c**	**17a**	**17b**	**17c**
P. aeruginosa	100	200	103	281	132	250
S. aureus	6.3	6.2	3.2	9	4	4
B. subtilis	25	25	26	18	17	16
C. albicans	6.3	13	0.5	35	33	16

Activities of the salts synthesised against various microorganisms are significantly different due to the anion type.

Massi *et al.* (2003) evaluated the antimicrobial properties of four series of new highly fluorinated bisammoniums (Quaterfluo® Tx, Quaterfluo® Bx, Quaterfluo® Cx, Quaterfluo® Dx). The reference compounds were Cetyl pyridinium chloride (CPC) and benzalkonium chloride (Bac 50). The minimal inhibitory concentration (MIC) values determined for prepared compounds were shown in **Table 6**.

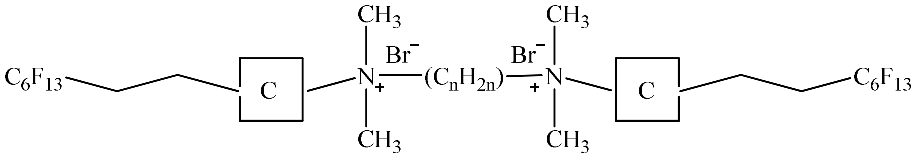

Quaterfluo® compound	**Type of connector**	**Spacer length (n)**
B3	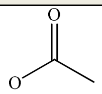	4
C3	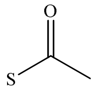	4
D3	No connector	4
T1	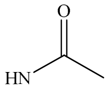	2
T2	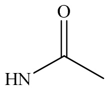	3

T3	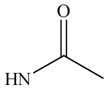	4
T4	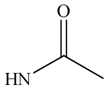	6

Table 6 MIC values (µM) for all tested biocides

Strains	**Quaterfluo® compounds**								
	B3	**C3**	**D3**	**T1**	**T2**	**T3**	**T4**	**CPC**	**Bac 50**
C. albicans	561.98	-	62.51	6.73	6.65	7.64	4.39	2.32	3.59
S. aureus	189.01	-	4.33	6.73	4.55	3.15	2.96	1.98	3.42
P. aeruginosa	-	-	7.31	5.80	5.19	5.94	5.52	17.60	47.72

Their activity was greatly affected by the type of connector; in this case, the results show that the amide connector was the most suitable for antimicrobial activity. The variation of this factor can lead to inactive structures (Quaterfluo® C3) or strong antimicrobial products (Quaterfluo® D3 and T3). The study of the variation of spacer length onto Quaterfluo® Tx series produced Quaterfluo® T1, T2, T3, T4. In view of the results, it appeared that the compounds from the T series are the most efficient products against bacterial and fungal strains compared with compounds from the B, C, and D series. Increasing the spacer length provided an increase in activity especially against *S. aureus* and *C. albicans*.

Ohkura *et al.* (2003) synthesized the bis-quaternary ammonium compounds (QACs) consisted of two identical alkylpyridinium rings and a bridge structure linking the rings to each other. The minimal inhibitory concentration (MIC) values and the median lethal dose (LD_{50}) with human normal epidermal keratinocytes from neonatal foreskin (NHEF(K)), normal skin fibroblast cell line (NB1RGB), human normal erythrocytes and JM cells as a model for the lymphocytes determined for prepared compounds were shown in **Table 7**.

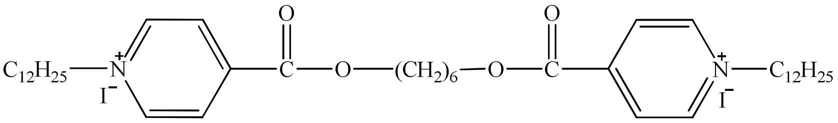

18

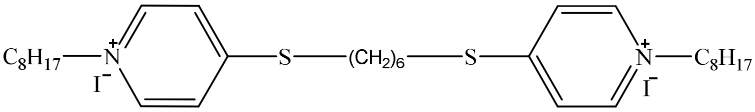

19

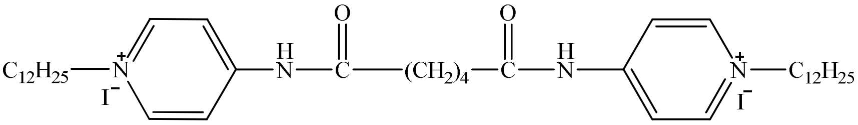

20

Table 7 MIC values (µM) and the LD_{50} (µM) of bis-quaternary ammonium compounds

Compounds	**LD_{50} in human cells***				**MIC**		
	NHEK(F)	**NB1RGB**	**Erythrocyte**	**JM**	*P. aeruginosa*	*S. aureus*	*B. subtilis*
18	13±2	52±3	11±3	50±5	80.0	3.3	-**
19	8±2	48±4	25±4	41±4	-	-	<0.2
20	16±5	53±3	12±2	30±4	12.5	-	-

* Means±SD (n=2)

** No activity

From the investigation of the relationship between the median lethal dose (LD_{50}) and the minimum inhibitory concentration (MIC) of these compounds, **19** as a disinfectant, seems to be very safe for human cells.

Demberelnyamba *et al.* (2004) synthesized three different series of quaternary imidazolium and pyrrolidinonium salts and evaluated their antibacterial and antifungal properties. The minimal inhibitory concentration (MIC) values determined for prepared compounds were shown in **Table 8**.

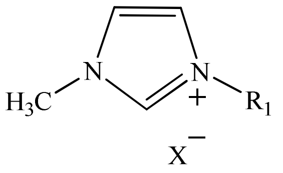

21

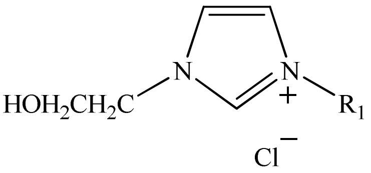

22

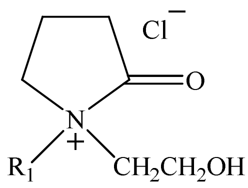

23

21a; $R_1 = C_8H_{17}$, X = Br
21b; $R_1 = C_{10}H_{21}$, X = Cl
21c; $R_1 = C_{12}H_{25}$, X = Br
21d; $R_1 = C_{14}H_{29}$, X = Cl
21e; $R_1 = C_{14}H_{29}$, X = Br
21f; $R_1 = C_{16}H_{33}$, X = Br
22a; $R_1 = C_{14}H_{29}$
22b; $R_1 = C_{16}H_{33}$
23a; $R_1 = C_{12}H_{25}$

Table 8 The MIC (μg/ml) of quaternary imidazolium and pyrrolidinonium salts

Strains	**Compounds**									
	21a	**21b**	**21c**	**21d**	**21e**	**21f**	**22a**	**22b**	**23a**	**BAC***
S. aureus	64	16	4	4	4	8	16	8	-	8
B. subtilis	500	125	8	4	4	4	16	8	4	8
C. albicans	250	250	32	8	8	8	64	8	-	-

* Benzalkonium chloride

Some of these compounds give results globally superior to the commercially available products benzalkonium chloride (BAC) and cetylpyridinium chloride (CPC) and used as references.

Denny *et al.* (2005) investigate the antimicrobial properties of a series of 1-alkyl-2-(4-pyridyl)pyridinium bromides (also known as 2,4'-bipyridyls) with varying lengths of alkyl chains (from C9 to C16). The minimal inhibitory concentration (MIC) values determined for prepared compounds were shown in **Table 9**.

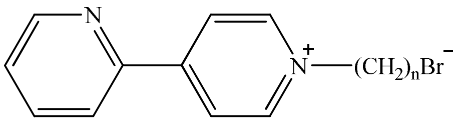

n = 9 – 16

Table 9 MIC (mg/l) of 1-alkyl-2-(4-pyridyl)pyridinium bromides series

	MIC number of strains						
	2	**4**	**8**	**16**	**32**	**64**	**>128**
MSSA (Methicillin-sensitive *S. aureus*)							
C9	-	-	-	+	+++	++	-
C10	-	+	+++	+	-	-	-
C11	+	+++	+	-	-	-	-
C12	+++	-	-	-	-	-	-
C13	+++	++	-	-	-	-	-
C14	+++	++	-	-	-	-	-
C16	+++	+	-	-	-	-	-
MRSA (Methicillin-resistant *S. aureus*)							
C9	-	-	-	+	+	+	+++
C10	-	-	++	-	+	++	++
C11	-	++	-	-	+	+++	-
C12	+	-	++	++	-	-	-
C13	+	-	+	++	+	-	-
C14	+	-	+	+++	-	-	-
C16	+	+	+	-	+++	-	-

-	: inactive
+	: low active
++	: moderately active
+++	: extremely active

The most active compounds had alkyl chain lengths of between 11 and 16 carbons. Methicillin-sensitive *S. aureus* was more susceptible to the inhibitors than Methicillin-resistant *S. aureus* (MRSA).

Sun *et al.* (2005) reported on the synthesis and antibacterial activity test of a novel series of perfluoroalkyl-containing quaternary ammonium salts **24-28**. The minimal inhibitory concentration (MIC) values determined for prepared compounds were shown in **Table 10**.

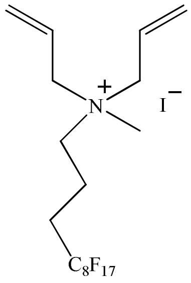

24

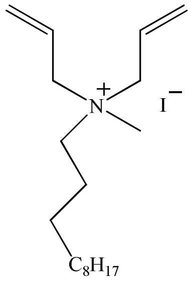

25

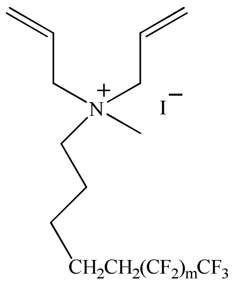

26; m = 5

27; m = 7

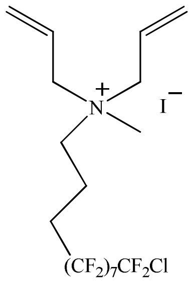

28

Table 10 The MIC values (µg/ml) for the compounds **1–5**

Strain	**Compounds**				
	24	**25**	**26**	**27**	**28**
S. aureus	2.5-5	20	10	2.5	2.5
C. albicans	50-100	50	100	100	>100

It can be concluded that the influence of the fluoroalkyl group is more effective than that of alkyl group for antibacterial activity. However, the length of the chains does not have an absolute connection with their antimicrobial activity.

Chelossi *et al.* (2006) reported a screening of the antibacterial efficacy of some compounds structurally related to poly-APS, both synthesized and extracted from marine sponge *Reniera sarai*. The minimal inhibitory concentration (MIC) values determined for prepared compounds were shown in **Table 11**.

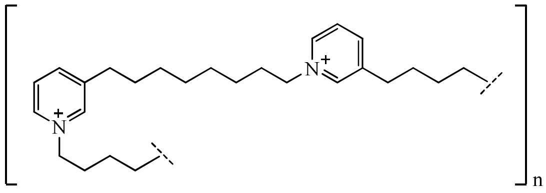

Poly-APS

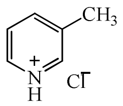

29

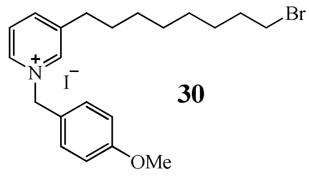

30

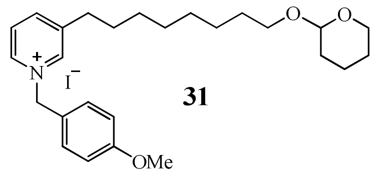

31

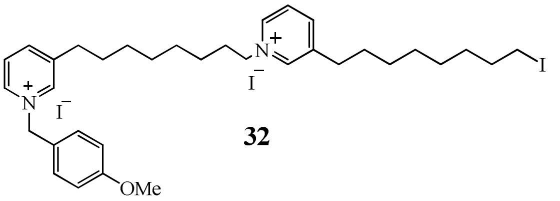

32

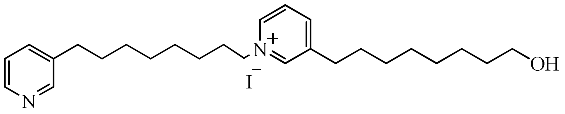

33

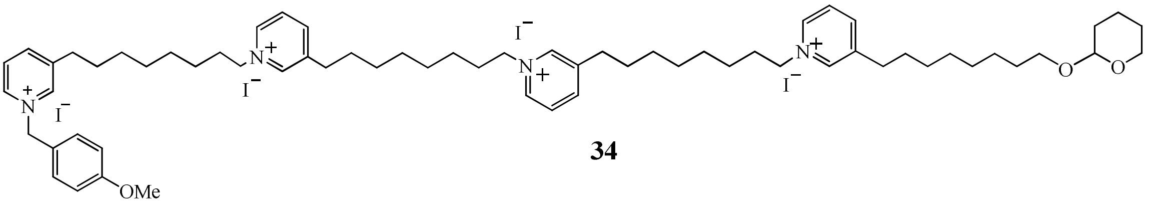

34

Table 11 MIC (mg/l) of natural and synthetic 3-alkylpyridinium salts against bacteria *in vitro*

Strains	**Compounds**						
	Poly-APS	**29**	**30**	**31**	**32**	**33**	**34**
S. aureus	25	>100	6	25	12.5	6	3
B. subtilis	25	>100	25	50	25	6	3
E. faecalis	25	50	50	25	50	25	12.5

The biological activity of synthetic alkylpyridinium analogues is related to their molecular structure. Compounds **32**, **33** and **34** have a di- or tetrameric structure, and their antibacterial ability seems to be enhanced by the presence of positive charges.

Pernak *et al.* (2006) synthesized and evaluate the antimicrobial of a novel class of chiral pyridinium salts. The minimal inhibitory concentration (MIC) values determined for prepared compounds were shown in **Table 12**.

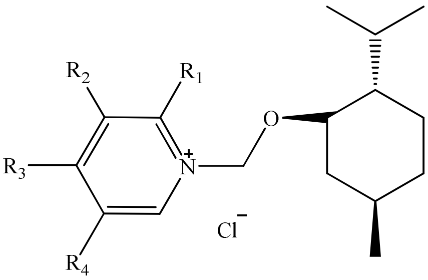

Compound	R_1	R_2	R_3	R_4
35a	H	H	H	H
35b	CH_3	H	H	H
35c	H	CH_3	H	H
35d	H	H	CH_3	H
35e	H	H	C_2H_5	H
35f	H	H	*tert*-Bu	H
35g	CH_3	H	H	OH
35h	H	$CONH_2$	H	H
35i	H	OH	H	H
35j	H	H	$N(CH_3)_2$	H
35k	H	$N(CH_3)_2$	H	H

Table 12 MIC (μM) of bis(pyridinium)alkanes

Compound	*S. aureus*	*P. aeruginosa*	*B. subtilis*	*C. albicans*
35a	882	>1,764	882	>1,764
35b	420	>1,681	1,681	>1,681
35c	840	>1,681	208	>1,681
35d	840	>1,681	1,681	>1,681
35e	803	>1,605	803	>1,605
35f	183	>1,473	183	1,473
35g	>584	>4,698	1,595	>4,699
35h	1,473	>13,837	>4,698	>13,840
35i	>1,669	>1,669	>1,669	1,669

35j	383	>5,113	>5,113	>5,112
35k	95	>15,661	>15,661	>15,656
BAC*	2.8	175	175	11

* Benzalkonium chloride

The restricted activity observed for most of chlorides **35** can be explained by the absence of a long substituent on the pyridine ring, which was accompanied by a low surface activity.

Clarissa *et al.* (2007) investigated a series of bispyridinium compounds. The minimal inhibitory concentration (MIC) values determined for prepared compounds were shown in **Table 13**.

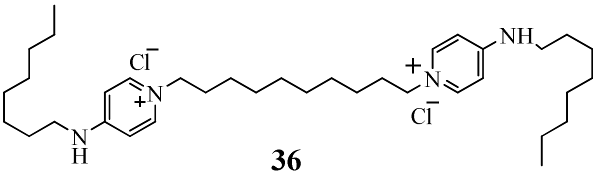
Cl⁻
Cl⁻
NH
N
H
+N
+
N

36

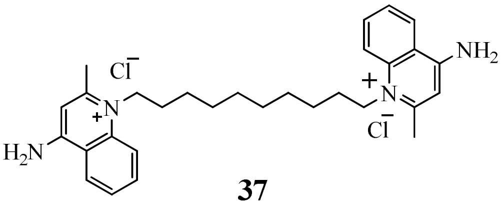
Cl⁻
NH₂
+
N
Cl⁻
H₂N
+N

37

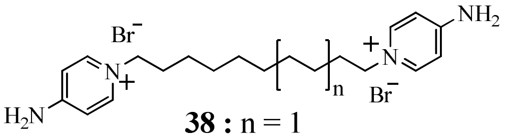
Br⁻
NH₂
+
N
n
Br⁻
N
+
H₂N

38 : n = 1
39 : n = 2
40 : n = 4

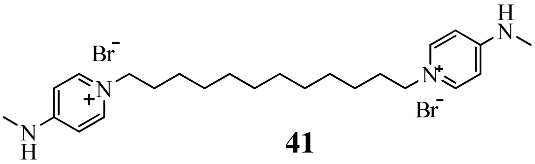
H
N
Br⁻
N+
Br⁻
N
+
N
H

41

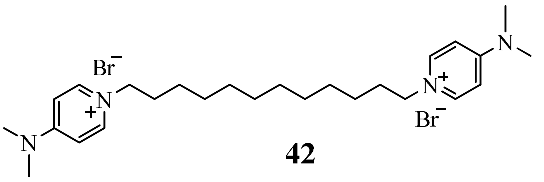

42

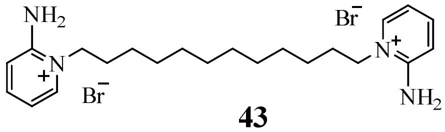
NH₂
Br⁻
N+
NH₂
N
+
Br⁻

43

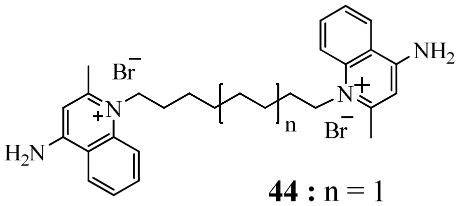
NH₂
Br⁻
N+
n
Br⁻
+N
H₂N

44 : n = 1

Table 13 MIC (µM) of bis(pyridinium)alkanes

Strain	**Compounds**								
	36	**37**	**38**	**39**	**40**	**41**	**42**	**43**	**44**
C. albicans	1.4	5.5	2.8	1.4	1.4	1.4	2.8	5.5	5.5

In the 4-aminopyridinium series of compounds (**38-40**), antifungal activity was found to increase as the distance between the headgroups was increased.

Eren *et. al.* (2008) synthesized and studied the activities of quaternary pyridinium functionalized polynorbornenes. The minimal inhibitory concentration (MIC) values determined for prepared compounds were shown in **Table 14**.

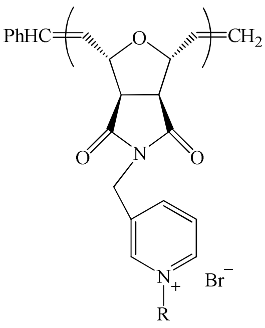

45a; R = ethyl
45b; R = butyl
45c; R = hexyl
45d; R = octyl
45e; R = decyl
45f; R = phenylethyl

Table 14 MIC (µg/ml) of pyridinium functionalized polynorbornenes against *B.subtilis*

Bacteria	**Compounds**					
	45a	**45b**	**45c**	**45d**	**45e**	**45f**
B.subtilis	200	200	4	4	6	12.5

When the alkyl substituent $\leq C_4$, the polymers are weakly active (and not hemolytic), but when the alkyl substituent $\geq C_6$, the polymers are quite potent.

Ohta *et al.* (2008) synthesized and evaluated the antibacterial of quaternary ammonium salt-type antibacterial agents with a phosphate group. The minimal inhibitory concentration (MIC) values determined for prepared compounds were shown in **Table 15**.

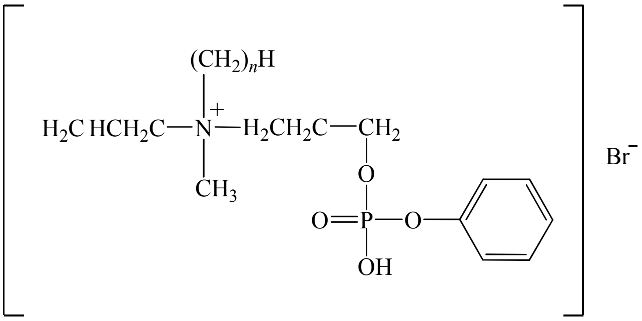

PPh-n-QAB (n = 8, 10, 12, 14, 16, 18)

Table 15 The MIC (µg/ml) values of PPh-n-QAB

Strains	**Compounds**					
	PPh-8-QAB	**PPh-10-QAB**	**PPh-12-QAB**	**PPh-14-QAB**	**PPh-16-QAB**	**PPh-18-QAB**
P. aeruginosa	400	>400	>400	>400	>400	>400
S. aureus	25	50	25	25	100	50
B. subtilis	50	50	50	25	>400	100
C. albicans	400	200	200	>400	>400	>400

PPh-12-QAB, among the six compounds synthesized, was highly effective against not only Gram-positive bacteria but also Gram-negative bacteria.

Xiao *et al.* (2008) synthesized three quaternary ammonium salts and determined *in vitro* antibacterial activities of these compounds against common pathogenic bacteria *S. aureus*. The minimal inhibitory concentration (MIC) values determined for prepared compounds were shown in **Table 16**.

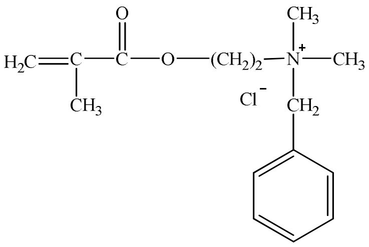

46

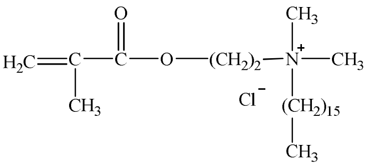

47

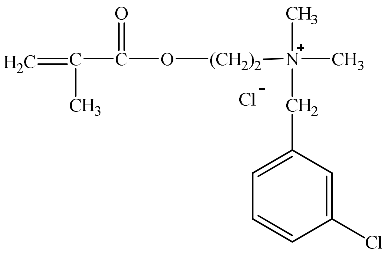

48

Table 16 MIC values (µg/ml) of three compounds

Bacterial strain	Compounds		
	46	**47**	**48**
S. aureus	1562.5	1.2	1562.5

Both **46** and **48** had similar MIC values and both are significantly higher than that of **47** which contains a 16-carbon alkyl chain. It has been shown that increasing the alkyl chain length of the substituents increased the hydrophobic interaction with the lipid bilayer of the cell wall, which increases the antibacterial activity of the compound.

Zhao and Sun (2008) explored the relationship between chemical structures and antimicrobial activities of quaternary ammonium salts particularly the impact of hydrophobicity of the salts on the antimicrobial functions.

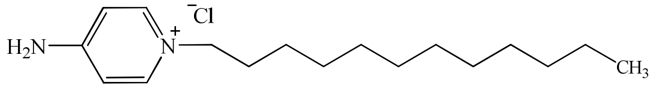

ADPC

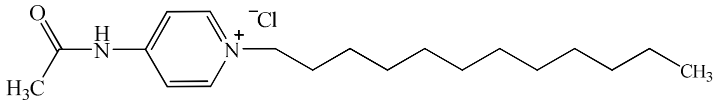

AADPC

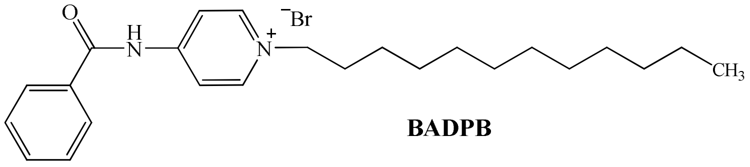

BADPB

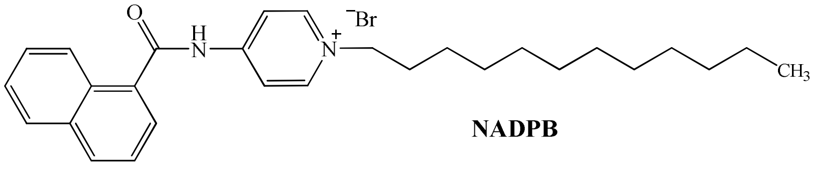

NADPB

The researchers investigated the effect of concentration and time on antimicrobial activities. This relation was shown in figures below.

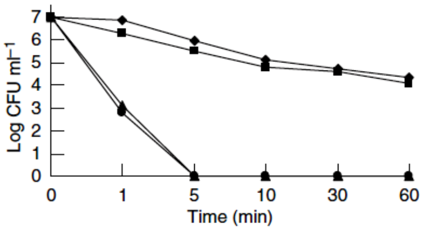

Figure 6 Effect of time on the antimicrobial activities of QASs in 10 ppm against *Staphylococcus aureus* [Symbols: (♦) ADPC, (■) AADPC, (▲) BADPB, (●) NADPB].

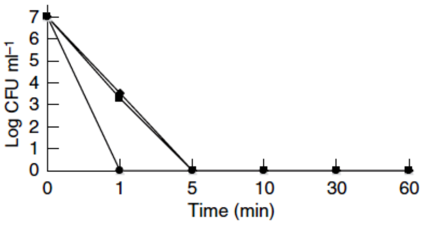

Figure 7 Effect of time on the antimicrobial activities of QASs in 50 ppm against *Staphylococcus aureus*. (♦) ADPC; (■) AADPC; (▲) BADPB and (●) NADPB.

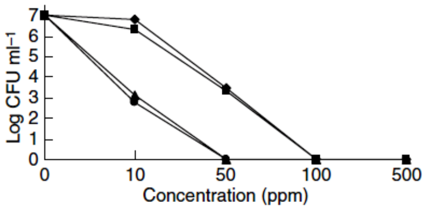

Figure 10 Effect of quaternary ammonium salt concentration on antimicrobial activities against *Staphylococcus aureus* in 1 min. (♦) ADPC; (■) AADPC; (▲) BADPB and (●) NADPB.

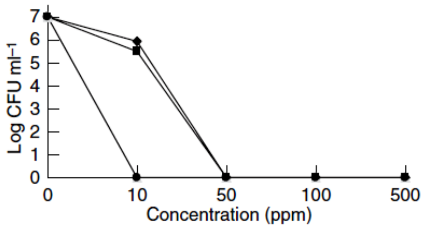

Figure 11 Effect of quaternary ammonium salt concentration on antimicrobial activities against *Staphylococcus aureus* in 5 min. (♦) ADPC; (■) AADPC; (▲) BADPB and (●) NADPB.

In this study, the long-chain alkyl group (C12) and the quaternary ammonium moiety are identical in this series; the difference in antimicrobial activities between the pyridinium salts are a result of hydrophobicity of another lipophilic moiety at the 4-(*para-*) position of the pyridinium ring. The highest bactericidal activity was achieved from the naphthoylamino derivative, the compound possessing the largest aromatic and hydrophobic group.

Caillier *et al.* (2009) synthesized the two series of surfactants monomers, with a quaternary ammonium group as polar head and an acrylic function as the polymerizable moiety and evaluated their antibacterial and antifungal properties. The minimal inhibitory concentration (MIC) values determined for prepared compounds were shown in **Table 17**.

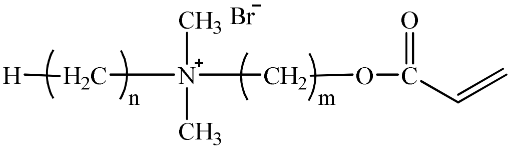

49

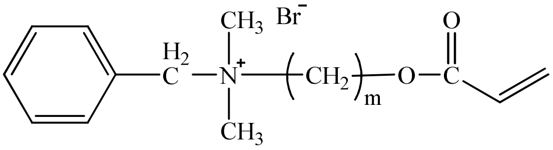

50

Compd.	n	m	Compd.	n	m
49a	$C_6H_5CH_2$	2	**50a**	$C_6H_5CH_2$	11
49b	10	2	**50b**	10	11
49c	12	2	**50c**	12	11
49d	14	2	**50d**	14	11
49e	16	2	**50e**	16	11

Table 17 MIC values (µM) for the synthesized compounds

Compd.	MIC (µM)		
	P. aeruginosa	*C. albicans*	*S. aureus*
49a	>2000	>2000	>2000
49b	355.8±3.8	277.6±3.0	355.8±3.8
49c	71.1±1.8	63.8±1.6	71.1±1.8
49d	112.4±1.9	18.1±0.3	178.1±3.0
49e	237.3±6.4	24.0±0.7	275.0±7.4
50a	153.9±3.2	153.9±3.2	243.8±5.0
50b	79.9±1.0	19.0±0.3	64.8±0.8
50c	58.4±3.4	14.8±0.5	34.7±1.2
50d	44.8±0.6	16.8±0.2	104.4±1.2
50e	131.7±2.7	27.1±0.6	208.6±4.3
BAC	93.0±1.8	8.3±0.2	3.2±0.1

The structure/activity study has shown that the length of the hydrocarbon spacer plays an important role in the biological activity because of its influence on the general hydrophobicity of the compounds. The MICs of undecylenic spacer (more hydrophobic) surfmers were systematically lower than the values recorded for surfactants with ethylenic spacers (less hydrophobic), whatever the nature of the hydrocarbon side chain ($C_{10}H_{21}$, $C_{12}H_{25}$, $C_{14}H_{29}$, $C_{16}H_{33}$ or C_6H_5–CH_2).

Massi *et al.* (2009) synthesized the fluorinated quaternary ammonium surfactants **51-66** and evaluated their antimicrobial activity using measurement of minimal inhibitory concentrations (MICs). The minimal inhibitory concentration (MIC) values determined for prepared compounds were shown in **Table 18**.

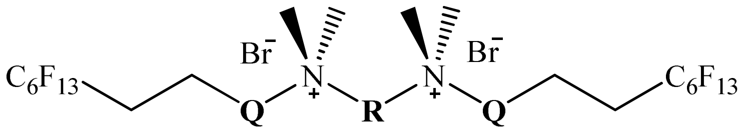

Compd.	**Q**	**R**	**Compd.**	**Q**	**R**
51	$NHC(O)CH_2$	$(CH_2)_2$	**59**	$NHC(O)CH_2$	$CH_2CH{=}CHCH_2$
52	$NHC(O)CH_2$	$(CH_2)_3$	**60**	$NHC(O)CH_2$	$CH_2CH(OH)CH_2$
53	$NHC(O)CH_2$	$(CH_2)_4$	**61**	$NHC(O)CH_2$	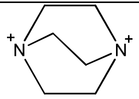
54	$NHC(O)CH_2$	$(CH_2)_6$	**62**	S-CH_2	$(CH_2)_4$
55	$NHC(O)CH_2$	$(CH_2)_8$	**63**	-	$(CH_2)_4$
56	$NHC(O)CH_2$	$(CH_2)_{10}$	**64**	$C(O)NHCH_2CH_2$	$(CH_2)_4$
57	$NHC(O)CH_2$	$(CH_2)_{12}$	**65**	$NHC(O)NHCH_2CH_2$	$(CH_2)_4$
58	$NHC(O)CH_2$	$(CH_2)_2$-S-S-$(CH_2)_2$	**66**	$NHC(O)OCH_2CH_2$	$(CH_2)_4$

Table 18 Antibacterial activity of **51-66** against *Pseudomonas aeruginosa* according to minimal inhibitory concentrations (MICs) expressed in μM

Compound	**MIC (μmol/L)**	**Compound**	**MIC (μmol/L)**
51	5.80	**59**	3.67
52	5.19	**60**	9.25
53	5.94	**61**	5.82
54	5.52	**62**	4.59
55	2.89	**63**	7.31
56	2.83	**64**	1.88
57	2.76	**65**	5.38
58	4.95	**66**	3.69

The variation of the nature of the connector between the charged nitrogen atoms (**Q**) and the fluorinated tails, particularly the presence of hydrogen bond donor group, and of the nature of the spacer (**R**) between the two quaternized nitrogen atoms modifies more largely the antibacterial effect.

1.6 Objective and outline of this study

The advantages of quaternary ammonium compounds (quats) in antimicrobial usage led to the design and synthesis the pyridinium disinfectants. Moreover, sulfa-mimetic structures were combined to improve the activities of the pyridinium quats. As a result, twenty four quaternary ammonium compounds disinfectant which are the derivatives of promising compounds naphthalenyl-ethenylpyridinium benzenesulfonate (**Fig. 4**) were synthesized in this study.

The compounds were consisted of two parts which were cation part and anion counter part. The cation part is naphthalenyl-ethenylpyridinium type containing pyridinium cation which was the well-known constituent of the herbicide, insecticide, some antibacterial drugs and disinfectants widely used in hospitals and industry due to its safeness (Maeda *et al.*, 1999). The extended aromatic system which was the naphthalenyl head group was introduced to increase the hydrophobicity in order to enhance the penetration through the cell wall of gram negative. In addition, the well-known antibacterial drugs sulfonamides also represent wide application in synthetic bioactive compounds and many representatives of this class of compounds were reported to have antibacterial activity. So the benzenesulfonate part, which was likely to form the similar interaction with the bacterial active site in their essential pathway, was added to mimic the sulfonamide drugs. All of the design strategy mentioned above was applied to these compounds to increase the possibility of achieving the antimicrobial active compounds.

In this study, the tested pathogenic bacteria were *S. aureus, B. subtilis, E. faecalis,* along with the two resistant-type bacteria Methicillin-Resistant *S. aureus* and Vancomycin-Resistant *E. faecalis* are the selected Gram-positive bacteria and *P. aeruginosa, S. typhi* and *S. sonnei* which are the Gram-negative bacteria. The only one tested fungus was *C. albicans*. All of the selected bacteria can cause severe infection diseases, especially Methicillin-Resistant *S. aureus* and Vancomycin-Resistant *E. faecalis* which can resist to the common widely used antibiotics.

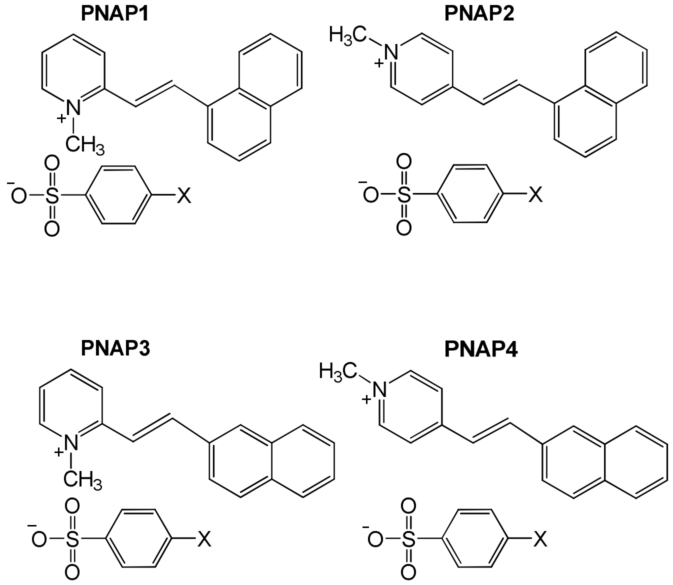

PNAP1M ; X = CH_3 **PNAP2M** ; X = CH_3
PNAP1O ; X = OCH_3 **PNAP2O** ; X = OCH_3
PNAP1C ; X = Cl **PNAP2C** ; X = Cl
PNAP1B ; X = Br **PNAP2B** ; X = Br
PNAP1N ; X = NH_2 **PNAP2N** ; X = NH_2
(For **PNAP1** *and* **PNAP2** *; Anion part is iodide (I^-))*

PNAP3M ; X = CH_3 **PNAP4M** ; X = CH_3
PNAP3O ; X = OCH_3 **PNAP4O** ; X = OCH_3
PNAP3C ; X = Cl **PNAP4C** ; X = Cl
PNAP3B ; X = Br **PNAP4B** ; X = Br
PNAP3N ; X = NH_2 **PNAP4N** ; X = NH_2
(For **PNAP3** *and* **PNAP4** *; Anion part is iodide (I^-))*

Figure 4 The naphthalenyl-ethenylpyridinium benzenesulfonate derivatives

In this study, focus shall be on the adducts of derivatives of naphthalenyl-ethenylpyridinium benzenesulfonate which are expected to exhibit the antimicrobial properties. Crystals of a size and quality suitable for single crystal X-ray diffraction studies are grown with the objective to study their structure in solid state.

This thesis is divided into four parts. Part one is the introduction, part two is the experimental, part three is the results and discussion and part four is the conclusion.

CHAPTER 2
EXPERIMENT

2.1 Instruments and chemicals

2.1.1 Instruments

Melting point was measured on a Fisher-Johns melting point apparatus. Ultraviolet (UV) absorption spectra were measured using a SPECORD S 100 (Analytikjena) spectrophotometer with methanol as solvent and principle bands (λ_{max}) were recorded as wavelengths (nm) and logε. Infrared spectra were recorded on a Perkin-Elmer FT-IR system Spectrum BX Spectrophotometer (KBr pellets) and major bands (ν) were recorded in wave numbers (cm^{-1}). Proton nuclear magnetic resonance spectra were recorded on FT-NMR Bruker Ultra Shield^{TM} 300 MHz. Spectra were recorded as δ value in ppm downfield from TMS (internal standard δ 0.00) and using deuterochloroform mixed with hexadeutero-dimethyl sulphoxide as solvents. Single crystal X-ray diffraction measurements were collected using SMART 1-K CCD diffractometer with monochromated MoK$_{\propto}$ radiation. (λ = 0.71073 Å) using ω scan mode and SHELXTL for structural solution and refinement. The antimicrobial assay were tested against gram-positive bacteria (which were *S. aureus, B. subtilis, E. faecalis,* Methicillin-Resistant *S. aureus* and Vancomycin-Resistant *E. faecalis*), gram-negative bacteria (which were *P. aeruginosa, S. typhi* and *S. sonnei*) and a fungus (*C. albicans*) by colorimetric microdilution assay using Alamar Blue indicator. The yields were reported as percentage of crude products.

2.1.2 Chemicals

All chemicals used in this study are AR grade and were used without further purification.

1) 2-Picoline from Fluka Chemica, Switzerland
2) 4-Picoline from Fluka Chemica, Switzerland
3) Piperidine from Fluka Chemica, Switzerland
4) Methyl iodide from Riedel-de Haën, Germany
5) 1-Naphthaldehyde from Fluka, Switzerland
6) 2-Naphthaldehyde from Aldrich, Germany
7) *p*-Toluenesulfonic acid monohydrate from Fluka Chemica, Switzerland
8) 4-Methoxybenzenesulfonyl chloride from Fluka Chemica, Switzerland
9) 4-Chlorobenzenesulfonyl chloride from Fluka Chemica, Switzerland
10) 4-Bromobenzenesulfonyl chloride from Fluka Chemica, Switzerland
11) Sulfanilic acid from Fluka, Switzerland
12) Silver nitrate from Merck, Germany
13) Sodium hydroxide from Lab-Scan, Ireland
14) Dichloromethane (AR grade) from Merck, Germany
15) Diethyl ether (AR grade) from Merck, Germany
16) Methanol (AR grade) from Merck, Germany
17) Ethanol (AR grade) from Merck, Germany
18) Acetone (AR grade) from Merck, Germany

2.2 *Synthesis of the starting materials*

2.2.1 1,2-dimethylpyridinium iodide (PO-ST)

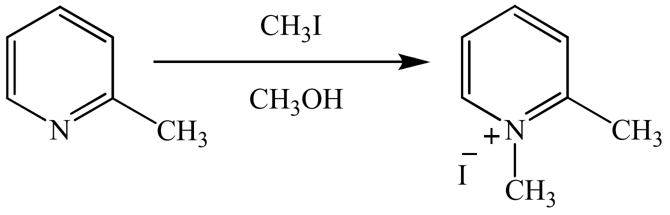

PO1 **PO-ST**

1,2-dimethylpyridinium iodide **(PO-ST)** and 1,4-dimethylpyridinium iodide **(PP-ST)** were prepared to be employed as starting material for the syntheses of related products. Methyl iodide (6.45 ml, 0.10 mol) was added drop wise to a stirred solution of 2-picoline **(PO1)** (10.00 ml, 0.10 mol) in cold methanol (15 ml) at 5 °C under nitrogen atmosphere for 1 hr and then refluxing for 1 hr. The mixture was cooled in an ice bath and the obtained crystalline solid was filtered, washed with cold methanol and dried in vacuum to give a white solid of 1,2-dimethylpyridinium iodide **(PO-ST)** (20.87 g, 87%), mp. 220-222 °C, UV-Vis (CH_3OH) λ_{max} (nm) (log ε): 218 (9,221), 256 (11,209), FT-IR (KBr) $\nu(cm^{-1})$: 1600 (C=C stretching), ^1H NMR ($CDCl_3$ + DMSO-d_6) (δ ppm) (300 MHz): 9.09 (1H, *d*, *J* = 6.9 Hz), 7.94 (1H, *t*, *J* = 6.9 Hz), 8.48 (1H, *t*, *J* = 6.9 Hz), 8.06 (1H, *t*, *J* = 6.9 Hz), 3.05 (3H, *s*), 4.65 (3H, *s*).

2.2.2 1,4-dimethylpyridinium iodide (PP-ST)

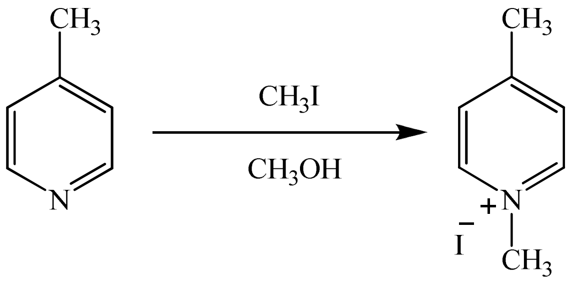

PP1 **PP-ST**

1,4-dimethylpyridinium iodide **(PP-ST)** were prepared to be employed as starting material for the syntheses of related products. Methyl iodide (6.45 ml, 0.10 mol) was added dropwise to a stirred solution of 4-picoline **(PP1)** (10.00 ml, 0.10 mol) in cold methanol (15 ml) at 5 °C under nitrogen atmosphere for 1 hr and then refluxing for 1 hr. The mixture was cooled in an ice bath and the obtained crystalline solid was filtered, washed with cold methanol and dried in vacuum to give a pale yellow solid of 1,4-dimethylpyridinium iodide **(PP-ST)** (15.50 g, 66%), mp. 140-142 °C, UV-Vis (CH_3OH) λ_{max} (nm) (log ε): 219.7 (3.78), 255.3 (3.16), FT-IR (KBr) ν(cm^{-1}): 1600-1500 (C=C stretching), ^1H NMR ($CDCl_3$ + DMSO-d_6) (δ ppm) (300 MHz): 9.13 (2H, *d*, J = 6.3 Hz), 7.88 (2H, *d*, J = 6.3 Hz), 4.62 (3H, *s*), 2.69 (3H, *s*).

2.3 Synthesis of cations parts

2.3.1 (*E*)-1-methyl-2-(2-(naphthalen-1-yl)vinyl)pyridinium iodide (PNAP1)

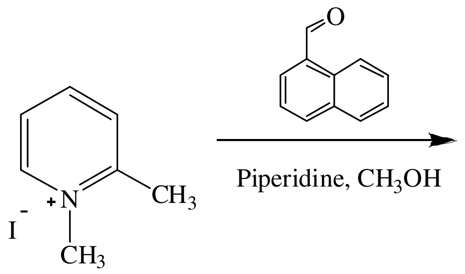

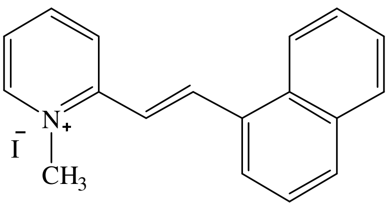

PO-ST **PNAP1**

The mixture of 1,2-dimethylpyridinium iodide **(PO-ST)** (2.00 g, 8.50 mmol), 1-naphthaldehyde (1.16 ml, 8.50 mmol) and piperidine (0.84 ml, 8.50 mmol) in methanol was refluxed under nitrogen atmosphere for 4 hrs. The solid formed was filtered off, washed with diethyl ether to give yellow solid of (*E*)-1-methyl-2-(2-(naphthalen-1-yl)vinyl)pyridinium iodide **(PNAP1)** (2.34 g, 80%), mp. 283-284 °C, UV-Vis (CH_3OH) λ_{max} (nm) (log ε): 221.69 (10,689), 277.79 (1,576), 354.17 (1,160), FT-IR (KBr) $\nu(cm^{-1})$: 3025 (sp^2 C-H aromatic stretching), 1609 (C=C aromatic stretching), 963 (C-H *trans*-RCH=CHR out of plane bending), ^{1}H NMR (see **Table 19**).

2.3.2 (*E*)-1-methyl-4-(2-(naphthalen-1-yl)vinyl)pyridinium iodide (PNAP2)

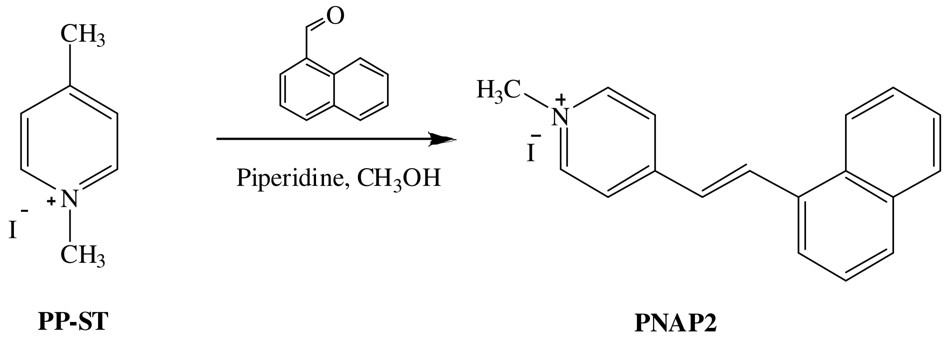

The mixture of 1,4-dimethylpyridinium iodide **(PP-ST)** (2.00 g, 8.50 mmol), 1-naphthaldehyde (1.16 ml, 8.50 mmol) and piperidine (0.84 ml, 8.50 mmol) in methanol was refluxed under nitrogen atmosphere for 3 hrs. The solid formed was filtered off, washed with diethyl ether to give yellow solid of (*E*)-1-methyl-4-(2-(naphthalen-1-yl)vinyl)pyridinium iodide **(PNAP2)** (2.38 g, 81%), mp. 287-288 °C, UV-Vis (CH_3OH) λ_{max} (nm) (log ε): 220.34 (8,521), 275.77 (2,048), 375.80 (741), FT-IR (KBr) ν(cm^{-1}): 3017 (*sp*^{2} C-H aromatic stretching), 1617 (C=C aromatic stretching), 974 (C-H *trans*-RCH=CHR out of plane bending), ^{1}H NMR (see **Table 20**).

2.3.3 (*E*)-1-methyl-2-(2-(naphthalen-2-yl)vinyl)pyridinium iodide (PNAP3)

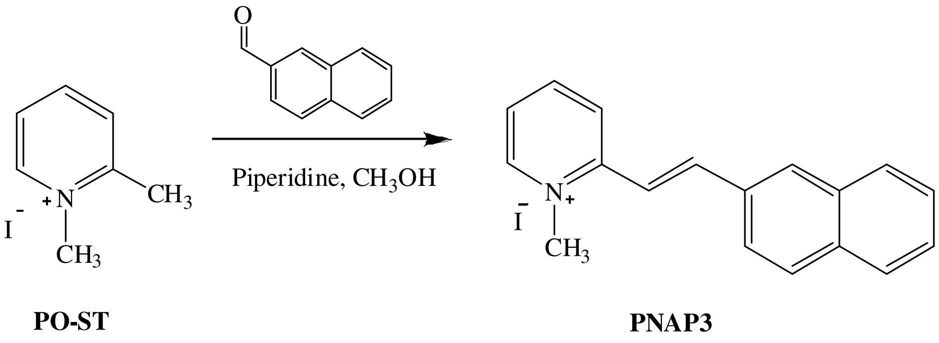

The mixture of 1,2-dimethylpyridinium iodide **(PO-ST)** (2.00 g, 8.50 mmol), 2-naphthaldehyde (1.33 g, 8.50 mmol) and piperidine (0.84 ml, 8.50 mmol) in methanol was refluxed under nitrogen atmosphere for 3 hrs. The solid formed was filtered off, washed with diethyl ether to give pale yellow solid of (*E*)-1-methyl-2-(2-(naphthalen-2-yl)vinyl)pyridinium iodide **(PNAP3)** (2.20 g, 75%), mp. 261-263 °C, UV-Vis (CH_3OH) λ_{max} (nm) (log ε): 223.57 (4,254), 339.43 (656), FT-IR (KBr) $\nu(cm^{-1})$: 3045 (sp^2 C-H aromatic stretching), 1612 (C=C aromatic stretching), 963 (C-H *trans*-RCH=CHR out of plane bending), ^{1}H NMR (see **Table 21**).

2.3.4 (*E*)-1-methyl-4-(2-(naphthalen-2-yl)vinyl)pyridinium iodide (PNAP4)

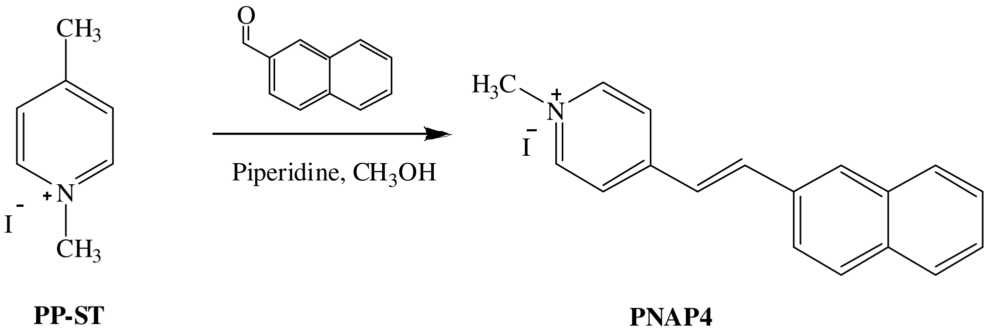

The mixture of 1,4-dimethylpyridinium iodide **(PP-ST)** (2.00 g, 8.50 mmol), 2-naphthaldehyde (1.33 g, 8.50 mmol) and piperidine (0.84 ml, 8.50 mmol) in methanol was refluxed under nitrogen atmosphere for 3 hrs. The solid formed was filtered off, washed with diethyl ether to give yellow solid of (*E*)-1-methyl-4-(2-(naphthalen-2-yl)vinyl)pyridinium iodide **(PNAP4)** (2.26 g, 77%), mp. 284-285 °C, UV-Vis (CH_3OH) λ_{max} (nm) (log ε): 225.56 (31,686), 356.83 (9,172), FT-IR (KBr) ν(cm^{-1}): 3019 (sp^2 C-H aromatic stretching), 1612 (C=C aromatic stretching), 971 (C-H *trans*-RCH=CHR out of plane bending), ^1H NMR (see **Table 22**).

2.4 Synthesis of anions counter parts

2.4.1 Silver (I) 4-methylbenzenesulfonate (ANM)

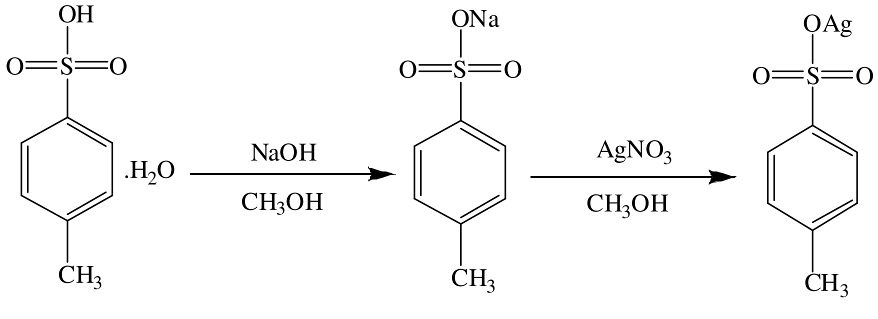

SM **ANM**

A solution of 4-methylbenzenesulfonic acid monohydrate **(SM)** (5.00 g, 26.30 mmol) in hot methanol was added to a stirred solution of sodium hydroxide (1.05 g, 26.30 mmol) in hot methanol, followed by addition of a solution of silver nitrate (4.47 g, 26.30 mmol) in hot methanol. A solution mixed with a solid was obtained which was filtered. The white crystalline solid of **ANM** (5.20 g, 71%) was collected after allowing the filtrate to stand in air for a few days, mp. 264-266 °C (decomp.), ^{1}H NMR ($CDCl_3$ + DMSO-d_6) (δ ppm) (300 MHz): 7.74 (2H, *d*, J = 8.1 Hz), 7.17 (2H, *d*, J = 8.1 Hz), 2.38 (1H, *s*).

2.4.2 Silver (I) 4-methoxybenzenesulfonate (ANOM)

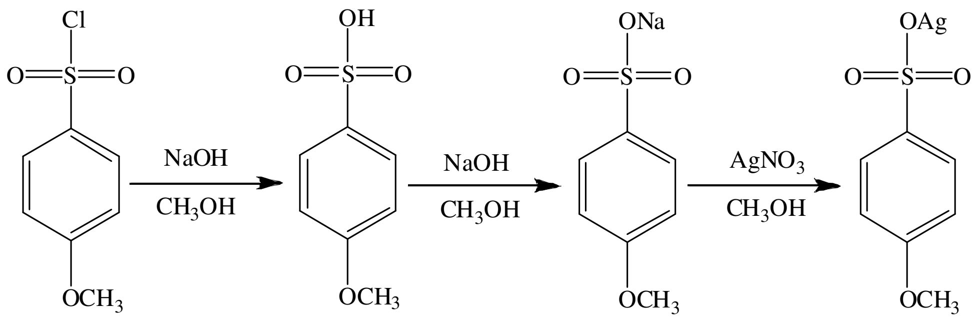

SOM **ANOM**

Silver (I) 4-methoxybenzenesulfonate **(ANOM)** was prepared by mixing a solution of 4-methoxybenzenesulfonyl chloride **(SOM)** (5.00 g, 24.20 mmol) and sodium hydroxide (0.97 g, 24.25 mmol) in hot methanol. A colorless solution mixed with a white solid of sodium chloride was obtained. The mixture was worked up by addition of water and extraction was dichloromethane. The dichloromethane part was evaporated and the resulting residue was dissolved in methanol, followed by addition of the solution of sodium hydroxide (0.96 g, 24.00 mmol) in hot methanol and a solution of silver nitrate (4.10 g, 24.14 mmol) in hot methanol. The colorless solution mixed with a solid of sodium nitrate was obtained, which was filtered and discarded. Compound **ANOM** (4.53 g, 63%) was obtained after allowing the resulting filtrate to stand in air for a few days, mp. 240-242 °C (decomp.), ^{1}H NMR ($CDCl_3$ + DMSO-d_6) (δ ppm) (300 MHz): 7.78 (2H, *d*, J = 8.7), 6.86 (2H, *d*, J = 8.7 Hz), 3.82 (1H, *s*).

2.4.3 Silver (I) 4-chlorobenzenesulfonate (ANCL)

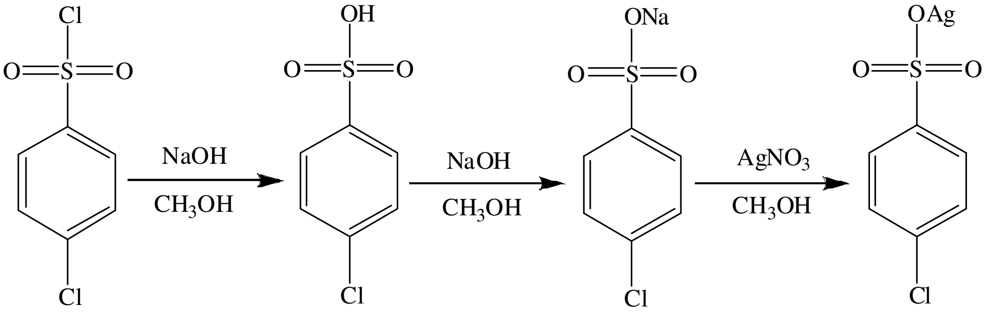

SCL **ANCL**

Silver (I) 4-chlorobenzenesulfonate **(ANCL)** was prepared to be employed as anionic part by mixing a solution (1:1 molar ratio) of 4-chlorobenzenesulfonyl chloride **(SCL)** (5.00 g, 19.57 mmol) and sodium hydroxide (0.78 g, 19.57 mmol) in hot methanol. A colorless solution mixed with a white solid of sodium chloride was obtained. The mixture was worked up by addition of water and extraction was dichloromethane. The dichloromethane part was evaporated and dissolved in methanol, followed by addition of the solution of sodium hydroxide (0.77 g, 19.32 mmol) in hot methanol and a solution of silver nitrate (3.32 g, 19.57 mmol) in hot methanol. The colorless solution mixed with a solid of sodium nitrate was obtained, which was filtered and discarded. Compound **ANCL** (4.56 g, 68%) was obtained after allowing the resulting filtrate to stand in air for a few days, mp. 227-229 °C (decomp.), ^{1}H NMR ($CDCl_3$ + DMSO-d_6) (δ ppm) (300 MHz): 7.76 (2H, *d*, J = 7.8), 7.50 (2H, *d*, J = 7.8 Hz).

2.4.4 Silver (I) 4-bromobenzenesulfonate (ANBR)

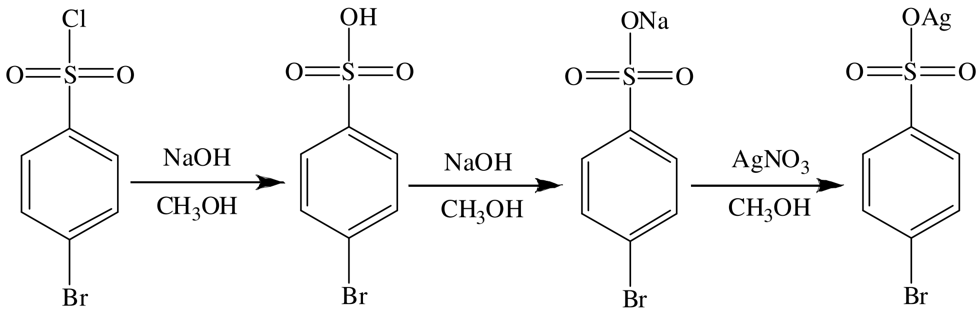

SBR

ANBR

Silver (I) 4-bromobenzenesulfonate **(ANBR)** was synthesized by mixing a solution of 4-bromobenzenesulfonyl chloride **(SBR)** (5.00 g, 23.69 mmol) and sodium hydroxide (0.95 g, 23.69 mmol) in hot methanol. A colorless solution mixed with a white solid of sodium chloride was obtained. The mixture was worked up by addition of water and extraction was dichloromethane. The dichloromethane part was evaporated and dissolved in methanol, followed by addition of the solution of sodium hydroxide (0.96 g, 23.64 mmol) in hot methanol and a solution of silver nitrate (4.00 g, 23.57 mmol) in hot methanol. The colorless solution mixed with a solid of sodium nitrate was obtained, which was filtered and discarded. Compound **ANBR** (4.36 g, 61%) was obtained after allowing the resulting filtrate to stand in air for a few days, mp. 230-232 °C decomposed, ^{1}H NMR ($CDCl_3$ + DMSO-d_6) (δ ppm) (300 MHz): 7.81 (2H, *d*, J = 8.4), 7.34 (2H, *d*, J = 8.4 Hz).

2.4.5 Silver (I) 4-aminobenzenesulfonate (ANNH)

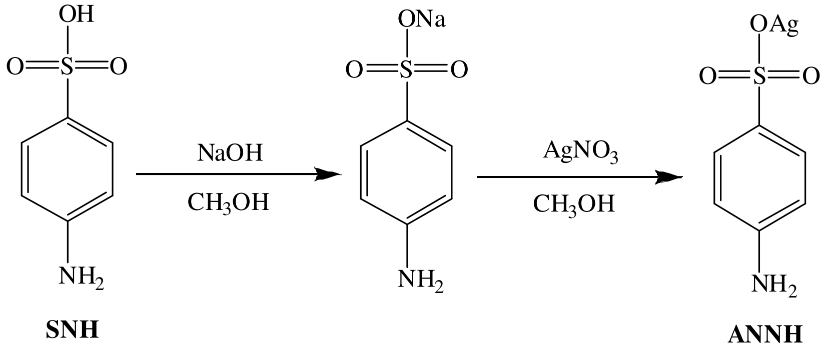

A solution of sulfanilic acid **(SNH)** (5.00 g, 28.75 mmol) in hot methanol was added to a stirred solution of sodium hydroxide (1.15 g, 28.75 mmol) in hot methanol, followed by addition of a solution of silver nitrate (4.88 g, 28.75 mmol) in hot methanol. A solution mixed with a solid was obtained which was filtered. The white crystalline solid of **ANNH** (4.83 g, 60%) was collected after allowing the filtrate to stand in air for a few days, mp. 279-280 °C (decomp.), ^{1}H NMR ($CDCl_3$ + DMSO-d_6) (δ ppm) (300 MHz): 7.26 (*d*, 2H, J = 8.1 Hz), 6.45 (*d*, 2H, J = 8.1 Hz), 5.19 (*s*, 2H).

2.5 Salt formations

2.5.1 (*E*)-1-methyl-2-(2-(naphthalen-1-yl)vinyl)pyridinium 4-methylbenzenesulfonate (PNAP1M)

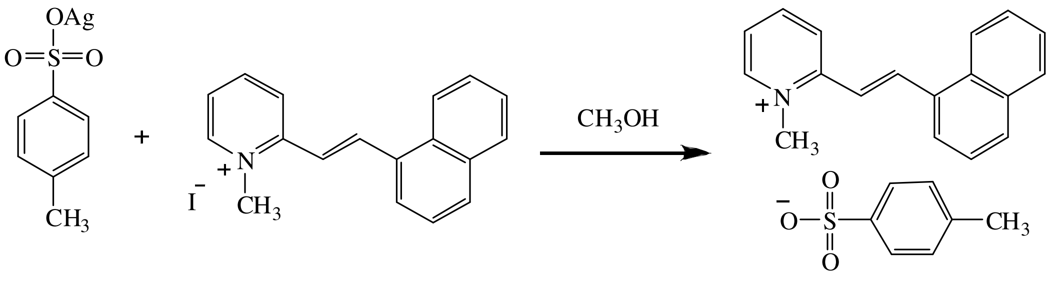

ANM **PNAP1** **PNAP1M**

(*E*)-1-methyl-2-(2-(naphthalen-1-yl)vinyl)pyridinium 4-methylbenzenesulfonate **(PNAP1M)** was synthesized by addition of a solution of silver (I) 4-methylbenzenesulfonate (0.20 g, 0.68 mmol) in hot methanol (20 ml) to a solution of compound **PNAP1** (0.26 g, 0.68 mmol) in hot methanol (45 ml). Upon addition a yellow solid of silver iodide was immediately formed which was removed by filtration and the yellow filtrate was evaporated under reduced pressure to yield a yellow solid. The yellow solid was recrystallized from methanol to give yellow crystals of compound **PNAP1M** (0.28 g, 98%), mp. 196-197 °C, UV-Vis (CH_3OH) λ_{max} (nm) (logε): 220.34(14,742), 275.09(2,150), 355.52(1,208), FT-IR (KBr) ν(cm^{-1}): 3025 (*sp*^{2} C-H aromatic stretching), 1611 (C=C aromatic stretching), 1195 (S=O stretching), ^{1}H NMR (see **Table 26**).

2.5.2 (*E*)-1-methyl-2-(2-(naphthalen-1-yl)vinyl)pyridinium 4-methoxybenzenesulfonate (PNAP1O)

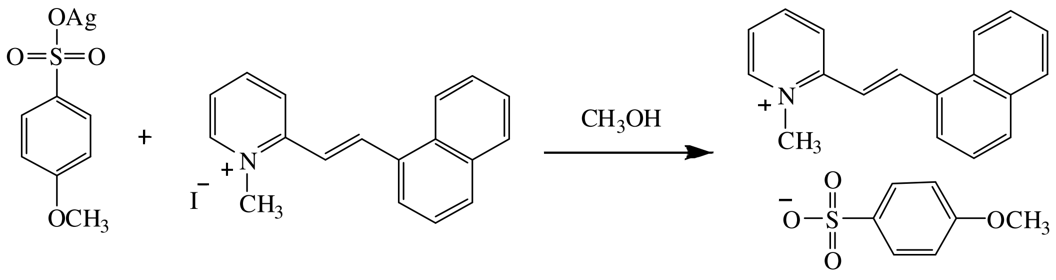

ANOM **PNAP1** **PNAP1O**

(*E*)-1-methyl-2-(2-(naphthalen-1-yl)vinyl)pyridinium 4-methoxybenzenesulfonate **(PNAP1O)** was synthesized by addition of a solution of silver (I) 4-methoxybenzenesulfonate (0.20 g, 0.67 mmol) in hot methanol (20 ml) to a solution of compound **PNAP1** (0.25 g, 0.67 mmol) in hot methanol (45 ml). Upon addition a yellow solid of silver iodide was immediately formed which was removed by filtration and the yellow filtrate was evaporated under reduced pressure to yield a yellow solid. The yellow solid was re-crystallized from methanol to give yellow crystals of compound **PNAP1O** (0.25 g, 86%), mp. 196-198 °C, UV-Vis (CH_3OH) λ_{max} (nm) (logε): 221.69 (9,801), 273.06 (1,565), 354.85 (654), FT-IR (KBr) ν(cm^{-1}): 2999 (sp^2 C-H aromatic stretching), 1601 (C=C aromatic stretching), 1208 (S=O stretching), 1194 (C-O in OCH_3 stretching), ^{1}H NMR (see **Table 27**).

2.5.3 (*E*)-1-methyl-2-(2-(naphthalen-1-yl)vinyl)pyridinium 4-chlorobenzenesulfonate (PNAP1C)

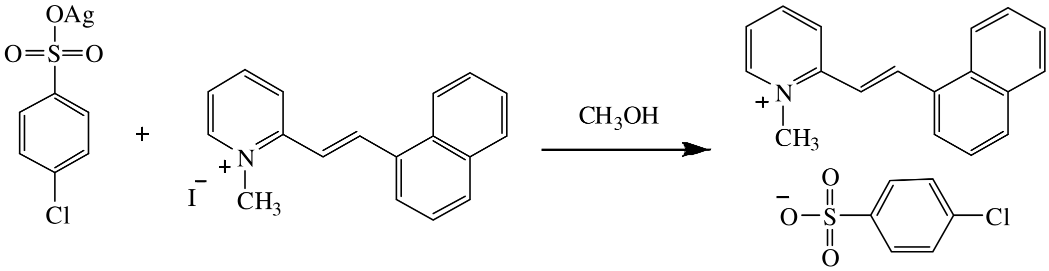

ANCL **PNAP1** **PNAP1C**

(*E*)-1-methyl-2-(2-(naphthalen-1-yl)vinyl)pyridinium 4-chlorobenzenesulfonate **(PNAP1C)** was synthesized by addition of a solution of silver (I) 4-chlorobenzenesulfonate (0.20 g, 0.67 mmol) in hot methanol (20 ml) to a solution of compound **PNAP1** (0.25 g, 0.67 mmol) in hot methanol (45 ml). Upon addition a yellow solid of silver iodide was immediately formed which was removed by filtration and the yellow filtrate was evaporated under reduced pressure to yield a yellow solid. The yellow solid was re-crystallized from methanol to give yellow crystals of compound **PNAP1C** (0.23 g, 80%), mp.(decompose) 270-272 °C, UV-Vis (CH_3OH) λ_{max} (nm) (logε): 221.02 (6,845), 274.42 (858), 358.23 (462), FT-IR (KBr) $\nu(cm^{-1})$: 3025 (sp^2 C-H aromatic stretching), 1598 (C=C aromatic stretching), 1218 (S=O stretching), ^1H NMR (see **Table 28**).

2.5.4 (*E*)-1-methyl-2-(2-(naphthalen-1-yl)vinyl)pyridinium 4-bromobenzenesulfonate (PNAP1B)

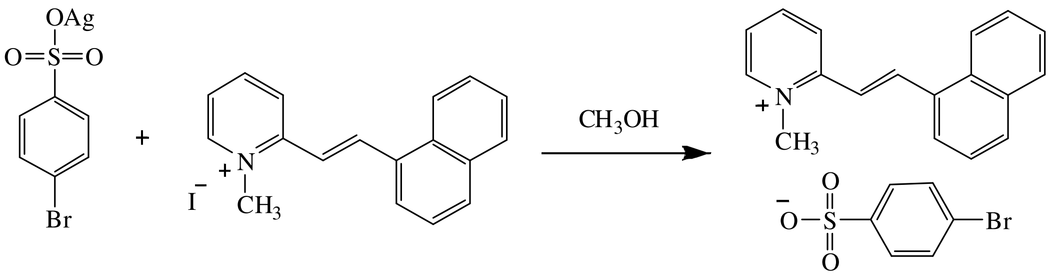

ANBR **PNAP1** **PNAP1B**

(*E*)-1-methyl-2-(2-(naphthalen-1-yl)vinyl)pyridinium 4-bromobenzenesulfonate **(PNAP1B)** was synthesized by addition of a solution of silver (I) 4-chlorobenzenesulfonate (0.20 g, 0.58 mmol) in hot methanol (20 ml) to a solution of compound **PNAP1** (0.22 g, 0.58 mmol) in hot methanol (45 ml). Upon addition a yellow solid of silver iodide was immediately formed which was removed by filtration and the yellow filtrate was evaporated under reduced pressure to yield a yellow solid. The yellow solid was re-crystallized from methanol to give yellow crystals of compound **PNAP1B** (0.28 g, 98%), mp. >300 °C, UV-Vis (CH_3OH) λ_{max} (nm) (logε): 221.02 (18,085), 273.74 (2,578), 356.87 (892), FT-IR (KBr) $\nu(cm^{-1})$: 3025 (sp^2 C-H aromatic stretching), 1600 (C=C aromatic stretching), 1220 (S=O stretching), ^{1}H NMR (see **Table 29**).

2.5.5 (*E*)-1-methyl-2-(2-(naphthalen-1-yl)vinyl)pyridinium 4-aminobenzenesulfonate (PNAP1N)

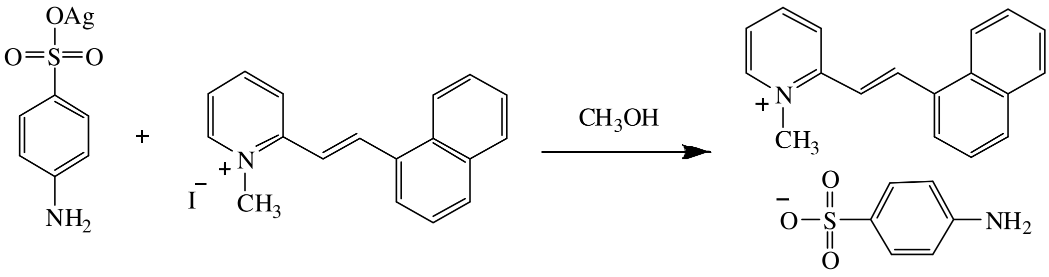

ANNH **PNAP1** **PNAP1N**

(*E*)-1-methyl-2-(2-(naphthalen-1-yl)vinyl)pyridinium 4-aminobenzenesulfonate **(PNAP1N)** was synthesized by addition of a solution of silver (I) 4-chlorobenzenesulfonate (0.20 g, 0.71 mmol) in hot methanol (20 ml) to a solution of compound **PNAP1** (0.27 g, 0.71 mmol) in hot methanol (45 ml). Upon addition a yellow solid of silver iodide was immediately formed which was removed by filtration and the yellow filtrate was evaporated under reduced pressure to yield a yellow solid. The yellow solid was re-crystallized from methanol to give yellow crystals of compound **PNAP1N** (0.16 g, 55%), mp. 232-233 °C, UV-Vis (CH_3OH) λ_{max} (nm) (logε): 220.92 (2,699), 255.35 (774), 364.59 (62), FT-IR (KBr) $\nu(cm^{-1})$: 3340 (N-H in primary amine stretching), 3091 (*sp*^{2} C-H aromatic stretching), 1617 (C=C aromatic stretching), 1183 (S=O stretching), ^{1}H NMR (see **Table 30**).

2.5.6 (*E*)-1-methyl-4-(2-(naphthalen-1-yl)vinyl)pyridinium 4-methylbenzenesulfonate (PNAP2M)

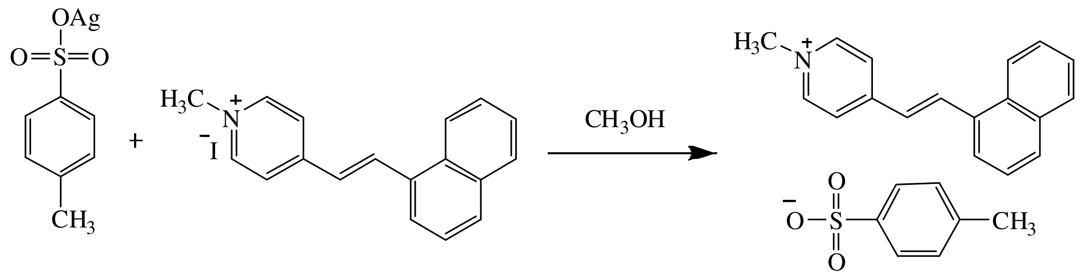

ANM **PNAP2** **PNAP2M**

(*E*)-1-methyl-4-(2-(naphthalen-1-yl)vinyl)pyridinium 4-methylbenzenesulfonate **(PNAP2M)** was synthesized by addition of a solution of silver (I) 4-methylbenzenesulfonate (0.20 g, 0.68 mmol) in hot methanol (20 ml) to a solution of compound **PNAP2** (0.26 g, 0.68 mmol) in hot methanol (45 ml). Upon addition a yellow solid of silver iodide was immediately formed which was removed by filtration and the yellow filtrate was evaporated under reduced pressure to yield a yellow solid. The yellow solid was re-crystallized from methanol to give yellow crystals of compound **PNAP2M** (0.24 g, 86%), mp. 178-180 °C, UV-Vis (CH_3OH) λ_{max} (nm) (logε): 220.34 (10,590), 276.44 (2,143), 377.15 (736), FT-IR (KBr) ν(cm^{-1}): 3048 (sp^2 C-H aromatic stretching), 1617 (C=C aromatic stretching), 1187 (S=O stretching), ^{1}H NMR (see **Table 31**).

2.5.7 (*E*)-1-methyl-4-(2-(naphthalen-1-yl)vinyl)pyridinium 4-methoxybenzenesulfonate (PNAP2O)

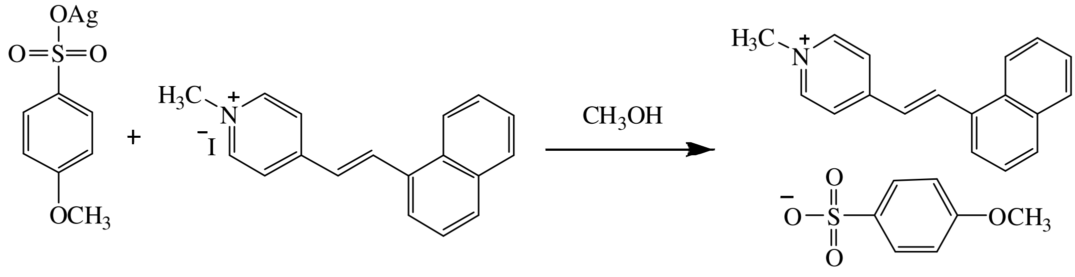

ANOM **PNAP2** **PNAP2O**

(*E*)-1-methyl-4-(2-(naphthalen-1-yl)vinyl)pyridinium 4-methoxybenzenesulfonate **(PNAP2O)** was synthesized by addition of a solution of silver (I) 4-methoxybenzenesulfonate (0.20 g, 0.67 mmol) in hot methanol (20 ml) to a solution of compound **PNAP2** (0.25 g, 0.67 mmol) in hot methanol (45 ml). Upon addition a yellow solid of silver iodide was immediately formed which was removed by filtration and the yellow filtrate was evaporated under reduced pressure to yield a yellow solid. The yellow solid was re-crystallized from methanol to give yellow crystals of compound **PNAP2O** (0.27 g, 92%), mp. 189-190 °C, UV-Vis (CH_3OH) λ_{max} (nm) (logε): 221.02 (5,020), 275.09 (985), 384.59 (244), FT-IR (KBr) ν(cm^{-1}): 3045 (sp^2 C-H aromatic stretching), 1618 (C=C aromatic stretching), 1207 (S=O stretching), 1190 (C-O in OCH_3 stretching), ^{1}H NMR (see **Table 32**).

2.5.8 (*E*)-1-methyl-4-(2-(naphthalen-1-yl)vinyl)pyridinium 4-chlorobenzenesulfonate (PNAP2C)

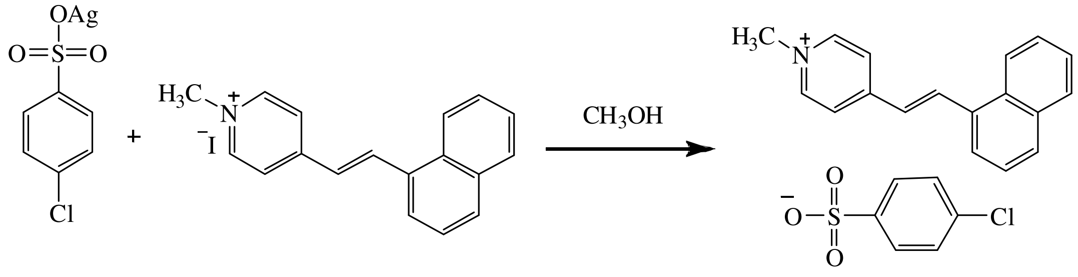

ANCL **PNAP2** **PNAP2C**

(*E*)-1-methyl-4-(2-(naphthalen-1-yl)vinyl)pyridinium 4-chlorobenzenesulfonate **(PNAP2C)** was synthesized by addition of a solution of silver (I) 4-chlorobenzenesulfonate (0.20 g, 0.67 mmol) in hot methanol (20 ml) to a solution of compound **PNAP2** (0.25 g, 0.67 mmol) in hot methanol (45 ml). Upon addition a yellow solid of silver iodide was immediately formed which was removed by filtration and the yellow filtrate was evaporated under reduced pressure to yield a yellow solid. The yellow solid was re-crystallized from methanol to give yellow crystals of compound **PNAP2C** (0.24 g, 82%), mp. 203-204 °C, UV-Vis (CH_3OH) λ_{max} (nm) ($\log\varepsilon$): 221.02 (13,460), 275.77 (2,518), 377.83 (867), FT-IR (KBr) $\nu(cm^{-1})$: 3047 (*sp*^{2} C-H aromatic stretching), 1623 (C=C aromatic stretching), 1209 (S=O stretching), ^{1}H NMR (see **Table 33**).

2.5.9 (*E*)-1-methyl-4-(2-(naphthalen-1-yl)vinyl)pyridinium 4-bromobenzenesulfonate (PNAP2B)

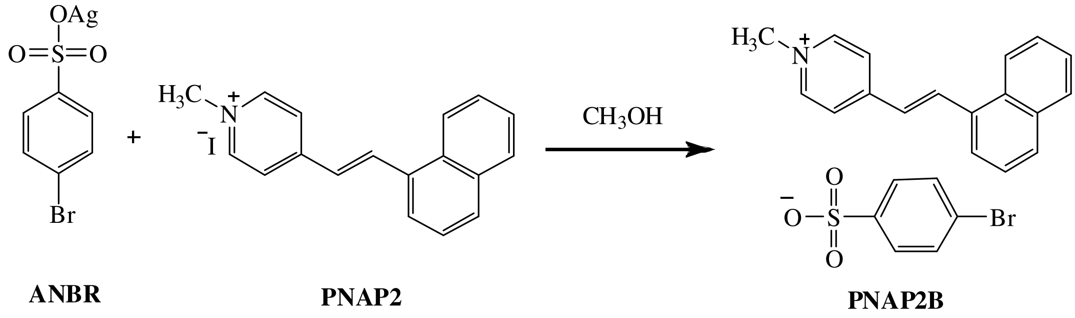

(*E*)-1-methyl-4-(2-(naphthalen-1-yl)vinyl)pyridinium 4-bromobenzenesulfonate **(PNAP2B)** was synthesized by addition of a solution of silver (I) 4-chlorobenzenesulfonate (0.20 g, 0.58 mmol) in hot methanol (20 ml) to a solution of compound **PNAP2** (0.22 g, 0.58 mmol) in hot methanol (45 ml). Upon addition a yellow solid of silver iodide was immediately formed which was removed by filtration and the yellow filtrate was evaporated under reduced pressure to yield a yellow solid. The yellow solid was re-crystallized from methanol to give yellow crystals of compound **PNAP2B** (0.25 g, 91%), mp. 222-223 °C, UV-Vis (CH_3OH) λ_{max} (nm) (logε): 220.34 (5,636), 275.09 (1,090), 383.23 (371), FT-IR (KBr) ν(cm^{-1}): 3045 (*sp*^{2} C-H aromatic stretching), 1618 (C=C aromatic stretching), 1203 (S=O stretching), ^{1}H NMR (see **Table 37**).

2.5.10 (*E*)-1-methyl-4-(2-(naphthalen-1-yl)vinyl)pyridinium 4-aminobenzenesulfonate (PNAP2N)

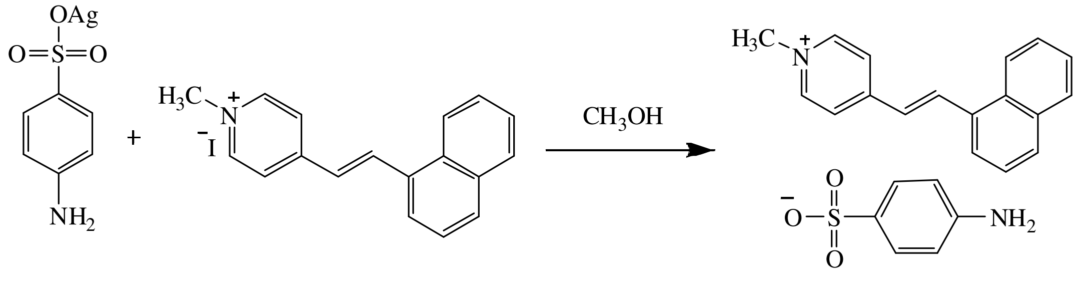

ANNH **PNAP2** **PNAP2N**

(*E*)-1-methyl-4-(2-(naphthalen-1-yl)vinyl)pyridinium 4-aminobenzenesulfonate **(PNAP2N)** was synthesized by addition of a solution of silver (I) 4-chlorobenzenesulfonate (0.20 g, 0.71 mmol) in hot methanol (20 ml) to a solution of compound **PNAP2** (0.27 g, 0.71 mmol) in hot methanol (45 ml). Upon addition a yellow solid of silver iodide was immediately formed which was removed by filtration and the yellow filtrate was evaporated under reduced pressure to yield a yellow solid. The yellow solid was re-crystallized from methanol to give yellow crystals of compound **PNAP2N** (0.13 g, 45%), mp. 240-241 °C, UV-Vis (CH_3OH) λ_{max} (nm) (logε): 220.92 (8,447), 253.36 (5,993), 347.38 (2,778), FT-IR (KBr) ν(cm^{-1}): 3385 (N-H in primary amine stretching), 3057 (*sp*^{2} C-H aromatic stretching), 1618 (C=C aromatic stretching), 1195 (S=O stretching), ^{1}H NMR (see **Table 41**).

2.5.11 (*E*)-1-methyl-2-(2-(naphthalen-2-yl)vinyl)pyridinium 4-methylbenzenesulfonate (PNAP3M)

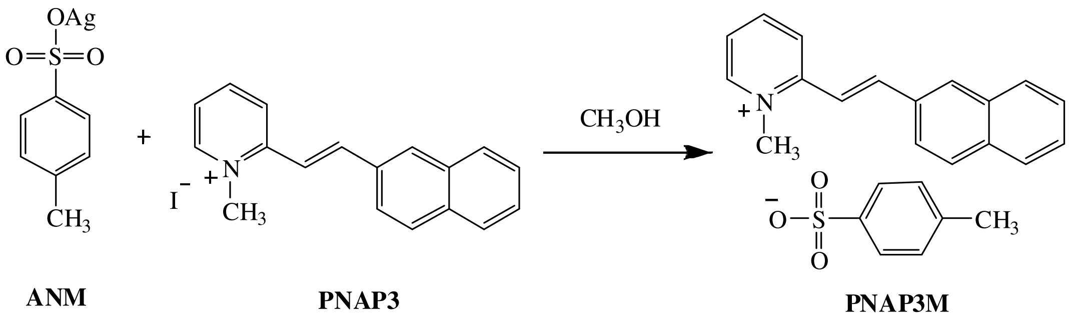

(*E*)-1-methyl-2-(2-(naphthalen-2-yl)vinyl)pyridinium 4-methylbenzenesulfonate **(PNAP3M)** was synthesized by addition of a solution of silver (I) 4-methylbenzenesulfonate (0.20 g, 0.68 mmol) in hot methanol (20 ml) to a solution of compound **PNAP3** (0.26 g, 0.68 mmol) in hot methanol (45 ml). Upon addition a yellow solid of silver iodide was immediately formed which was removed by filtration and the yellow filtrate was evaporated under reduced pressure to yield a yellow solid. The yellow solid was re-crystallized from methanol to give yellow crystals of compound **PNAP3M** (0.23 g, 81%), mp. 176-177 °C, UV-Vis (CH_3OH) λ_{max} (nm) (logε): 223.57 (34,917), 342.24 (9,573), FT-IR (KBr) ν(cm^{-1}): 3045 (*sp*^{2} C-H aromatic stretching), 1610 (C=C aromatic stretching), 1186 (S=O stretching), 963 (C-H *trans*-RCH=CHR out of plane bending), ^{1}H NMR (see **Table 42**).

2.5.12 (*E*)-1-methyl-2-(2-(naphthalen-2-yl)vinyl)pyridinium 4-methoxybenzenesulfonate (PNAP3O)

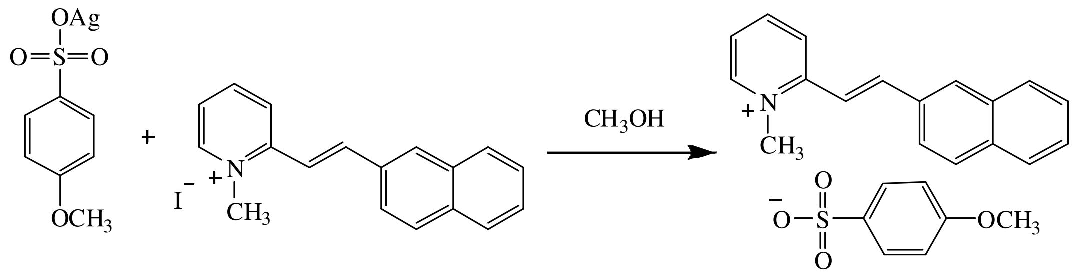

ANOM **PNAP3** **PNAP3O**

(*E*)-1-methyl-2-(2-(naphthalen-2-yl)vinyl)pyridinium 4-methoxybenzenesulfonate **(PNAP3O)** was synthesized by addition of a solution of silver (I) 4-methoxybenzenesulfonate (0.20 g, 0.67 mmol) in hot methanol (20 ml) to a solution of compound **PNAP3** (0.25 g, 0.67 mmol) in hot methanol (45 ml). Upon addition a yellow solid of silver iodide was immediately formed which was removed by filtration and the yellow filtrate was evaporated under reduced pressure to yield a yellow solid. The yellow solid was re-crystallized from methanol to give yellow crystals of compound **PNAP3O** (0.19 g, 67%), mp. 232-234 °C, UV-Vis (CH_3OH) λ_{max} (nm) ($\log\varepsilon$): 228.21 (35,620), 341.58 (5,479), FT-IR (KBr) $\nu(cm^{-1})$: 3060 (sp^2 C-H aromatic stretching), 1601 (C=C aromatic stretching), 1186 (S=O stretching), 1136 (C-O in OCH_3 stretching), ^1H NMR (see **Table 43**).

2.5.13 (*E*)-1-methyl-2-(2-(naphthalen-2-yl)vinyl)pyridinium 4-chlorobenzenesulfonate (PNAP3C)

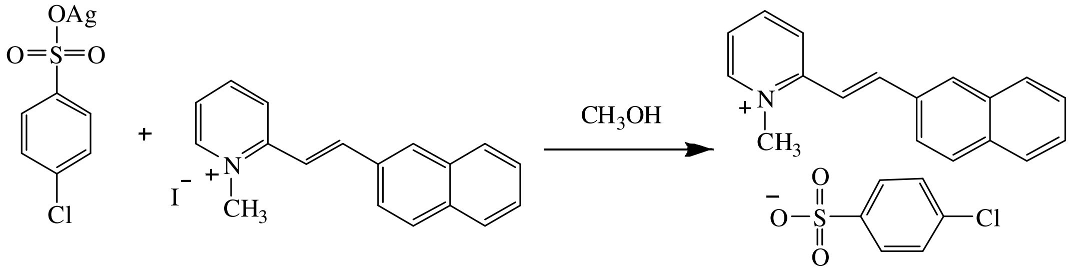

ANCL **PNAP3** **PNAP3C**

(*E*)-1-methyl-2-(2-(naphthalen-2-yl)vinyl)pyridinium 4-chlorobenzenesulfonate **(PNAP3C)** was synthesized by addition of a solution of silver (I) 4-chlorobenzenesulfonate (0.20 g, 0.67 mmol) in hot methanol (20 ml) to a solution of compound **PNAP3** (0.25 g, 0.67 mmol) in hot methanol (45 ml). Upon addition a yellow solid of silver iodide was immediately formed which was removed by filtration and the yellow filtrate was evaporated under reduced pressure to yield a yellow solid. The yellow solid was re-crystallized from methanol to give yellow crystals of compound **PNAP3C** (0.21 g, 73%), mp. >300 °C, UV-Vis (CH_3OH) λ_{max} (nm) (logε): 222.91 (32,990), 340.92 (4,804), FT-IR (KBr) ν(cm^{-1}): 1618 (C=C aromatic stretching), 1176 (S=O stretching), ^{1}H NMR (see **Table 44**).

2.5.14 (*E*)-1-methyl-2-(2-(naphthalen-2-yl)vinyl)pyridinium 4-bromobenzenesulfonate (PNAP3B)

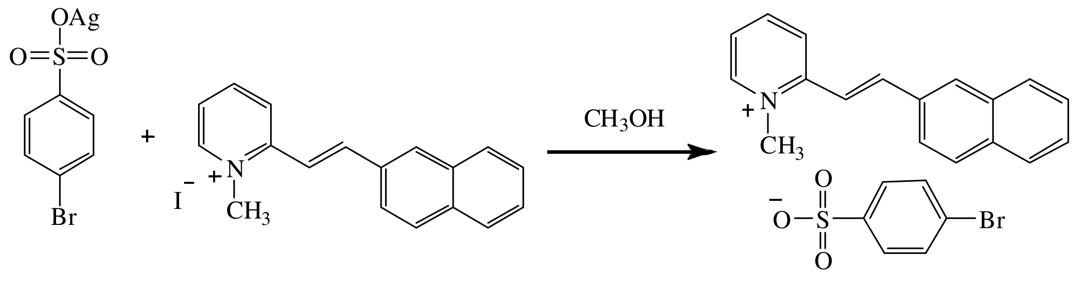

ANBR **PNAP3** **PNAP3B**

(*E*)-1-methyl-2-(2-(naphthalen-2-yl)vinyl)pyridinium 4-bromobenzenesulfonate **(PNAP3B)** was synthesized by addition of a solution of silver (I) 4-chlorobenzenesulfonate (0.20 g, 0.58 mmol) in hot methanol (20 ml) to a solution of compound **PNAP3** (0.22 g, 0.58 mmol) in hot methanol (45 ml). Upon addition a yellow solid of silver iodide was immediately formed which was removed by filtration and the yellow filtrate was evaporated under reduced pressure to yield a yellow solid. The yellow solid was re-crystallized from methanol to give yellow crystals of compound **PNAP3B** (0.24 g, 86%), mp. 249-251 °C, UV-Vis (CH_3OH) λ_{max} (nm) ($\log\varepsilon$): 226.23 (44,180), 342.24 (11,235), FT-IR (KBr) $\nu(cm^{-1})$: 3076 (sp^2 C-H aromatic stretching), 1609 (C=C aromatic stretching), 1215 (S=O stretching), ^1H NMR (see **Table 45**).

2.5.15 (*E*)-1-methyl-2-(2-(naphthalen-2-yl)vinyl)pyridinium 4-aminobenzenesulfonate (PNAP3N)

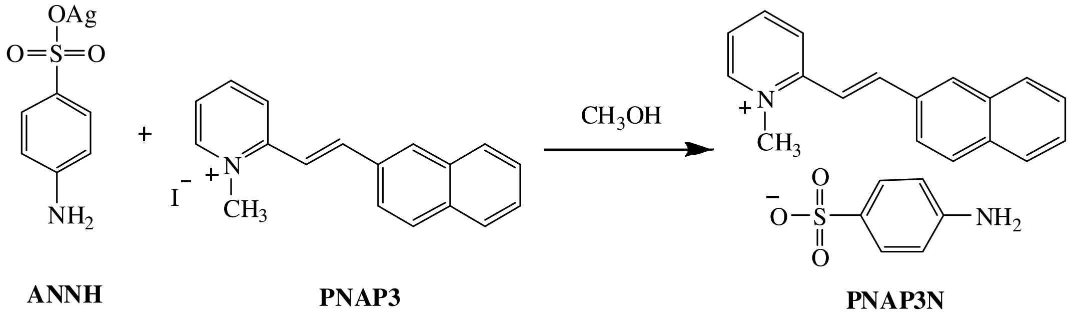

(*E*)-1-methyl-2-(2-(naphthalen-2-yl)vinyl)pyridinium 4-aminobenzenesulfonate **(PNAP3N)** was synthesized by addition of a solution of silver (I) 4-chlorobenzenesulfonate (0.20 g, 0.71 mmol) in hot methanol (20 ml) to a solution of compound **PNAP3** (0.27 g, 0.71 mmol) in hot methanol (45 ml). Upon addition a yellow solid of silver iodide was immediately formed which was removed by filtration and the yellow filtrate was evaporated under reduced pressure to yield a yellow solid. The yellow solid was re-crystallized from methanol to give yellow crystals of compound **PNAP3N** (0.18 g, 60%), mp. 215-217 °C, UV-Vis (CH_3OH) λ_{max} (nm) ($\log\varepsilon$): 226.89 (30,262), 341.58 (8,137), FT-IR (KBr) $\nu(cm^{-1})$: 3334 (N-H in primary amine stretching), 3046 (sp^2 C-H aromatic stretching), 1600 (C=C aromatic stretching), 1270 (C-N in aromatic amine stretching), 1197 (S=O stretching), ^1H NMR (see **Table 46**).

2.5.16 (*E*)-1-methyl-4-(2-(naphthalen-2-yl)vinyl)pyridinium 4-methylbenzenesulfonate (PNAP4M)

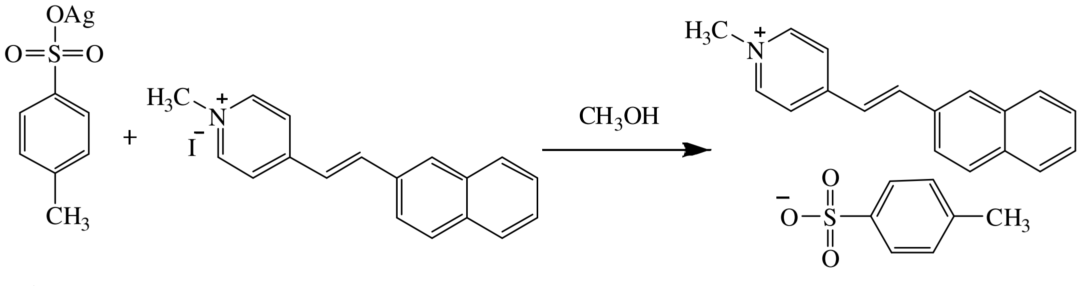

ANM **PNAP4** **PNAP4M**

(*E*)-1-methyl-4-(2-(naphthalen-2-yl)vinyl)pyridinium 4-methylbenzenesulfonate **(PNAP4M)** was synthesized by addition of a solution of silver (I) 4-methylbenzenesulfonate (0.20 g, 0.68 mmol) in hot methanol (20 ml) to a solution of compound **PNAP4** (0.26 g, 0.68 mmol) in hot methanol (45 ml). Upon addition a yellow solid of silver iodide was immediately formed which was removed by filtration and the yellow filtrate was evaporated under reduced pressure to yield a yellow solid. The yellow solid was re-crystallized from methanol to give yellow crystals of compound **PNAP4M** (0.21 g, 74%), mp. 212-214 °C, UV-Vis (CH_3OH) λ_{max} (nm) (logε): 222.91 (14,078), 356.83 (3,373), FT-IR (KBr) ν(cm^{-1}): 3045 (*sp*^{2} C-H aromatic stretching), 1618 (C=C aromatic stretching), 1196 (S=O stretching), ^{1}H NMR (see **Table 47**).

2.5.17 (*E*)-1-methyl-4-(2-(naphthalen-2-yl)vinyl)pyridinium 4-methoxybenzenesulfonate (PNAP4O)

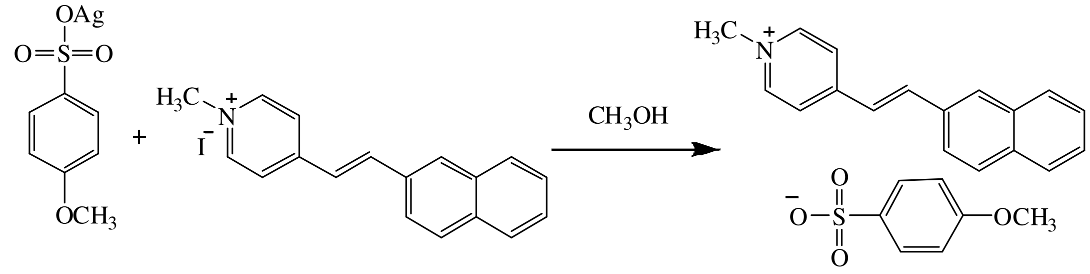

ANOM **PNAP4** **PNAP4O**

(*E*)-1-methyl-4-(2-(naphthalen-2-yl)vinyl)pyridinium 4-methoxybenzenesulfonate **(PNAP4O)** was synthesized by addition of a solution of silver (I) 4-methoxybenzenesulfonate (0.20 g, 0.67 mmol) in hot methanol (20 ml) to a solution of compound **PNAP4** (0.25 g, 0.67 mmol) in hot methanol (45 ml). Upon addition a yellow solid of silver iodide was immediately formed which was removed by filtration and the yellow filtrate was evaporated under reduced pressure to yield a yellow solid. The yellow solid was re-crystallized from methanol to give yellow crystals of compound **PNAP4O** (0.24 g, 83%), mp. 203-204 °C, UV-Vis (CH_3OH) λ_{max} (nm) (logε): 232.19 (41,756), 356.17 (13,111), FT-IR (KBr) ν(cm^{-1}): 3046 (*sp*^{2} C-H aromatic stretching), 1618 (C=C aromatic stretching), 1208 (S=O stretching), 1190 (C-O in OCH_3 stretching), ^{1}H NMR (see **Table 48**).

2.5.18 (*E*)-1-methyl-4-(2-(naphthalen-2-yl)vinyl)pyridinium 4-chlorobenzenesulfonate (PNAP4C)

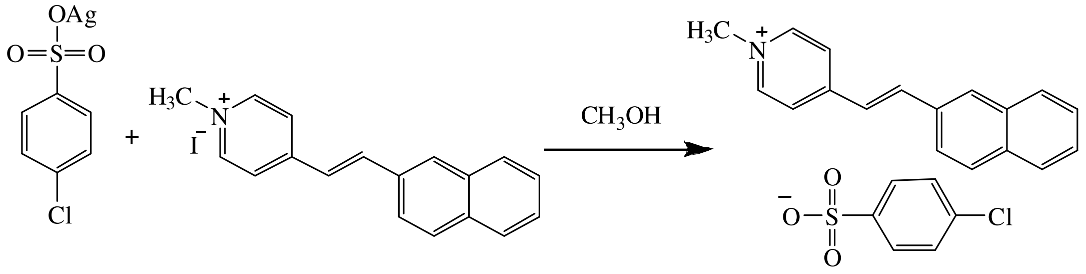

ANCL **PNAP4** **PNAP4C**

(*E*)-1-methyl-4-(2-(naphthalen-2-yl)vinyl)pyridinium 4-chlorobenzenesulfonate **(PNAP4C)** was synthesized by addition of a solution of silver (I) 4-chlorobenzenesulfonate (0.20 g, 0.67 mmol) in hot methanol (20 ml) to a solution of compound **PNAP4** (0.25 g, 0.67 mmol) in hot methanol (45 ml). Upon addition a yellow solid of silver iodide was immediately formed which was removed by filtration and the yellow filtrate was evaporated under reduced pressure to yield a yellow solid. The yellow solid was re-crystallized from methanol to give yellow crystals of compound **PNAP4C** (0.23 g, 79%), mp.(decompose) 260-261 °C, UV-Vis (CH_3OH) λ_{max} (nm) (logε): 223.57 (36,669), 355.50 (4,795), FT-IR (KBr) ν(cm^{-1}): 1618, (C=C aromatic stretching), 1385 (S=O stretching), ^{1}H NMR (see **Table 49**).

2.5.19 (*E*)-1-methyl-4-(2-(naphthalen-2-yl)vinyl)pyridinium 4-bromobenzenesulfonate (PNAP4B)

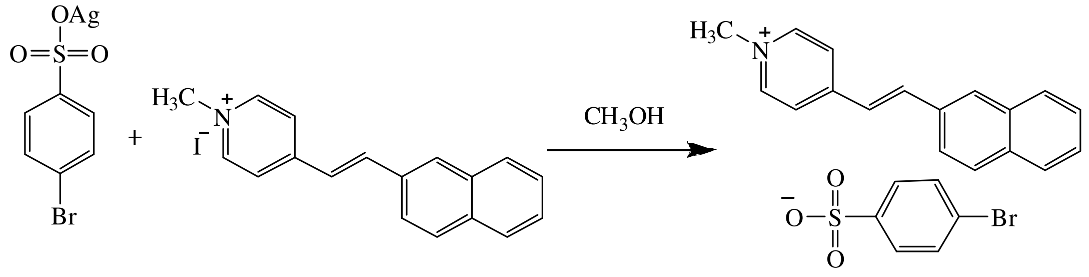

ANBR **PNAP4** **PNAP4B**

(*E*)-1-methyl-4-(2-(naphthalen-2-yl)vinyl)pyridinium 4-bromobenzenesulfonate **(PNAP4B)** was synthesized by addition of a solution of silver (I) 4-chlorobenzenesulfonate (0.20 g, 0.58 mmol) in hot methanol (20 ml) to a solution of compound **PNAP4** (0.22 g, 0.58 mmol) in hot methanol (45 ml). Upon addition a yellow solid of silver iodide was immediately formed which was removed by filtration and the yellow filtrate was evaporated under reduced pressure to yield a yellow solid. The yellow solid was re-crystallized from methanol to give yellow crystals of compound **PNAP4B** (0.25 g, 89%), mp. 235-237 °C, UV-Vis (CH_3OH) λ_{max} (nm) (logε): 226.89 (42,880), 356.17 (11,360), FT-IR (KBr) ν(cm^{-1}): 3044 (sp^2 C-H aromatic stretching), 1617 (C=C aromatic stretching), 1219 (S=O stretching), ^{1}H NMR (see **Table 50**).

2.5.20 (*E*)-1-methyl-4-(2-(naphthalen-2-yl)vinyl)pyridinium 4-aminobenzenesulfonate (PNAP4N)

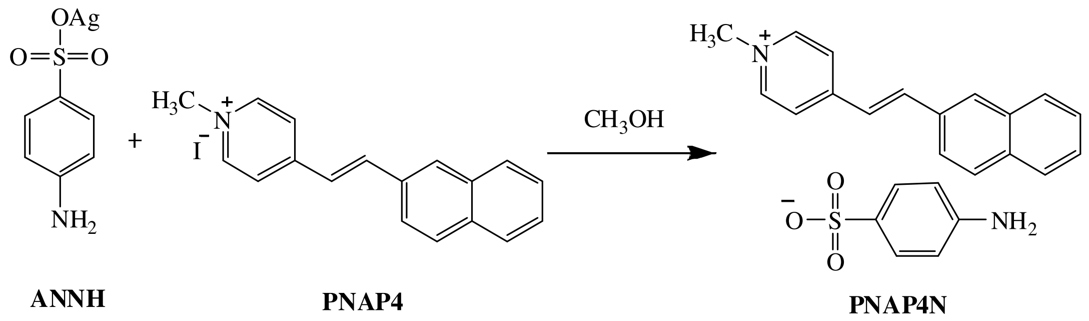

(*E*)-1-methyl-4-(2-(naphthalen-2-yl)vinyl)pyridinium 4-aminobenzenesulfonate **(PNAP4N)** was synthesized by addition of a solution of silver (I) 4-chlorobenzenesulfonate (0.20 g, 0.71 mmol) in hot methanol (20 ml) to a solution of compound **PNAP4** (0.27 g, 0.71 mmol) in hot methanol (45 ml). Upon addition a yellow solid of silver iodide was immediately formed which was removed by filtration and the yellow filtrate was evaporated under reduced pressure to yield a yellow solid. The yellow solid was re-crystallized from methanol to give yellow crystals of compound **PNAP4N** (0.16 g, 54%), mp. 248-250 °C, UV-Vis (CH_3OH) λ_{max} (nm) (logε): 230.20 (38,170), 354.18 (10,205), FT-IR (KBr) ν(cm^{-1}): 3337 (N-H in primary amine stretching), 3042 (sp^2 C-H aromatic stretching), 1617 (C=C aromatic stretching), 1181 (S=O stretching), ^1H NMR (see **Table 51**).

2.6 Antimicrobial assay

All the pure compounds were tested against gram-positive bacteria (which were *S. aureus, B. subtilis, E. faecalis,* Methicillin-Resistant *S. aureus* and Vancomycin-Resistant *E. faecalis*), gram-negative bacteria (which were *P. aeruginosa, S. typhi* and *S. sonnei*) and a fungus (*C. albicans*). Bacteria *S. typhi*, *S. sonei, B. subtilis* and *P. aeruginosa* were obtained from culture collections, Department of Industrial Biotechnology and Department of Pharmacognosy and Botany, Prince of Songkla University. Methicillin-Resistant *S. aureus* (MRSA) ATCC 43300, Vancomycin-Resistant *E. faecalis* (VRE) ATCC 51299, *S. aureus* TISTR517 and *E. faecalis* TISTR459 were obtained from Microbial Research Center (MIRCEN), Bangkok, Thailand. *Candida albicans* was obtained from Department of Pharmacognosy and Botany, PSU. The antimicrobial assay employed was the colorimetric microdilution broth technique using RPMI1640 medium and Alamar Blue as an indicator. Microbial inocula were prepared as suspension in RPMI1640 medium and mixed with 1% 100x Alamar Blue indicator. The cell suspension was then transferred into a 96-well microliter plate (100 µl/well except for first row which contained 190 µl/well). Each compound (10 µl) dissolved in DMSO at a concentration of 25 mg/ml and was then added to each well of the first row and mixed well with a micropipette. Half of the mixtures of cell suspension and compounds in the first rows were then transferred to the next well in the second row to perform a half-fold dilution. The dilution process was repeated as a sequence until the compounds were diluted 128 times in the last row. The excess 100 µl of the mixture in the last row was discarded. The plates were incubated at 37°C for 8–12 hrs. The antimicrobial activity was determined as the MIC value which was the least concentration of the compound that could inhibit the change of Alamar Blue indicator from blue to red. All assays were repeated at least three times.

CHAPTER 3

RESULTS AND DISCUSSION

3.1 Structural elucidation of starting materials

3.1.1 1,2-dimethylpyridinium iodide (PO-ST)

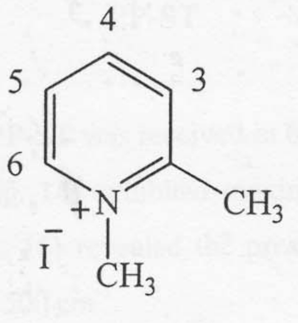

PO-ST

A white solid of **PO-ST** was received in 87% yield, mp. 220-222 °C. The UV-Vis absorption spectra (**Fig. 11**) exhibited maximum bands at 218 and 256 nm. The FT-IR spectrum (**Fig. 12**) revealed the presence of stretching vibration of C=C in aromatic ring at 1600 cm^{-1}.

The ^{1}H NMR spectrum (**Fig. 13**) showed the signals of protons H-3, H-4, H-5 and H-6 at δ 8.06 (1H, *d*, J = 6.9 Hz), δ 8.48 (1H, *t*, J = 6.9 Hz), δ 7.94 (1H, *t*, J = 6.9 Hz) and δ 9.09 (1H, *d*, J = 6.9 Hz), respectively. Two *singlet* signals of *N*-CH_3 and 2-CH_3 appeared at δ 4.65 and δ 3.05 respectively. The possible structure of a white solid was 1,2-dimethylpyridinium iodide **(PO-ST)**.

3.1.2 1,4-dimethylpyridinium iodide (PP-ST)

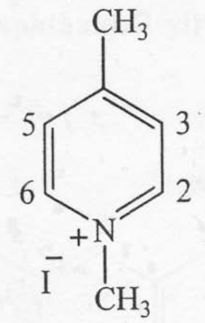

PP-ST

A pale yellow solid of **PP-ST** was received in 66% yield, mp. 140-142 °C. The UV-Vis absorption spectra (**Fig. 14**) exhibited maximum bands at 219.7 and 255.3 nm. The FT-IR spectrum (**Fig. 15**) revealed the presence of stretching vibration of C=C in aromatic ring at 1600-1500 cm^{-1}.

The ^{1}H NMR spectrum (**Fig. 16**) showed two *doublet* signals of equivalent protons H-2, H-6 and H-3, H-5 at δ 9.09 (2H, J = 6.6 Hz) and δ 7.92 (2H, J = 6.6 Hz) respectively. Two *singlet* signals of N-CH_3 and 4-CH_3 appeared at δ 4.55 and δ 2.71 respectively. The possible structure of a pale yellow solid was 1,4-dimethylpyridinium iodide **(PP-ST)**.

3.2 Structural elucidation of cation parts

3.2.1 (*E*)-1-methyl-2-(2-(naphthalen-1-yl)vinyl)pyridinium iodide (PNAP1)

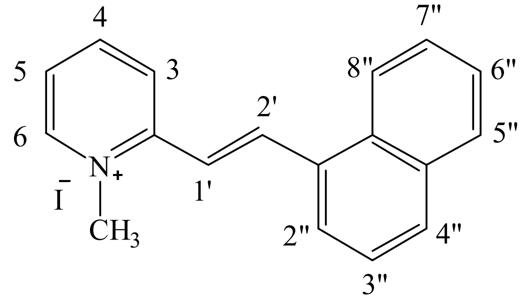

PNAP1

The yellow solid of **PNAP1** was prepared (80% yield), mp.283-284 °C. The UV-Vis spectrum (**Fig. 17**) showed maxima at 221.6, 277.7 and 354.1 nm. The *sp*^{2} C-H aromatic stretching vibration was observed in the FT-IR spectrum (**Fig. 18**) at 3025 cm^{-1} and the C=C aromatic stretching vibration was observed at 963 cm^{-1}.

The ^{1}H NMR spectrum (**Fig. 19,** see **Table 19**) consisted of *singlet* signals of *N*-CH_3 protons at δ 4.47 ppm (3H). Two *doublets* of H-1′ (δ 7.71, J = 15.6 Hz) and H-2′ (δ 8.74, J = 15.6 Hz) were assigned to be *trans*-disubstituted double bonds. Resonances of aromatic protons H-3, H-4, H-5 and H-6 were also shown at δ 8.84 (*d*, J = 8.1 Hz), δ 8.57 (*d*, J = 8.1 Hz), δ 7.98 (*t*, J = 8.1 Hz) and δ 9.00 (*d*, J = 8.1 Hz), respectively. There are also signals of naphthalenyl protons H-2″- H-8″ at δ 7.94 (*d*, J = 7.5 Hz), δ 7.61 (*t*, J = 7.5 Hz), δ 8.20 (*d*, J = 7.5 Hz), δ 8.06 (*d*, J = 6.3 Hz), δ 7.62 (*t*, J = 6.3 Hz), δ 7.66 (*t*, J = 6.3 Hz) and δ 8.51 (*d*, J = 6.3 Hz), respectively. Thus, these assignments clearly support the proposed structure which was (*E*)-1-methyl-2-(2-(naphthalen-1-yl)vinyl)pyridinium iodide (**PNAP1**).

Table 19 ^{1}H NMR of compound **PNAP1**

Position	**δ_H (ppm), *mult*, *J* (Hz)**
1-CH_3	4.47 (3H, *s*)
3	8.84 (1H, *d*, 8.1)
4	8.57 (1H, *d*, 8.1)
5	7.98 (1H, *t*, 8.1)
6	9.00 (1H, *d*, 8.1)
1′	7.71 (1H, *d*, 15.6)
2′	8.74 (1H, *d*, 15.6)
2″	7.94 (1H, *d*, 7.5)
3″	7.61 (1H, *t*, 7.5)
4″	8.20 (1H, *d*, 7.5)
5″	8.06 (1H, *d*, 6.3)
6″	7.62 (1H, *t*, 6.3)
7″	7.66 (1H, *t*, 6.3)
8″	8.51 (1H, *d*, 6.3)

3.2.2 (*E*)-1-methyl-4-(2-(naphthalen-1-yl)vinyl)pyridinium iodide (PNAP2)

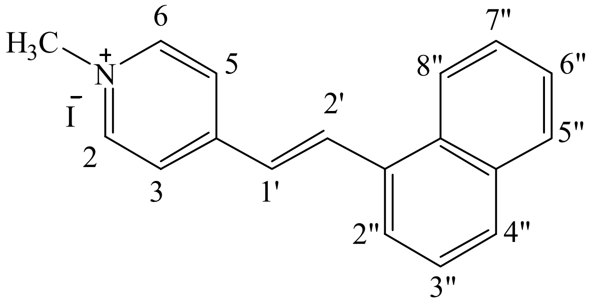

PNAP2

The yellow solid of **PNAP2** was prepared (81% yield), mp.287-288 °C. The UV-Vis spectrum (**Fig. 20**) showed maxima at 220.3, 275.7 and 375.8 nm. The *sp*^{2} C-H aromatic stretching vibration was observed in the FT-IR spectrum (**Fig. 21**) at 3017 cm^{-1} and the C=C aromatic stretching vibration was observed at 1168 cm^{-1}.

The ^{1}H NMR spectrum (**Fig. 22,** see **Table 20**) consisted of *singlet* signals of *N*-CH$_3$ protons at δ 4.44 ppm (3H). Two *doublets* of H-1′ (δ 7.52, J = 15.9 Hz) and H-2′ (δ 8.80, J = 15.9 Hz) were assigned to be *trans*-disubstituted double bonds and two *doublets* at δ 8.97 (2H, J = 6.6 Hz) and δ 8.41 (2H, J = 6.6 Hz) were the signals of equivalent H-2, H-6 and H-3, H-5, respectively. Resonances of naphthalenyl protons H-2″- H-8″ were also shown at δ 7.98 (*d, J* = 7.8 Hz), δ 8.04 (*t, J* = 7.8 Hz), δ 8.02 (*d, J* = 7.8 Hz), δ 8.06 (*d, J* = 7.5 Hz), δ 7.65 (*t, J* = 7.5 Hz), δ 7.63 (*t, J* = 7.5 Hz) and δ 8.49 (*d, J* = 7.5 Hz), respectively. Accordingly, compound **PNAP2** was assigned to be (*E*)-1-methyl-4-(2-(naphthalen-1-yl)vinyl)pyridinium iodide.

Table 20 ^{1}H NMR of compound **PNAP2**

Position	**δ_H (ppm), *mult*, *J* (Hz)**
1-CH_3	4.44 (3H, *s*)
2 6	8.97 (2H, *d*, 6.6)
3 5	8.41 (2H, *d*, 6.6)
1′	7.52 (1H, *d*, 15.9)
2′	8.80 (1H, *d*, 15.9)
2″	7.98 (1H, *d*, 7.8)
3″	8.04 (1H, *t*, 7.8)
4″	8.02 (1H, *d*, 7.8)
5″	8.06 (1H, *d*, 7.5)
6″	7.65 (1H, *t*, 7.5)
7″	7.63 (1H, *t*, 7.5)
8″	8.49 (1H, *d*, 7.5)

3.2.3 (*E*)-1-methyl-2-(2-(naphthalen-2-yl)vinyl)pyridinium iodide (PNAP3)

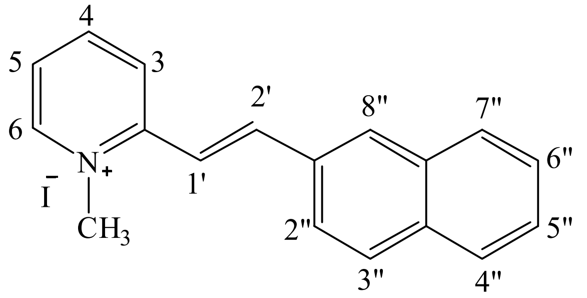

PNAP3

The pale yellow solid of **PNAP3** was prepared (75% yield), mp.261-263 °C. The UV-Vis spectrum (**Fig. 23**) showed maxima at 223.5 and 339.4 nm. The *sp*^{2} C-H aromatic stretching vibration was observed in the FT-IR spectrum (**Fig. 24**) at 3045 cm^{-1} and the C=C aromatic stretching vibration was observed at 1612 cm^{-1}.

The ^{1}H NMR spectrum (**Fig. 25,** see **Table 21**) consisted of *singlet* signals of *N*-CH_3 protons at δ 4.43 ppm (3H). Two *doublets* of H-1′ (δ 7.69, J = 15.9 Hz) and H-2′ (δ 8.04, J = 15.9 Hz) were assigned to be *trans*-disubstituted double bonds. Resonances of aromatic protons of the pyridinium ring H-3, H-4, H-5 and H-6 were also shown at δ 8.54 (*d*, J = 8.1 Hz), δ 8.46 (*d*, J = 8.1 Hz), δ 8.03 (*t*, J = 8.1 Hz) and δ 8.94 (*d*, J = 8.1 Hz), respectively. There are also signals of naphthalenyl protons H-2″- H-8″ at δ 7.86 (*d*, J = 9.6 Hz), δ 7.87 (*d*, J = 9.6 Hz), δ 7.92 (*d*, J = 8.4 Hz), δ 7.54 (*t*, J = 8.4 Hz), δ 7.53 (*t*, J = 8.4 Hz), δ 7.89 (*d*, J = 8.4 Hz) and δ 8.23 (*s*), respectively. Thus, these assignments clearly support the proposed structure which was (*E*)-1-methyl-2-(2-(naphthalen-2-yl)vinyl)pyridinium iodide (**PNAP3**).

Table 21 ^{1}H NMR of compound **PNAP3**

Position	**δ_H (ppm), *mult*, *J* (Hz)**
1-CH_3	4.43 (3H, *s*)
3	8.54 (1H, *d*, 8.1)
4	8.46 (1H, *t*, 8.1)
5	8.03 (1H, *t*, 8.1)
6	8.94 (1H, *d*, 8.1)
1′	7.69 (1H, *d*, 15.9)
2′	8.04 (1H, *d*, 15.9)
2″	7.86 (1H, *d*, 9.6)
3″	7.87 (1H, *d*, 9.6)
4″	7.92 (1H, *d*, 8.4)
5″	7.54 (1H, *t*, 8.4)
6″	7.53 (1H, *t*, 8.4)
7″	7.89 (1H, *d*, 8.4)
8″	8.23 (1H, *s*)

3.2.4 (*E*)-1-methyl-4-(2-(naphthalen-2-yl)vinyl)pyridinium iodide (PNAP4)

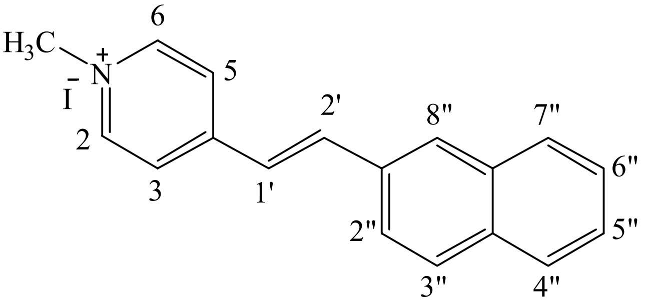

PNAP4

The yellow solid of **PNAP4** was prepared (77% yield), mp.284-285 °C. The UV-Vis spectrum (**Fig. 26**) showed maxima at 225.5 and 356.8 nm. The *sp*^{2} C-H aromatic stretching vibration was observed in the FT-IR spectrum (**Fig. 27**) at 3019 cm^{-1} and the C=C aromatic stretching vibration was observed at 1612 cm^{-1}.

The ^{1}H NMR spectrum (**Fig. 28,** see **Table 22**) consisted of *singlet* signals of *N*-CH_3 protons at δ 4.41 ppm (3H). Two *doublets* of H-1′ (δ 7.46, *J* = 16.5 Hz) and H-2′ (δ 8.03, *J* = 16.5 Hz) were assigned to be *trans*-disubstituted double bonds and two *doublets* at δ 8.91 (2H, *J* = 6.3 Hz) and δ 8.19 (2H, *J* = 6.3 Hz) were the signals of equivalent H-2, H-6 and H-3, H-5, respectively. Resonances of naphthalenyl protons H-2″- H-8″ were also shown at δ 7.56 (d, J = 8.7 Hz), δ 7.54 (*d, J* = 8.7 Hz), δ 7.89 (*d, J* = 8.4 Hz), δ 7.91 (*t, J* = 8.4 Hz), δ 7.88 (*t, J* = 8.4 Hz), δ 7.89 (*d, J* = 8.4 Hz) and 8.14 (*s*), respectively. Accordingly, compound **PNAP4** was assigned to be (*E*)-1-methyl-4-(2-(naphthalen-2-yl)vinyl)pyridinium iodide.

Table 22 ^{1}H NMR of compound **PNAP4**

Position	**δ_H (ppm), *mult*, *J* (Hz)**
1-CH_3	4.41 (3H, *s*)
2 6	8.91 (2H, *d*, 6.3)
3 5	8.19 (2H, *d*, 6.3)
1′	7.46 (1H, *d*, 16.5)
2′	8.03 (1H, *d*, 16.5)
2″	7.56 (1H, *d*, 8.7)
3″	7.54 (1H, *d*, 8.7)
4″	7.89 (1H, *d*, 8.4)
5″	7.91 (1H, *t*, 8.4)
6″	7.88 (1H, *t*, 8.4)
7″	7.90 (1H, *d*, 8.4)
8″	8.14 (1H, *s*)

The crystal structure of **PNAP4** is illustrated in **Fig. 5** and **Fig. 6** which show the packing diagram of **PNAP4** and intermolecular hydrogen bondings. The crystal and experiment data are given in **Table 23**. Bond lengths and angles are shown in **Table 24**. Hydrogen-bond geometry is shown in **Table 25**. The X-ray study shows that **PNAP4** crystallized out in centrosymmetric space group **$P2_1/c$.**

Fig. 5 shows the asymmetric unit of the title compound which consists of a $C_{18}H_{16}N^+$ cation and a I^- anion. The whole cation is disordered over two sites; the major component *A* and the minor component *B*, with the refined site-occupancy ratio of 0.554 (7)/0.446 (7). The cation exists in the *E* configuration with respect to the C6═C7 double bond. The napthalenyl moiety is essentially planar in both disorder components as indicated by the interplanar angle between the two aromatic C8-C10/C15-C17 and C10–C15 rings [1.5 (8)° for the major component *A* and 3.2 (9)° for the minor component *B*]. The major component *A* of cation is slightly twisted with the dihedral angle between the pyridinium and the mean plane through the napthalenyl moiety (C8–C17) being 4.7 (6)° whereas the minor component *B* is almost planar [dihedral angle 1.6 (8)°]. The C4–C5–C6–C7 and C6–C7–C8–C17 torsion angles [0.4 (10)° and 2.1 (10)° in the major component and -179.4 (8)° and 179.9 (8)° in the minor component] in both disorder components indicate that the orientations of the ethynyl moiety in these components are related by 180° rotation about the long axis of the molecule.

In the crystal packing (**Fig. 6**), centrosymmetrically related cations are stacked along the *a* axis, with significant π-π interactions between pyridinium ring and naphthalene ring system [centroid-centroid distance is 3.442 (9) Å]. The iodide ions are located between adjacent coloumns of cations. The cations are linked to the iodide ions by C—H···I weak interactions. The crystal structure is further stabilized by C—H···π interactions involving the methyl group (**Table 24**).

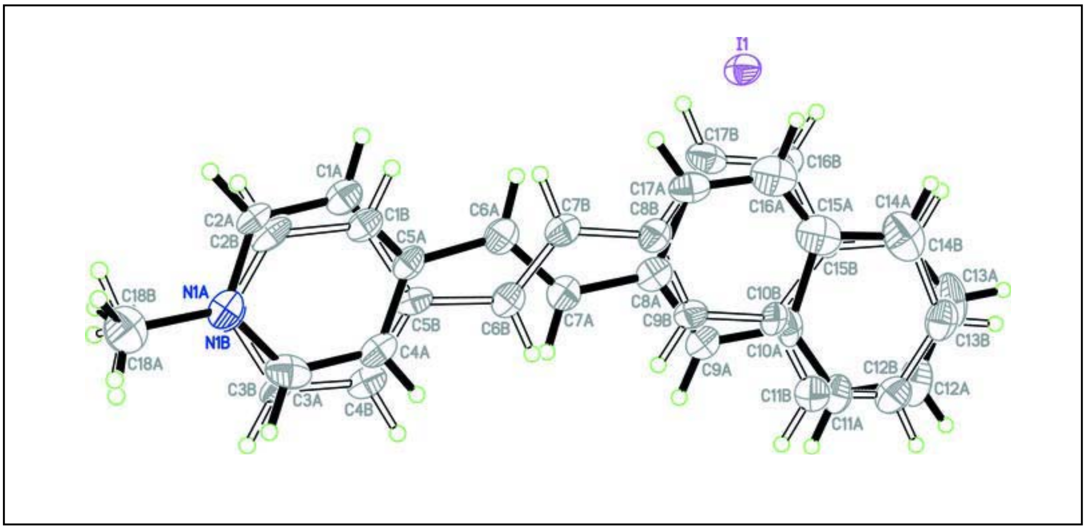
I1
C17B
C16B
C1A
C2A
C2B
C1B
C6A
C7B
C17A
C8B
C16A
C15A
C14A
C5A
C15B
C14B
C13A
C18B
N1A
C10B
N1B
C5B
C6B
C7A
C8A
C9B
C13B
C18A
C4A
C10A
C9A
C12B
C12A
C3B
C3A
C4B
C11B
C11A

Figure 5 X-ray ORTEP diagram of the compound **PNAP4**

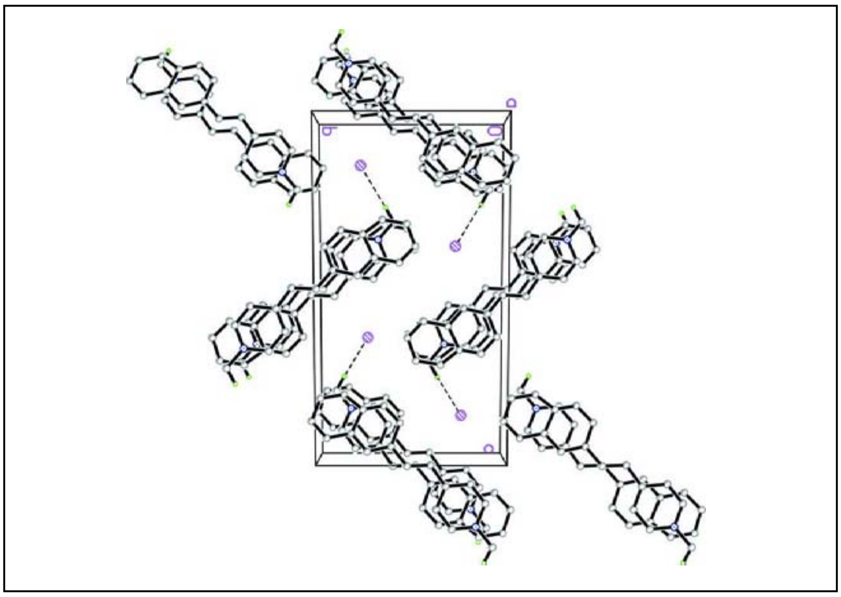

Figure 6 Packing diagram of **PNAP4** viewed down the *a* axis with H-bonds shown as dashed lines.

Table 23 Crystal data of **PNAP4**.

Identification code	**PNAP4**	
Empirical formula	$C_{18}H_{16}N^{+}I^{-}$	
Formula weight	373.29	
Temperature	100.0(1) K	
Wavelength	0.71073 Å	
Crystal system, space group	Monoclinic, $P2_1/c$	
Unit cell dimensions	a = 7.2789(1) Å	α = 90 °
	b = 10.9363(2) Å	β = 101.280(1) °
	c = 20.0883(4) Å	γ = 90 °
Volume	1568.22(5) $Å^3$	
Z, Calculated density	4, 1.581 Mg/m^3	
Absorption coefficient	2.03 mm^{-1}	
F(000)	736	
Crystal size	0.53 x 0.30 x 0.29 mm	
Theta range for data collection	2.1 to 35.0 °	
Limiting indices	-11<=h<=11, -17<=k<=16, -32<=l<=27	
Reflections collected / unique	34203 / 6896 [*R*(int) = 0.028]	
Completeness to theta = 35.00	99.9 %	
Max. and min. transmission	0.838 and 0.412	
Refinement method	Full-matrix least-squares on F^2	
Data / restraints / parameters	6896 / 91 / 338	
Goodness-of-fit on F^2	1.060	
Final *R* indices [I>2σ(I)]	*R1* = 0.555 *wR2* = 0.1395	
R indices (all data)	*R1* = 0.0701, *wR2* = 0.1475	
Largest diff. peak and hole	3.511 and -2.416 e.$Å^{-3}$	

Table 24 Bond lengths [Å] and angles [°] for **PNAP4**

N1A-C3A	1.34(3)	N1B-C2B	1.31(6)
N1A-C2A	1.38(4)	N1B-C3B	1.36(4)
N1A-C18A	1.45(4)	N1B-C18B	1.50(5)
C1A-C2A	1.354(13)	C1B-C5B	1.385(12)
C1A-C5A	1.408(10)	C1B-C2B	1.393(18)
C1A-H1AA	0.93	C1B-H1BA	0.93
C2A-H2AA	0.93	C2B-H2BA	0.93
C3A-C4A	1.390(17)	C3B-C4B	1.350(17)
C3A-H3AA	0.93	C3B-H3BA	0.93
C4A-C5A	1.378(10)	C4B-C5B	1.393(12)
C4A-H4AA	0.93	C4B-H4BA	0.93
C5A-C6A	1.467(8)	C5B-C6B	1.456(11)
C6A-C7A	1.337(8)	C6B-C7B	1.342(10)
C6A-H6AA	0.93	C6B-H6BA	0.93
C7A-C8A	1.460(9)	C7B-C8B	1.465(11)
C7A-H7AA	0.93	C7B-H7BA	0.93
C8A-C9A	1.386(10)	C8B-C9B	1.404(12)
C8A-C17A	1.442(10)	C8B-C17B	1.432(12)
C9A-C10A	1.429(15)	C9B-C10B	1.397(19)
C9A-H9AA	0.93	C9B-H9BA	0.93
C10A-C11A	1.417(16)	C10B-C11B	1.385(19)
C10A-C15A	1.51(2)	C10B-C15B	1.41(2)
C11A-C12A	1.360(11)	C11B-C12B	1.378(15)
C11A-H11A	0.93	C11B-H11B	0.93
C12A-C13A	1.416(17)	C12B-C13B	1.424(17)
C12A-H12A	0.93	C12B-H12B	0.93
C13A-C14A	1.38(3)	C13B-C14B	1.40(2)
C13A-H13A	0.93	C13B-H13B	0.93
C14A-C15A	1.43(2)	C14B-C15B	1.435(15)
C14A-H14A	0.93	C14B-H14B	0.93
C15A-C16A	1.23(2)	C15B-C16B	1.52(2)

Table 24 (Continued)

C16A-C17A	1.372(18)	C16B-C17B	1.313(19)
C16A-H16A	0.93	C16B-H16B	0.93
C17A-H17A	0.93	C17B-H17B	0.93
C18A-H18A	0.96	C18B-H18G	0.96
C18A-H18B	0.96	C18B-H18D	0.96
C18A-H18C	0.96	C18B-H18E	0.96

C3A-N1A-C2A	117(3)	C9A-C8A-C7A	117.2(7)
C3A-N1A-C18A	123(3)	C17A-C8A-C7A	122.0(7)
C2A-N1A-C18A	119(2)	C8A-C9A-C10A	118.7(10)
C2A-C1A-C5A	122.2(7)	C8A-C9A-H9AA	120.6
C2A-C1A-H1AA	118.9	C10A-C9A-H9AA	120.6
C5A-C1A-H1AA	118.9	C11A-C10A-C9A	119.1(14)
C1A-C2A-N1A	120.9(15)	C11A-C10A-C15A	125.2(12)
C1A-C2A-H2AA	119.5	C9A-C10A-C15A	115.3(11)
N1A-C2A-H2AA	119.5	C12A-C11A-C10A	121.0(12)
N1A-C3A-C4A	123(2)	C12A-C11A-H11A	119.5
N1A-C3A-H3AA	118.4	C10A-C11A-H11A	119.5
C4A-C3A-H3AA	118.4	C11A-C12A-C13A	119.0(13)
C5A-C4A-C3A	120.0(9)	C11A-C12A-H12A	120.5
C5A-C4A-H4AA	120.0	C13A-C12A-H12A	120.5
C3A-C4A-H4AA	120.0	C14A-C13A-C12A	117.7(18)
C4A-C5A-C1A	116.0(6)	C14A-C13A-H13A	121.1
C4A-C5A-C6A	123.9(7)	C12A-C13A-H13A	121.1
C1A-C5A-C6A	120.0(7)	C13A-C14A-C15A	132(2)
C7A-C6A-C5A	123.4(6)	C13A-C14A-H14A	114.2
C7A-C6A-H6AA	118.3	C15A-C14A-H14A	114.2
C5A-C6A-H6AA	118.3	C16A-C15A-C14A	131.7(17)
C6A-C7A-C8A	127.9(6)	C16A-C15A-C10A	123.1(14)
C6A-C7A-H7AA	116.1	C14A-C15A-C10A	105.1(14)
C8A-C7A-H7AA	116.1	C15A-C16A-C17A	123.3(14)

Table 24 (Continued)

C9A-C8A-C17A	120.8(6)	C15A-C16A-H16A	118.4
C17A-C16A-H16A	118.4	C17B-C8B-C7B	120.3(9)
C16A-C17A-C8A	118.6(10)	C10B-C9B-C8B	121.8(11)
C16A-C17A-H17A	120.7	C10B-C9B-H9BA	119.1
C8A-C17A-H17A	120.7	C8B-C9B-H9BA	119.1
C2B-N1B-C3B	120(3)	C11B-C10B-C9B	123.3(17)
C2B-N1B-C18B	123(3)	C11B-C10B-C15B	114.6(13)
C3B-N1B-C18B	116(4)	C9B-C10B-C15B	121.6(13)
C5B-C1B-C2B	118.5(10)	C12B-C11B-C10B	121.5(13)
C5B-C1B-H1BA	120.7	C12B-C11B-H11B	119.3
C2B-C1B-H1BA	120.7	C10B-C11B-H11B	119.3
N1B-C2B-C1B	123(2)	C11B-C12B-C13B	120.7(13)
N1B-C2B-H2BA	118.7	C11B-C12B-H12B	119.7
C1B-C2B-H2BA	118.7	C13B-C12B-H12B	119.7
C4B-C3B-N1B	120(2)	C14B-C13B-C12B	123.1(17)
C4B-C3B-H3BA	120.2	C14B-C13B-H13B	118.4
N1B-C3B-H3BA	120.2	C12B-C13B-H13B	118.4
C3B-C4B-C5B	122.4(9)	C13B-C14B-C15B	110.9(17)
C3B-C4B-H4BA	118.8	C13B-C14B-H14B	124.6
C5B-C4B-H4BA	118.8	C15B-C14B-H14B	124.6
C1B-C5B-C4B	116.6(8)	C10B-C15B-C14B	129.0(13)
C1B-C5B-C6B	124.0(8)	C10B-C15B-C16B	114.3(9)
C4B-C5B-C6B	119.5(8)	C14B-C15B-C16B	116.6(12)
C7B-C6B-C5B	127.8(7)	C17B-C16B-C15B	122.9(12)
C7B-C6B-H6BA	116.1	C17B-C16B-H16B	118.5
C5B-C6B-H6BA	116.1	C15B-C16B-H16B	118.5
C6B-C7B-C8B	124.5(7)	C16B-C17B-C8B	120.8(11)
C6B-C7B-H7BA	117.8	C16B-C17B-H17B	119.6
C8B-C7B-H7BA	117.8	C8B-C17B-H17B	119.6
C9B-C8B-C17B	118.4(8)	N1B-C18B-H18G	109.5

Table 24 (Continued)

C9B-C8B-C7B	121.3(8)	N1B-C18B-H18D	109.5
H18G-C18B-H18D	109.5	H18G-C18B-H18E	109.5
N1B-C18B-H18E	109.5	H18D-C18B-H18E	109.5

Table 25 Hydrogen-bond geometry [Å, °] of **PNAP4**

D—H···*A*	D—H	H···*A*	D···*A*	D—H···*A*
C18*A*—H18*A*···I1$^{\mathrm{i}}$	0.96	3.05	3.928(17)	152
C18*A*—H18*B*···*Cg*1$^{\mathrm{i}}$	0.96	2.63	3.513(18)	153
C18*A*—H18*B*···*Cg*2$^{\mathrm{i}}$	0.96	2.65	3.517(18)	150
C18*B*—H18*E*···*Cg*1$^{\mathrm{i}}$	0.96	2.62	3.44(2)	143
C18*B*—H18*E*···*Cg*2$^{\mathrm{i}}$	0.96	2.66	3.45(2)	139

Symmetry codes: (i) -*x*+1, -*y*+1, -*z*+2. *Cg*1 and *Cg*2 are centroids of the C10*A*-C15*A* and C10B-C15B rings, respectively.

3.3 Structural elucidation of anions counter part

3.3.1 Silver (I) 4-methylbenzenesulfonate (ANM)

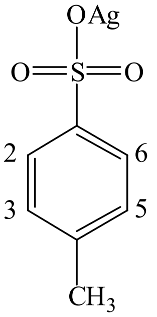

ANM

A white solid of compound **ANM** was obtained in 71% yield which decomposed at 264-266 °C. The ^{1}H NMR spectrum (**Fig. 29**) showed equivalent protons of *p*-disubstituted aromatic at δ 7.74 (2H, *d*, J = 8.1 Hz, H-2, H-6) and 7.17 (2H, *d*, J = 8.1 Hz, H-3, H-5). A *singlet* signal of 4-CH_3 was observed at δ 2.38. Therefore, compound **ANM** was identified to be silver (I) 4-methylbenzenesulfonate.

3.3.2 Silver (I) 4-methoxybenzenesulfonate (ANOM)

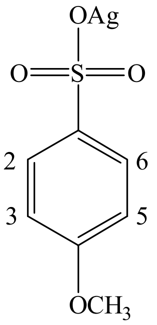

ANOM

Compound **ANOM** was obtained as a white solid in 63%, decomposed at 240-242°C. The ^{1}H NMR spectrum (**Fig. 30**) showed two *doublet* signals of H-2, H-6 and H-3, H-5 at δ 7.78 (2H, J = 8.7 Hz) and δ 6.86 (2H, J = 8.7 Hz) respectively.

The *singlet* signal of 4-OCH_3 appeared at δ 3.82 (3H). Therefore, compound **ANOM** was proposed to be silver (I) 4-methoxybenzenesulfonate.

3.3.3 Silver (I) 4-chlorobenzenesulfonate (ANCL)

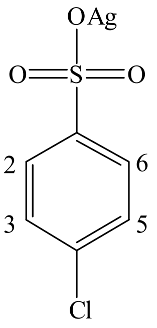

ANCL

Compound **ANCL** was synthesized as a white solid in 68%, decomposed at 227-229 °C. The ^1H NMR spectrum (**Fig. 31**) exhibited only two *doublet* signals of AA′ BB′ pattern at δ 7.76 (H-2, H-6) and δ 7.50 (H-3, H-5) with coupling constant of 7.8 Hz which indicated the location of Cl at C-4. Thus, compound **ANCL** was considered to be silver (I) 4-chlorobenzenesulfonate.

3.3.4 Silver (I) 4-bromobenzenesulfonate (ANBR)

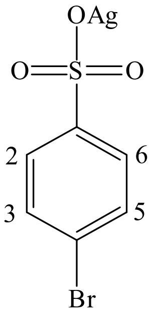

ANBR

Compound **ANBR** was received as a white solid in 61%, decomposed at 230-232 °C. The ^1H NMR spectrum (**Fig. 32**) exhibited only two *doublet*s of AA′ BB′ pattern at δ 7.81 (H-2, H-6) and δ 7.34 (H-3, H-5) with coupling constant of 8.4

Hz which indicated the location of Br at C-4. Accordingly, compound **ANBR** was assigned as silver (I) 4-bromobenzenesulfonate.

3.3.5 Silver (I) 4-aminobenzenesulfonate (ANNH)

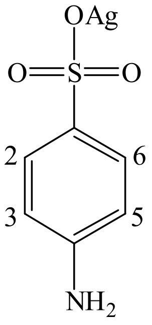

ANNH

Compound **ANNH** was received as a white solid in 60%, decomposed at 279-280 °C. The ^1H NMR spectrum (**Fig. 33**) exhibited only two *doublet*s of AA′ BB′ pattern at δ 7.26 (H-2, H-6) and δ 6.45 (H-3, H-5) with coupling constant of 8.1 Hz. The *broad singlet* signal of 4-NH_2 appeared at δ 5.19 (2H). Accordingly, compound **ANNH** was assigned as silver (I) 4-aminobenzenesulfonate.

3.4 Structural elucidation of Salt formations

3.4.1 (*E*)-1-methyl-2-(2-(naphthalen-1-yl)vinyl)pyridinium 4-methylbenzenesulfonate (PNAP1M)

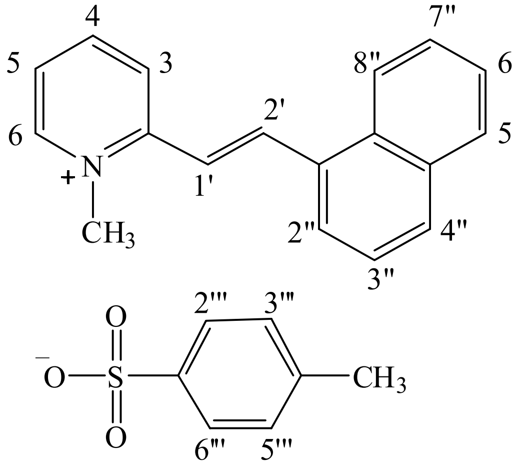

PNAP1M

Compound **PNAP1M** was obtained as a yellow solid (98% yield), mp. 196-197 °C. The UV-Vis absorption bands (**Fig. 34**) were shown at 220.34, 275.09 and 355.52 nm. The FT-IR spectrum (**Fig. 35**) exhibited stretching vibrations of C=C (1611 cm^{-1}) and S=O in sulfonates (1195 cm^{-1}).

The ^{1}H NMR spectrum (**Fig. 36,** see **Table 26**) showed two fragments of cationic and anionic parts. The former showed characteristic of *trans*-disubstituted double bonds at δ 7.69 (1H, *d*, J = 15.6 Hz, H-1′) and δ 8.74 (1H, *d*, J = 15.6 Hz, H-2′). The *singlet* signals at δ 4.46 (3H) was assigned as *N*-CH$_3$. Four signals of 2-substituted pyridinium part pattern at δ 8.82 (1H, *d*, J = 8.1 Hz), δ 8.55 (1H, *d*, J = 8.1 Hz), δ 7.98 (1H, *d*, J = 8.1 Hz) and δ 8.99 (1H, *d*, J = 8.1 Hz) were assigned to be H-3, H-4, H-5 and H-6, respectively. Resonances of aromatic protons of naphthalenyl part H-2″ to H-8″ were also shown at δ 7.92 (*d*, J = 6.6 Hz), δ 7.56 (*d*, J =6.6 Hz), δ 8.19 (*d*, J = 6.6 Hz), δ 8.05 (*d*, J = 8.1 Hz), δ 7.56 (*d*, J = 8.1 Hz), δ 7.63 (*t*, J = 8.1 Hz) and δ 8.49 (*d*, J = 8.1 Hz), respectively. ^{1}H NMR spectrum showed signals of anionic part. Equivalent protons of *p*-disubstituted aromatic appeared as two *doublets* at *δ* 7.56 (2H, *J* = 8.1 Hz, H-2‴, H-6‴) and *δ* 7.10 (2H, *J* = 8.1 Hz, H-3‴, H-5‴). The *singlet* signal of 4‴-CH_3 was observed at *δ* 2.31 (3H). These spectroscopic data confirmed that **PNAP1M** is (*E*)-1-methyl-2-(2-(naphthalen-1-yl)vinyl)pyridinium 4-methylbenzenesulfonate.

Table 26 ^{1}H NMR of compound **PNAP1M**

Position	**δ_H (ppm), *mult*, *J* (Hz)**
1-CH_3	4.46 (3H, *s*)
3	8.82 (1H, *d*, 8.1)
4	8.55 (1H, *d*, 8.1)
5	7.98 (1H, *t*, 8.1)
6	8.99 (1H, *d*, 8.1)
1′	7.69 (1H, *d*, 15.6)
2′	8.74 (1H, *d*, 15.6)
2″	7.92 (1H, *d*, 6.6)
3″	7.65 (1H, *t*, 6.6)
4″	8.19 (1H, *d*, 6.6)
5″	8.05 (1H, *d*, 8.1)
6″	7.56 (1H, *d*, 8.1)
7″	7.63 (1H, *t*, 8.1)
8″	8.49 (1H, *d*, 8.1)
2‴ 6‴	7.56 (2H, *d*, 8.1)
3‴ 5‴	7.10 (2H, *d*, 8.1)
4‴-CH_3	2.31 (3H, *s*)

3.4.2 (*E*)-1-methyl-2-(2-(naphthalen-1-yl)vinyl)pyridinium 4-methoxy-benzenesulfonate (PNAP1O)

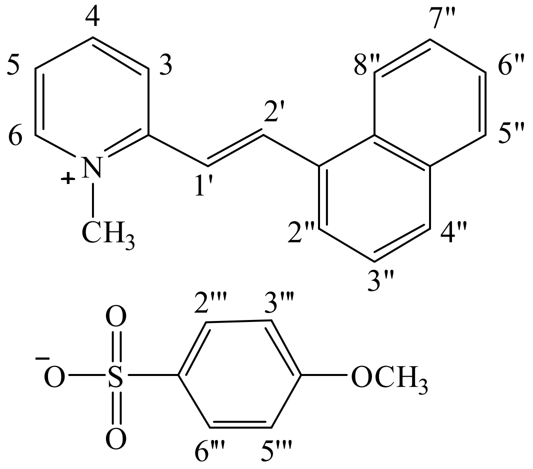

PNAP1O

Compound **PNAP1O** was obtained as a yellow solid (86% yield), mp. 196-198 °C. The UV-Vis absorption bands (**Fig. 37**) were shown at 221.69, 273.06 and 354.85 nm. The FT-IR spectrum (**Fig. 38**) exhibited stretching vibrations of C=C (1601 cm^{-1}) and S=O in sulfonates (1208 cm^{-1}).

The ^1H NMR spectrum (**Fig. 39,** see **Table 27**) showed two fragments of cationic and anionic parts. The former showed characteristic of *trans*-disubstituted double bonds at δ 7.69 (1H, *d*, *J* = 15.9 Hz, H-1′) and δ 8.72 (1H, *d*, *J* = 15.9 Hz, H-2′). The *singlet* signals at δ 4.47 (3H) was assigned as *N*-CH_3. Four signals of 2-substituted pyridinium part at δ 8.79 (1H, *d*, *J* = 8.4 Hz), δ 8.53 (1H, *t*, *J* = 8.4 Hz), δ 7.97 (1H, *t*, *J* = 8.4 Hz) and δ 8.99 (1H, *d*, *J* = 8.4 Hz) were assigned to be H-3, H-4, H-5 and H-6, respectively. Resonances of aromatic protons of naphthalenyl part H-2″ to H-8″ were also shown at δ 7.91 (*d*, *J* = 6.3 Hz), δ 7.58 (*d*, *J* =6.3 Hz), δ 8.17 (*d*, *J* = 6.3 Hz), δ 8.04 (*d*, *J* = 7.8 Hz), δ 7.61 (*d*, *J* = 7.8 Hz), δ 7.64 (*t*, *J* = 7.8 Hz) and δ 8.47 (*d*, *J* = 7.8 Hz), respectively. ^1H NMR spectrum showed signals of anionic part. Equivalent protons of *p*-disubstituted aromatic appeared as two *doublets* at δ 7.61 (2H, *J* = 6.9 Hz, H-2‴, H-6‴) and δ 6.82 (2H, *J* = 6.9 Hz, H-3‴, H-5‴). The *singlet* signal of 4‴-OCH_3 was observed at δ 3.77 (3H). These spectroscopic data confirmed that **PNAP1O** is (*E*)-1-methyl-2-(2-(naphthalen-1-yl)vinyl)pyridinium 4-methoxybenzenesulfonate.

Table 27 ^{1}H NMR of compound **PNAP1O**

Position	**δ_H (ppm), *mult*, *J* (Hz)**
1-CH_3	4.47 (3H, *s*)
3	8.79 (1H, *d*, 8.4)
4	8.53 (1H, *t*, 8.4)
5	7.97 (1H, *t*, 8.4)
6	8.99 (1H, *d*, 8.4)
1′	7.69 (1H, *d*, 15.9)
2′	8.72 (1H, *d*, 15.9)
2″	7.91 (1H, *d*, 6.3)
3″	7.58 (1H, *d*, 6.3)
4″	8.17 (1H, *d*, 6.3)
5″	8.04 (1H, *d*, 7.8)
6″	7.61 (1H, *d*, 7.8)
7″	7.64 (1H, *t*, 7.8)
8″	8.47 (1H, *d*, 7.8)
2‴ 6‴	7.61 (2H, *d*, 6.9)
3‴ 5‴	6.82 (2H, *d*, 6.9)
4‴-OCH_3	3.77 (3H, *s*)

3.4.3 (*E*)-1-methyl-2-(2-(naphthalen-1-yl)vinyl)pyridinium 4-chlorobenzenesulfonate (PNAP1C)

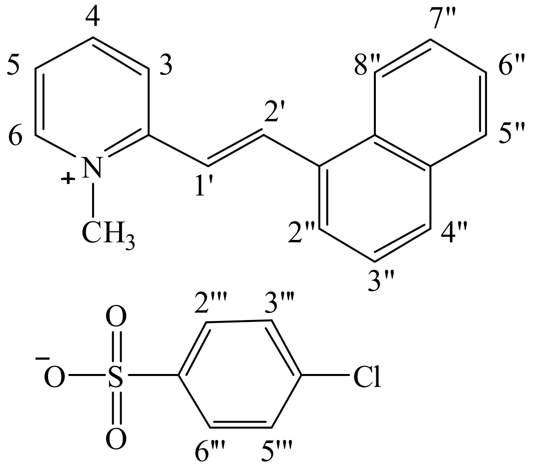

PNAP1C

Compound **PNAP1C** was obtained as a yellow solid (80% yield), mp. 270-272 °C. The UV-Vis absorption bands (**Fig. 40**) were shown at 221.02, 274.42 and 358.23 nm. The FT-IR spectrum (**Fig. 41**) exhibited stretching vibrations of C=C (1598 cm^{-1}) and S=O in sulfonates (1218 cm^{-1}).

The ^1H NMR spectrum (**Fig. 42,** see **Table 28**) showed two fragments of cationic and anionic parts. The former showed characteristic of *trans*-disubstituted double bonds at δ 7.17 (1H, *d*, J = 15.0 Hz, H-1′) and δ 8.73 (1H, *d*, J = 15.0 Hz, H-2′). The *singlet* signals at δ 4.44 (3H) was assigned as N-CH_3. Four signals of 2-substituted pyridinium part at δ 8.82 (1H, *d*, J = 6.0 Hz), δ 8.50 (1H, *d*, J = 6.0 Hz), δ 7.97 (1H, *d*, J = 6.0 Hz) and δ 9.07 (1H, *d*, J = 6.0 Hz) were assigned to be H-3, H-4, H-5 and H-6, respectively. Resonances of aromatic protons of naphthalenyl part H-2″ to H-8″ were also shown at δ 7.90 (*d*, J = 8.4 Hz), δ 7.27 (*d*, J = 8.4 Hz), δ 8.13 (*d*, J = 8.4 Hz), δ 8.02 (*d*, J = 5.4 Hz), δ 7.61 (*d*, J = 5.4 Hz), δ 7.62 (*d*, J = 5.4 Hz) and δ 8.44 (*d*, J = 5.4 Hz), respectively. ^1H NMR spectrum showed signals of anionic part. Equivalent protons of *p*-disubstituted aromatic appeared as two *doublets* at δ 7.68 (2H, J = 7.2 Hz, H-2‴, H-6‴) and δ 7.33 (2H, J = 7.2 Hz, H-3‴, H-5‴). These spectroscopic data confirmed that **PNAP1C** is (*E*)-1-methyl-2-(2-(naphthalen-1-yl)vinyl)pyridinium 4-chlorobenzenesulfonate.

Table 28 ^{1}H NMR of compound **PNAP1C**

Position	**δ_H (ppm), *mult*, *J* (Hz)**
1-CH_3	4.44 (3H, *s*)
3	8.82 (1H, *d*, 6.0)
4	8.50 (1H, *d*, 6.0)
5	7.97 (1H, *d*, 6.0)
6	9.07 (1H, *d*, 6.0)
1′	7.17 (1H, *d*, 15.0)
2′	8.73 (1H, *d*, 15.0)
2″	7.90 (1H, *d*, 8.4)
3″	7.27 (1H, *d*, 8.4)
4″	8.13 (1H, *d*, 8.4)
5″	8.02 (1H, *d*, 5.4)
6″	7.61 (1H, *d*, 5.4)
7″	7.62 (1H, *d*, 5.4)
8″	8.44 (1H, *d*, 5.4)
2‴ 6‴	7.68 (2H, *d*, 7.2)
3‴ 5‴	7.33 (2H, *d*, 7.2)

3.4.4 (*E*)-1-methyl-2-(2-(naphthalen-1-yl)vinyl)pyridinium 4-bromobenzenesulfonate (PNAP1B)

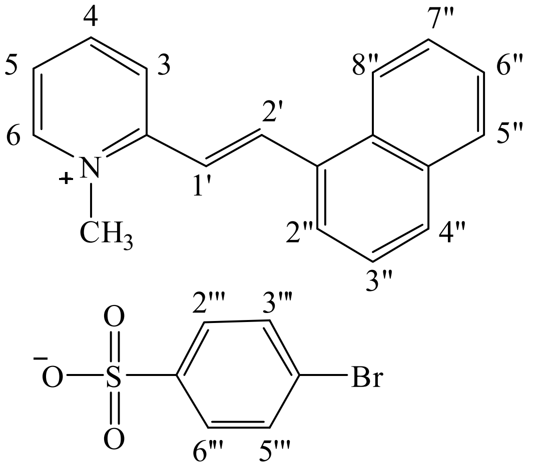

PNAP1B

Compound **PNAP1B** was obtained as a yellow solid (91% yield), mp. 222-223 °C. The UV-Vis absorption bands (**Fig. 43**) were shown at 220.34, 275.09 and 383.23 nm. The FT-IR spectrum (**Fig. 44**) exhibited stretching vibrations of C=C (1618 cm^{-1}) and S=O in sulfonates (1203 cm^{-1}).

The ^1H NMR spectrum (**Fig. 45,** see **Table 29**) showed two fragments of cationic and anionic parts. The former showed characteristic of *trans*-disubstituted double bonds at δ 7.69 (1H, *d*, J = 15.0 Hz, H-1′) and δ 8.72 (1H, *d*, J = 15.0 Hz, H-2′). The *singlet* signals at δ 4.47 (3H) was assigned as *N*-CH_3. Four signals of 2-substituted pyridinium part at δ 8.79 (1H, *d*, J = 8.4 Hz), δ 8.54 (1H, *t*, J = 8.4 Hz), δ 7.90 (1H, *d*, J = 8.4 Hz) and δ 9.09 (1H, *d*, J = 8.4 Hz) were assigned to be H-3, H-4, H-5 and H-6, respectively. Resonances of aromatic protons of naphthalenyl part H-2″ to H-8″ were also shown at δ 7.86 (*d*, J = 6.3 Hz), δ 7.17 (*d*, J = 6.3 Hz), δ 8.16 (*d*, J = 6.3 Hz), δ 8.00 (*d*, J = 7.5 Hz), δ 7.31 (*t*, J = 7.5 Hz), δ 7.61 (*d*, J = 7.5 Hz) and δ 8.45 (*d*, J = 7.5 Hz), respectively. ^1H NMR spectrum showed signals of anionic part. Equivalent protons of *p*-disubstituted aromatic appeared as two *doublets* at δ 7.65 (2H, J = 8.4 Hz, H-2‴, H-6‴) and δ 7.47 (2H, J = 8.4 Hz, H-3‴, H-5‴). These spectroscopic data confirmed that **PNAP1B** is (*E*)-1-methyl-2-(2-(naphthalen-1-yl)vinyl)pyridinium 4-bromobenzenesulfonate.

Table 29 ^{1}H NMR of compound **PNAP1B**

Position	**δ_H (ppm), *mult*, *J* (Hz)**
1-CH_3	4.47 (3H, *s*)
3	8.79 (1H, *d*, 8.4)
4	8.54 (1H, *t*, 8.4)
5	7.90 (1H, *t*, 8.4)
6	9.09 (1H, *d*, 8.4)
1′	7.69 (1H, *d*, 15.0)
2′	8.72 (1H, *d*, 15.0)
2″	7.86 (1H, *d*, 6.3)
3″	7.17 (1H, *d*, 6.3)
4″	8.16 (1H, *d*, 6.3)
5″	8.00 (1H, *d*, 7.5)
6″	7.31 (1H, *t*, 7.5)
7″	7.61 (1H, *d*, 7.5)
8″	8.45 (1H, *d*, 7.5)
2‴ 6‴	7.65 (2H, *d*, 8.4)
3‴ 5‴	7.47 (2H, *d*, 8.4)

3.4.5 (*E*)-1-methyl-2-(2-(naphthalen-1-yl)vinyl)pyridinium 4-aminobenzenesulfonate (PNAP1N)

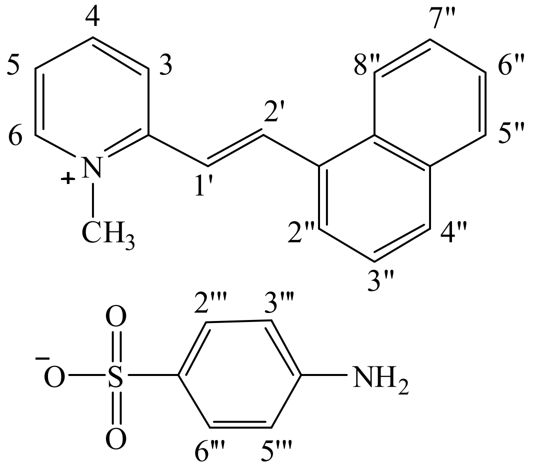

PNAP1N

Compound **PNAP1N** was obtained as a yellow solid (55% yield), mp. 232-233 °C. The UV-Vis absorption bands (**Fig. 46**) were shown at 220.92, 255.35 and 364.59 nm. The FT-IR spectrum (**Fig. 47**) exhibited stretching vibrations of C=C (1617 cm^{-1}) and S=O in sulfonates (1183 cm^{-1}).

The ^1H NMR spectrum (**Fig. 48,** see **Table 30**) showed two fragments of cationic and anionic parts. The former showed characteristic of *trans*-disubstituted double bonds at δ 7.67 (1H, *d*, J = 15.9 Hz, H-1′) and δ 8.72 (1H, *d*, J = 15.9 Hz, H-2′). The *singlet* signals at δ 4.49 (3H) was assigned as *N*-CH_3. Four signals of 2-substituted pyridinium part at δ 8.78 (1H, *d*, J = 7.6 Hz), δ 8.52 (1H, *t*, J = 7.6 Hz), δ 7.99 (1H, *t*, J = 7.6 Hz) and δ 9.01 (1H, *d*, J = 7.6 Hz) were assigned to be H-3, H-4, H-5 and H-6, respectively. Resonances of aromatic protons of naphthalenyl part H-2″ to H-8″ were also shown at δ 7.92 (*d*, J = 8.4 Hz), δ 7.45 (*d*, J = 8.4 Hz), δ 8.14 (*d*, J = 8.4 Hz), δ 8.05 (*d*, J = 7.5 Hz), δ 7.58 (*d*, J = 7.5 Hz), δ 7.62 (*t*, J = 7.5 Hz) and δ 8.43 (*d*, J = 7.5 Hz), respectively. ^1H NMR spectrum showed signals of anionic part. Equivalent protons of *p*-disubstituted aromatic appeared as two *doublets* at δ 7.46 (2H, J = 8.4 Hz, H-2‴, H-6‴) and δ 6.52 (2H, J = 8.4 Hz, H-3‴, H-5‴). These spectroscopic data confirmed that **PNAP1N** is (*E*)-1-methyl-2-(2-(naphthalen-1-yl)vinyl)pyridinium 4-aminobenzenesulfonate.

Table 30 ^{1}H NMR of compound **PNAP1N**

Position	δ_H **(ppm), *mult*, *J* (Hz)**
1-CH_3	4.49 (3H, *s*)
3	8.78 (1H, *d*, 7.6)
4	8.52 (1H, *t*, 7.6)
5	7.99 (1H, *t*, 7.6)
6	9.01 (1H, *d*, 7.6)
1′	7.67 (1H, *d*, 15.9)
2′	8.72 (1H, *d*, 15.9)
2″	7.92 (1H, *d*, 8.4)
3″	7.45 (1H, *d*, 8.4)
4″	8.14 (1H, *d*, 8.4)
5″	8.05 (1H, *d*, 7.5)
6″	7.58 (1H, *d*, 7.5)
7″	7.62 (1H, *t*, 7.5)
8″	8.43 (1H, *d*, 7.5)
2‴ 6‴	7.46 (2H, *d*, 8.4)
3‴ 5‴	6.52 (2H, *d*, 8.4)
4‴-NH_2	4.79 (2H, *br s*)

3.4.6 (*E*)-1-methyl-4-(2-(naphthalen-1-yl)vinyl)pyridinium 4-methylbenzenesulfonate (PNAP2M)

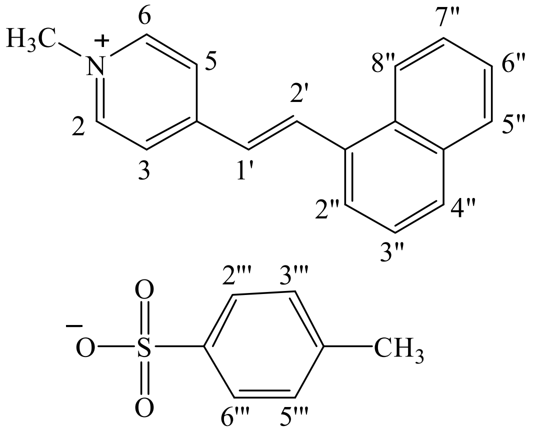

PNAP2M

Compound **PNAP2M** was obtained as yellow crystals (86% yield), mp. 178-180 °C. The UV-Vis absorption spectra (**Fig. 49**) showed maximum bands at 220.34, 276.44 and 377.15 nm. The FT-IR spectrum (**Fig. 50**) exhibited stretching vibrations of C=C (1617 cm^{-1}) and S=O in sulfonates (1187 cm^{-1}).

The ^{1}H NMR spectrum (**Fig. 51,** see **Table 31**) showed two fragments of cationic and anionic parts. The former showed characteristic of *trans*-disubstituted double bonds at δ 7.57 (1H, *d*, J = 16.2 Hz, H-1′) and δ 8.81 (1H, *d*, J = 16.2 Hz, H-2′). The *singlet* signal at δ 4.31 (3H) was assigned as *N*-CH$_3$. Equivalent protons of *p*-disubstituted aromatic appeared as two *doublet* signals at δ 8.91 (2H, J = 6.0 Hz, H-2, H-6) and δ 8.43 (2H, J = 6.0 Hz, H-3, H-5). Resonances of aromatic protons of naphthalenyl part H-2″ to H-8″ were also shown at δ 7.96 (*d*, J = 8.1 Hz), δ 8.06 (*t*, J = 8.1 Hz), δ 7.99 (*d*, J = 8.1 Hz), δ 8.03 (*d*, J = 7.2 Hz), δ 7.63 (*d*, J = 7.2 Hz), δ 7.60 (*d*, J = 7.2 Hz) and δ 8.55 (*d*, J = 7.2 Hz), respectively. ^{1}H NMR spectrum also showed resonances of aromatic protons of anionic part at δ 7.53 (2H, *d*, J = 8.1 Hz, H-2‴, H-6‴) and δ 7.10 (2H, *d*, J = 8.1 Hz, H-3‴, H-5‴). These observations confirmed that **PNAP2M** is (*E*)-1-methyl-4-(2-(naphthalen-1-yl)vinyl)pyridinium 4-methylbenzenesulfonate.

Table 31 ^{1}H NMR of compound **PNAP2M**

Position	**δ_H (ppm), *mult*, *J* (Hz)**
1-CH_3	4.31 (3H, *s*)
2 6	8.91 (2H, *d*, 6.0)
3 5	8.43 (2H, *d*, 6.0)
1′	7.57 (1H, *d*, 15.2)
2′	8.81 (1H, *d*, 15.2)
2″	7.96 (1H, *d*, 8.1)
3″	8.06 (1H, *t*, 8.1)
4″	7.99 (1H, *d*, 8.1)
5″	8.03 (1H, *d*, 7.2)
6″	7.63 (1H, *d*, 7.2)
7″	7.60 (1H, *d*, 7.2)
8″	8.55 (1H, *d*, 7.2)
2‴ 6‴	7.53 (2H, *d*, 8.1)
3‴ 5‴	7.10 (2H, *d*, 8.1)
4‴-CH_3	2.39 (3H, *s*)

3.4.7 (*E*)-1-methyl-4-(2-(naphthalen-1-yl)vinyl)pyridinium 4-methoxybenzenesulfonate (PNAP2O)

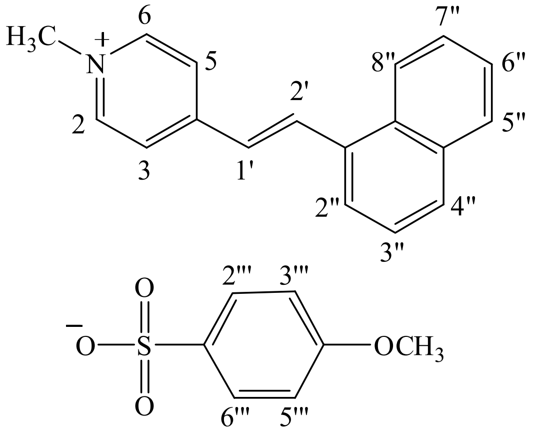

PNAP2O

Compound **PNAP2O** was obtained as a yellow crystals (92% yield), mp. 189-190 °C. The UV-Vis absorption spectra (**Fig. 52**) showed maximum bands at 221.02, 275.09 and 384.59 nm. The FT-IR spectrum (**Fig. 53**) exhibited stretching vibrations of C=C (1618 cm^{-1}), C-O in OCH_3 (1190 cm^{-1}) and S=O in sulfonates (1207 cm^{-1}).

The ^1H NMR spectrum (**Fig. 54,** see **Table 32**) showed two fragments of cationic and anionic parts. The former showed characteristic of *trans*-disubstituted double bonds at δ 7.59 (1H, *d*, J = 15.9 Hz, H-1′) and δ 8.81 (1H, *d*, J = 15.9 Hz, H-2′). The *singlet* signal at δ 4.30 (3H) was assigned as *N*-CH_3. Equivalent protons of *p*-disubstituted aromatic appeared as two *doublet* signals at δ 8.90 (2H, J = 6.6 Hz, H-2, H-6) and δ 8.43 (2H, J = 6.6 Hz, H-3, H-5). Resonances of aromatic protons of naphthalenyl part H-2″ to H-8″ were also shown at δ 8.00 (*d*, J = 7.5 Hz), δ 8.08 (*d*, J = 7.5 Hz), δ 8.03 (*d*, J = 7.5 Hz), δ 8.06 (*d*, J = 7.2 Hz), δ 7.68 (*d*, J = 7.2 Hz), δ 7.67 (*d*, J = 7.2 Hz) and δ 8.56 (*d*, J = 7.2 Hz), respectively. ^1H NMR spectrum also showed resonances of aromatic protons of anionic part at δ 7.56 (2H, *d*, J = 8.7 Hz, H-2‴, H-6‴) and δ 6.84 (2H, *d*, J = 8.7 Hz, H-3‴, H-5‴). These observations confirmed that **PNAP2O** is (*E*)-1-methyl-4-(2-(naphthalen-1-yl)vinyl)pyridinium 4-methoxybenzenesulfonate.

Table 32 ^{1}H NMR of compound **PNAP2O**

Position	**δ_H (ppm), *mult*, *J* (Hz)**
1-CH_3	4.30 (3H, *s*)
2 6	8.90 (2H, *d*, 6.6)
3 5	8.43 (2H, *d*, 6.6)
1′	7.59 (1H, *d*, 15.9)
2′	8.81 (1H, *d*, 15.9)
2″	8.00 (1H, *d*, 7.5)
3″	8.08 (1H, *d*, 7.5)
4″	8.03 (1H, *d*, 7.5)
5″	8.06 (1H, *d*, 7.2)
6″	7.68 (1H, *d*, 7.2)
7″	7.67 (1H, *d*, 7.2)
8″	8.56 (1H, *d*, 7.2)
2‴ 6‴	7.56 (2H, *d*, 8.7)
3‴ 5‴	6.84 (2H, *d*, 8.7)
4‴-OCH_3	3.75 (3H, *s*)

3.4.8 (*E*)-1-methyl-4-(2-(naphthalen-1-yl)vinyl)pyridinium 4-chlorobenzenesulfonate (PNAP2C)

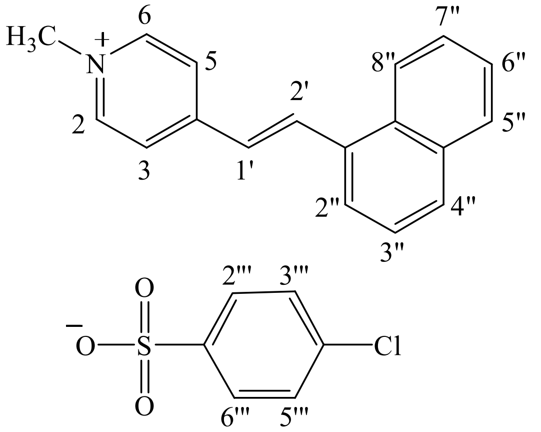

PNAP2C

Compound **PNAP2C** was obtained as brown crystal (82% yield), mp. 203-204 °C. The UV-Vis absorption spectra (**Fig. 55**) showed maximum bands at 221.02, 275.77 and 377.83 nm. The FT-IR spectrum (**Fig. 56**) exhibited stretching vibrations of C=C (1623 cm^{-1}) and S=O in sulfonates (1209 cm^{-1}).

The ^{1}H NMR spectrum (**Fig. 57,** see **Table 33**) showed two fragments of cationic and anionic parts. The former showed characteristic of *trans*-disubstituted double bonds at δ 7.55 (1H, *d*, J = 16.8 Hz, H-1′) and δ 8.80 (1H, *d*, J = 16.8 Hz, H-2′). The *singlet* signal at δ 4.34 (3H) was assigned as N-CH$_3$. Equivalent protons of *p*-disubstituted aromatic appeared as two *doublet* signals at δ 8.91 (2H, J = 6.6 Hz, H-2, H-6) and δ 8.41 (2H, J = 6.6 Hz, H-3, H-5). Resonances of aromatic protons of naphthalenyl part H-2″ to H-8″ were also shown at δ 7.97 (*d*, J = 9.6 Hz), δ 7.98 (*t*, J = 9.6 Hz), δ 8.00 (*d*, J = 9.6 Hz), δ 8.06 (*d*, J = 7.2 Hz), δ 7.60 (*d*, J = 7.2 Hz), δ 7.58 (*d*, J = 7.2 Hz) and δ 8.52 (*d*, J = 7.2 Hz), respectively. ^{1}H NMR spectrum also showed resonances of aromatic protons of anionic part at δ 7.69 (2H, *d*, J = 8.4 Hz, H-2‴, H-6‴) and δ 7.33 (2H, *d*, J = 8.4 Hz, H-3‴, H-5‴). These observations confirmed that **PNAP2C** is (*E*)-1-methyl-4-(2-(naphthalen-1-yl)vinyl)pyridinium 4-chlorobenzenesulfonate.

Table 33 ^{1}H NMR of compound **PNAP2C**

Position	**δ_H (ppm), *mult*, *J* (Hz)**
1-CH_3	4.34 (3H, *s*)
2 6	8.91 (2H, *d*, 6.6)
3 5	8.41 (2H, *d*, 6.6)
1′	7.55 (1H, *d*, 16.8)
2′	8.80 (1H, *d*, 16.8)
2″	7.97 (1H, *d*, 9.6)
3″	7.98 (1H, *t*, 9.6)
4″	8.00 (1H, *d*, 9.6)
5″	8.06 (1H, *d*, 7.2)
6″	7.60 (1H, *d*, 7.2)
7″	7.58 (1H, *d*, 7.2)
8″	8.52 (1H, *d*, 7.2)
2‴ 6‴	7.69 (2H, *d*, 8.4)
3‴ 5‴	7.33 (2H, *d*, 8.4)

The crystal structure of **PNAP2C** is illustrated in **Fig. 7** and **Fig. 8** which show the packing diagram of **PNAP2C** and intermolecular hydrogen bondings. The crystal and experiment data are given in **Table 34**. Bond lengths and angles are shown in **Table 35**. Hydrogen-bond geometry are shown in **Table 36**. The X-ray study shows that **PNAP2C** crystallized out in non-centrosymmetric space group $\boldsymbol{Pna}\mathbf{2}_1$.

Figure 7 shows the asymmetric unit of **PNAP2C** which consists of a $C_{18}H_{16}N^+$ cation and a $C_6H_4ClO_3S^-$ anion. The cation exists in an *E* configuration with respect to the C11═C12 double bond [1.341 (4) Å] and the torsion angle C10–C11–C12–C13 is 179.6 (3)°. The naphthalenyl moiety is slightly bend which can be reflected by the dihedral angle between the two aromatic C1–C4/C9–C10 and C4–C9 rings being 3.68 (14)°. The whole molecule of cation is twisted with dihedral angles between the pyridinium and the two aromatic C1–C4/C9–C10 and C4–C9 rings being 47.44 (14) and 50.81 (14)°, respectively. The orientation of the ethenyl unit can be described as atom C11 lies on the same plane with naphthalenyl moiety with the rms deviation of 0.028 (3) Å whereas atom C12 lies on the same plane with the pyridinium ring with the rms deviation of 0.017 (3) Å and the torsion angles C8–C9–C10–C11 of -0.5 (4)° and C11–C12–C13–C17 of -11.4 (5)°. The cation and anion are inclined to each other with a dihedral angle of 68.21 (13)° between the pyridinium and C19–C24 rings.

In the crystal packing (**Fig. 8**), all O atoms of the sulfonate group are involved in weak C—H···O interactions (**Table 36**). The cations and anions are alternately arranged with the cations stacked in an antiparallel manner along the *c* axis and the anions linked together into chains along the same direction. The cations are linked to the anions by weak C—H···O interactions (**Table 36**) forming 3D network. The crystal structure is further stabilized by C—H···π interactions (Table 35). π···π interactions with the distances Cg1···Cg2 = 3.6733 (17) Å and Cg1···Cg3 = 3.6374 (16) Å are also observed (symmetry code for both Cg···Cg interactions: 2-x, 1-y,-1/2+z); Cg1, Cg2, Cg3 and Cg4 are the centroids of the N1/C13–C17, C1–C4/C9–C10, C4–C9 and C19–C24 rings, respectively. A short Cl1···O2 [3.108 (2) Å] contact is also present.

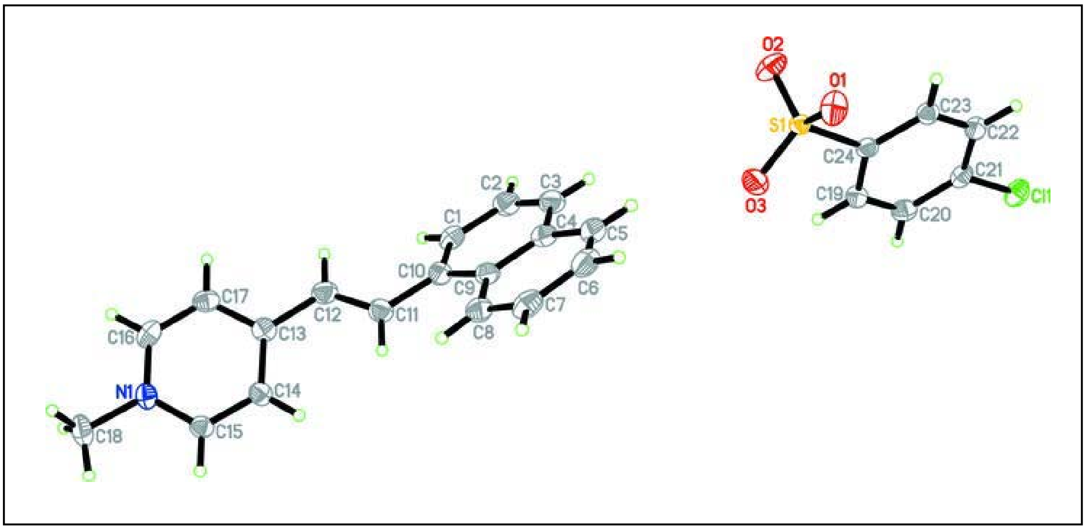
O2
O1
S1
C23
C22
C24
C21
Cl1
O3
C19
C20
C2
C3
C1
C4
C5
C10
C9
C6
C17
C12
C11
C7
C8
C16
C13
N1
C14
C18
C15

Figure 7 X-ray ORTEP diagram of the compound **PNAP2C**

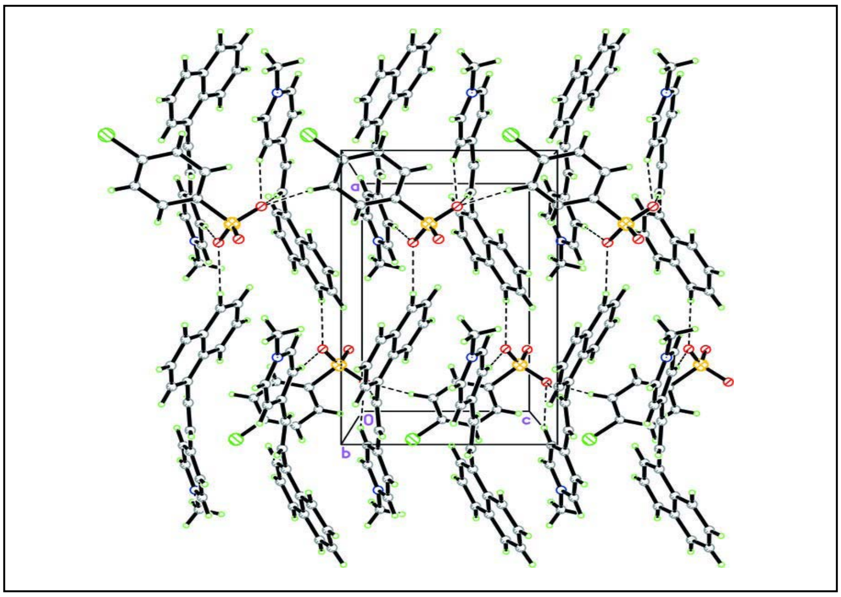

Figure 8 The crystal packing of the compound **PNAP2C** viewed down the *b* axis. Weak C—H···O interactions are shown as dashed lines.

Table 34 Crystal data of **PNAP2C**

Identification code	**PNAP2C**
Empirical formula	$C_{18}H_{16}N^{+}\cdot C_6H_4ClO_3S^{-}$
Formula weight	437.93
Temperature	100.0(1) K
Wavelength	0.71073 Å
Crystal system, space group	Orthorhombic, $Pna2_1$
Unit cell dimensions	a = 12.3379(8) Å α = 90 °
	b = 21.8466(16) Å β = 90 °
	c = 7.5032(5) Å γ = 90 °
Volume	2022.4(2) $Å^3$
Z, Calculated density	4, 1.438 Mg/m^3
Absorption coefficient	0.32 mm^{-1}
F(000)	912
Crystal size	0.52 x 0.15 x 0.03 mm
Theta range for data collection	2.5 to 30.0 °
Limiting indices	-17<=h<=17, -25<=k<=30, -10<=l<=10
Reflections collected / unique	26247 / 5881 [R(int) = 0.045]
Completeness to theta = 30.00	99.9 %
Max. and min. transmission	0.990 and 0.852
Refinement method	Full-matrix least-squares on F^2
Data / restraints / parameters	5881 / 1 / 272
Goodness-of-fit on F^2	1.029
Final R indices [I>2σ(I)]	$R1$ = 0.0497, $wR2$ = 0.1131
R indices (all data)	$R1$ = 0.0615, $wR2$ = 0.1194
Largest diff. peak and hole	0.79 and -0.32 e.$Å^3$

Table 35 Bond lengths [Å] and angles [°] for **PNAP2C**

Cl1-C21	1.740(3)	C10-C11	1.455(4)
S1-O1	1.446(2)	C11-C12	1.341(4)
S1-O3	1.446(2)	C11-H11A	0.93
S1-O2	1.4514(18)	C12-C13	1.480(4)
S1-C24	1.792(3)	C12-H12A	0.93
N1-C15	1.350(3)	C13-C14	1.396(4)
N1-C16	1.358(4)	C13-C17	1.400(4)
N1-C18	1.468(3)	C14-C15	1.375(3)
C1-C10	1.389(4)	C14-H14A	0.93
C1-C2	1.395(4)	C15-H15A	0.93
C1-H1A	0.93	C16-C17	1.364(4)
C2-C3	1.351(4)	C16-H16A	0.93
C2-H2A	0.93	C17-H17A	0.93
C3-C4	1.429(4)	C18-H18A	0.96
C3-H3A	0.93	C18-H18B	0.96
C4-C9	1.410(4)	C18-H18C	0.96
C4-C5	1.419(4)	C19-C24	1.388(4)
C5-C6	1.367(4)	C19-C20	1.389(4)
C5-H5A	0.93	C19-H19A	0.93
C6-C7	1.402(4)	C20-C21	1.392(4)
C6-H6A	0.93	C20-H20A	0.93
C7-C8	1.376(4)	C21-C22	1.384(4)
C7-H7A	0.93	C22-C23	1.393(4)
C8-C9	1.425(4)	C22-H22A	0.93
C8-H8A	0.93	C23-C24	1.395(3)
C9-C10	1.441(4)	C23-H23A	0.93
O1-S1-O3	114.45(13)	O3-S1-C24	105.43(12)
O1-S1-O2	112.79(13)	O2-S1-C24	104.70(11)
O3-S1-O2	113.43(12)	C15-N1-C16	120.2(2)
O1-S1-C24	104.83(11)	C15-N1-C18	119.8(2)

Table 35 (Continued)

C16-N1-C18	120.0(2)	C12-C11-C10	124.1(2)
C10-C1-C2	121.4(3)	C12-C11-H11A	118.0
C10-C1-H1A	119.3	C10-C11-H11A	118.0
C2-C1-H1A	119.3	C11-C12-C13	124.8(2)
C3-C2-C1	120.4(3)	C11-C12-H12A	117.6
C3-C2-H2A	119.8	C13-C12-H12A	117.6
C1-C2-H2A	119.8	C14-C13-C17	117.1(2)
C2-C3-C4	120.6(3)	C14-C13-C12	122.8(2)
C2-C3-H3A	119.7	C17-C13-C12	120.0(2)
C4-C3-H3A	119.7	C15-C14-C13	121.0(2)
C9-C4-C5	119.4(3)	C15-C14-H14A	119.5
C9-C4-C3	120.2(3)	C13-C14-H14A	119.5
C5-C4-C3	120.4(3)	N1-C15-C14	120.1(2)
C6-C5-C4	120.9(3)	N1-C15-H15A	119.9
C6-C5-H5A	119.6	C14-C15-H15A	119.9
C4-C5-H5A	119.6	N1-C16-C17	121.2(2)
C5-C6-C7	119.8(3)	N1-C16-H16A	119.4
C5-C6-H6A	120.1	C17-C16-H16A	119.4
C7-C6-H6A	120.1	C16-C17-C13	120.2(2)
C8-C7-C6	120.9(3)	C16-C17-H17A	119.9
C8-C7-H7A	119.5	C13-C17-H17A	119.9
C6-C7-H7A	119.5	N1-C18-H18A	109.5
C7-C8-C9	120.2(3)	N1-C18-H18B	109.5
C7-C8-H8A	119.9	H18A-C18-H18B	109.5
C9-C8-H8A	119.9	N1-C18-H18C	109.5
C4-C9-C8	118.6(2)	H18A-C18-H18C	109.5
C4-C9-C10	117.9(2)	H18B-C18-H18C	109.5
C8-C9-C10	123.4(2)	C24-C19-C20	120.3(2)
C1-C10-C9	119.4(2)	C24-C19-H19A	119.8
C1-C10-C11	121.0(3)	C20-C19-H19A	119.8
C9-C10-C11	119.6(2)	C19-C20-C21	119.1(3)

Table 35 (Continued)

C19-C20-H20A	120.5	C23-C22-H22A	120.4
C21-C20-H20A	120.5	C22-C23-C24	120.0(3)
C22-C21-C20	121.3(2)	C22-C23-H23A	120.0
C22-C21-Cl1	119.7(2)	C24-C23-H23A	120.0
C20-C21-Cl1	119.0(2)	C19-C24-C23	120.0(2)
C21-C22-C23	119.2(2)	C19-C24-S1	120.30(18)
C21-C22-H22A	120.4	C23-C24-S1	119.6(2)

Table 36 Hydrogen-bond geometry [Å, °] of **PNAP2C**

D—H···*A*	D—H	H···*A*	D···*A*	D—H···*A*
C5—H5*A*···O3	0.93	2.51	3.370(3)	153
C11—H11*A*···O1^{i}	0.93	2.34	3.267(3)	178
C14—H14*A*··· O1^{i}	0.93	2.38	3.260(3)	158
C15—H15*A*···O2^{ii}	0.93	2.42	3.285(3)	155
C17—H17*A*···O3^{iii}	0.93	2.43	3.348(3)	171
C18—H18*A*···O2^{ii}	0.96	2.45	3.372(4)	160
C20—H20*A*···O1^{iv}	0.93	2.34	3.226(4)	159
C22—H22*A*···O2^{v}	0.93	2.52	3.277(3)	139
C1—H1*A*···*Cg*4^{iii}	0.93	2.98	3.682(3)	133
C3—H3*A*···*Cg*4^{vi}	0.93	2.87	3.651(3)	142
C6—H6*A*···*Cg*3^{vii}	0.93	2.82	3.593(3)	141

Symmetry codes: (i) -*x*+1, -*y*+1, *z*-1/2; (ii) -*x*+3/2, *y*+1/2, *z*-1/2; (iii) *x*+1, *y*, *z*; (iv) *x*, *y*, *z*-1; (v) *x*-1/2, -*y*+1/2, *z*; (vi) *x*+1/2, -*y*+1/2, *z*; (vii) -*x*+1, -*y*+1, *z*+1/2. *Cg*1, *Cg*2, *Cg*3 and *Cg*4 are the centroids of the N1/C13–C17, C1–C4/C9/C10, C4–C9 and C19–C24 rings, respectively.

3.4.9 (*E*)-1-methyl-4-(2-(naphthalen-1-yl)vinyl)pyridinium 4-bromobenzenesulfonate (PNAP2B)

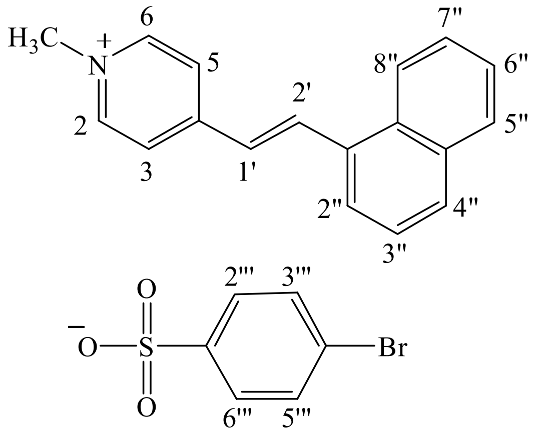

PNAP2B

Compound **PNAP2B** was obtained as brown crystal (91% yield), mp. 222-223 °C. The UV-Vis absorption spectra (**Fig. 58**) showed maximum bands at 220.34, 275.09 and 383.23 nm. The FT-IR spectrum (**Fig. 59**) exhibited stretching vibrations of C=C (1618 cm^{-1}) and S=O in sulfonates (1203 cm^{-1}).

The ^{1}H NMR spectrum (**Fig. 60,** see **Table 37**) showed two fragments of cationic and anionic parts. The former showed characteristic of *trans*-disubstituted double bonds at δ 7.53 (1H, *d*, *J* = 16.5 Hz, H-1′) and δ 8.81 (1H, *d*, *J* = 16.5 Hz, H-2′). The *singlet* signal at δ 4.31 (3H) was assigned as *N*-CH$_3$. Equivalent protons of *p*-disubstituted aromatic appeared as two *doublet* signals at δ 8.91 (2H, *J* = 6.3 Hz, H-2, H-6) and δ 8.66 (2H, *J* = 6.3 Hz, H-3, H-5). Resonances of aromatic protons of naphthalenyl part H-2″ to H-8″ were also shown at δ 7.97 (*d*, *J* = 8.4 Hz), δ 8.08 (*d*, *J* = 8.4 Hz), δ 8.00 (*d*, *J* = 8.4 Hz), δ 8.06 (*d*, *J* = 8.7 Hz), δ 7.60 (*d*, *J* = 8.7 Hz), δ 7.59 (*d*, *J* = 8.7 Hz) and δ 8.43 (*d*, *J* = 8.7 Hz), respectively. ^{1}H NMR spectrum also showed resonances of aromatic protons of anionic part at δ 7.49 (2H, *d*, *J* = 7.2 Hz, H-2‴, H-6‴) and δ 7.11 (2H, *d*, *J* = 7.2 Hz, H-3‴, H-5‴). These observations confirmed that **PNAP2B** is (*E*)-1-methyl-4-(2-(naphthalen-1-yl)vinyl)pyridinium 4-bromobenzenesulfonate.

Table 37 ^{1}H NMR of compound **PNAP2B**

Position	δ_H **(ppm),** ***mult*****,** ***J*** **(Hz)**
1-CH_3	4.31 (3H, *s*)
2 6	8.91 (2H, *d*, 6.3)
3 5	8.66 (2H, *d*, 6.3)
1′	7.53 (1H, *d*, 16.5)
2′	8.81 (1H, *d*, 16.5)
2″	7.97 (1H, *d*, 8.4)
3″	8.08 (1H, *d*, 8.4)
4″	8.00 (1H, *d*, 8.4)
5″	8.06 (1H, *d*, 8.7)
6″	7.60 (1H, *d*, 8.7)
7″	7.59 (1H, *d*, 8.7)
8″	8.43 (1H, *d*, 8.7)
2‴ 6‴	7.49 (2H, *d*, 7.2)
3‴ 5‴	7.11 (2H, *d*, 7.2)

The crystal structure of **PNAP2B** is illustrated in **Fig. 9** and **Fig. 10** which show the packing diagram of **PNAP2B** and intermolecular hydrogen bondings. The crystal and experiment data are given in **Table 38**. Bond lengths and angles are shown in **Table 39**. Hydrogen-bond geometry are shown in **Table 40**. The X-ray study shows that **PNAP2B** crystallized out in non-centrosymmetric space group ***Pna*2$_1$**.

Fig. 9 shows the asymmetric unit of **PNAP2B** which consists of a $C_{18}H_{16}N^+$ cation and a $C_6H_4BrO_3S^-$ anion. The whole molecule of the cation is disordered over two sites; the major component *A* and the minor component *B*, with the refined site-occupancy ratio of 0.733 (1)/0.267 (1). The cation exists in the *E* configuration with respect to the C11═C12 double bond. The naphthalenyl moiety is not planar as indicated by the interplanar angle between the two aromatic C1–C6 and C1/C6–C10 rings being 5.0 (5)° (for the major component *A*) and 5.7 (10)° (for the minor component *B*). The cation is twisted with the dihedral angle between the pyridinium and the two aromatic C1–C6 and C1/C6–C10 rings being 56.3 (5)° and 51.4 (5)°, respectively (for the major component *A*); 52.2 (11)° and 53.4 (11)°, respectively (for the minor component *B*) and the torsion angles C19–C10–C11–C12 = -26.5 (14)° and C11–C12–C13–C17 = -9.3 (15)° for the major component *A*; whereas the corresponding values are -6(2)° and 4(3)° for the minor component *B*. The cation and anion are inclined to each other with interplanar angles of 85.0 (4)° and 71.5 (9)° respectively between the benzene ring and the pyridinium units of the major and minor disorder components.

In the crystal packing (**Fig. 10**), all O atoms of the sulfonate group are involved in weak C—H···O interactions (**Table 39**). The cations and anions are alternately arranged with the cations (both the major *A* and minor *B* components) stacked in an antiparallel manner along the *c* axis and the anions linked together into chains along the same direction. The cations are linked to the anions into chains along the [1 0 2] direction by weak C—H···O interactions (**Table 40**). The crystal structure is further stabilized by C—H···π interactions (**Table 39**). π–π interaction with the distances Cg1···Cg2 = 3.698 (6) Å and Cg1···Cg3 = 3.502 (9) Å are also observed (symmetry code for both Cg···Cg interactions: 1-x, 1-y,-1/2+z); Cg1, Cg2, Cg3 and Cg4 are the centroids of the N1A/C13A–C17A, C1A–C6A, C1B–C6B and C19–C24 rings, respectively. A short Br1···O3 [3.029 (4) Å] contact is also present.

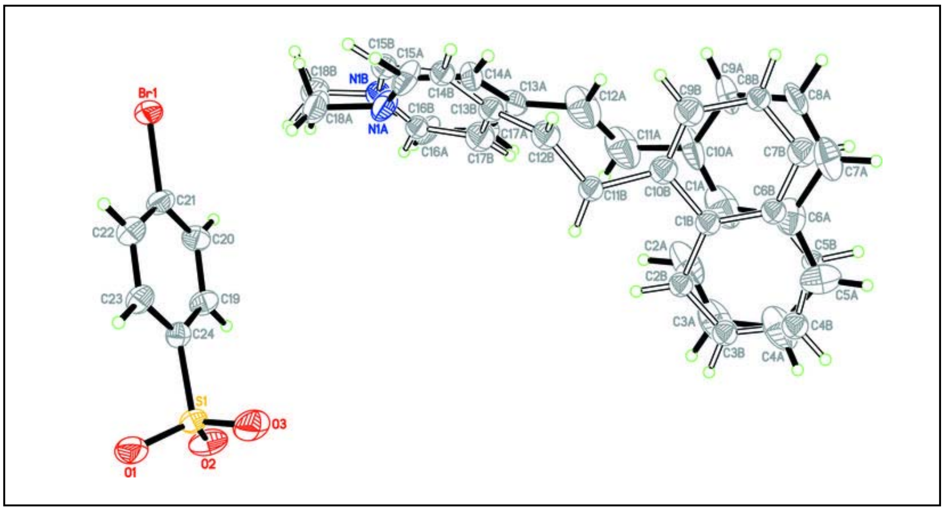
Br1
C21
C22
C20
C23
C19
C24
S1
O3
O1
O2
C15B
C15A
C18B
N1B
C14B
C14A
C13A
C12A
C9B
C9A
C8B
C8A
C18A
N1A
C16B
C13B
C17A
C16A
C17B
C12B
C11A
C10A
C7B
C7A
C11B
C10B
C1A
C6B
C1B
C6A
C2A
C5B
C2B
C5A
C3A
C4B
C3B
C4A

Figure 9 X-ray ORTEP diagram of the compound **PNAP2B**

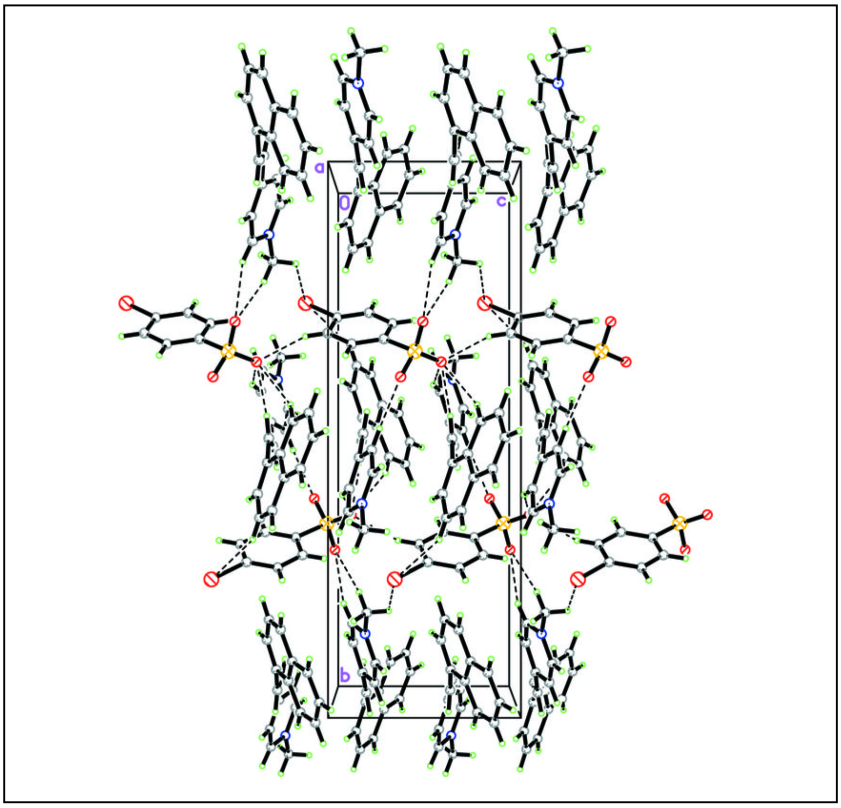

Figure 10 Packing diagram of **PNAP2B** viewed down the *a* axis with weak C—H···O interactions shown as dashed lines.

Table 38 Crystal data of **PNAP2B**

Identification code	**PNAP2B**
Empirical formula	$C_{18}H_{16}N^{+}I^{-}{\cdot}C_6H_4BrO_3S^{-}$
Formula weight	482.38
Temperature	100.0(1) K
Wavelength	0.71073 Å
Crystal system, space group	Orthorhombic, $Pna2_1$
Unit cell dimensions	a = 12.2195(2) Å α = 90 °
	b = 21.9907(4) Å β = 90 °
	c = 7.6256(1) Å γ = 90 °
Volume	2049.12(6) $Å^3$
Z, Calculated density	4, 1.564 Mg/m^3
Absorption coefficient	2.14 mm^{-1}
F(000)	984
Crystal size	0.46 x 0.15 x 0.14 mm
Theta range for data collection	2.5 to 30.0 °
Limiting indices	-12<=h<=17, -30<=k<=25, -10<=l<=10
Reflections collected / unique	15171 / 5563 [*R*(int) = 0.044]
Completeness to theta = 30.00	99.8 %
Max. and min. transmission	0.753 and 0.437
Refinement method	Full-matrix least-squares on F^2
Data / restraints / parameters	5563 / 11 / 326
Goodness-of-fit on F^2	1.029
Final *R* indices [I>2σ(I)]	*R1* = 0.0449, *wR2* = 0.0825
R indices (all data)	*R1* = 0.0762, *wR2* = 0.0938
Largest diff. peak and hole	1.11 and -0.48 e.$Å^3$

Table 39 Bond lengths [Å] and angles [°] for **PNAP2B**

Br1-C21	1.906(4)	C13A-C17A	1.381(14)
S1-O2	1.433(3)	C13A-C14A	1.384(8)
S1-O1	1.437(3)	C14A-C15A	1.357(9)
S1-O3	1.452(3)	C14A-H14A	0.95
S1-C24	1.782(4)	C15A-H15A	0.95
N1A-C15A	1.356(10)	C16A-C17A	1.342(15)
N1A-C16A	1.404(11)	C16A-H16A	0.95
N1A-C18A	1.486(9)	C17A-H17A	0.95
C1A-C6A	1.407(11)	C18A-H18A	0.98
C1A-C10A	1.423(10)	C18A-H18B	0.98
C1A-C2A	1.467(9)	C18A-H18C	0.98
C2A-C3A	1.352(14)	N1B-C16B	1.16(3)
C2A-H2AA	0.95	N1B-C15B	1.40(3)
C3A-C4A	1.391(18)	N1B-C18B	1.51(3)
C3A-H3AA	0.95	C1B-C2B	1.40(2)
C4A-C5A	1.247(19)	C1B-C6B	1.43(3)
C4A-H4AA	0.95	C1B-C10B	1.489(18)
C5A-C6A	1.433(14)	C2B-C3B	1.40(3)
C5A-H5AA	0.95	C2B-H2BA	0.95
C6A-C7A	1.441(13)	C3B-C4B	1.42(3)
C7A-C8A	1.396(11)	C3B-H3BA	0.95
C7A-H7AA	0.95	C4B-C5B	1.64(4)
C8A-C9A	1.396(8)	C4B-H4BA	0.95
C8A-H8AA	0.95	C5B-C6B	1.33(3)
C9A-C10A	1.363(9)	C5B-H5BA	0.95
C9A-H9AA	0.95	C6B-C7B	1.40(4)
C10A-C11A	1.457(9)	C7B-C8B	1.39(2)
C11A-C12A	1.372(9)	C7B-H7BA	0.95
C11A-H11A	0.95	C8B-C9B	1.41(2)
C12A-C13A	1.459(9)	C8B-H8BA	0.95
C12A-H12A	0.95	C9B-C10B	1.31(2)

Table 39 (Continued)

C9A-C8A-H8AA	119.6	C2B-C1B-C10B	122.7(14)
C10A-C9A-C8A	121.3(7)	C6B-C1B-C10B	115.2(16)
C10A-C9A-H9AA	119.4	C1B-C2B-C3B	123.2(17)
C8A-C9A-H9AA	119.4	C1B-C2B-H2BA	118.4
C9A-C10A-C1A	119.1(6)	C3B-C2B-H2BA	118.4
C9A-C10A-C11A	122.5(7)	C2B-C3B-C4B	123(2)
C1A-C10A-C11A	118.3(6)	C2B-C3B-H3BA	118.7
C12A-C11A-C10A	122.4(6)	C4B-C3B-H3BA	118.7
C12A-C11A-H11A	118.8	C3B-C4B-C5B	109.4(19)
C10A-C11A-H11A	118.8	C3B-C4B-H4BA	125.3
C11A-C12A-C13A	122.3(6)	C5B-C4B-H4BA	125.3
C11A-C12A-H12A	118.8	C6B-C5B-C4B	127(3)
C13A-C12A-H12A	118.8	C6B-C5B-H5BA	116.7
C17A-C13A-C14A	116.7(7)	C4B-C5B-H5BA	116.7
C17A-C13A-C12A	124.9(7)	C5B-C6B-C7B	120(3)
C14A-C13A-C12A	118.1(6)	C5B-C6B-C1B	116(3)
C15A-C14A-C13A	121.5(6)	C7B-C6B-C1B	124(2)
C15A-C14A-H14A	119.2	C8B-C7B-C6B	115.9(19)
C13A-C14A-H14A	119.2	C8B-C7B-H7BA	122.1
N1A-C15A-C14A	120.0(6)	C6B-C7B-H7BA	122.1
N1A-C15A-H15A	120.0	C7B-C8B-C9B	121.5(18)
C14A-C15A-H15A	120.0	C7B-C8B-H8BA	119.2
C17A-C16A-N1A	117.5(9)	C9B-C8B-H8BA	119.2
C17A-C16A-H16A	121.2	C10B-C9B-C8B	123.4(16)
N1A-C16A-H16A	121.2	C10B-C9B-H9BA	118.3
C16A-C17A-C13A	123.4(9)	C8B-C9B-H9BA	118.3
C16A-C17A-H17A	118.3	C9B-C10B-C1B	118.6(15)
C13A-C17A-H17A	118.3	C9B-C10B-C11B	125.5(13)
C16B-N1B-C15B	118(2)	C1B-C10B-C11B	115.6(12)
C16B-N1B-C18B	121(2)	C12B-C11B-C10B	117.6(11)
C15B-N1B-C18B	118.5(17)	C12B-C11B-H11B	121.2

Table 39 (Continued)

C2B-C1B-C6B	121.7(17)	C10B-C11B-H11B	121.2
C13B-C12B-C11B	116.8(12)	N1B-C18B-H18F	109.5
C13B-C12B-H12B	121.6	H18D-C18B-H18F	109.5
C11B-C12B-H12B	121.6	H18E-C18B-H18F	109.5
C14B-C13B-C17B	117.3(19)	C20-C19-C24	121.5(3)
C14B-C13B-C12B	115.9(15)	C20-C19-H19A	119.3
C17B-C13B-C12B	125.2(19)	C24-C19-H19A	119.3
C15B-C14B-C13B	122.3(17)	C19-C20-C21	118.2(4)
C15B-C14B-H14B	118.8	C19-C20-H20A	120.9
C13B-C14B-H14B	118.8	C21-C20-H20A	120.9
C14B-C15B-N1B	118.0(17)	C22-C21-C20	121.5(3)
C14B-C15B-H15B	121.0	C22-C21-Br1	119.7(3)
N1B-C15B-H15B	121.0	C20-C21-Br1	118.8(3)
N1B-C16B-C17B	131(3)	C23-C22-C21	119.2(4)
N1B-C16B-H16B	114.3	C23-C22-H22A	120.4
C17B-C16B-H16B	114.3	C21-C22-H22A	120.4
C16B-C17B-C13B	110(2)	C22-C23-C24	120.4(4)
C16B-C17B-H17B	125.2	C22-C23-H23A	119.8
C13B-C17B-H17B	125.2	C24-C23-H23A	119.8
N1B-C18B-H18D	109.5	C19-C24-C23	119.2(4)
N1B-C18B-H18E	109.5	C19-C24-S1	120.6(3)
H18D-C18B-H18E	109.5	C23-C24-S1	120.1(3)

Table 40 Hydrogen-bond geometry [Å, °] of **PNAP2B**

D—H···*A*	D—H	H···*A*	D···*A*	D—H···*A*
C2*A*—H2*AA*···O1$^{\mathrm{i}}$	0.95	2.53	3.392(11)	151
C5*A*—H5*AA*···O2$^{\mathrm{ii}}$	0.95	2.47	3.362(10)	157
C11*A*—H11*A*···O1$^{\mathrm{i}}$	0.95	2.34	3.282(10)	175
C14*A*—H14*A*···O2$^{\mathrm{iii}}$	0.95	2.44	3.373(7)	169
C16*A*—H16*A*···O3$^{\mathrm{iv}}$	0.95	2.49	3.361(11)	153
C17*A*—H17*A*···O1$^{\mathrm{i}}$	0.95	2.35	3.227(14)	153
C18*A*—H18*A*···O3$^{\mathrm{iv}}$	0.98	2.57	3.501(8)	159
C19—H19*A*···O2	0.95	2.56	2.930(5)	103
C20—H20*A*···O1$^{\mathrm{iv}}$	0.95	2.34	3.252(5)	161
C22—H22*A*···O3$^{\mathrm{v}}$	0.95	2.51	3.274(6)	137
C4*A*—H4*AA*···*Cg*2$^{\mathrm{vi}}$	0.95	2.84	3.659(14)	145
C7*A*—H7*AA*···*Cg*4$^{\mathrm{vii}}$	0.95	2.88	3.657(9)	140
C4*B*—H4*BA*···*Cg*2$^{\mathrm{vi}}$	0.95	2.90	3.59(2)	130

Symmetry codes: (i) *x*-1/2, -*y*+3/2, *z*-1; (ii) –*x*+1/2, *y*-1/2, *z*-1/2; (iii) -*x*+3/2, *y*-1/2, *z*-1/2; (iv) *x*, *y*, *z*-1; (v) *x*+1/2, -*y*+3/2, *z*; (vi) -*x*, -*y*+1, *z*+1/2 ; (vii) -*x*+1, -*y*+1, *z*-1/2. *Cg*2 and *Cg*4 are the centroids of the C1*A*–C6*A* and C19–C24 rings, respectively.

3.4.10 (*E*)-1-methyl-4-(2-(naphthalen-1-yl)vinyl)pyridinium 4-aminobenzenesulfonate (PNAP2N)

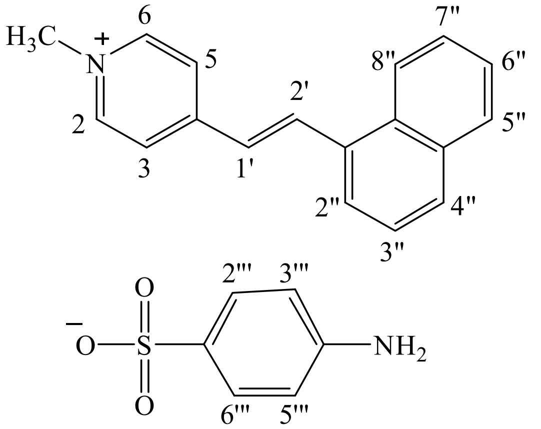

PNAP2N

Compound **PNAP2N** was obtained as brown crystal (45% yield), mp. 240-241 °C. The UV-Vis absorption spectra (**Fig. 61**) showed maximum bands at 220.92, 253.36 and 347.38 nm. The FT-IR spectrum (**Fig. 62**) exhibited stretching vibrations of C=C (1618 cm^{-1}) and S=O in sulfonates (1195 cm^{-1}).

The ^{1}H NMR spectrum (**Fig. 63,** see **Table 41**) showed two fragments of cationic and anionic parts. The former showed characteristic of *trans*-disubstituted double bonds at δ 7.56 (1H, *d*, J = 16.2 Hz, H-1′) and δ 8.80 (1H, *d*, J = 16.2 Hz, H-2′). The *singlet* signal at δ 4.32 (3H) was assigned as *N*-CH_3. Equivalent protons of *p*-disubstituted aromatic appeared as two *doublet* signals at δ 8.91 (2H, J = 6.9 Hz, H-2, H-6) and δ 8.42 (2H, J = 6.9 Hz, H-3, H-5). Resonances of aromatic protons of naphthalenyl part H-2″ to H-8″ were also shown at δ 7.97 (*d*, J = 8.4 Hz), δ 8.05 (*t*, J = 8.4 Hz), δ 7.97 (*d*, J = 8.4 Hz), δ 8.01 (*d*, J = 6.6 Hz), δ 7.63 (*t*, J = 6.6 Hz), δ 7.61 (*t*, J = 6.6 Hz) and δ 8.54 (*t*, J = 6.6 Hz), respectively. ^{1}H NMR spectrum also showed resonances of aromatic protons of anionic part at δ 7.35 (2H, *d*, J = 8.4 Hz, H-2‴, H-6‴) and δ 6.48 (2H, *d*, J = 8.4 Hz, H-3‴, H-5‴). The *singlet* signal of 4‴-NH_2 was observed at δ 5.03 (2H). These observations confirmed that **PNAP2N** is (*E*)-1-methyl-4-(2-(naphthalen-1-yl)vinyl)pyridinium 4-aminobenzenesulfonate.

Table 41 ^{1}H NMR of compound **PNAP2N**

Position	**δ_H (ppm), *mult*, *J* (Hz)**
1-CH_3	4.32 (3H, *s*)
2	8.91 (2H, *d*, 6.9)
6	
3	8.42 (2H, *d*, 6.9)
5	
1′	7.56 (1H, *d*, 16.2)
2′	8.80 (1H, *d*, 16.2)
2″	7.97 (1H, *d*, 8.4)
3″	8.04 (1H, *t*, 8.4)
4″	7.97 (1H, *d*, 8.4)
5″	8.01 (1H, *d*, 6.6)
6″	7.63 (1H, *t*, 6.6)
7″	7.61 (1H, *t*, 6.6)
8″	8.54 (1H, *t*, 6.6)
2‴	7.35 (2H, *d*, 8.4)
6‴	
3‴	6.48 (2H, *d*, 8.4)
5‴	
4‴-NH_2	5.03 (3H, *br s*)

3.4.11 (*E*)-1-methyl-2-(2-(naphthalen-2-yl)vinyl)pyridinium 4-methylbenzenesulfonate (PNAP3M)

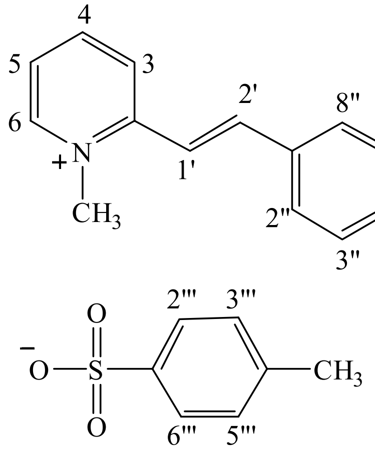

PNAP3M

Compound **PNAP3M** was obtained as a yellow solid (81% yield), mp. 176-177 °C. The UV-Vis absorption bands (**Fig. 64**) were shown at 223.57 and 342.24 nm. The FT-IR spectrum (**Fig. 65**) exhibited stretching vibrations of C=C (1610 cm^{-1}) and S=O in sulfonates (1186 cm^{-1}).

The ^{1}H NMR spectrum (**Fig. 66,** see **Table 42**) showed two fragments of cationic and anionic parts. The former showed characteristic of *trans*-disubstituted double bonds at δ 7.74 (1H, *d*, J = 15.9 Hz, H-1′) and δ 8.11 (1H, *d*, J = 15.9 Hz, H-2′). The *singlet* signals at δ 4.42 (3H) was assigned as *N*-CH_3. Four signals of 2-substituted pyridinium part pattern at δ 8.58 (1H, *d*, J = 7.8 Hz), δ 8.52 (1H, *t*, J = 7.8 Hz), δ 8.02 (1H, *t*, J = 7.8 Hz) and δ 8.93 (1H, *d*, J = 7.8 Hz) were assigned to be H-3, H-4, H-5 and H-6, respectively. Resonances of aromatic protons of naphthalenyl part H-2″ to H-8″ were also shown at δ 7.88 (*d*, J = 6.9 Hz), δ 7.93 (*d*, J =6.9 Hz), δ 8.03 (*d*, J = 8.7 Hz), δ 7.61 (*t*, J = 8.7 Hz), δ 7.60 (*t*, J = 8.7 Hz), δ 7.98 (*d*, J = 8.7 Hz) and δ 8.30 (*s*, 3H), respectively. ^{1}H NMR spectrum showed signals of anionic part. Equivalent protons of *p*-disubstituted aromatic appeared as two *doublets* at δ 7.50 (2H, J = 8.1 Hz, H-2‴, H-6‴) and δ 7.11 (2H, J = 8.1 Hz, H-3‴, H-5‴). The *singlet* signal of 4‴-CH_3 was observed at δ 2.29 (3H). These spectroscopic data confirmed that **PNAP3M** is (*E*)-1-methyl-2-(2-(naphthalen-2-yl)vinyl)pyridinium 4-methylbenzenesulfonate.

Table 42 ^{1}H NMR of compound **PNAP3M**

Position	δ_H **(ppm),** ***mult*****,** ***J*** **(Hz)**
1-CH_3	4.42 (3H, *s*)
3	8.58 (1H, *d*, 7.8)
4	8.52 (1H, *t*, 7.8)
5	8.02 (1H, *t*, 7.8)
6	8.93 (1H, *d*, 7.8)
1′	7.74 (1H, *d*, 15.9)
2′	8.11 (1H, *d*, 15.9)
2″	7.88 (1H, *d*, 6.9 Hz)
3″	7.93 (1H, *d*, 6.9 Hz)
4″	8.03 (1H, *d*, 8.7 Hz)
5″	7.61 (1H, *t*, 8.7 Hz)
6″	7.60 (1H, *t*, 8.7 Hz)
7″	7.98 (1H, *d*, 8.7 Hz)
8″	8.30 (1H, *s*)
2‴ 6‴	7.50 (2H, *d*, 8.1)
3‴ 5‴	7.11 (2H, *d*, 8.1)
4‴-CH_3	2.29 (3H, *s*)

3.4.12 (*E*)-1-methyl-2-(2-(naphthalen-2-yl)vinyl)pyridinium 4-methoxybenzenesulfonate (PNAP3O)

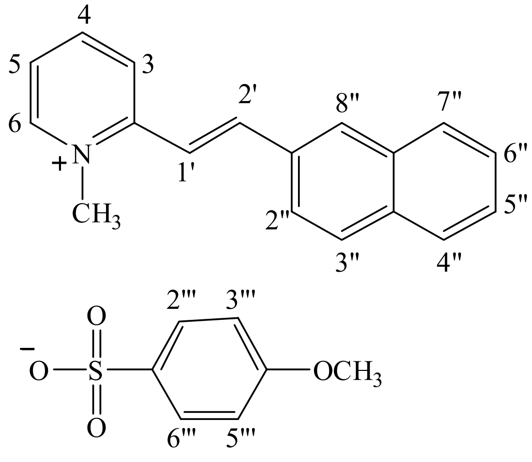

PNAP3O

Compound **PNAP3O** was obtained as a yellow solid (67% yield), mp. 232-234 °C. The UV-Vis absorption bands (**Fig. 67**) were shown at 228.21 and 341.58 nm. The FT-IR spectrum (**Fig. 68**) exhibited stretching vibrations of C=C (1601 cm^{-1}) and S=O in sulfonates (1186 cm^{-1}).

The ^{1}H NMR spectrum (**Fig. 69,** see **Table 43**) showed two fragments of cationic and anionic parts. The former showed characteristic of *trans*-disubstituted double bonds at δ 7.74 (1H, *d*, J = 15.9 Hz, H-1′) and δ 8.09 (1H, *d*, J = 15.9 Hz, H-2′). The *singlet* signals at δ 4.45 (3H) was assigned as *N*-CH$_3$. Four signals of 2-substituted pyridinium part pattern at δ 8.58 (1H, *d*, J = 8.4 Hz), δ 8.51 (1H, *t*, J = 8.4 Hz), δ 8.08 (1H, *d*, J = 8.4 Hz) and δ 8.96 (1H, *d*, J = 8.4 Hz) were assigned to be H-3, H-4, H-5 and H-6, respectively. Resonances of aromatic protons of naphthalenyl part H-2″ to H-8″ were also shown at δ 7.89 (*d*, J = 7.8 Hz), δ 7.91 (*d*, J = 7.8 Hz), δ 7.99 (*d*, J = 8.1 Hz), δ 7.62 (*t*, J = 8.1 Hz), δ 7.60 (*t*, J = 8.1 Hz), δ 7.99 (*d*, J = 8.1 Hz) and δ 8.28 (*s*, 3H), respectively. ^{1}H NMR spectrum showed signals of anionic part. Equivalent protons of *p*-disubstituted aromatic appeared as two *doublets* at δ 7.61 (2H, J = 8.4 Hz, H-2‴, H-6‴) and δ 6.83 (2H, J = 8.4 Hz, H-3‴, H-5‴). The *singlet* signal of 4‴-OCH$_3$ was observed at δ 3.76 (3H). These spectroscopic data confirmed that **PNAP3O** is (*E*)-1-methyl-2-(2-(naphthalen-2-yl)vinyl)pyridinium 4-methoxybenzenesulfonate.

Table 43 ^{1}H NMR of compound **PNAP3O**

Position	**δ_H (ppm), *mult*, *J* (Hz)**
1-CH_3	4.45 (3H, *s*)
3	8.58 (1H, *d*, 8.4)
4	8.51 (1H, *t*, 8.4)
5	8.08 (1H, *d*, 8.4)
6	8.96 (1H, *d*, 8.4)
1′	7.74 (1H, *d*, 15.9)
2′	8.09 (1H, *d*, 15.9)
2″	7.89 (1H, *d*, 7.8 Hz)
3″	7.91 (1H, *d*, 7.8 Hz)
4″	7.99 (1H, *d*, 8.1 Hz)
5″	7.62 (1H, *t*, 8.1 Hz)
6″	7.60 (1H, *t*, 8.1 Hz)
7″	7.98 (1H, *d*, 8.1 Hz)
8″	8.28 (1H, *s*)
2‴ 6‴	7.61 (2H, *d*, 8.4)
3‴ 5‴	6.83 (2H, *d*, 8.4)
4‴-OCH_3	3.76 (3H, *s*)

3.4.13 (*E*)-1-methyl-2-(2-(naphthalen-2-yl)vinyl)pyridinium 4-chlorobenzenesulfonate (PNAP3C)

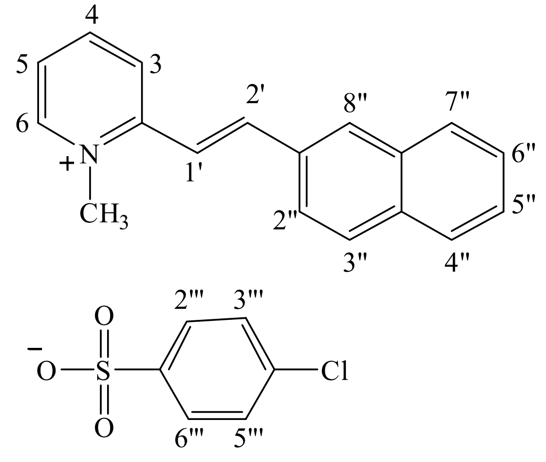

PNAP3C

Compound **PNAP3C** was obtained as a yellow solid (73% yield), mp. >300 °C. The UV-Vis absorption bands (**Fig. 70**) were shown at 222.91 and 340.92 nm. The IR spectrum (**Fig. 71**) exhibited stretching vibrations of C=C (1618 cm^{-1}) and S=O in sulfonates (1176 cm^{-1}).

The ^{1}H NMR spectrum (**Fig. 72, **see **Table 44**) showed two fragments of cationic and anionic parts. The former showed characteristic of *trans*-disubstituted double bonds at δ 7.71 (1H, *d*, J = 15.9 Hz, H-1′) and δ 7.98 (1H, *d*, J = 15.9 Hz, H-2′). The *singlet* signals at δ 4.51 (3H) was assigned as *N*-CH$_3$. Four signals of 2-substituted pyridinium part pattern at δ 8.54 (1H, *d*, J = 8.4 Hz), δ 8.48 (1H, *t*, J = 8.4 Hz), δ 8.03 (1H, *t*, J = 8.4 Hz) and δ 9.00 (1H, *d*, J = 8.4 Hz) were assigned to be H-3, H-4, H-5 and H-6, respectively. Resonances of aromatic protons of naphthalenyl part H-2″ to H-8″ were also shown at δ 7.86 (*d*, J = 8.1 Hz), δ 7.88 (*d*, J = 8.1 Hz), δ 7.91 (*d*, J = 7.5 Hz), δ 7.57 (*t*, J = 7.5 Hz), δ 7.58 (*t*, J = 7.5 Hz), δ 7.90 (*d*, J = 7.5 Hz) and δ 8.24 (*s*, 3H), respectively. ^{1}H NMR spectrum showed signals of anionic part. Equivalent protons of *p*-disubstituted aromatic appeared as two *doublets* at δ 7.77 (2H, J = 8.4 Hz, H-2‴, H-6‴) and δ 7.31 (2H, J = 8.4 Hz, H-3‴, H-5‴). These spectroscopic data confirmed that **PNAP3C** is (*E*)-1-methyl-2-(2-(naphthalen-2-yl)vinyl)pyridinium 4-chlorobenzenesulfonate.

Table 44 ^{1}H NMR of compound **PNAP3C**

Position	**δ_H (ppm), *mult*, *J* (Hz)**
1-CH_3	4.42 (3H, *s*)
3	8.54 (1H, *d*, 8.4)
4	8.48 (1H, *t*, 8.4)
5	8.03 (1H, *t*, 8.4)
6	9.00 (1H, *d*, 8.4)
1′	7.71 (1H, *d*, 15.9)
2′	7.98 (1H, *d*, 15.9)
2″	7.86 (1H, *d*, 8.1 Hz)
3″	7.88 (1H, *d*, 8.1 Hz)
4″	7.91 (1H, *d*, 7.5 Hz)
5″	7.57 (1H, *t*, 7.5 Hz)
6″	7.58 (1H, *t*, 7.5 Hz)
7″	7.90 (1H, *t*, 7.5 Hz)
8″	8.24 (1H, *s*)
2‴	7.77 (2H, *d*, 8.4)
6‴	
3‴	7.31 (2H, *d*, 8.4)
5‴	

3.4.14 (*E*)-1-methyl-2-(2-(naphthalen-2-yl)vinyl)pyridinium 4-bromobenzenesulfonate (PNAP3B)

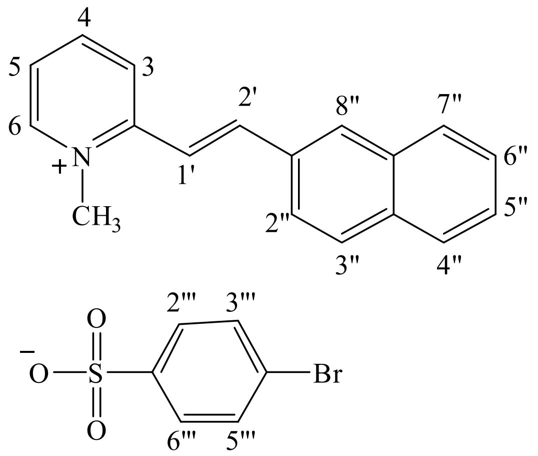

PNAP3B

Compound **PNAP3B** was obtained as a yellow solid (86% yield), mp. 249-251 °C. The UV-Vis absorption bands (**Fig. 73**) were shown at 226.23 and 342.24 nm. The FT-IR spectrum (**Fig. 74**) exhibited stretching vibrations of C=C (1609 cm^{-1}) and S=O in sulfonates (1215 cm^{-1}).

The ^{1}H NMR spectrum (**Fig. 75,** see **Table 45**) showed two fragments of cationic and anionic parts. The former showed characteristic of *trans*-disubstituted double bonds at δ 7.75 (1H, *d*, *J* = 15.3 Hz, H-1′) and δ 8.11 (1H, *d*, *J* = 15.3 Hz, H-2′). The *singlet* signals at δ 4.44 (3H) was assigned as *N*-$\mathrm{CH_3}$. Four signals of 2-substituted pyridinium part pattern at δ 8.59 (1H, *d*, *J* = 8.4 Hz), δ 8.52 (1H, *t*, *J* = 8.4 Hz), δ 8.02 (1H, *d*, *J* = 8.4 Hz) and δ 8.95 (1H, *d*, *J* = 8.4 Hz) were assigned to be H-3, H-4, H-5 and H-6, respectively. Resonances of aromatic protons of naphthalenyl part H-2″ to H-8″ were also shown at δ 7.90-8.05 (*m*, 3H, H-2″ – H-4″ and H-7″), δ 7.61 (*d*, *J* = 5.7 Hz, H-5″), δ 7.60 (*d*, *J* = 5.7 Hz, H-6″) and δ 8.31 (*s*, 3H, H-8″), respectively. ^{1}H NMR spectrum showed signals of anionic part. Equivalent protons of *p*-disubstituted aromatic appeared as two *doublets* at δ 7.57 (2H, *J* = 8.7 Hz, H-2‴, H-6‴) and δ 7.50 (2H, *J* = 8.7 Hz, H-3‴, H-5‴). These spectroscopic data confirmed that **PNAP3B** is (*E*)-1-methyl-2-(2-(naphthalen-2-yl)vinyl)pyridinium 4-bromobenzenesulfonate.

Table 45 ^{1}H NMR of compound **PNAP3B**

Position	**δ_H (ppm), *mult*, *J* (Hz)**
1-CH_3	4.44 (3H, *s*)
3	8.59 (1H, *d*, 8.4)
4	8.52 (1H, *t*, 8.4)
5	8.02 (1H, *d*, 8.4)
6	8.95 (1H, *d*, 8.4)
1′	7.75 (1H, *d*, 15.3)
2′	8.11 (1H, *d*, 15.3)
2″	7.90-8.05 (3H, *m*)
3″	
4″	
5″	7.61 (1H, *d*, 5.7 Hz)
6″	7.60 (1H, *d*, 5.7 Hz)
7″	7.90-8.05 (1H, *m*)
8″	8.31 (1H, *s*)
2‴	7.57 (2H, *d*, 8.7)
6‴	
3‴	7.50 (2H, *d*, 8.7)
5‴	

3.4.15 (*E*)-1-methyl-2-(2-(naphthalen-2-yl)vinyl)pyridinium 4-aminobenzenesulfonate (PNAP3N)

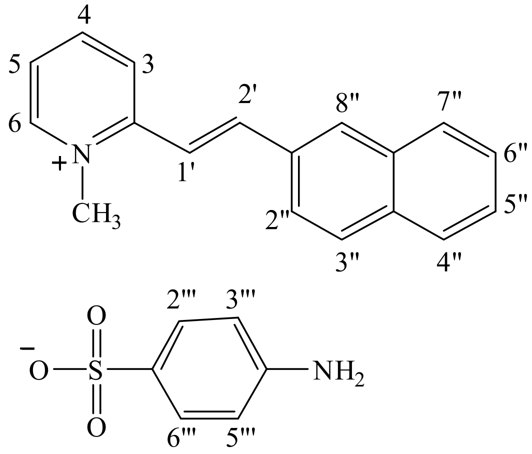

PNAP3N

Compound **PNAP3N** was obtained as a yellow solid (60% yield), mp. 215-217 °C. The UV-Vis absorption bands (**Fig. 76**) were shown at 226.89 and 341.58 nm. The FT-IR spectrum (**Fig. 77**) exhibited stretching vibrations of C=C (1600 cm^{-1}) and S=O in sulfonates (1197 cm^{-1}).

The ^{1}H NMR spectrum (**Fig. 78,** see **Table 46**) showed two fragments of cationic and anionic parts. The former showed characteristic of *trans*-disubstituted double bonds at δ 7.74 (1H, *d*, *J* = 15.9 Hz, H-1′) and δ 8.11 (1H, *d*, *J* = 15.9 Hz, H-2′). The *singlet* signals at δ 4.43 (3H) was assigned as *N*-CH_3. Four signals of 2-substituted pyridinium part pattern at δ 8.58 (1H, *d*, *J* = 8.4 Hz), δ 8.54 (1H, *t*, *J* = 8.4 Hz), δ 8.10 (1H, *d*, *J* = 8.4 Hz) and δ 8.94 (1H, *d*, *J* = 8.4 Hz) were assigned to be H-3, H-4, H-5 and H-6, respectively. Resonances of aromatic protons of naphthalenyl part H-2″ to H-8″ were also shown at δ 7.93 (*d*, *J* = 8.7 Hz), δ 7.97 (*d*, *J* = 8.7 Hz), δ 8.01 (*d*, *J* = 9.3 Hz), δ 7.60 (*d*, *J* = 9.3 Hz), δ 7.59 (*d*, *J* = 9.3 Hz), δ 7.98 (*d*, *J* = 9.3 Hz) and δ 8.30 (*s*, 3H), respectively. ^{1}H NMR spectrum showed signals of anionic part. Equivalent protons of *p*-disubstituted aromatic appeared as two *doublets* at δ 7.31 (2H, *J* = 8.4 Hz, H-2‴, H-6‴) and δ 6.46 (2H, *J* = 8.4 Hz, H-3‴, H-5‴). The *singlet* signal of 4‴-NH_2 was observed at δ 5.10 (*br s*, 2H). These spectroscopic data confirmed that **PNAP3N** is (*E*)-1-methyl-2-(2-(naphthalen-2-yl)vinyl)pyridinium 4-aminobenzenesulfonate.

Table 46 ^{1}H NMR of compound **PNAP3N**

Position	δ_H **(ppm),** ***mult*****,** ***J*** **(Hz)**
1-CH_3	4.43 (3H, *s*)
3	8.58 (1H, *d*, 8.4)
4	8.54 (1H, *t*, 8.4)
5	8.10 (1H, *d*, 8.4)
6	8.94 (1H, *d*, 8.4)
1′	7.74 (1H, *d*, 15.9)
2′	8.11 (1H, *d*, 15.9)
2″	7.93 (1H, *d*, 8.7 Hz)
3″	7.97 (1H, *d*, 8.7 Hz)
4″	8.01 (1H, *d*, 9.3 Hz)
5″	7.60 (1H, *d*, 9.3 Hz)
6″	7.59 (1H, *d*, 9.3 Hz)
7″	7.98 (1H, *d*, 9.3 Hz)
8″	8.30 (1H, *s*)
2‴ 6‴	7.31 (2H, *d*, 8.4)
3‴ 5‴	6.46 (2H, *d*, 8.4)
4‴-NH_2	5.10 (2H, *br s*)

3.4.16 (*E*)-1-methyl-4-(2-(naphthalen-2-yl)vinyl)pyridinium 4-methylbenzenesulfonate (PNAP4M)

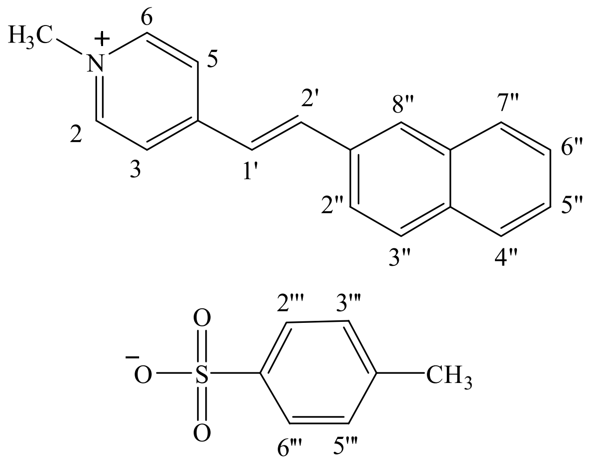

PNAP4M

Compound **PNAP4M** was obtained as yellow solid (74% yield), mp. 212-214°C. The UV-Vis absorption spectra (**Fig. 79**) showed maximum bands at 222.91 and 356.83 nm. The FT-IR spectrum (**Fig. 80**) exhibited stretching vibrations of C=C (1618 cm^{-1}) and S=O in sulfonates (1196 cm^{-1}).

The ^{1}H NMR spectrum (**Fig. 81,** see **Table 47**) showed two fragments of cationic and anionic parts. The former showed characteristic of *trans*-disubstituted double bonds at δ 7.45 (1H, *d*, J = 16.2 Hz, H-1′) and δ 8.06 (1H, *d*, J = 16.2 Hz, H-2′). The *singlet* signal at δ 4.35 (3H) was assigned as N-CH$_3$. Equivalent protons of *p*-disubstituted aromatic appeared as two *doublet* signals at δ 8.85 (2H, J = 6.3 Hz, H-2, H-6) and δ 8.20 (2H, J = 6.3 Hz, H-3, H-5). Resonances of aromatic protons of naphthalenyl part H-2″ to H-8″ were also shown at δ 7.56 (*d*, J = 8.4 Hz), δ 7.55 (*d*, J = 8.4 Hz), δ 7.78 (*d*, J = 6.3 Hz), δ 7.93 (*t*, J = 6.3 Hz), δ 7.92 (*t*, J = 6.3 Hz), δ 7.82 (*d*, J = 6.3 Hz) and δ 8.15 (*s*, 1H), respectively. ^{1}H NMR spectrum also showed resonances of aromatic protons of anionic part at δ 7.64 (2H, *d*, J = 8.1 Hz, H-2‴, H-6‴) and δ 7.11 (2H, *d*, J = 8.1 Hz, H-3‴, H-5‴). The *singlet* signal of 4‴-CH$_3$ was observed at δ 2.32 (3H). These observations confirmed that **PNAP4M** is (*E*)-1-methyl-4-(2-(naphthalen-2-yl)vinyl)pyridinium 4-methylbenzenesulfonate.

Table 47 ^{1}H NMR of compound **PNAP4M**

Position	**δ_H (ppm), *mult*, *J* (Hz)**
1-CH_3	4.35 (3H, *s*)
2	8.85 (2H, *d*, 6.3)
6	
3	8.20 (2H, *d*, 6.3)
5	
1′	7.45 (1H, *d*, 16.2)
2′	8.06 (1H, *d*, 16.2)
2″	7.56 (1H, *d*, 8.4 Hz)
3″	7.55 (1H, *d*, 8.4 Hz)
4″	7.78 (1H, *d*, 6.3 Hz)
5″	7.93 (1H, *t*, 6.3 Hz)
6″	7.92 (1H, *t*, 6.3 Hz)
7″	7.82 (1H, *t*, 6.3 Hz)
8″	8.15 (1H, *s*)
2‴	7.64 (2H, *d*, 8.1)
6‴	
3‴	7.11 (2H, *d*, 8.1)
5‴	
4‴-CH_3	2.32 (3H, *s*)

3.4.17 (*E*)-1-methyl-4-(2-(naphthalen-2-yl)vinyl)pyridinium 4-methoxybenzenesulfonate (PNAP4O)

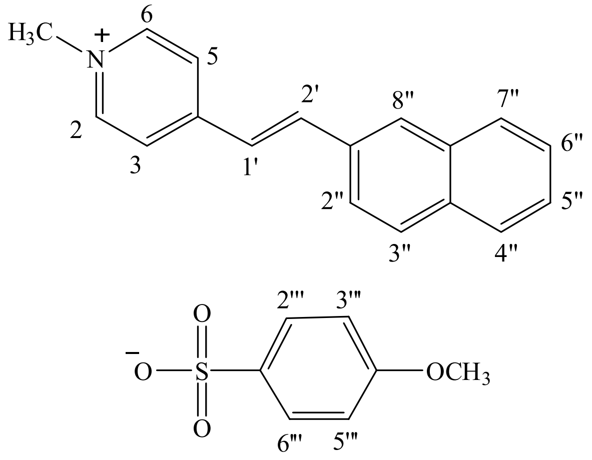

PNAP4O

Compound **PNAP4O** was obtained as yellow solid (83% yield), mp. 203-204°C. The UV-Vis absorption spectra (**Fig. 82**) showed maximum bands at 232.19 and 356.17 nm. The FT-IR spectrum (**Fig. 83**) exhibited stretching vibrations of C=C (1618 cm^{-1}), C-O in OCH$_3$ (1190 cm^{-1}) and S=O in sulfonates (1208 cm^{-1}).

The ^{1}H NMR spectrum (**Fig. 84,** see **Table 48**) showed two fragments of cationic and anionic parts. The former showed characteristic of *trans*-disubstituted double bonds at δ 7.58 (1H, *d*, J = 13.8 Hz, H-1′) and δ 8.15 (1H, *d*, J = 13.8 Hz, H-2′). The *singlet* signal at δ 4.32 (3H) was assigned as *N*-CH$_3$. Equivalent protons of *p*-disubstituted aromatic appeared as two *doublet* signals at δ 8.89 (2H, J = 6.9 Hz, H-2, H-6) and δ 8.24 (2H, J = 6.3 Hz, H-3, H-5). Resonances of aromatic protons of naphthalenyl part H-2″ to H-8″ were also shown at δ 7.56 (*d*, J = 8.7 Hz, H-2″), δ 7.59 (*d*, J = 8.7 Hz, H-3″), δ 7.78-7.98 (*m*, 4H, H-4″-H-7″) and δ 8.12 (*s*, 1H), respectively. ^{1}H NMR spectrum also showed resonances of aromatic protons of anionic part at δ 7.63 (2H, *d*, J = 8.7 Hz, H-2‴, H-6‴) and δ 6.82 (2H, *d*, J = 8.7 Hz, H-3‴, H-5‴). The *singlet* signal of 4‴-OCH$_3$ was observed at δ 3.77 (3H). These observations confirmed that **PNAP4O** is (*E*)-1-methyl-4-(2-(naphthalen-2-yl)vinyl)pyridinium 4-methoxybenzenesulfonate.

Table 48 ^{1}H NMR of compound **PNAP4O**

Position	***δ*$_H$ (ppm), *mult*, *J* (Hz)**
1-CH_3	4.32 (3H, *s*)
2 6	8.89 (2H, *d*, 6.9)
3 5	8.24 (2H, *d*, 6.9)
1′	7.58 (1H, *d*, 13.8)
2′	8.15 (1H, *d*, 13.8)
2″	7.56 (1H, *d*, 8.7 Hz)
3″	7.59 (1H, *d*, 8.7 Hz)
4″ 5″ 6″ 7″	7.78-7.98 (4H, *m*)
8″	8.12 (1H, *s*)
2‴ 6‴	7.63 (2H, *d*, 8.7)
3‴ 5‴	6.82 (2H, *d*, 8.7)
4‴-OCH_3	3.77 (3H, *s*)

3.4.18 (*E*)-1-methyl-4-(2-(naphthalen-2-yl)vinyl)pyridinium 4-chlorobenzenesulfonate (PNAP4C)

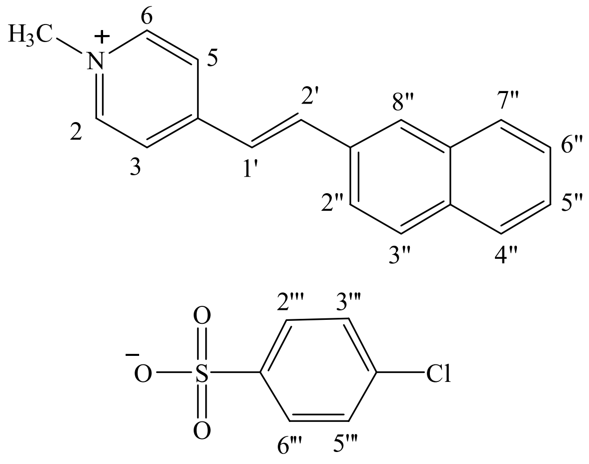

PNAP4C

Compound **PNAP4C** was obtained as yellow solid (79% yield), mp. 260-261°C. The UV-Vis absorption spectra (**Fig. 85**) showed maximum bands at 223.57 and 355.50 nm. The FT-IR spectrum (**Fig. 86**) exhibited stretching vibrations of C=C (1618 cm^{-1}) and S=O in sulfonates (1385 cm^{-1}).

The ^{1}H NMR spectrum (**Fig. 87,** see **Table 49**) showed two fragments of cationic and anionic parts. The former showed characteristic of *trans*-disubstituted double bonds at δ 7.52 (1H, *d*, J = 15.9 Hz, H-1′) and δ 8.08 (1H, *d*, J = 15.9 Hz, H-2′). The *singlet* signal at δ 4.37 (3H) was assigned as N-CH$_3$. Equivalent protons of *p*-disubstituted aromatic appeared as two *doublet* signals at δ 8.89 (2H, J = 6.9 Hz, H-2, H-6) and δ 8.22 (2H, J = 6.9 Hz, H-3, H-5). Resonances of aromatic protons of naphthalenyl part H-2″ to H-8″ were also shown at δ 7.56 (*d*, J = 7.8 Hz), δ 7.50 (*d*, J = 7.8 Hz), δ 7.82 (*d*, J = 9.0 Hz), δ 7.92 (*t*, J = 9.0 Hz), δ 7.84 (*t*, J = 9.0 Hz), δ 7.89 (*d*, J = 9.0 Hz) and δ 8.16 (*s*, 1H), respectively. ^{1}H NMR spectrum also showed resonances of aromatic protons of anionic part at δ 7.76 (2H, *d*, J = 8.4 Hz, H-2‴, H-6‴) and δ 7.31 (2H, *d*, J = 8.4 Hz, H-3‴, H-5‴). These observations confirmed that **PNAP4C** is (*E*)-1-methyl-4-(2-(naphthalen-2-yl)vinyl)pyridinium 4-chlorobenzene sulfonate.

Table 49 ^{1}H NMR of compound **PNAP4C**

Position	**δ_H (ppm), *mult*, *J* (Hz)**
1-CH_3	4.38 (3H, *s*)
2	8.89 (2H, *d*, 6.9)
6	
3	8.22 (2H, *d*, 6.9)
5	
1′	7.52 (1H, *d*, 15.9)
2′	8.08 (1H, *d*, 15.9)
2″	7.56 (1H, *d*, 7.8 Hz)
3″	7.50 (1H, *d*, 7.8 Hz)
4″	7.82 (1H, *d*, 9.0 Hz)
5″	7.92 (1H, *t*, 9.0 Hz)
6″	7.84 (1H, *t*, 9.0 Hz)
7″	7.89 (1H, *d*, 9.0 Hz)
8″	8.16 (1H, *s*)
2‴	7.76 (2H, *d*, 8.4)
6‴	
3‴	7.31 (2H, *d*, 8.4)
5‴	

3.4.19 (*E*)-1-methyl-4-(2-(naphthalen-2-yl)vinyl)pyridinium 4-bromobenzenesulfonate (PNAP4B)

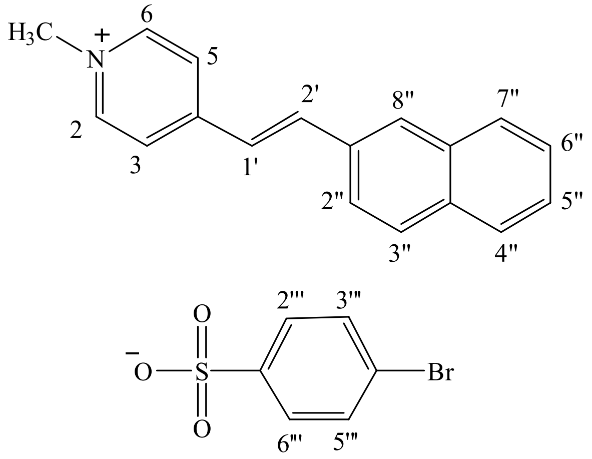

PNAP4B

Compound **PNAP4B** was obtained as yellow solid (89% yield), mp. 235-237 °C. The UV-Vis absorption spectra (**Fig. 88**) showed maximum bands at 226.89 and 356.17 nm. The FT-IR spectrum (**Fig. 89**) exhibited stretching vibrations of C=C (1617 cm^{-1}) and S=O in sulfonates (1219 cm^{-1}).

The ^{1}H NMR spectrum (**Fig. 90,** see **Table 50**) showed two fragments of cationic and anionic parts. The former showed characteristic of *trans*-disubstituted double bonds at δ 7.50 (1H, *d*, J = 15.6 Hz, H-1′) and δ 8.11 (1H, *d*, J = 15.6 Hz, H-2′). The *singlet* signal at δ 4.34 (3H) was assigned as *N*-CH$_3$. Equivalent protons of *p*-disubstituted aromatic appeared as two *doublet* signals at δ 8.89 (2H, J = 6.6 Hz, H-2, H-6) and δ 8.23 (2H, J = 6.6 Hz, H-3, H-5). Resonances of aromatic protons of naphthalenyl part H-2″ to H-8″ were also shown at δ 7.57 (*d*, J = 7.2 Hz), δ 7.53 (*d*, J = 7.2 Hz), δ 7.90 (*d*, J = 6.6 Hz), δ 7.94 (*t*, J = 6.6 Hz), δ 7.82 (*t*, J = 6.6 Hz), δ 7.92 (*d*, J = 6.6 Hz) and δ 8.16 (*s*, 1H), respectively. ^{1}H NMR spectrum also showed resonances of aromatic protons of anionic part at δ 7.65 (2H, *d*, J = 7.8 Hz, H-2‴, H-6‴) and δ 7.46 (2H, *d*, J = 7.8 Hz, H-3‴, H-5‴). These observations confirmed that **PNAP4B** is (*E*)-1-methyl-4-(2-(naphthalen-2-yl)vinyl)pyridinium 4-bromobenzene sulfonate.

Table 50 ^{1}H NMR of compound **PNAP4B**

Position	***δ*$_H$ (ppm), *mult*, *J* (Hz)**
1-CH$_3$	4.34 (3H, *s*)
2 6	8.89 (2H, *d*, 6.6)
3 5	8.23 (2H, *d*, 6.6)
1′	7.50 (1H, *d*, 15.6)
2′	8.11 (1H, *d*, 15.6)
2″	7.57 (1H, *d*, 7.2 Hz)
3″	7.53 (1H, *d*, 7.2 Hz)
4″	7.90 (1H, *d*, 6.6 Hz)
5″	7.94 (1H, *t*, 6.6 Hz)
6″	7.82 (1H, *t*, 6.6 Hz)
7″	7.92 (1H, *d*, 6.6 Hz)
8″	8.16 (1H, *s*)
2‴ 6‴	7.65 (2H, *d*, 7.8)
3‴ 5‴	7.46 (2H, *d*, 7.8)

3.4.20 (*E*)-1-methyl-4-(2-(naphthalen-2-yl)vinyl)pyridinium 4-aminobenzenesulfonate (PNAP4N)

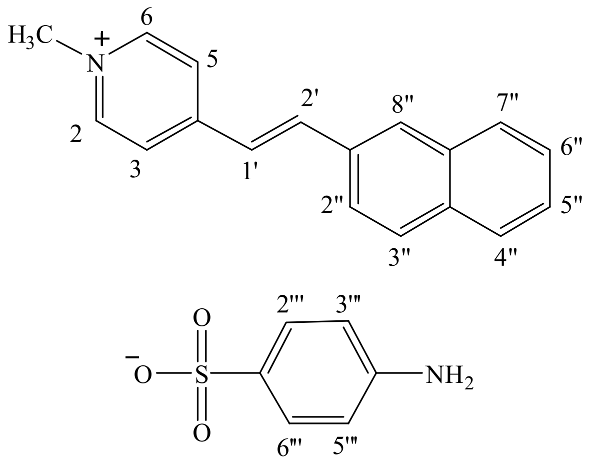

PNAP4N

Compound **PNAP4N** was obtained as yellow solid (54% yield), mp. 248-250 °C. The UV-Vis absorption spectra (**Fig. 91**) showed maximum bands at 230.20 and 354.18 nm. The FT-IR spectrum (**Fig. 92**) exhibited stretching vibrations of C=C (1617 cm^{-1}) and S=O in sulfonates (1181 cm^{-1}).

The ^{1}H NMR spectrum (**Fig. 93,** see **Table 51**) showed two fragments of cationic and anionic parts. The former showed characteristic of *trans*-disubstituted double bonds at δ 7.64 (1H, *d*, J = 16.5 Hz, H-1′) and δ 8.16 (1H, *d*, J = 16.5 Hz, H-2′). The *singlet* signal at δ 4.28 (3H) was assigned as *N*-CH$_3$. Equivalent protons of *p*-disubstituted aromatic appeared as two *doublet* signals at δ 8.87 (2H, J = 6.9 Hz, H-2, H-6) and δ 8.26 (2H, J = 6.9 Hz, H-3, H-5). Resonances of aromatic protons of naphthalenyl part H-2″ to H-8″ were also shown at δ 7.61 (*d*, J = 6.0 Hz, H-2″), δ 7.98 (*d*, J = 6.0 Hz, H-3″), δ 7.89-8.03 (*m*, 4H, H-4″-H-7″) and δ 8.21 (*s*, 1H), respectively. ^{1}H NMR spectrum also showed resonances of aromatic protons of anionic part at δ 7.30 (2H, *d*, J = 8.4 Hz, H-2‴, H-6‴) and δ 6.46 (2H, *d*, J = 8.4 Hz, H-3‴, H-5‴). These observations confirmed that **PNAP4N** is (*E*)-1-methyl-4-(2-(naphthalen-2-yl)vinyl)pyridinium 4-aminobenzenesulfonate.

Table 51 ^{1}H NMR of compound **PNAP4N**

Position	**δ_H (ppm), *mult*, *J* (Hz)**
1-CH_3	4.28 (3H, *s*)
2	8.87 (2H, *d*, 6.9)
6	
3	8.26 (1H, *d*, 6.9)
5	
1′	7.64 (1H, *d*, 16.5)
2′	8.16 (1H, *d*, 16.5)
2″	7.61 (1H, *d*, 6.0 Hz)
3″	7.98 (1H, *d*, 6.0 Hz)
4″	7.89-8.03 (4H, *m*)
5″	
6″	
7″	
8″	8.21 (1H, *s*)
2‴	7.30 (2H, *d*, 8.4)
6‴	
3‴	6.46 (2H, *d*, 8.4)
5‴	
4‴-NH_2	5.12 (2H, *br s*)

3.5 The antimicrobial activity

Table 52 Antibacterial activity of silver (I) salts of anionic parts

Compounds	MIC (µg/mL)								
	Gram-positive bacteria						**Gram-negative bacteria**		
	MRSA*	***S. aureus***	***B. subtilis***	**VRE****	***E. faecalis***		***S. sonnei***	***P. aeruginosa***	***S. typhi***
ANM	2.34	2.34	2.34	2.34	2.34		2.34	300	150
ANOM	2.34	2.34	2.34	2.34	2.34		2.34	-[a]	300
ANCL	9.37	9.37	18.75	9.37	18.75		18.75	150	300
ANBR	37.5	18.75	75	37.5	75		75	300	300
ANNH	2.34	2.34	4.68	2.34	4.68		4.68	300	300
Vancomycin	2.34	2.34	2.34	9.37	2.34		4.68	2.34	4.68

[a] No activity was observed up to 300 µg/mL

* Methicillin-Resistant *S. aureus* ATCC 43300

** Vancomycin-Resistant *E. faecalis* ATCC 51299

The results of antibacterial activity in Table 52 showed that most of the silver salts of anionic parts were more effective against Gram-positive than Gram-negative bacteria. The obtained data clearly suggested that the activities of these compounds depended on the electron donating ability of *para*-substituents. Overall, the antibacterial activities of the compounds containing electron donating groups (**ANM**, **ANOM** and **ANNH**) were considerable whereas the activities of compounds containing electron withdrawing groups (**ANCL** and **ANBR**) were poor.

Among the compounds containing electron donating *para*-substituents (**ANM**, **ANOM** and **ANNH**), compound **ANM** and **ANOM** showed the most potent activity against all tested Gram-positive bacteria and one Gram-negative bacteria i.e. *S. sonnei*. The activity of compound **ANNH** was expressed in the similar way as of **ANM** and **ANOM** with a bit lower efficiency.

For compounds containing electron withdrawing *para*-substituents (**ANCL** and **ANBR**), the MIC values of these two compounds distinctly indicated the decrease in antibacterial activity of compounds containing electron withdrawing *para*-substituents. For compound **ANCL** which contains *para*-Cl groups, the activities against all of the tested bacteria (except *P. aeruginosa* and *S. typhi*) were ≈ 2-4 times less than those of **ANM**. Compound **ANCL** was totally inactive against *P. aeruginosa* and *S. typhi*. Compound **ANBR** showed a very low activity especially against MRSA, *B. subtilis*, *E. faecalis* and *S. sonnei* with the MIC values ≈ 9-16 times greater than that of **ANM**. Compound **ANBR** was inactive against *P. aeruginosa* and *S. typhi*. These values suggested that electron withdrawing substituent groups Cl and Br diminish the antibacterial activity of the silver (I) 4-substitutedbenzenesulfonate compounds.

Noteworthy, for the antibiotic resistant bacteria, compounds **ANM**, **ANOM** and **ANNH** showed the very potent activity against MRSA and VRE with the MICs of 2.34 µg/mL. Moreover, compounds **ANM** and **ANOM** indicated the same MIC values against both susceptible and resistant *S. aureus* and *E. faecalis*. The low MIC values of compounds **ANM**, **ANOM** and **ANNH** showed a good sign of breaking through the resistant mechanism which has limited the use of commercial drugs such as Methicillin and Vancomycin for a long time.

Table 53 Antibacterial activity of naphthalenyl-ethenylpyridinium benzenesulfonate derivatives

Compounds	**MIC (µg/mL)**							
	Gram-positive bacteria					**Gram-negative bacteria**		
	MRSA*	***S. aureus***	***B. subtilis***	**VRE****	***E. faecalis***	***S. sonnei***	***P. aeruginosa***	***S. typhi***
PNAP1 series								
PNAP1	37.5	37.5	150	150	150	300	-[a]	-
PNAP1M	18.75	37.5	75	37.5	300	-	75	-
PNAP1O	-	-	-	-	-	-	300	-
PNAP1B	75	150	-	300	-	-	-	-
PNAP1C	75	150	-	300	-	-	-	-
PNAP1N	75	-	-	300	300	300	-	-
PNAP2 series								
PNAP2	-	-	300	-	300	300	-	-
PNAP2M	-	300	37.5	-	37.5	150	300	-
PNAP2O	-	300	37.5	-	37.5	150	300	-
PNAP2B	-	-	-	-	300	300	-	-
PNAP2C	-	-	300	-	300	300	-	-
PNAP2N	75	300	300	300	300	300	-	-

Table 53 (cont.)

Compounds	MIC (µg/mL)								
	Gram-positive bacteria						Gram-negative bacteria		
	MRSA*	*S. aureus*	*B. subtilis*	VRE**	*E. faecalis*		*S. sonnei*	*P. aeruginosa*	*S. typhi*
PNAP3 series									
PNAP3	-	-	-	-	-		-	-	-
PNAP3M	-	-	-	-	-		-	-	-
PNAP3O	-	-	-	-	-		-	-	-
PNAP3B	-	300	-	-	300		300	-	-
PNAP3C	-	-	300	-	300		-	-	-
PNAP3N	37.5	300	300	300	300		300	-	-
PNAP4 series									
PNAP4	-	-	150	-	150		300	300	-
PNAP4M	-	300	37.5	-	37.5		75	300	-
PNAP4O	-	-	-	-	-		-	-	-
PNAP4B	-	-	300	-	-		-	-	-
PNAP4C	-	-	150	-	150		300	-	-
PNAP4N	-	75	150	75	150		150	-	-

[a] No activity was observed up to 300 µg/mL

* Methicillin-Resistant *S. aureus* ATCC 43300

** Vancomycin-Resistant *E. faecalis* ATCC 51299

The antibacterial activities of cationic parts (**PNAP1-PNAP4**, Table 53) were moderate to low against Gram-positive bacteria whereas they were inactive against Gram-negative bacteria. Cationic part **PNAP3** was inactive against all the tested bacteria.

PNAP1 and **PNAP2** series displayed the dominant antibacterial activity. The introduction of 4-substitutedbenzenesulfonate group moiety to the pyridinium stilbene parts caused a little enhancement to the antibacterial activity displayed by the comparison between iodide-containing and 4-substitutedbenzenesulfonate containing compound in the same series. For example, the changing from iodide ion to 4-methylbenzenesulfonate in **PNAP1** series (**PNAP1** and **PNAP1M**) led to the one-fold-better of antibacterial activity against MRSA (MIC of **PANP1** and **PNAP1M** were 37.5 and 18.75 µg/ml, respectively). In addition, for **PNAP2-PNAP3** series, the introduction of 4-aminobenzenesulfonate part brought about the enhancement in the antibacterial against MRSA (see table 53). From the result, it might be concluded that the 4-substitutedbenzenesulfonate affect the antibacterial activities of the quats.

However, the introduction of naphthalenyl part expecting for the better activity against Gram-negative bacteria seems not to cause any enhancement. From Table 53, the MIC values of the compounds against *S. sonnei*, *P. aeruginosa*, and *S. typhi* indicated that all compounds were inactive against the tested Gram-negative bacteria.

Table 54 Antifungal activity (*C. albicans*) of silver salts of anionic parts

Compounds	MIC (µg/mL)
ANM	-
ANC	300
ANB	-
ANOM	-
ANNH	300

Table 55 Antifungal activity (*C. albicans*) of naphthalenyl-ethenylpyridinium benzenesulfonate derivatives

Compounds	MIC (µg/mL)	Compounds	MIC (µg/mL)	Compounds	MIC (µg/mL)	Compounds	MIC (µg/mL)
PNAP1	150	**PNAP2**	-	**PNAP3**	-	**PNAP4**	300
PNAP1M	150	**PNAP2M**	300	**PNAP3M**	-	**PNAP4M**	150
PNAP1O	-	**PNAP2O**	300	**PNAP3O**	-	**PNAP4O**	-
PNAP1B	-	**PNAP2B**	-	**PNAP3B**	-	**PNAP4B**	-
PNAP1C	-	**PNAP2C**	-	**PNAP3C**	-	**PNAP4C**	-
PNAP1N	-	**PNAP2N**	-	**PNAP3N**	-	**PNAP4N**	300

From the data in Table 54 and 55 showing that all synthesized compounds were inactive against *C. albicans*.

CHAPTER 4
CONCLUSION

Twenty four new naphthalenyl-ethenylpyridinium benzenesulfonate derivatives were successfully synthesized. Their structures were elucidated by spectroscopic techniques. Three structures of these compounds namely:

(*E*)-1-methyl-4-(2-(naphthalen-2-yl)vinyl)pyridinium iodide (**PNAP4**),

(*E*)-1-methyl-4-(2-(naphthalen-1-yl)vinyl)pyridinium 4-bromobenzenesulfonate (**PNAP2B**), and

(*E*)-1-methyl-4-(2-(naphthalen-1-yl)vinyl)pyridinium 4-chlorobenzenesulfonate (**PNAP2C**) were also determined by the single crystal X-ray diffraction. Compounds **PNAP2B** and **PNAP2C** crystallized out in the $Pna2_1$ space group whereas compound **PNAP4** crystallized out in the $P2_1/c$ space group.

All twenty four new naphthalenyl-ethenylpyridinium benzenesulfonate derivatives were evaluated for antimicrobial activities against some pathogenic Gram-positive bacteria i.e. *S. aureus, B. subtilis, E. faecalis,* Methicillin-Resistant *S. aureus*, Vancomycin-Resistant *E. faecalis*, Gram-negative bacteria i.e. *P. aeruginosa, S. typhi*, *S. sonnei* and one fungus which was *C. albicans*. It was found that the twelve compounds in both **PNAP1** and **PNAP2** series exhibited the moderate to low activity against the tested bacteria whereas the compounds in **PNAP3** and **PNAP4** showed either very low activity or inactive. In addition, all the synthesized compounds were inactive against the *C. albicans* fungi.

By comparison between **PNAP1** and **PNAP3** series, which contained 1,2-disubstituted pyridinium part, it was found that **PNAP1** series exhibited more potent antibacterial activity than that of **PNAP3** series. This may be due to the different positional attachment of the naphthalenyl part. In **PNAP1** series, the 1-naphthalenyl part was present in the molecule while 2-naphthalenyl was in **PNAP2** series. These may affect the bacterial cell penetration or the attachment with the target site. Due to the same reason mentioned above, **PNAP2** series displayed more potent antibacterial activity than **PNAP4** series. In addition, there was no significant difference between the activities of **PNAP3** and **PNAP4** series and both of them were inactive. The last comparison occurred between **PNAP1** and **PNAP2** series and it appeared that **PNAP1** series was better than **PNAP2**. The reason may be the difference of substitution position in pyridinium part.

In addition, when considering the effect from introducing benzenesulfonate part in **PNAP1** series, it can be concluded that the benzenesulfonate part enhance the activity of these quats. For example, the changing from iodide ion to 4-methylbenzenesulfonate in **PNAP1** series (**PNAP1** and **PNAP1M**) led to the two-fold-better of antibacterial activity against MRSA (MIC of **PANP1** and **PNAP1M** were 37.5 and 18.75 µg/ml, respectively). However, all compounds were still inactive against the tested Gram-negative bacteria although the naphthalenyl part was introduced to the structure.

PNAP1

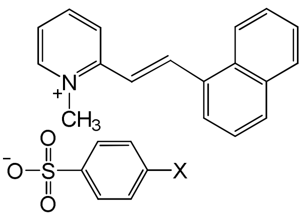

PNAP2

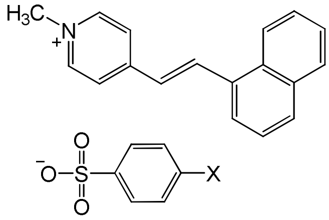

PNAP1M ; $X = CH_3$
PNAP1O ; $X = OCH_3$
PNAP1C ; X = Cl
PNAP1B ; X = Br
PNAP1N ; $X = NH_2$

PNAP2M ; $X = CH_3$
PNAP2O ; $X = OCH_3$
PNAP2C ; X = Cl
PNAP2B ; X = Br
PNAP2N ; $X = NH_2$

*(For **PNAP1** and **PNAP2** ; Anion part is iodide (I^-))*

PNAP3

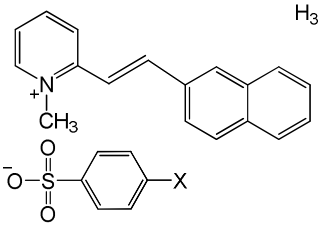

PNAP4

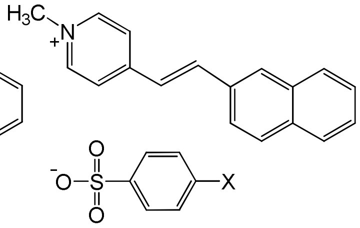

PNAP3M ; $X = CH_3$
PNAP3O ; $X = OCH_3$
PNAP3C ; X = Cl
PNAP3B ; X = Br
PNAP3N ; $X = NH_2$

PNAP4M ; $X = CH_3$
PNAP4O ; $X = OCH_3$
PNAP4C ; X = Cl
PNAP4B ; X = Br
PNAP4N ; $X = NH_2$

*(For **PNAP3** and **PNAP4** ; Anion part is iodide (I^-))*

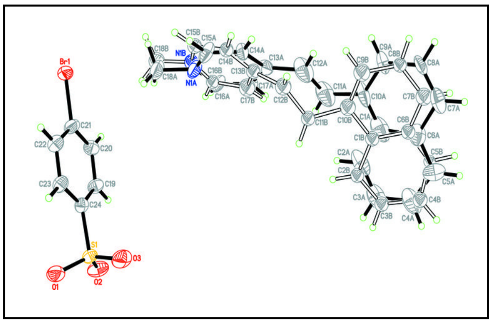

PNAP2B

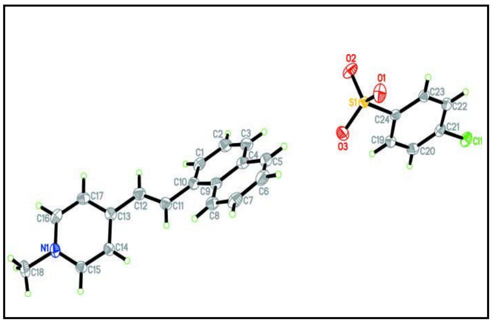

PNAP2C

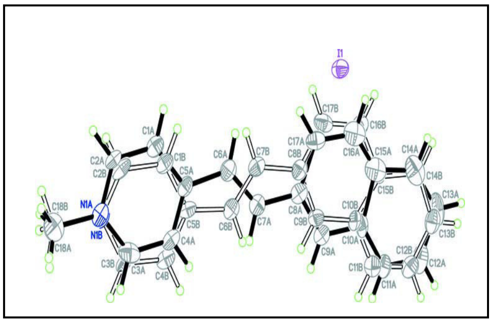

PNAP4

REFERENCES

Archer, G. L. 1998. "*Staphylococcus aureus*: A well-armed pathogen". *Clinical Infectious Diseases*. **26**:1179–1181.

Block, S. S. 1991. *Disinfection, Sterilization and Preservation*. 4th edition. Lea & Febiger: Philadelphia.

Caillier, L., de Givenchy, E. T., Levy, R., Vandenberghe, Y., Géribaldi, S. and Guittard, F. 2009. "Synthesis and antimicrobial properties of polymerizable quaternary ammoniums". *European Journal of Medicinal Chemistry*. **44**: 3201-3208.

Chelossi, E., Mancini, I., Sepčić, K., Turk, T. and Faimali, M. 2006. "Comparative antibacterial activity of polymeric 3-alkylpyridinium salts isolated from the Mediterranean sponge *Reniera sarai* and their synthetic analogues". *Biomolecular Engineering*. **23**: 317-323.

Clarissa, K. L. Ng., Singhal, V., Widmer, F., Wright, L. C., Tania, C. S. and Jolliffe, K. A. 2007. "Synthesis, antifungal and haemolytic activity of a series of bis(pyridinium)alkanes". *Bioorganic & Medicinal Chemistry*. **15**: 3422-3429.

Collier, H. O. J., Potter, M. D. and Taylor, E. P. 1953. "Antibacterial activities of some bis*iso*quinolinium salts". *British Journal of Pharmacology*, **8**: 34-37.

Collier, H. O. J., Potter, M. D. and Taylor, E. P. 1955. "Antifungal activities of bisisoquinolinium and bisquinolinium salts". *British Journal of Pharmacology*. **10**: 343-348.

Demberelnyamba, D., Kim, K. S., Choi, S., Park, S. Y., Lee, H., Kim, C. J. and Yoo, I. D. 2004. "Synthesis and antimicrobial properties of imidazolium and pyrrolidinonium salts". *Bioorganic & Medicinal Chemistry.* **12**: 853-857.

Denny, B. J., Novotny, L., West, P.W.J., Blesova, M. and Zamocka, J. 2005. "Antimicrobial Activity of a Series of 1-Alkyl-2-(4-Pyridyl)Pyridinium

Bromides against Gram-Positive and Gram-Negative Bacteria". *Medical Principles and Practice*. **14**: 377-381.

Doyle, R. J., Keller, K. F. and Ezzell, J. W. 1985. *Manual of clinical microbiology*. 4th edition. American Society for Microbiology: Washington D. C.

Eren, T., Som, A., Rennie, J. R., Nelson, C. F., Urgina, Y., Nüsslein, K., Coughlin, E. B. and Tew, G. N. 2008. "Antibacterial and hemolytic activities of quaternary pyridinium functionalized polynorbornenes". *Macromolecular Chemistry and Physics*. **209**: 516-524.

Gamage, B. 2003. *A guide to selection and use of disinfectants*. BC Centre for disease control: British Columbia.

Halliday, A. 1821. "Observations on the use of the different preparations of iodine as a remedy for bronchocele, and in the treatment of scrofula" *London Medical Repository*. **16**: 199.

Hameed, S., Saeed, M., Khan, A., Nizami, S. S. and Kazmi, M. H. 1994. "Synthesis and antibacterial activity of picoline derivatives". *Journal of Islamic Academy of Sciences*. **7**: 26-29.

Maeda, T., Manabe, Y., Yamamoto, M., Yoshida, M., Okazaki, K., Nagamune, H. and Kourai, H. 1999. "Synthesis and antimicrobial characteristics of novel biocides, 4,4 '-(1,6-hexamethylenedioxydicarbonyl)bis(1-alkylpyridinium iodide)s". *Chemical & Pharmaceutical Bulletin*. **47**: 1020-1023.

Massi, L., Guittard, F., Géribaldi, S., Levy, R. and Duccini, Y. 2003. "Antimicrobial properties of highly fluorinated bis-ammonium salts". *International Journal of Antimicrobial Agents*. **21**: 20-26.

Massi, L., Guittard, F., Levy, R. and Géribaldi, S. 2009. "Enhanced activity of fluorinated quaternary ammonium surfactants against *Pseudomonas aeruginosa*". *European Journal of Medicinal Chemistry*. **44**: 1615-1622.

McGowan, J. E. Jr., Tenover, F. C. 2004. “Confronting bacterial resistance in healthcare settings – a crucial role for the microbiologist”. *Nature Reviews Microbiology*, **2**: 251- 258.

Moote, A. L. M.; Dorothy, C. 2004. “The Great plague: The Story of London’s Most Deadly Year”, Johns Hopkins University Press: Baltimore.

Munoz, C., Baqar, S., de Verg, L., Thupari, J., Goldblum, S., Olson, J. G. Taylor, D. N., Heresi, G. P. and Murphy, J. R. 1995. “Characteristics of *Shigella sonnei* infection of volunteers: signs, symtoms, immune responses, changes in selected cytokines and acute-phase substances”. *American Journal of Tropical Medicine and Hygiene*. **53**: 47-54.

Ohkura, K., Sukeno, A., Yamamoto, K., Nagamune, H., Maeda, T. and Kourai, H. 2003. “Analysis of structural features of bis-quaternary ammonium antimicrobial agents 4,4’-(α,ω-polymethylenedithio)bis(1-alkylpyridinium iodide)s using computational simulation”. *Bioorganic & Medicinal Chemistry.* **11**: 5035-5043.

Ohta, Y., Kondo, Y., Kawada, K., Teranaka, T. and Yoshino, N. 2008. “Synthesis and antibacterial activity of quaternary ammonium salt-type antibacterial agents with a phosphate group”. *Journal of Oleo Science.* **57**: 445-452.

Pernak, J. and Feder-Kubis, J. 2006. “Chiral pyridinium-based ionic liquids containing the(1*R*,2*S*,5*R*)-(-)-menthyl group”. *Tetrahedron: Asymmetry*. **17**: 1728-1737.

Pernak, J., Kalewska, J., Ksycifiska, H. and Cybulski, J. 2001. “Synthesis and anti-microbial activities of some pyridinium salts with alkoxymethyl hydrophobic group”. *European Journal of Medicinal Chemistry*, **36**: 899-907.

Pernak, J., Rogoza, J. and Mirska, I. 2001. “Synthesis and antimicrobial activities of new pyridinium and benzimidazolium chlorides”. *European Journal of Medicinal Chemistry.* **36**: 313-320.

Rutala, W. A. 1995. “APIC guidelines for selection and use of disinfectants”. *American Journal of Infection Control*, **23**: 313–342.

Sun, J. Y., Li, J., Qiu, X. L. and Qing, F. L. 2005. “Synthesis and structure-activity relationship (SAR) of novel perfluoroalkyl-containing quaternary ammonium salts”. *Journal of Fluorine Chemistry*. **126**: 1425-1431.

Xiao, Y. H., Chen, J. H., Fang, M., Xing, X. D., Wang, H., Wang, Y. J. and Li, F. 2008. “Antibacterial effects of three experimental quaternary ammonium salt (QAS) monomers on bacteria associated with oral infections”. *Journal of Oral Science*. **50**: 323-327.

Zhao, T. and Sun, G. 2007. “Hydrophobicity and antimicrobial activities of quaternary pyridinium salts”. *Journal of Applied Microbiology*. **104**: 824-830.

APPENDIX

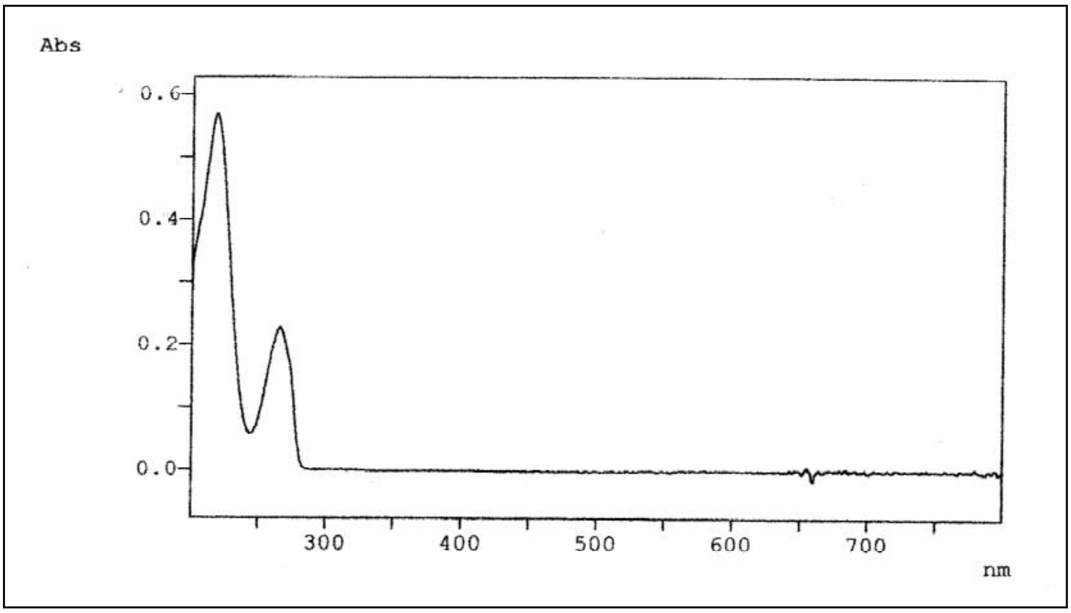

Figure 11 UV-Vis (CH_3OH) spectrum of compound **PO-ST**

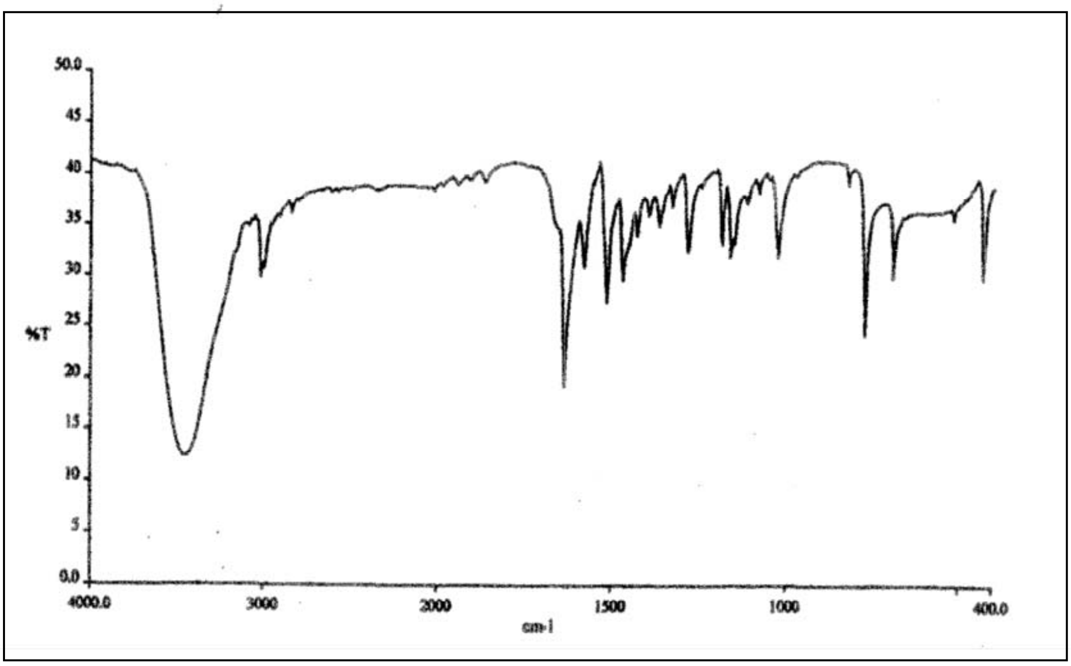

Figure 12 FT-IR (KBr) spectrum of compound **PO-ST**

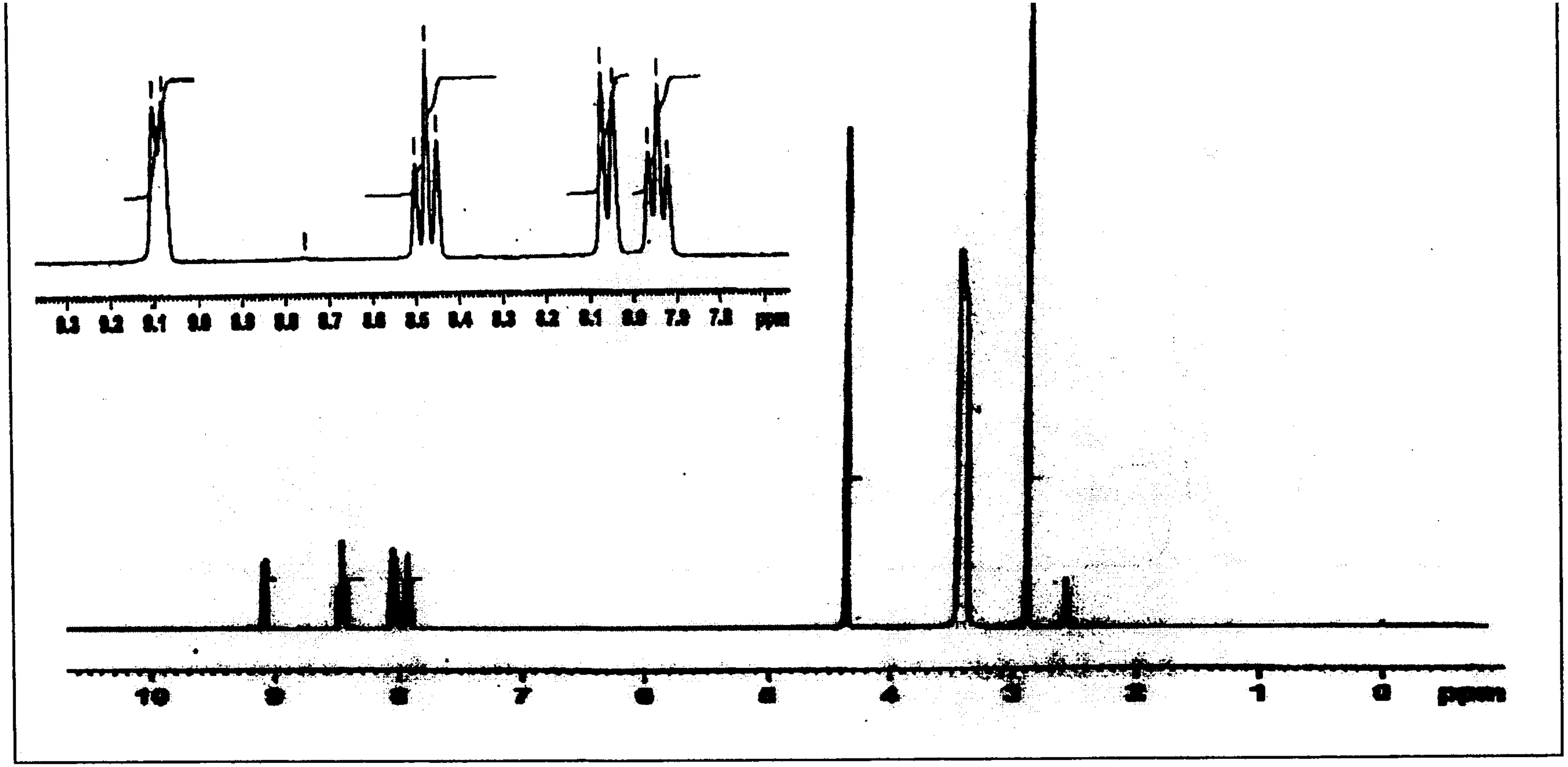

Figure 13 ^{1}H NMR (300 MHz, $CDCl_3$ + DMSO-d_6) spectrum of compound **PO-ST**

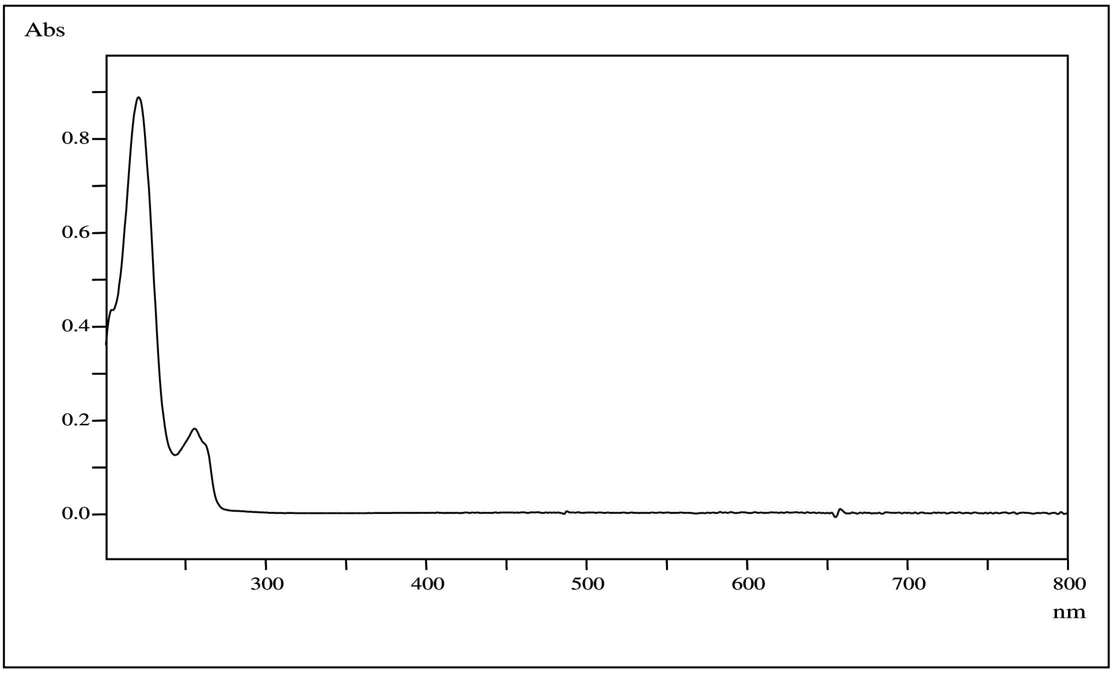

Figure 14 UV-Vis (CH_3OH) spectrum of compound **PP-ST**

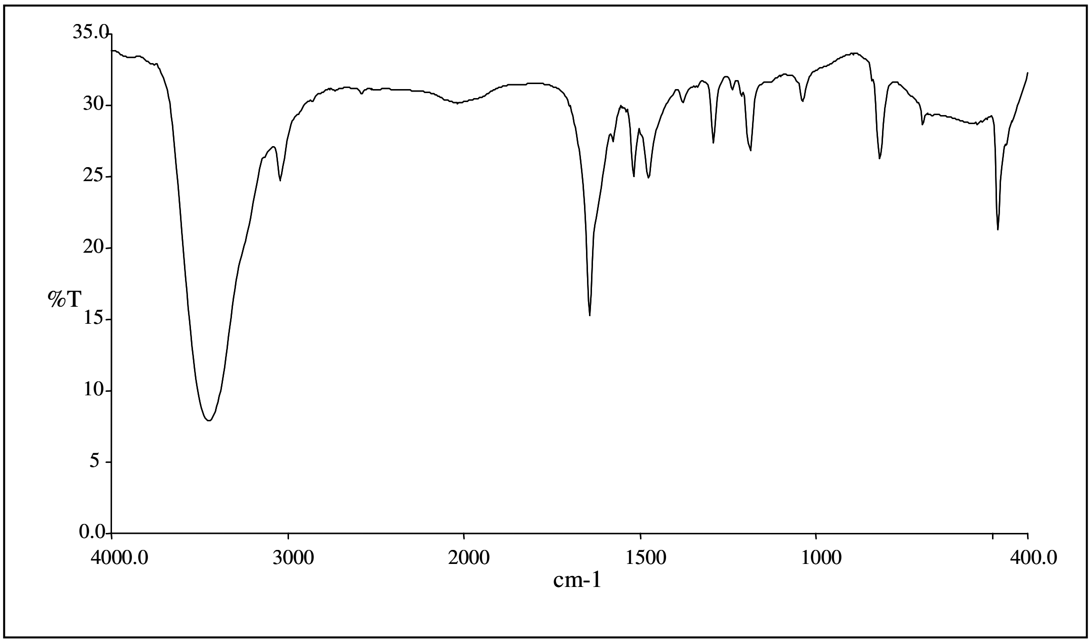

Figure 15 FT-IR (KBr) spectrum of compound **PP-ST**

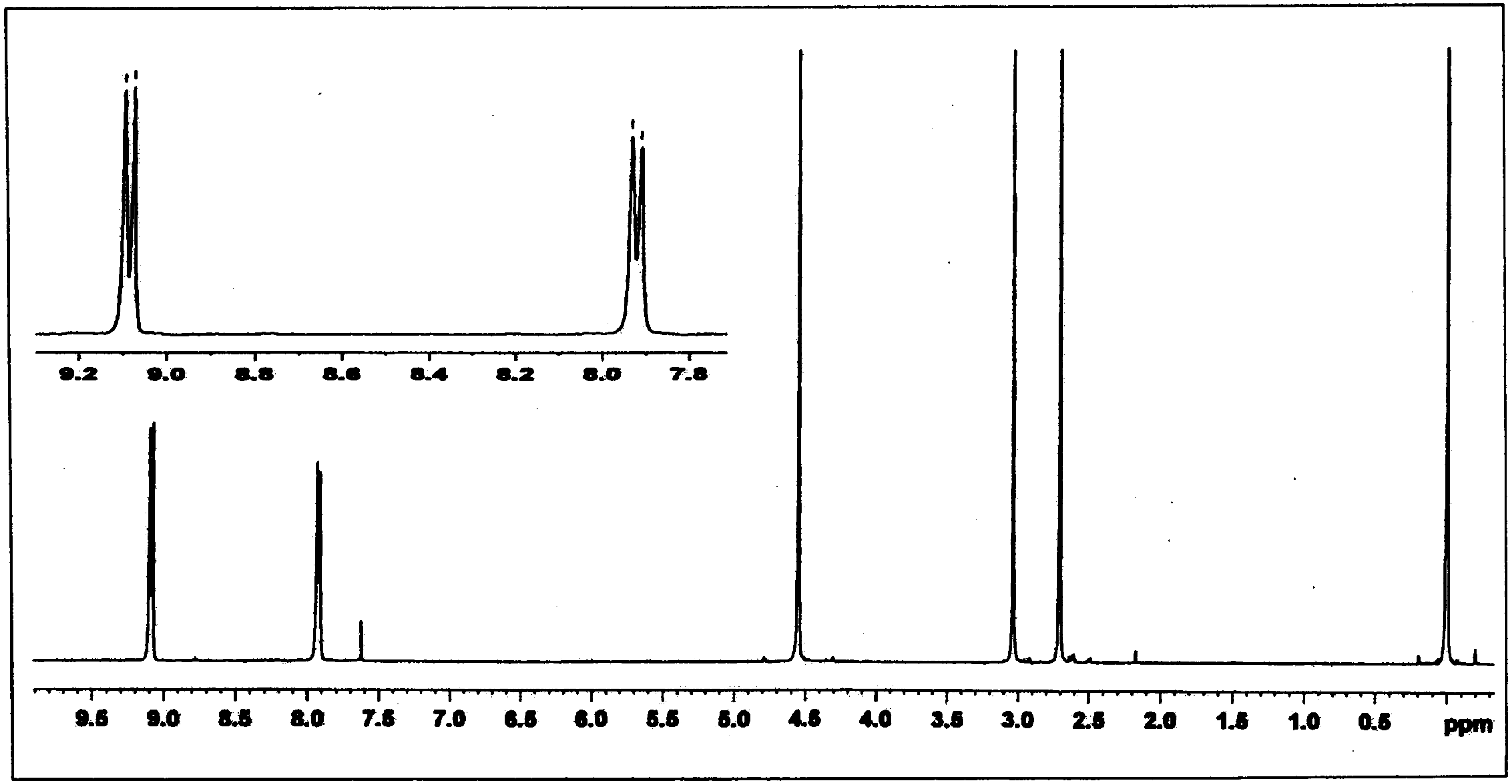

Figure 16 ^{1}H NMR (300 MHz, $CDCl_3$ + DMSO-d_6) spectrum of compound **PP-ST**

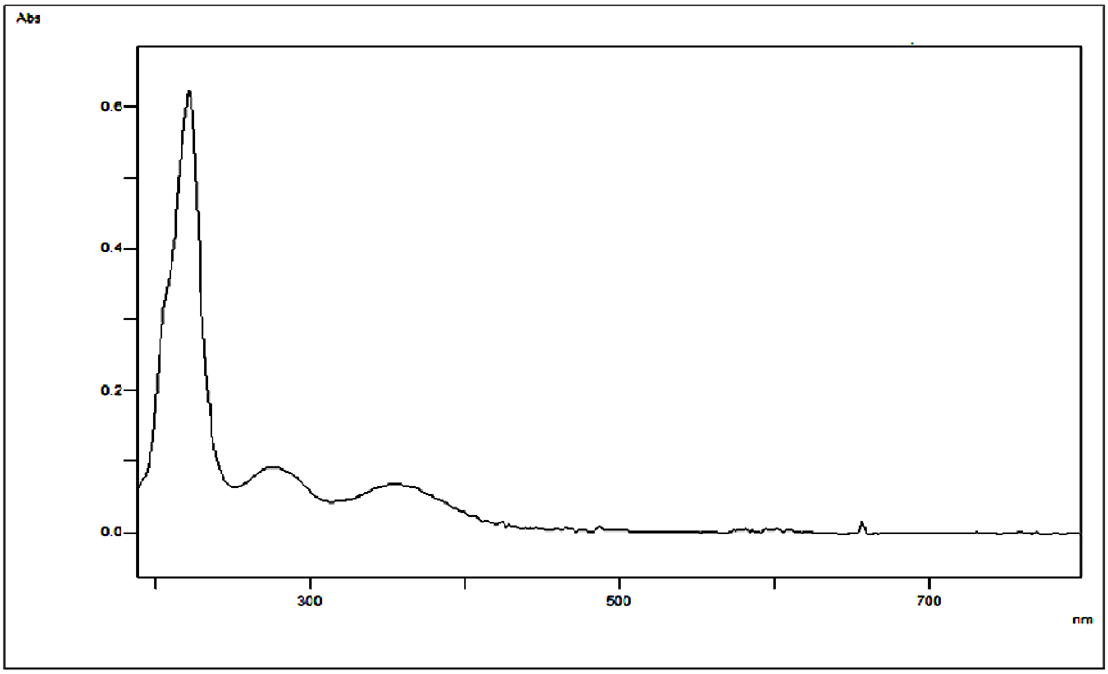

Figure 17 UV-Vis (CH_3OH) spectrum of compound **PNAP1**

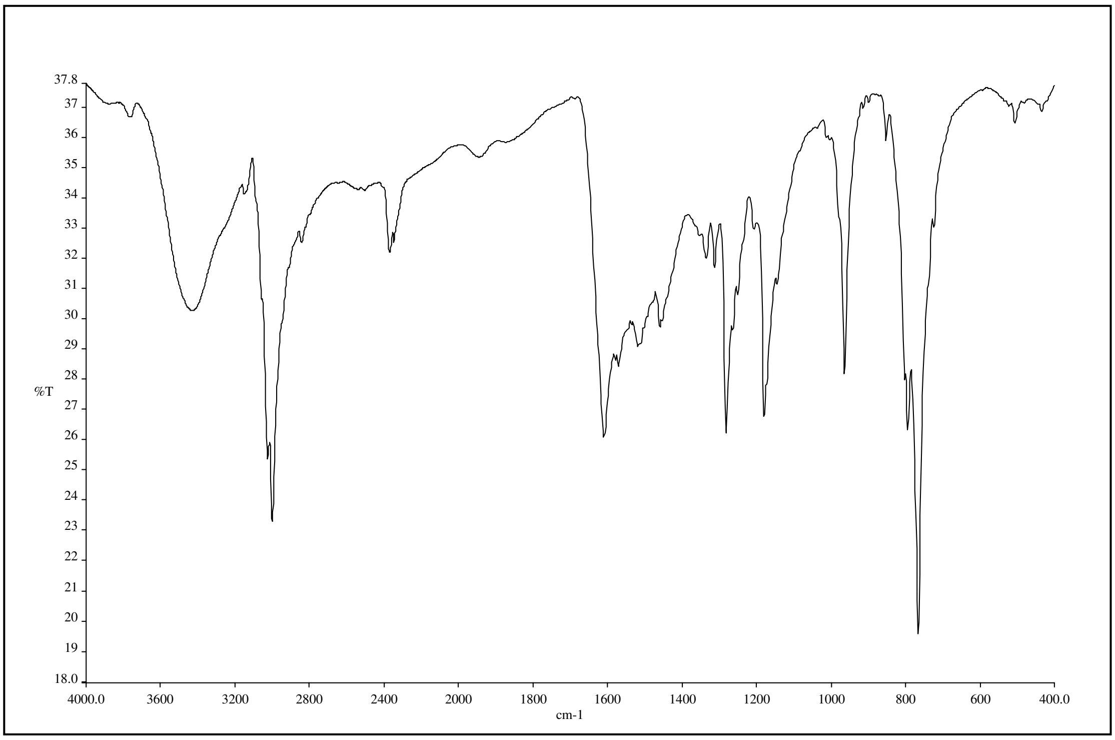

Figure 18 FT-IR (KBr) spectrum of compound **PNAP1**

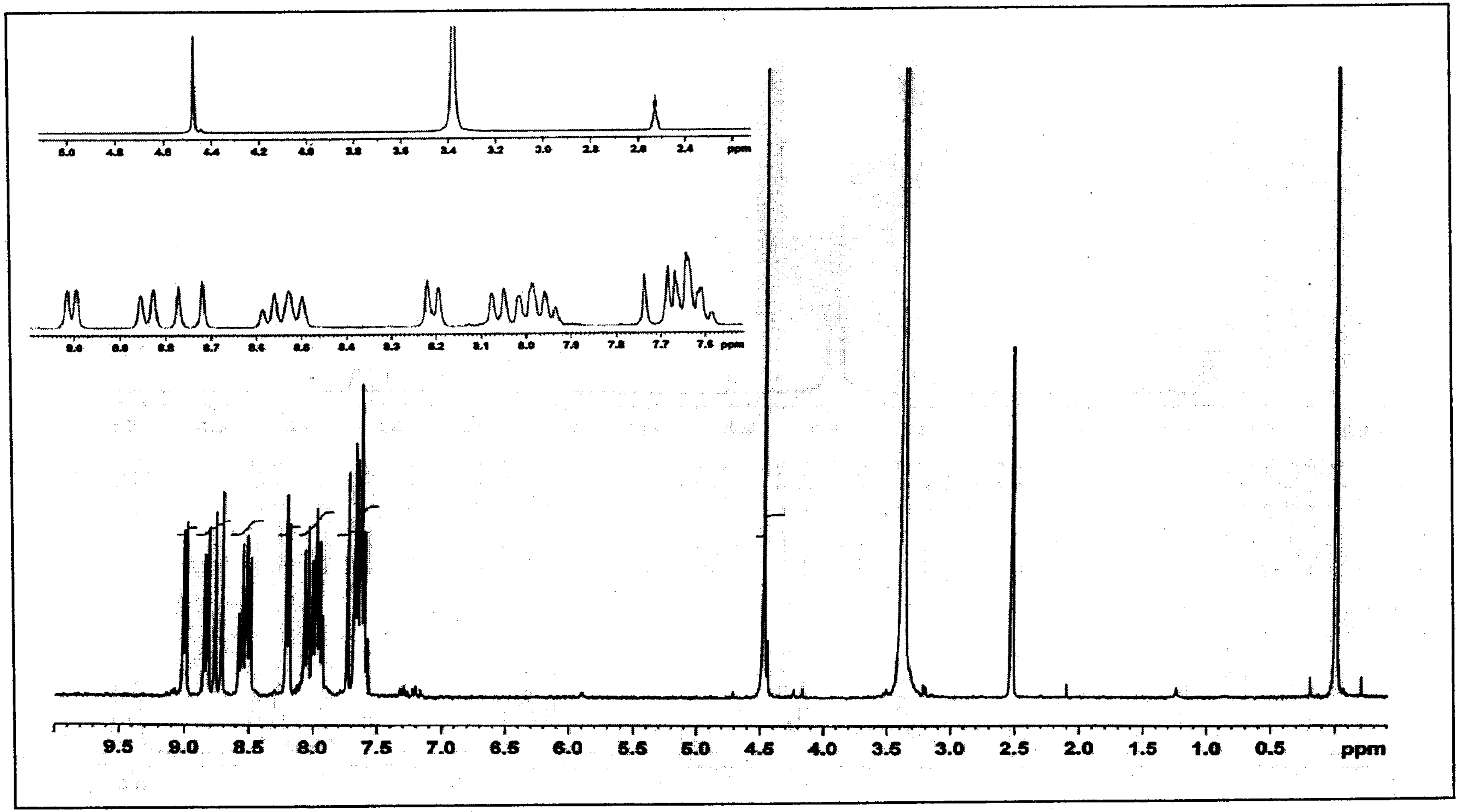

Figure 19 ^{1}H NMR (300 MHz, $CDCl_3$ + DMSO-d_6) spectrum of compound **PNAP1**

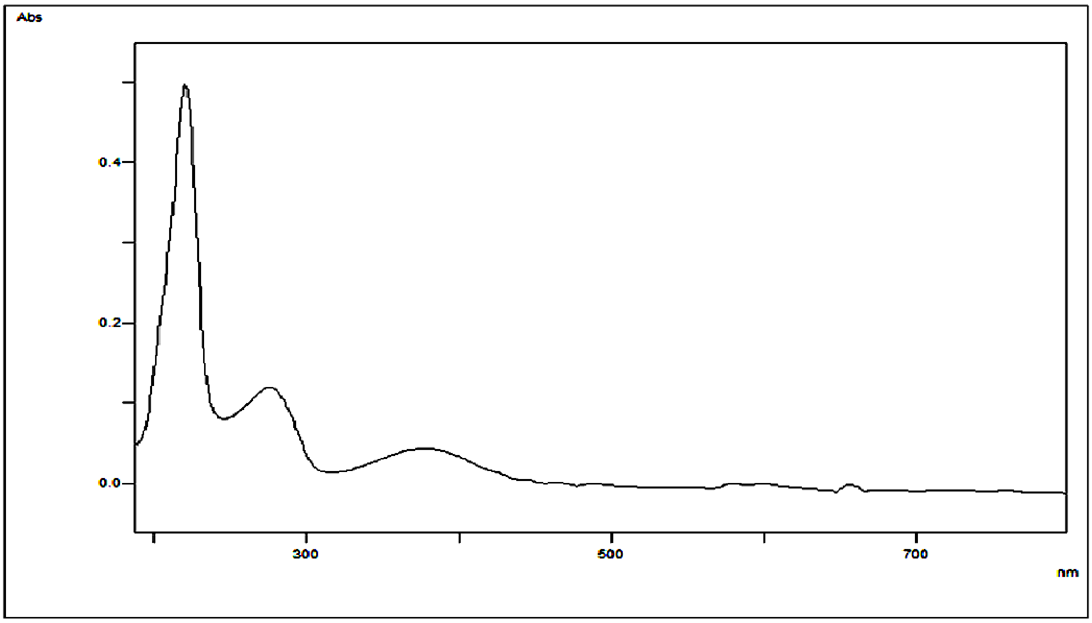

Figure 20 UV-Vis (CH_3OH) spectrum of compound **PNAP2**

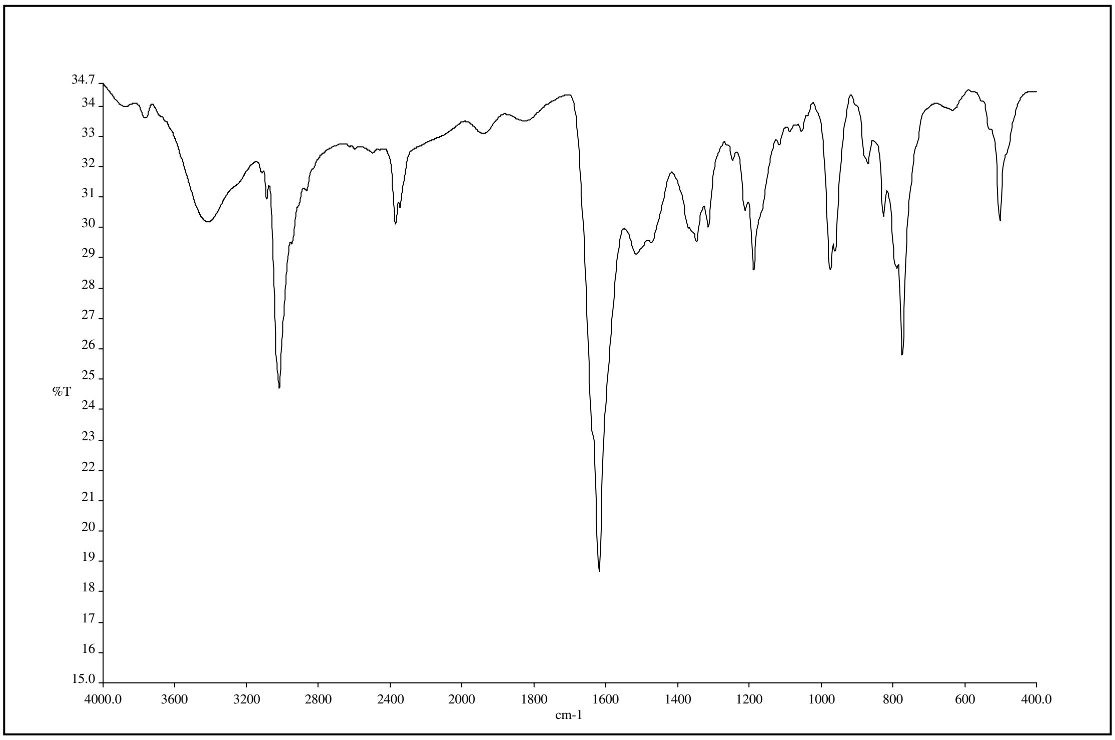

Figure 21 FT-IR (KBr) spectrum of compound **PNAP2**

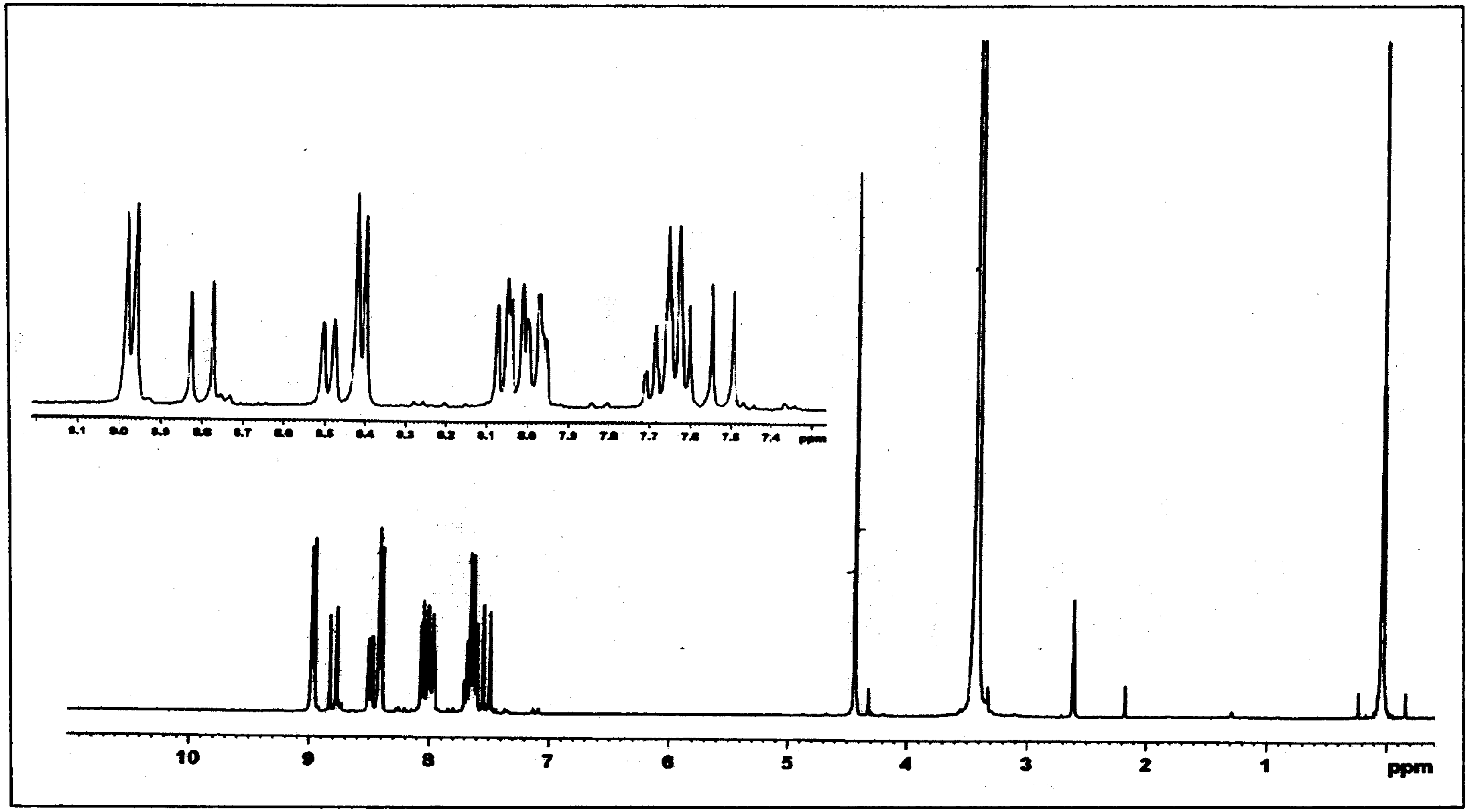

Figure 22 ^{1}H NMR (300 MHz, $CDCl_3$ + DMSO-d_6) spectrum of compound **PNAP2**

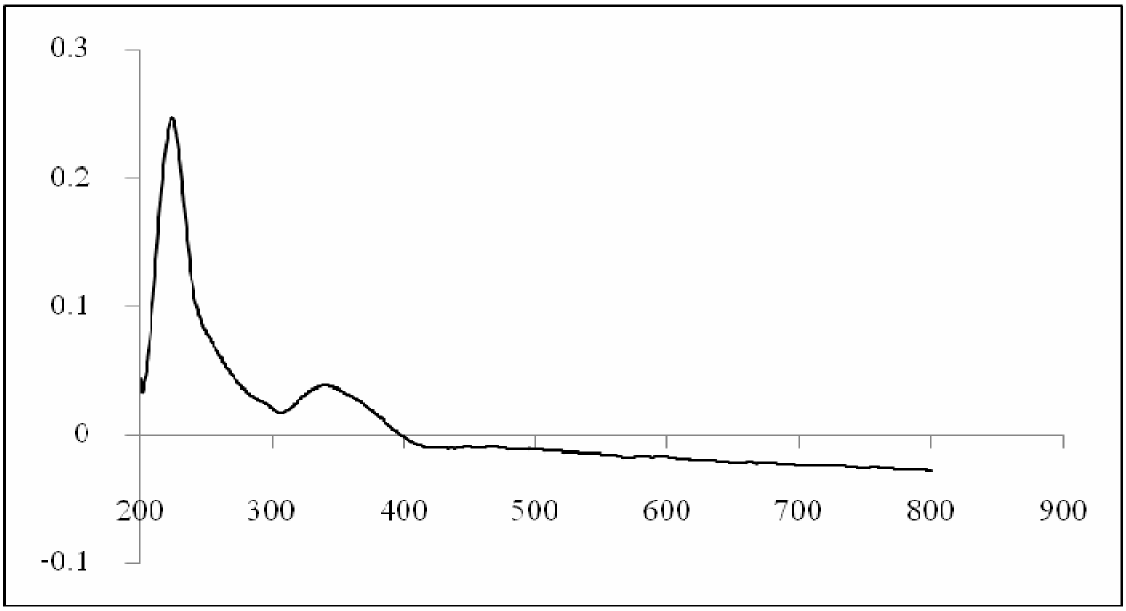

Figure 23 UV-Vis (CH_3OH) spectrum of compound **PNAP3**

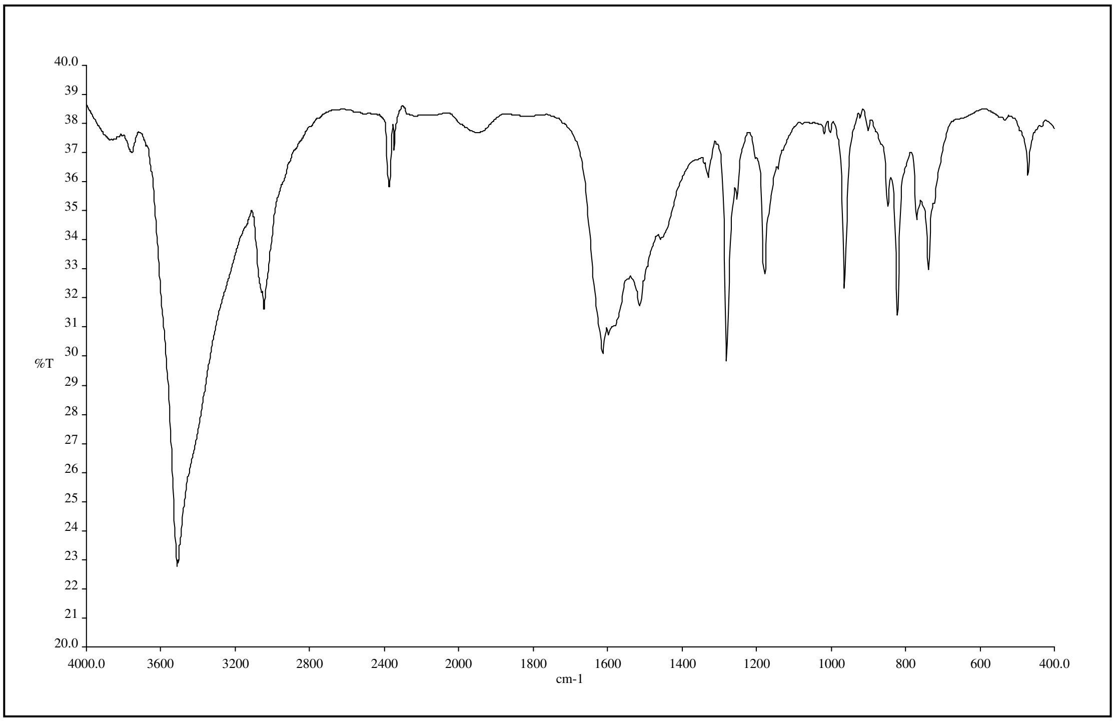

Figure 24 FT-IR (KBr) spectrum of compound **PNAP3**

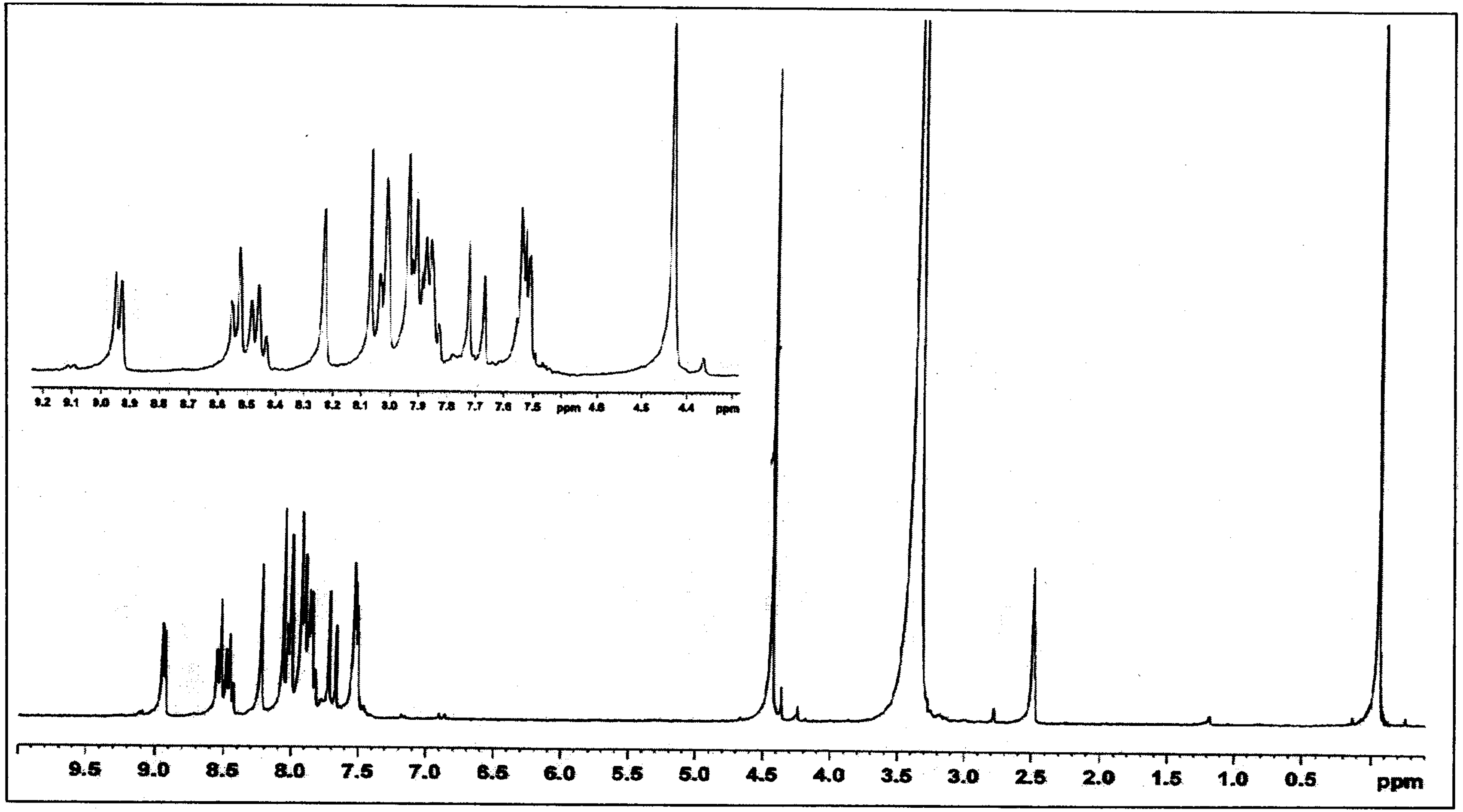

Figure 25 ^{1}H NMR (300 MHz, $CDCl_3$ + DMSO-d_6) spectrum of compound **PNAP3**

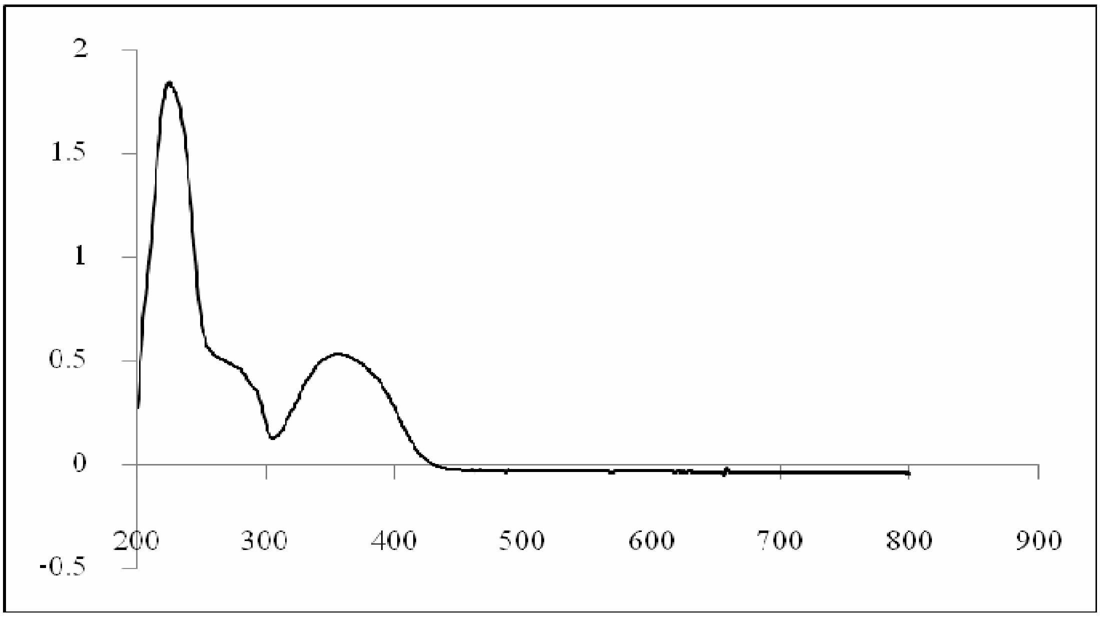

Figure 26 UV-Vis (CH_3OH) spectrum of compound **PNAP4**

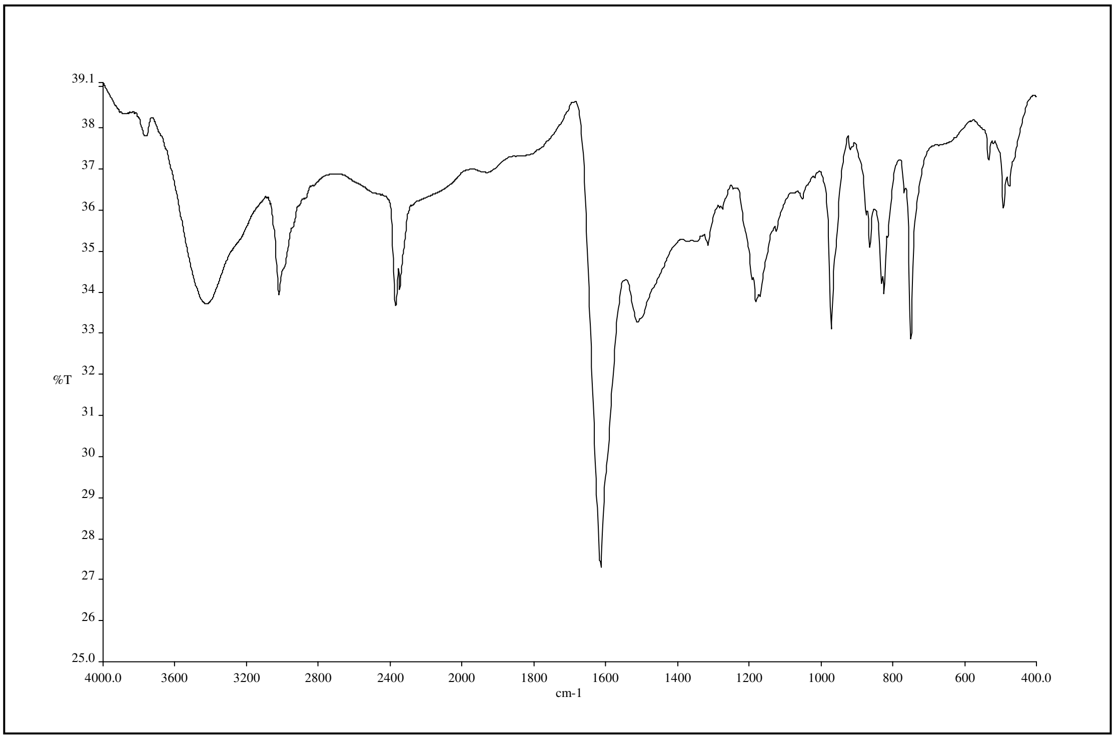

Figure 27 FT-IR (KBr) spectrum of compound **PNAP4**

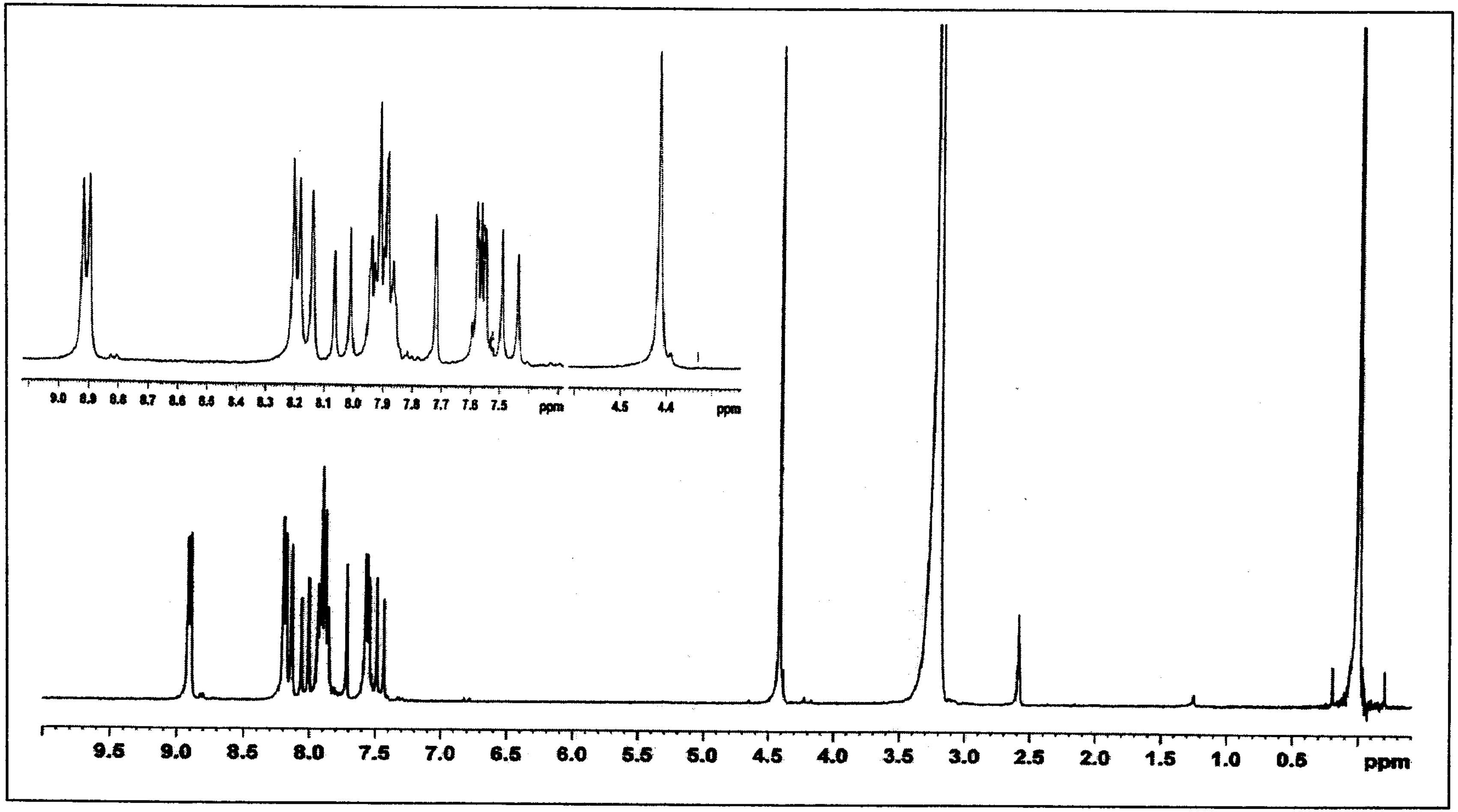

Figure 28 ^{1}H NMR (300 MHz, $CDCl_3$ + DMSO-d_6) spectrum of compound **PNAP4**

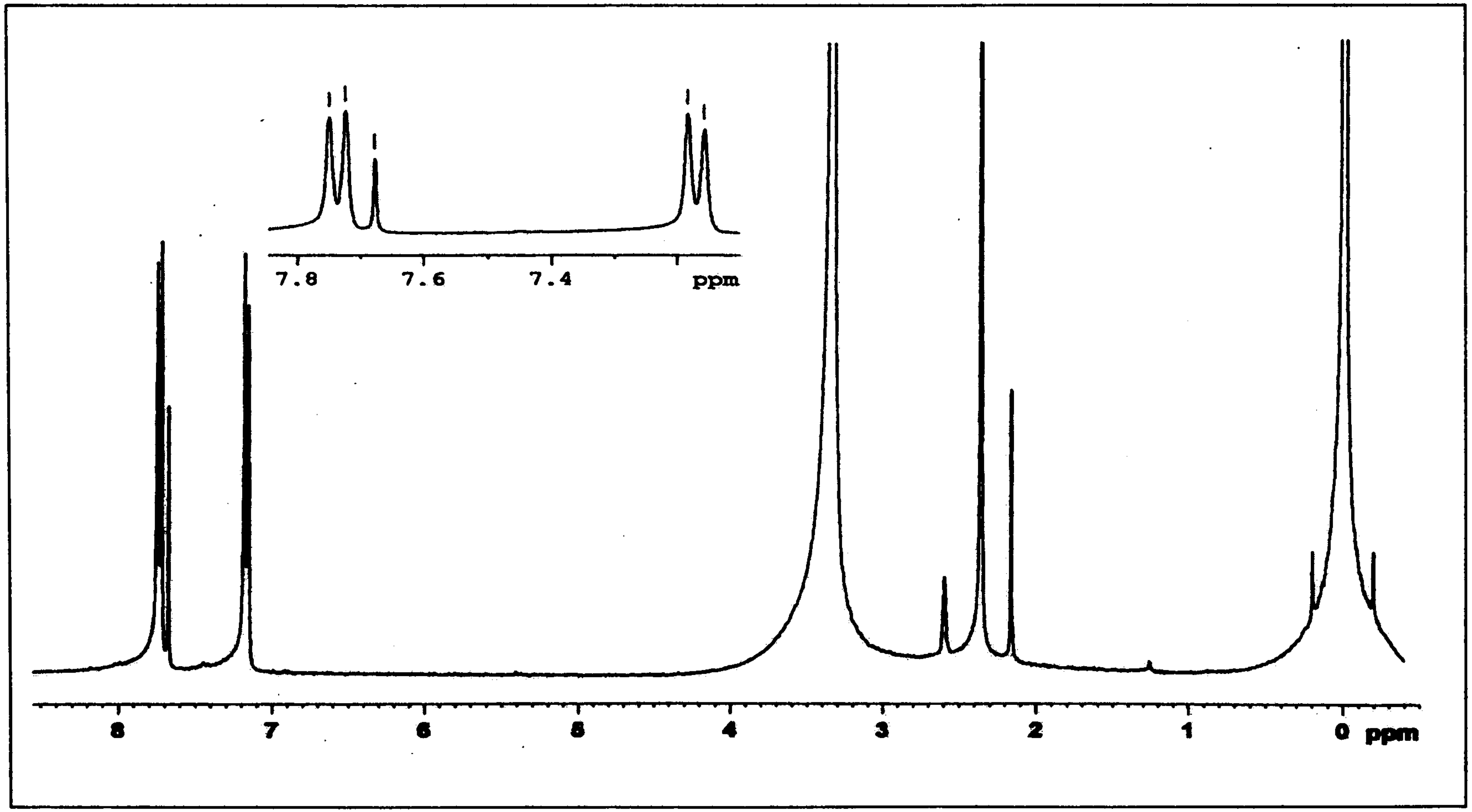

Figure 29 ^{1}H NMR (300 MHz, $CDCl_3$ + DMSO-d_6) spectrum of compound ANM

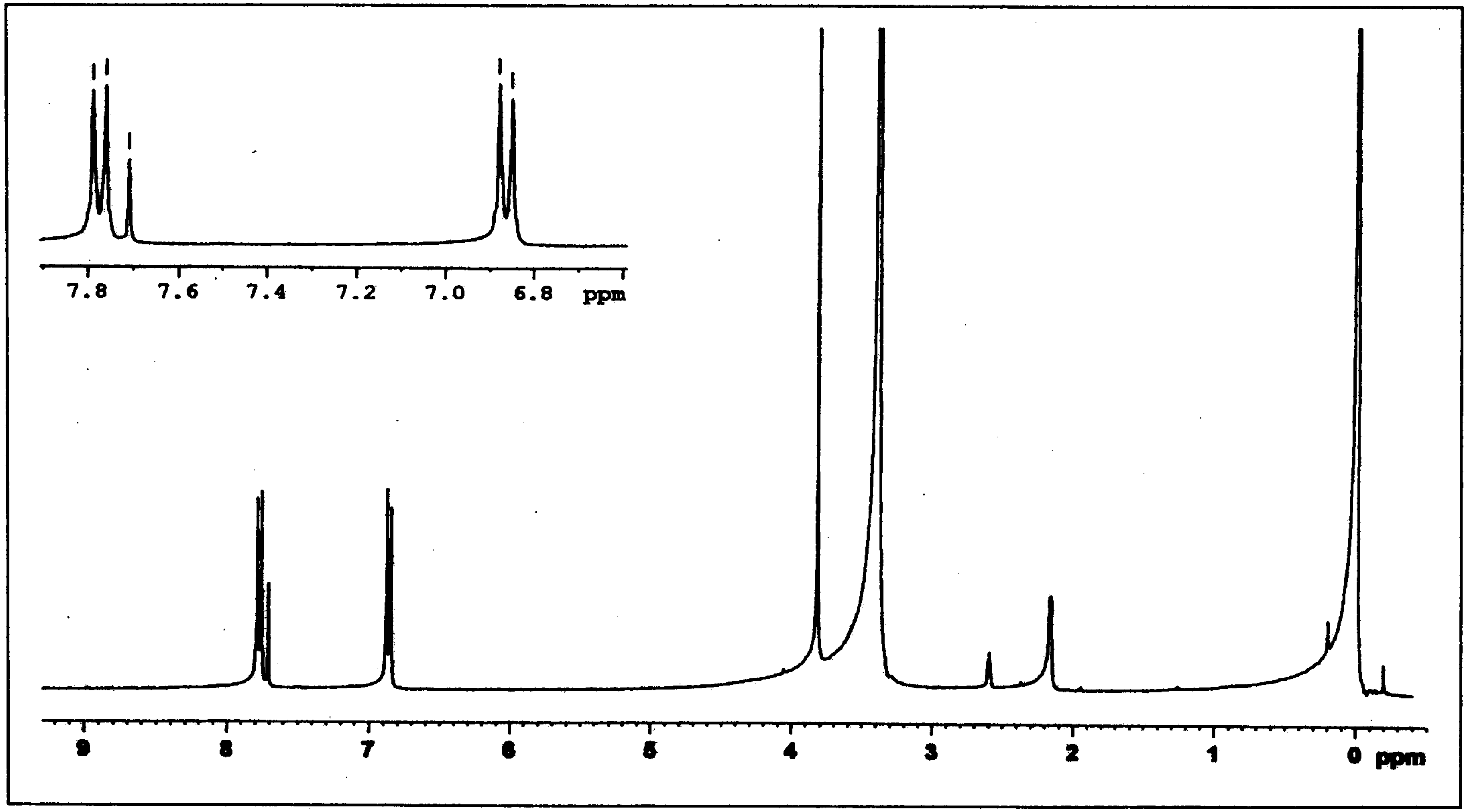

Figure 30 ^{1}H NMR (300 MHz, $CDCl_3$ + DMSO-d_6) spectrum of compound ANOM

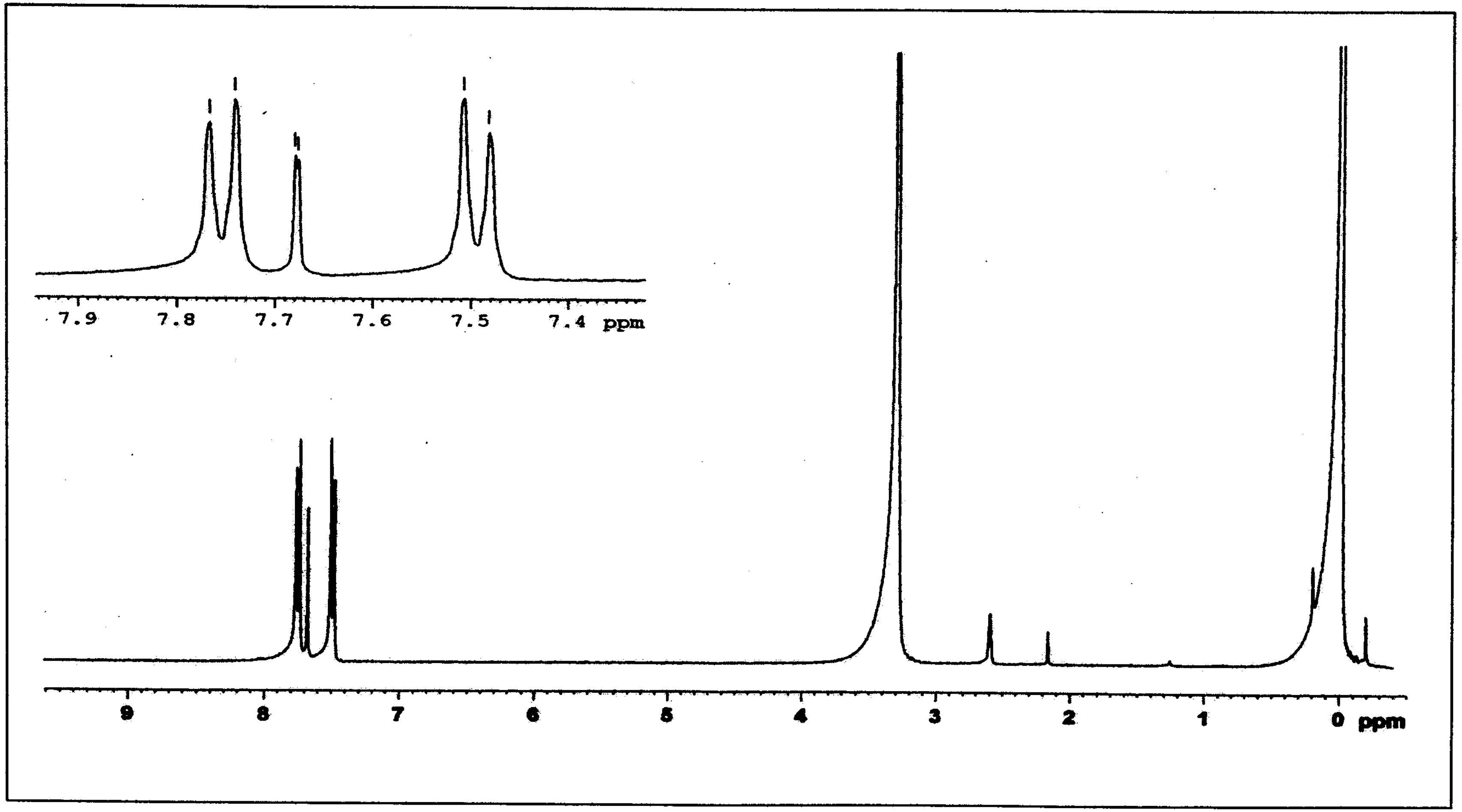

Figure 31 ^{1}H NMR (300 MHz, $CDCl_3$ + DMSO-d_6) spectrum of compound **ANCL**

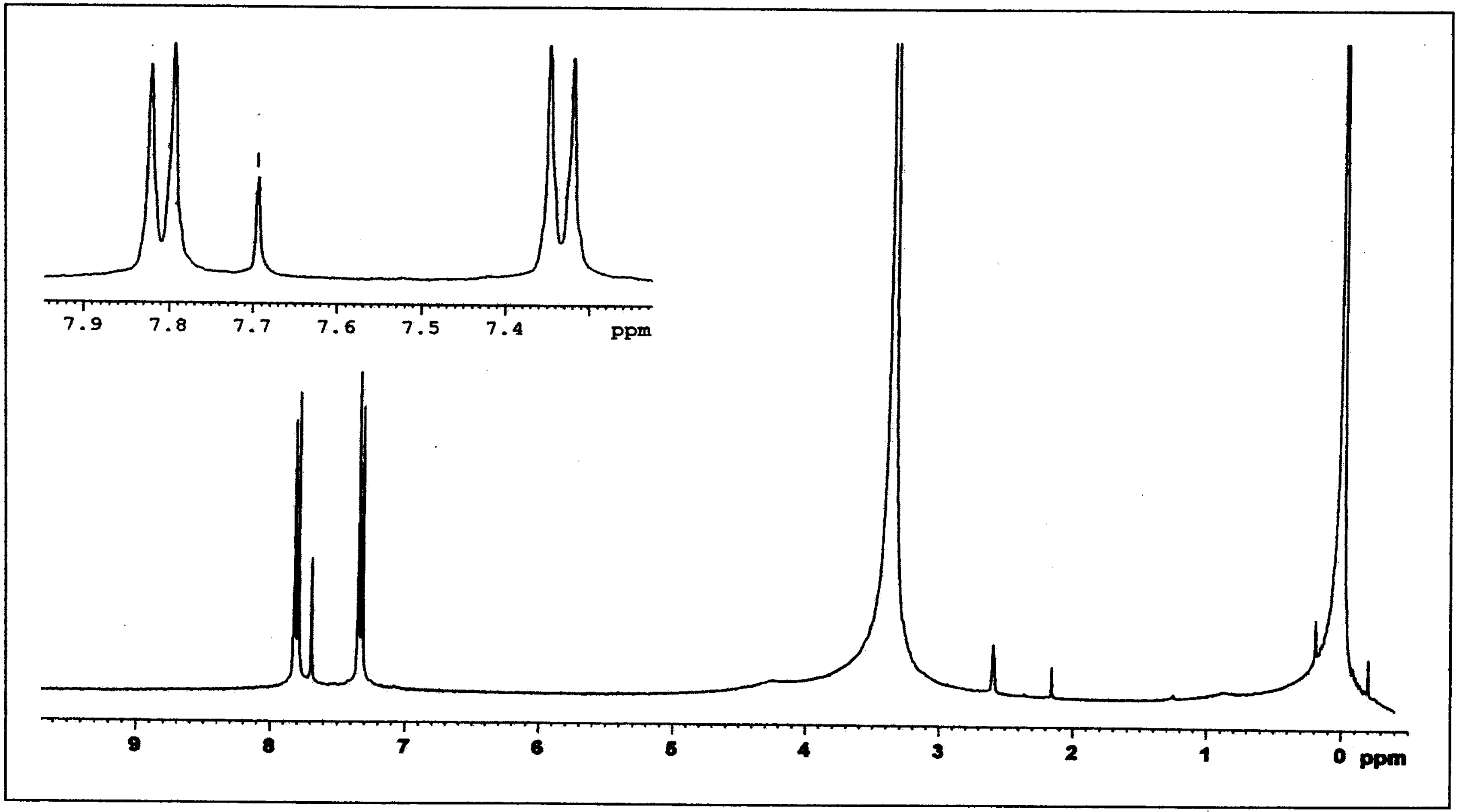

Figure 32 ^{1}H NMR (300 MHz, $CDCl_3$ + DMSO-d_6) spectrum of compound **ANBR**

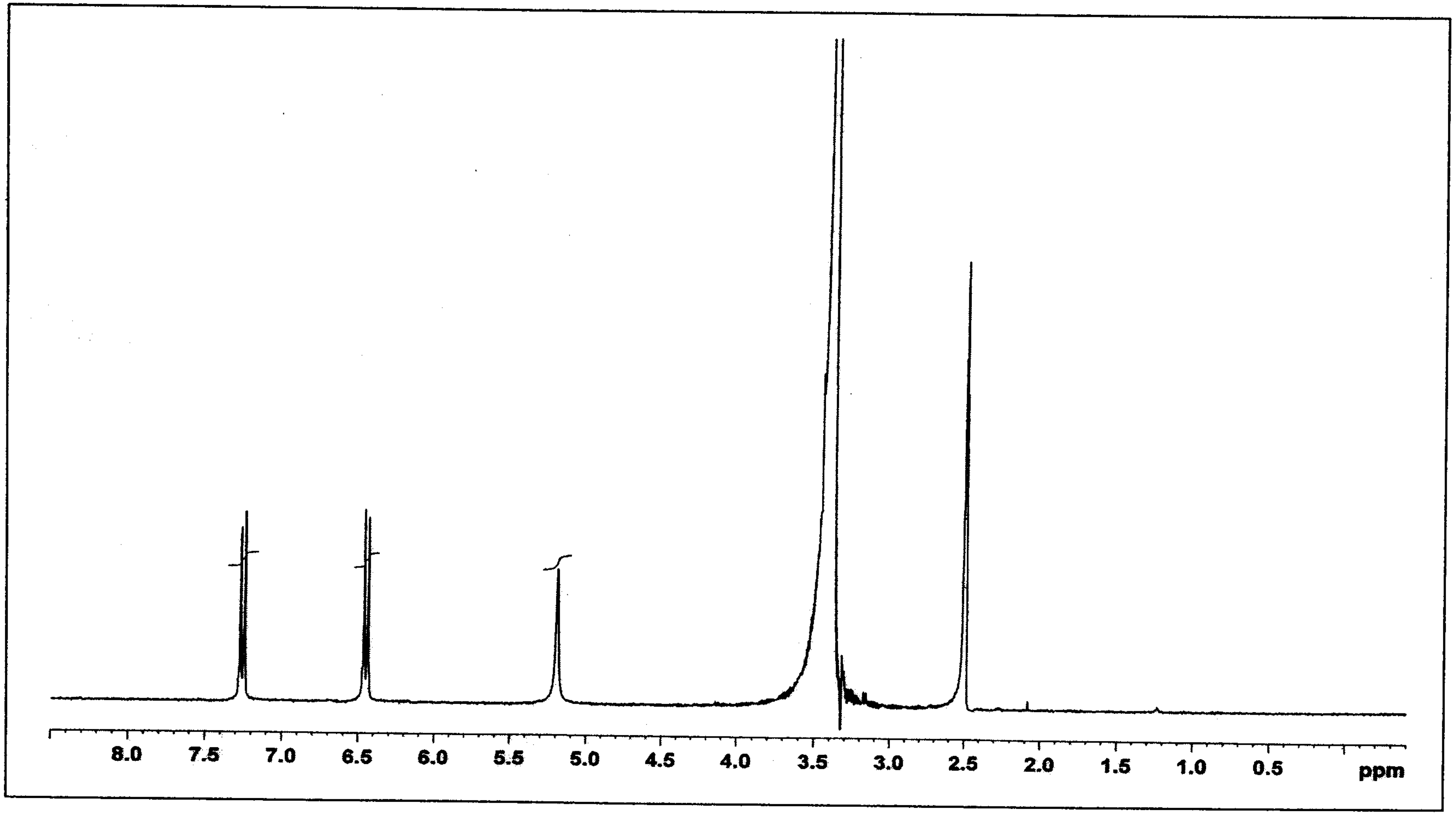

Figure 33 ^{1}H NMR (300 MHz, $CDCl_3$ + DMSO-*d*$_6$) spectrum of compound **ANNH**

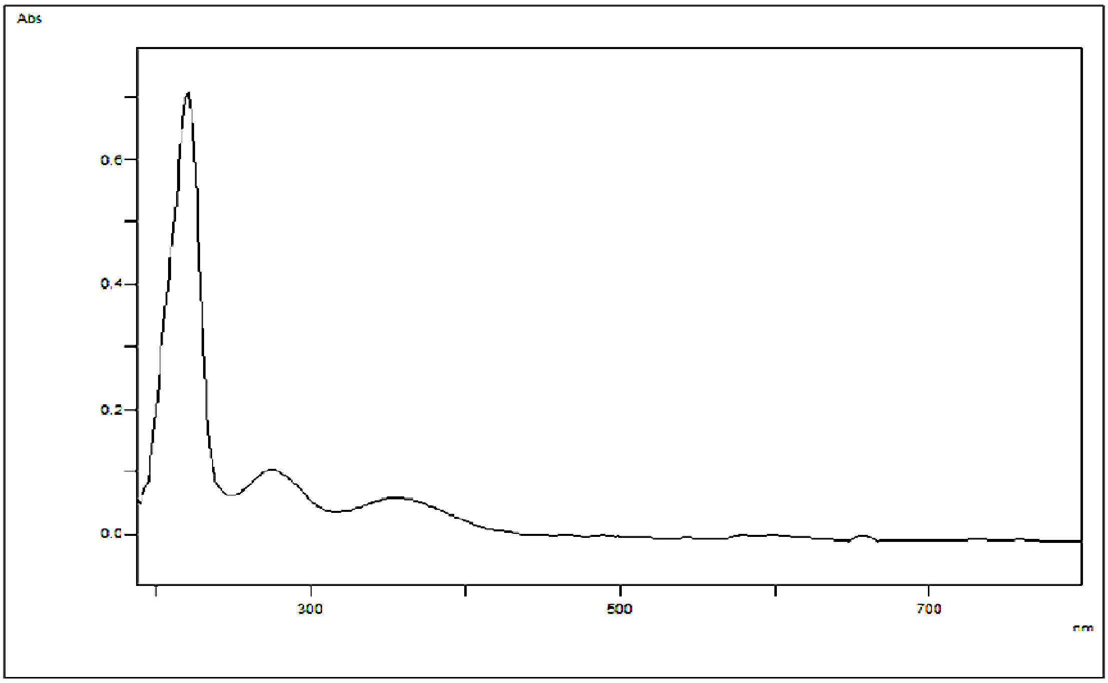

Figure 34 UV-Vis (CH_3OH) spectrum of compound **PNAP1M**

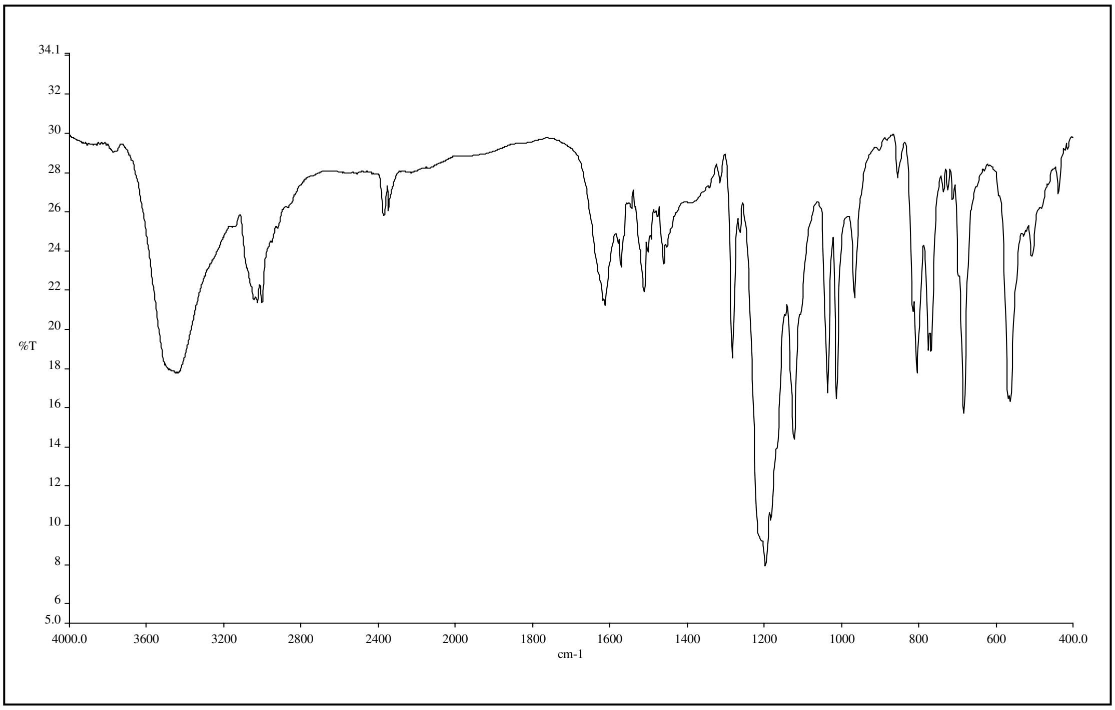

Figure 35 FT-IR (KBr) spectrum of compound **PNAP1M**

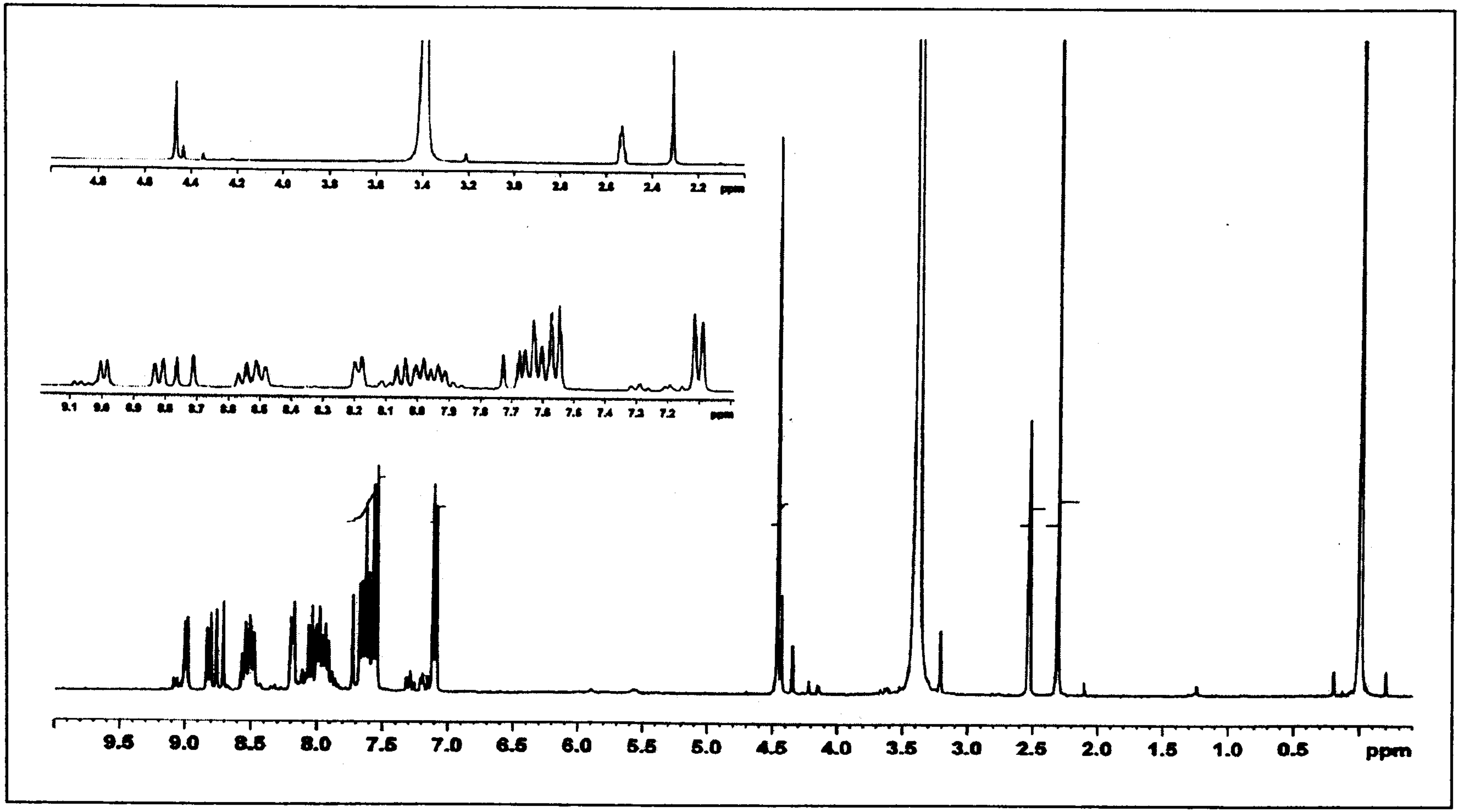

Figure 36 ^{1}H NMR (300 MHz, $CDCl_3$ + DMSO-d_6) spectrum of compound **PNAP1M**

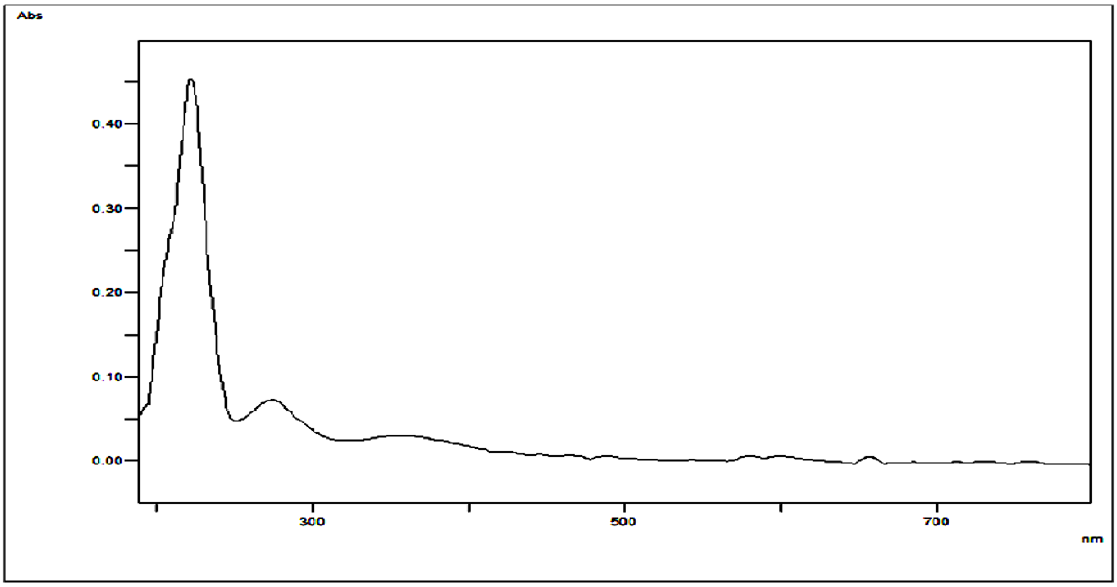

Figure 37 UV-Vis (CH_3OH) spectrum of compound **PNAP1O**

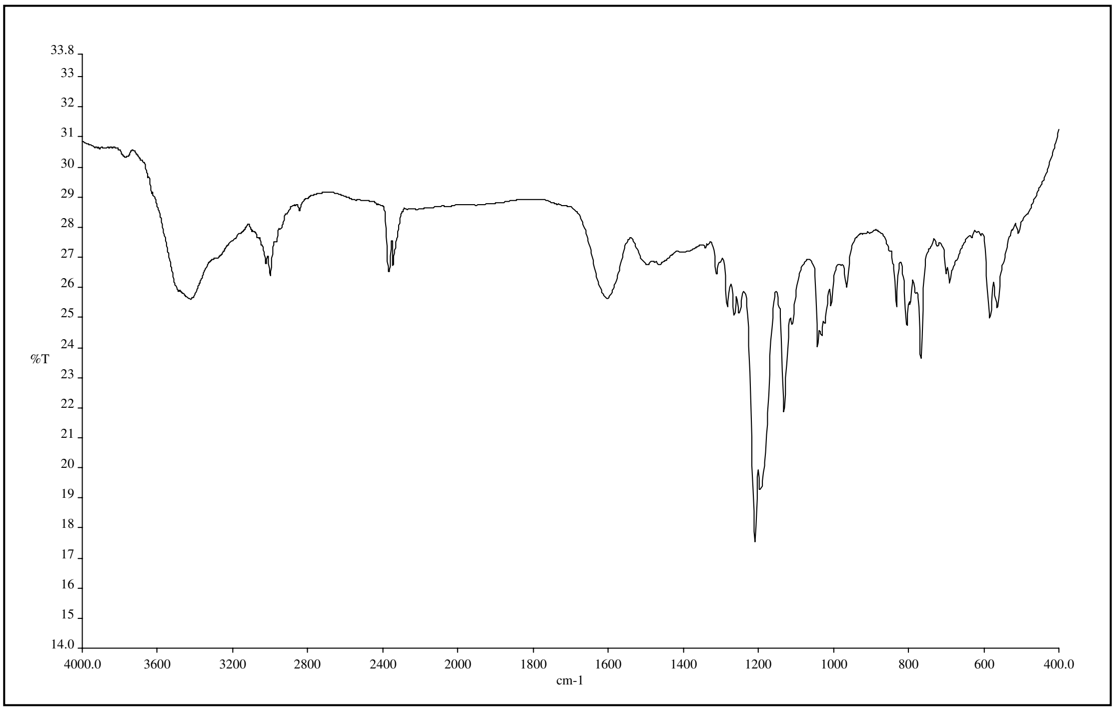

Figure 38 FT-IR (KBr) spectrum of compound **PNAP1O**

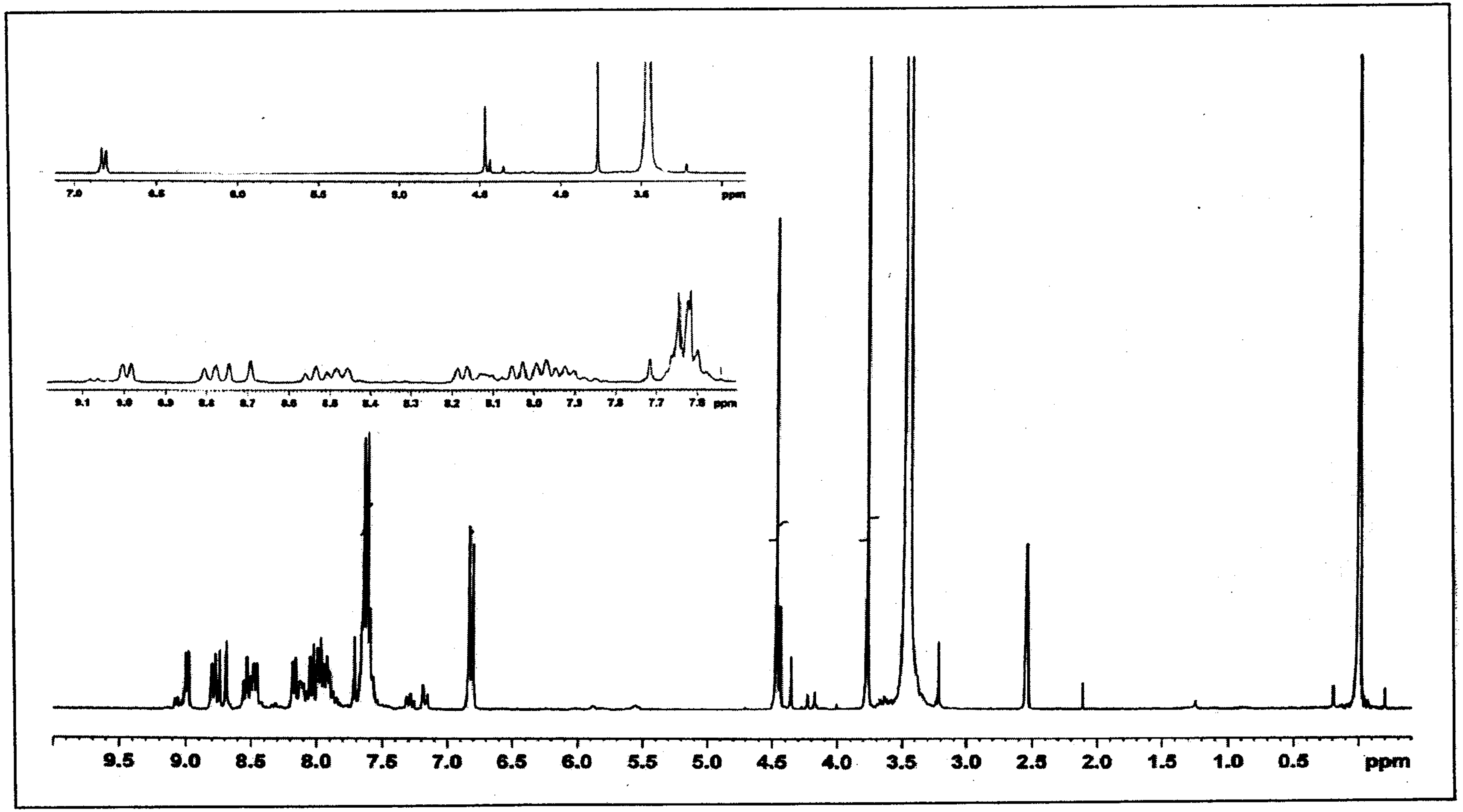

Figure 39 ^{1}H NMR (300 MHz, $CDCl_3$ + DMSO-d_6) spectrum of compound **PNAP1O**

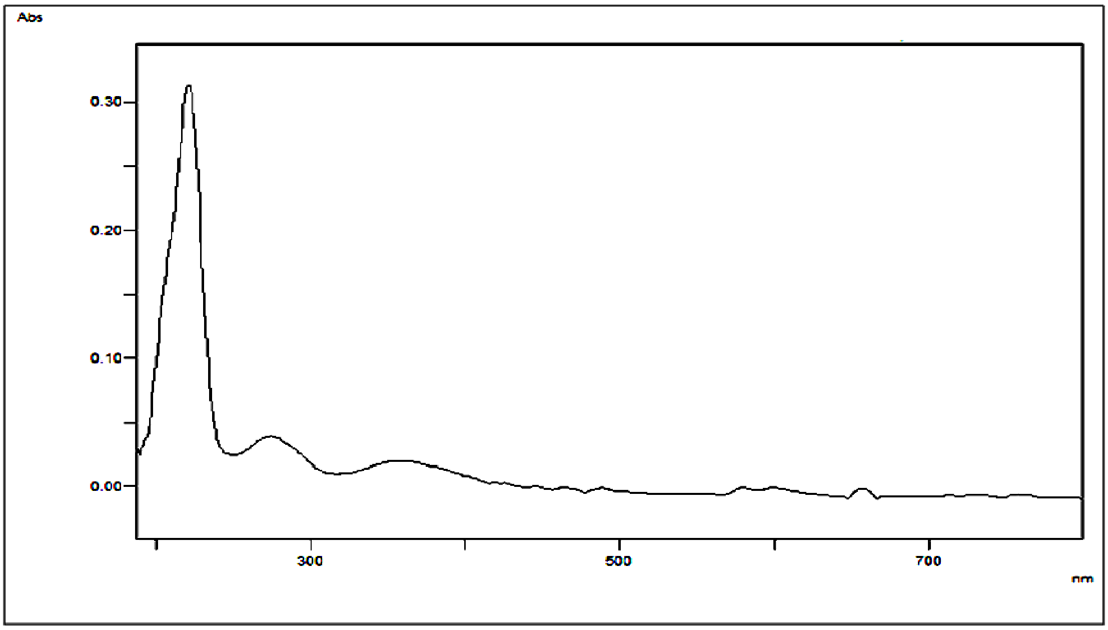

Figure 40 UV-Vis (CH_3OH) spectrum of compound **PNAP1C**

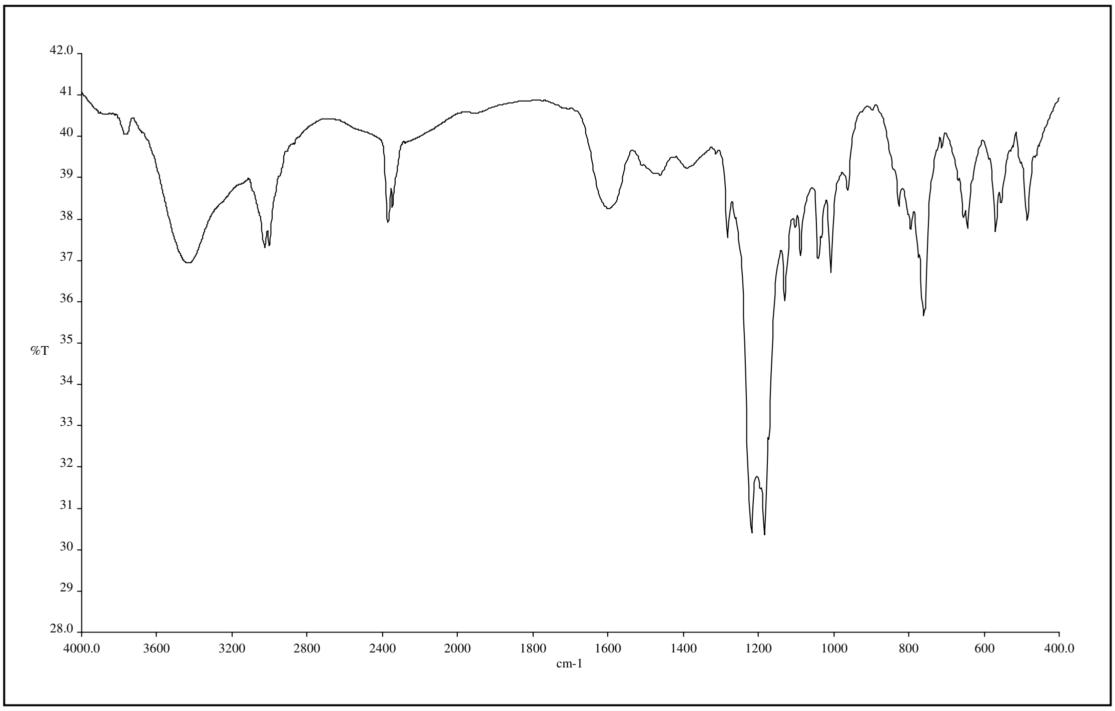

Figure 41 FT-IR (KBr) spectrum of compound **PNAP1C**

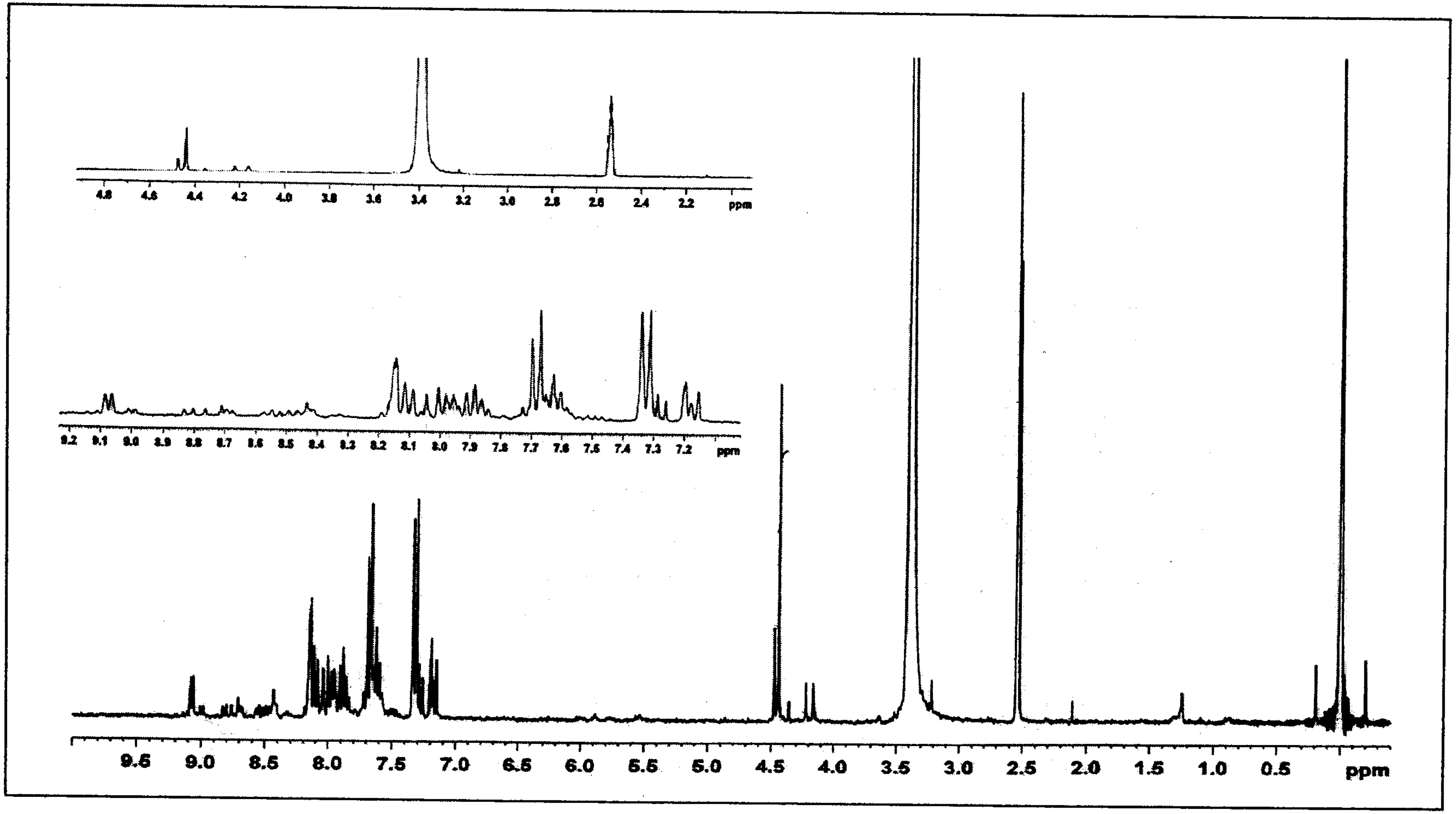

Figure 42 ^{1}H NMR (300 MHz, $CDCl_3$ + DMSO-d_6) spectrum of compound **PNAP1C**

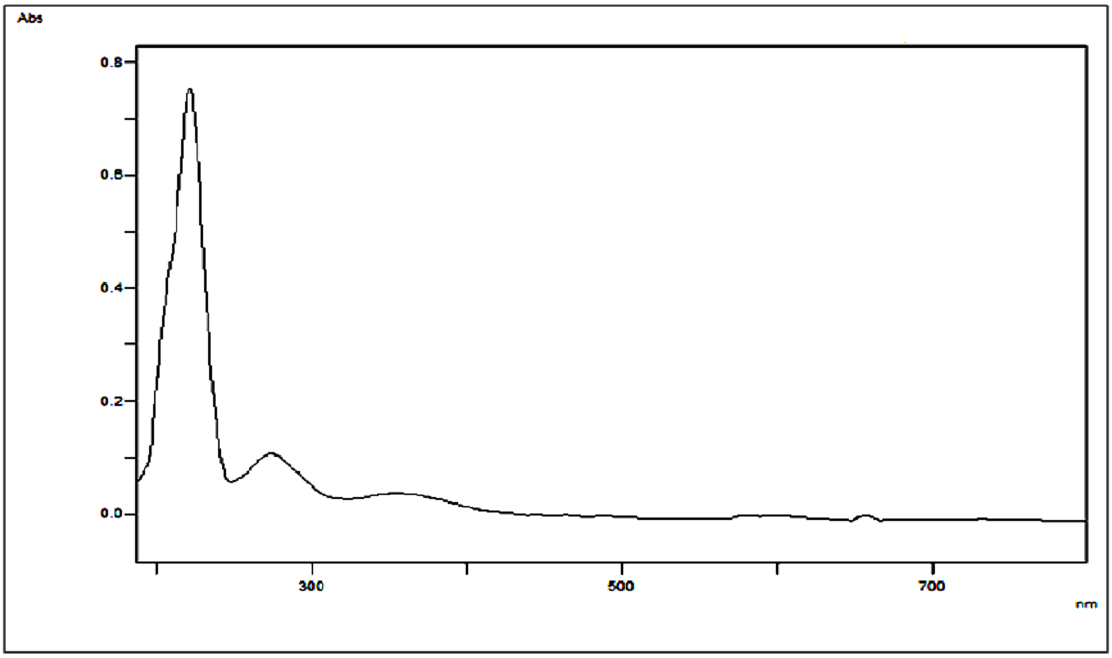

Figure 43 UV-Vis (CH_3OH) spectrum of compound **PNAP1B**

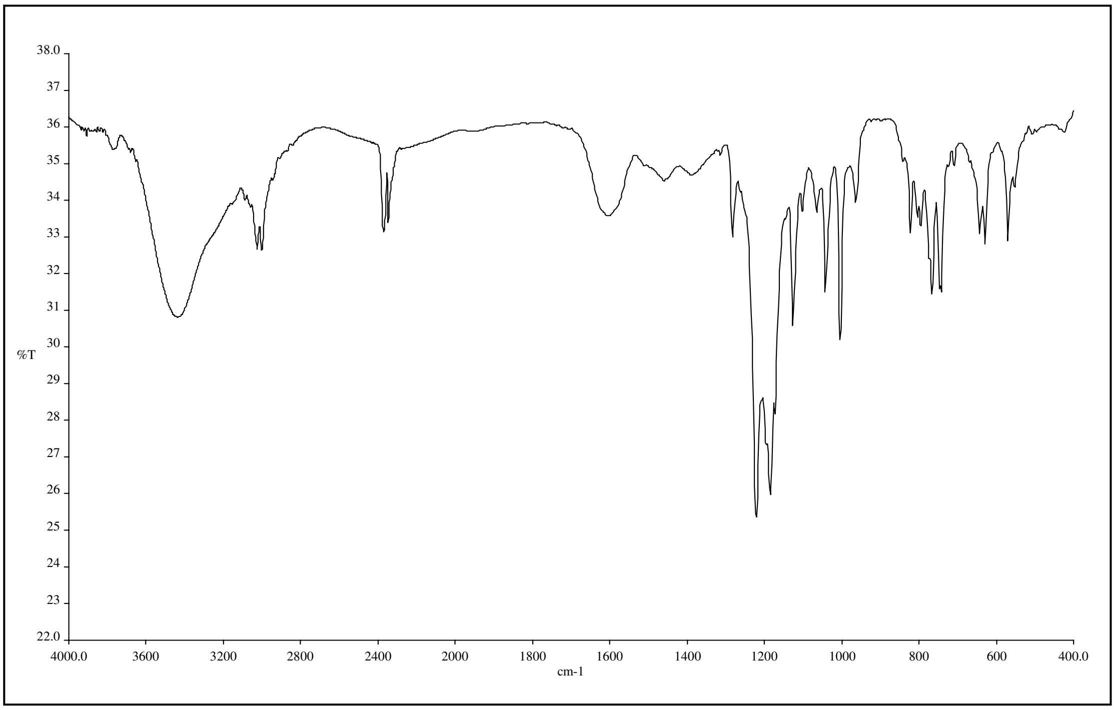

Figure 44 FT-IR (KBr) spectrum of compound **PNAP1B**

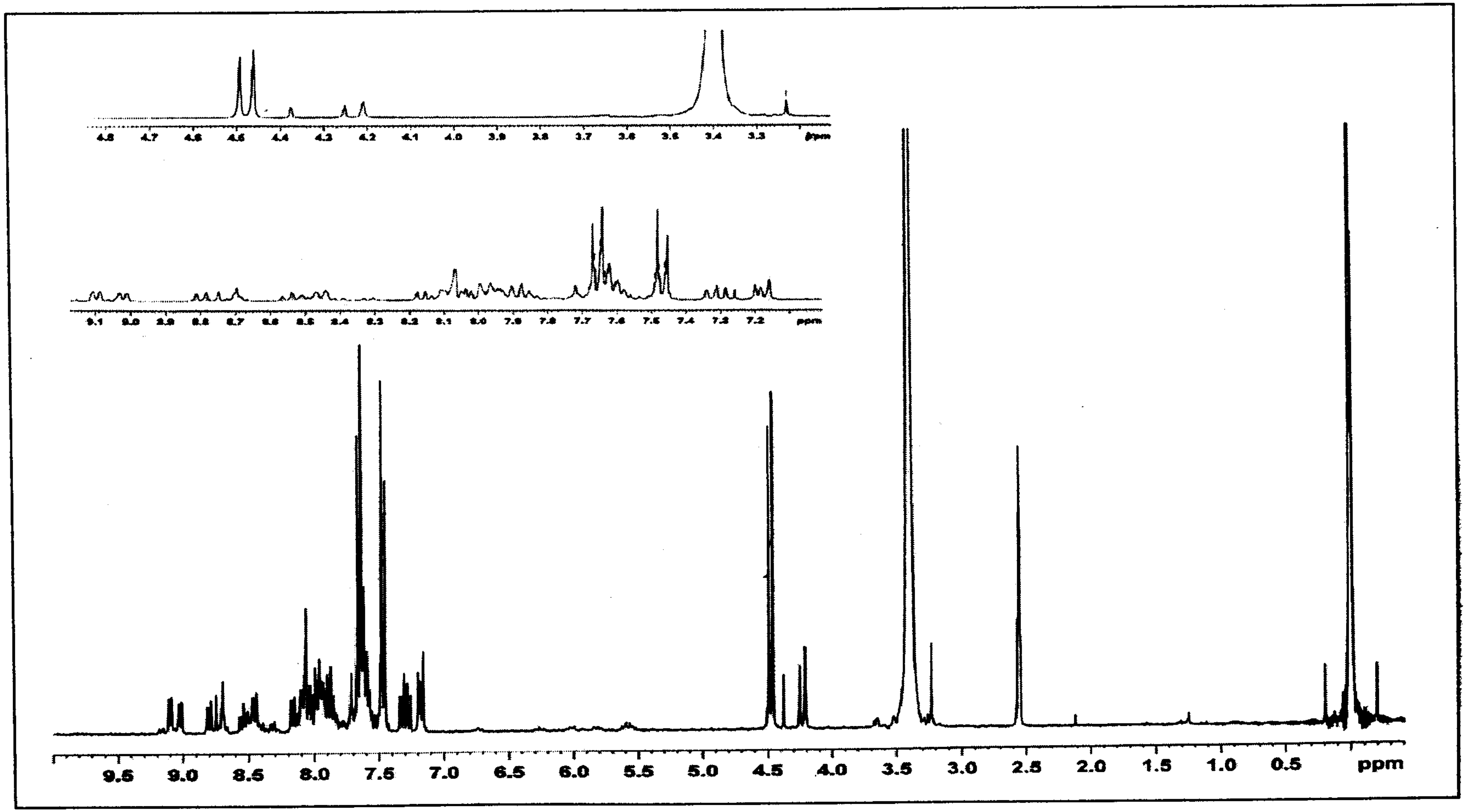

Figure 45 ^{1}H NMR (300 MHz, $CDCl_3$ + DMSO-d_6) spectrum of compound **PNAP1B**

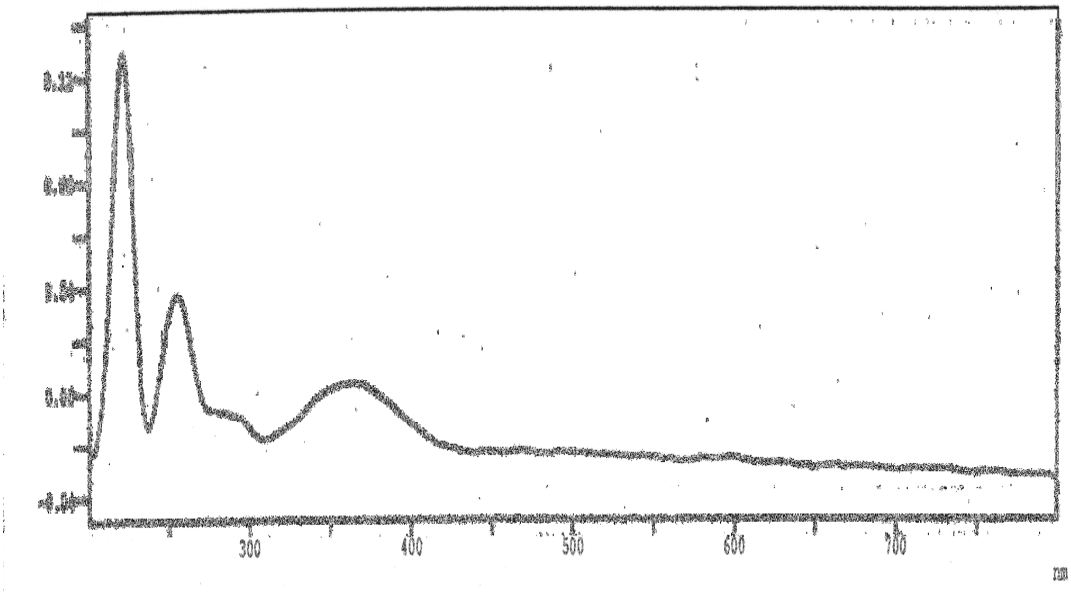

Figure 46 UV-Vis (CH_3OH) spectrum of compound **PNAP1N**

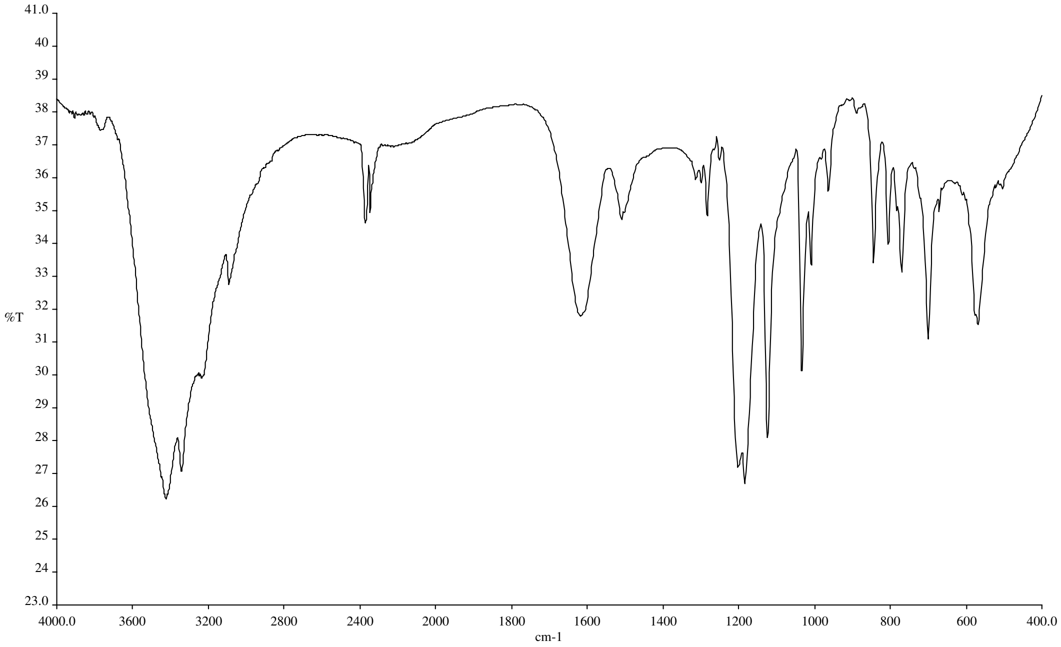

Figure 47 FT-IR (KBr) spectrum of compound **PNAP1N**

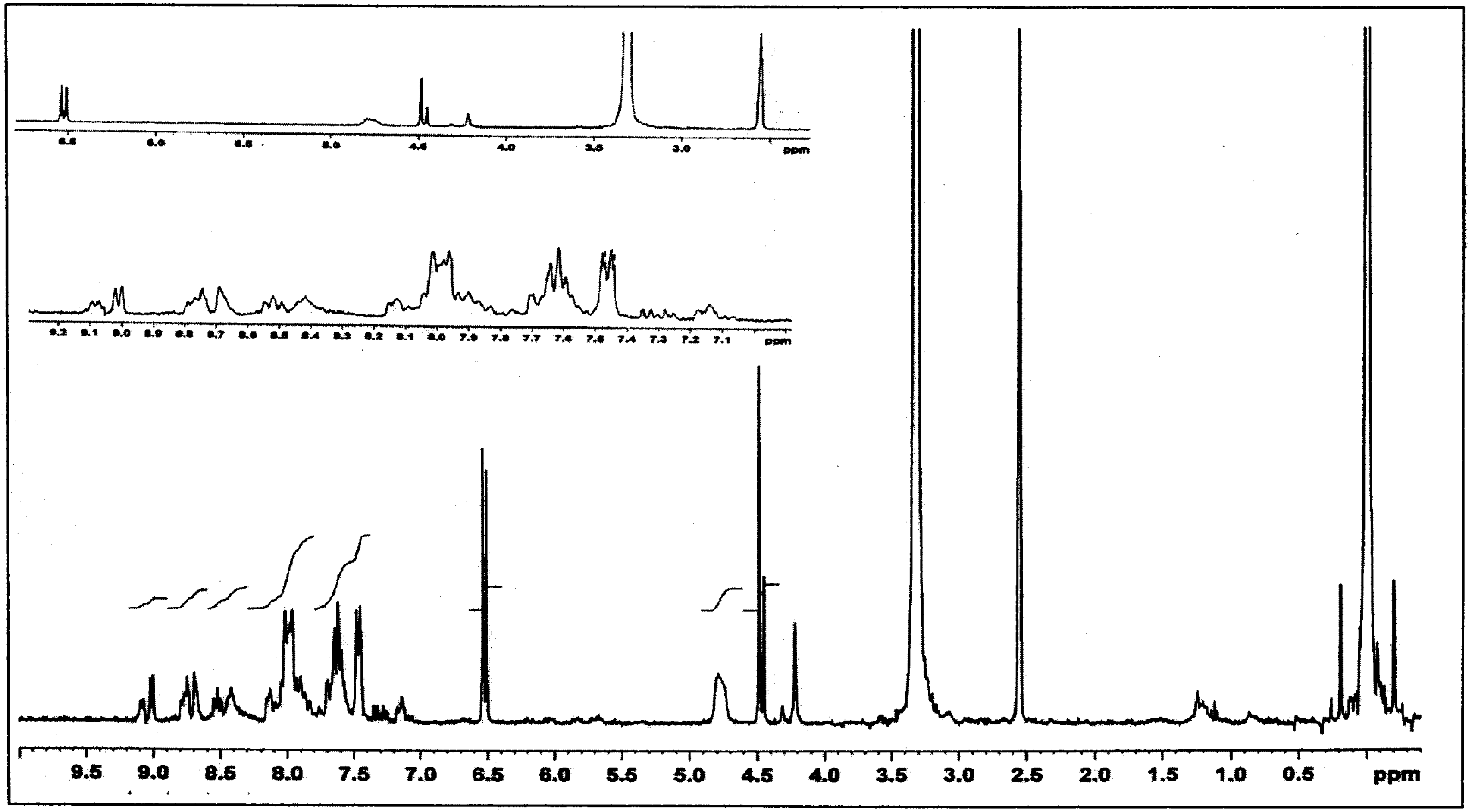

Figure 48 ^{1}H NMR (300 MHz, $CDCl_3$ + DMSO-d_6) spectrum of compound **PNAP1N**

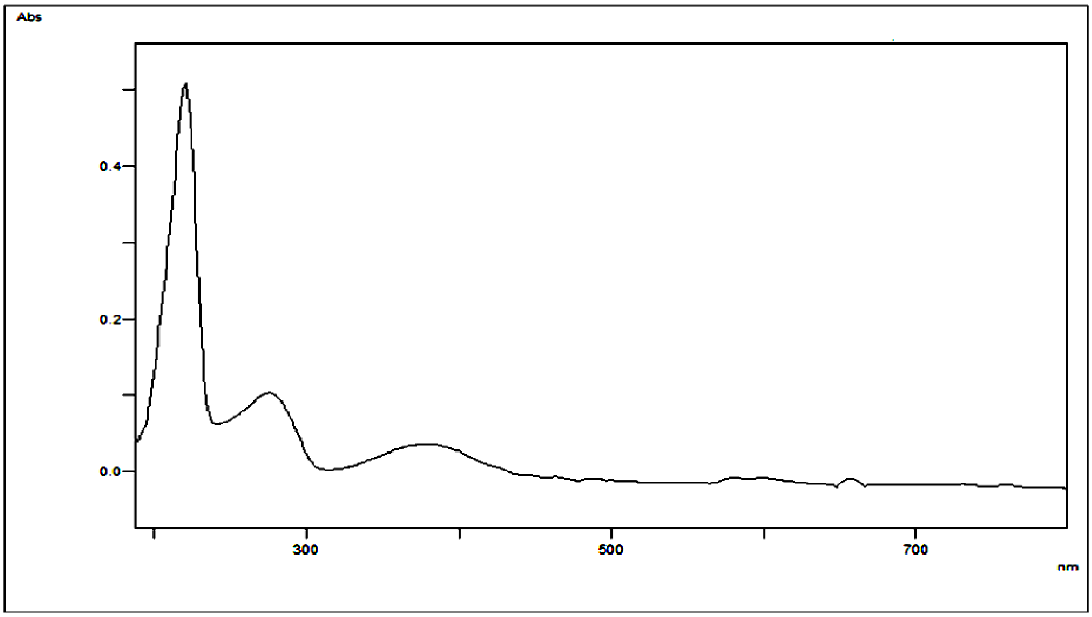

Figure 49 UV-Vis (CH_3OH) spectrum of compound **PNAP2M**

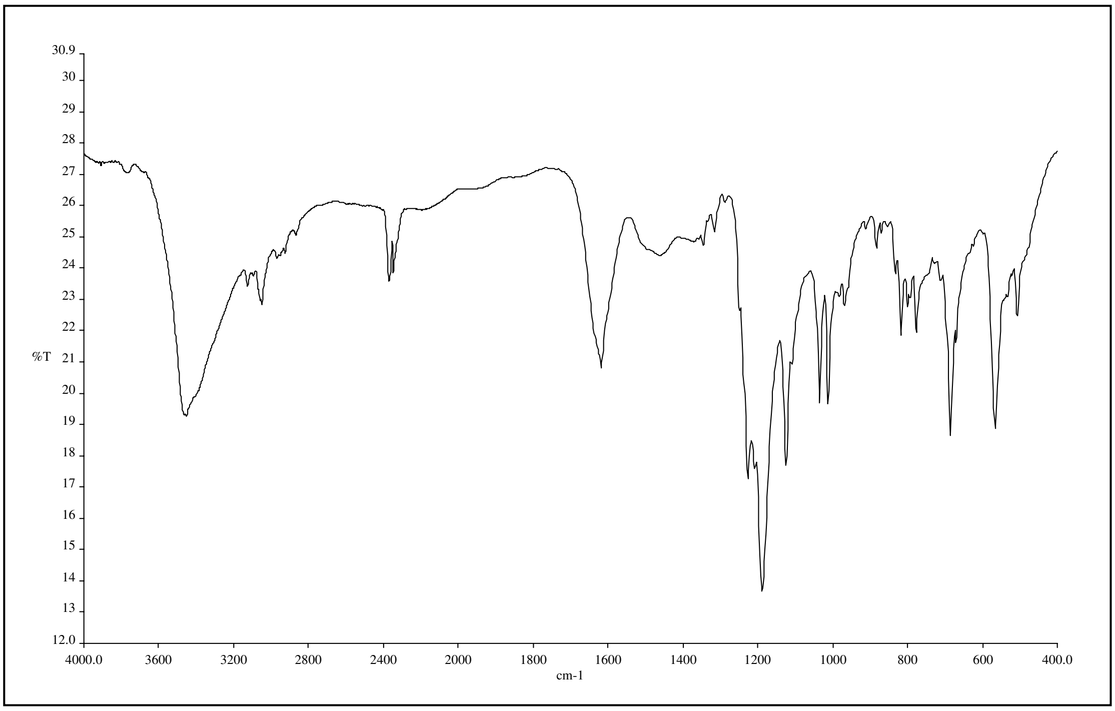

Figure 50 FT-IR (KBr) spectrum of compound **PNAP2M**

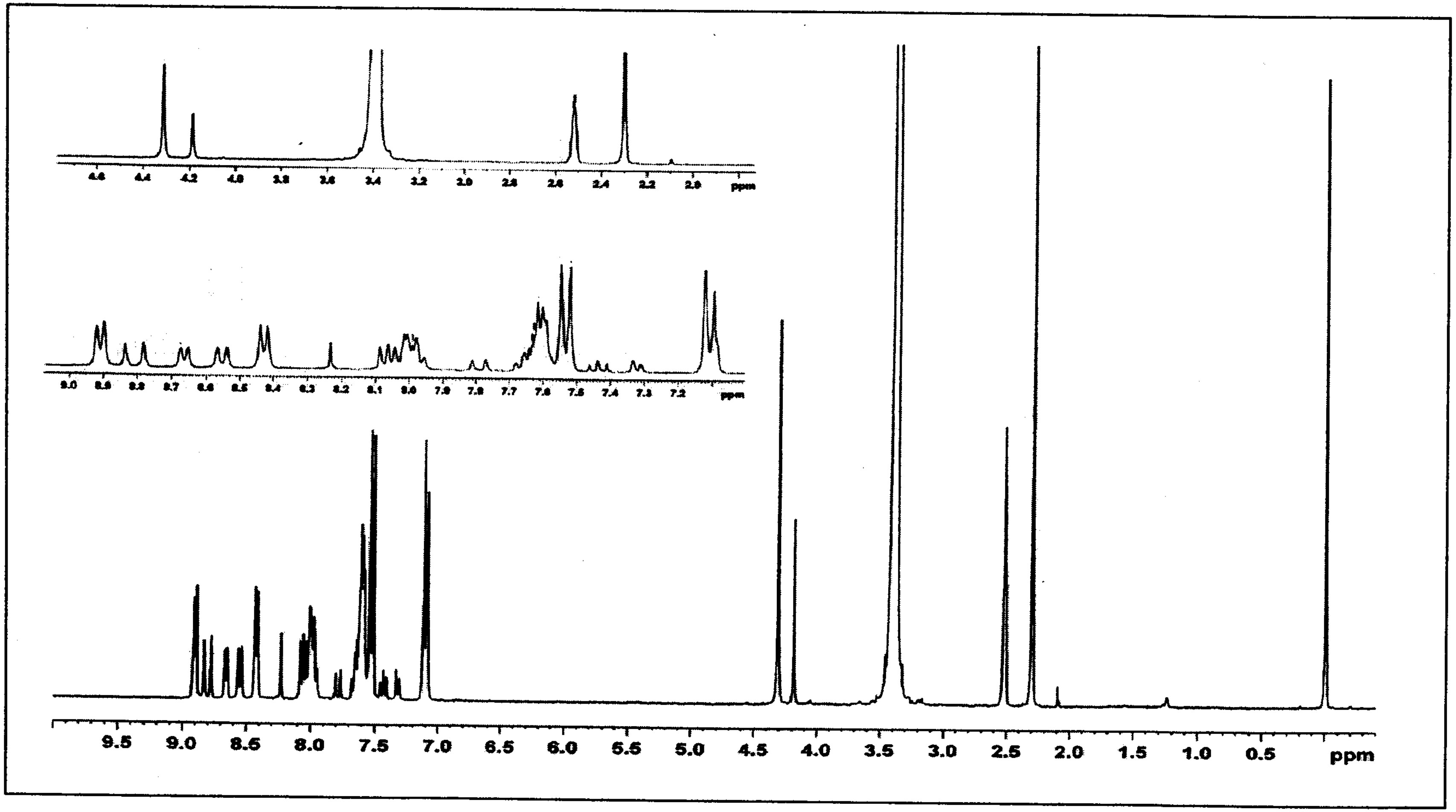

Figure 51 ^{1}H NMR (300 MHz, $CDCl_3$ + DMSO-d_6) spectrum of compound **PNAP2M**

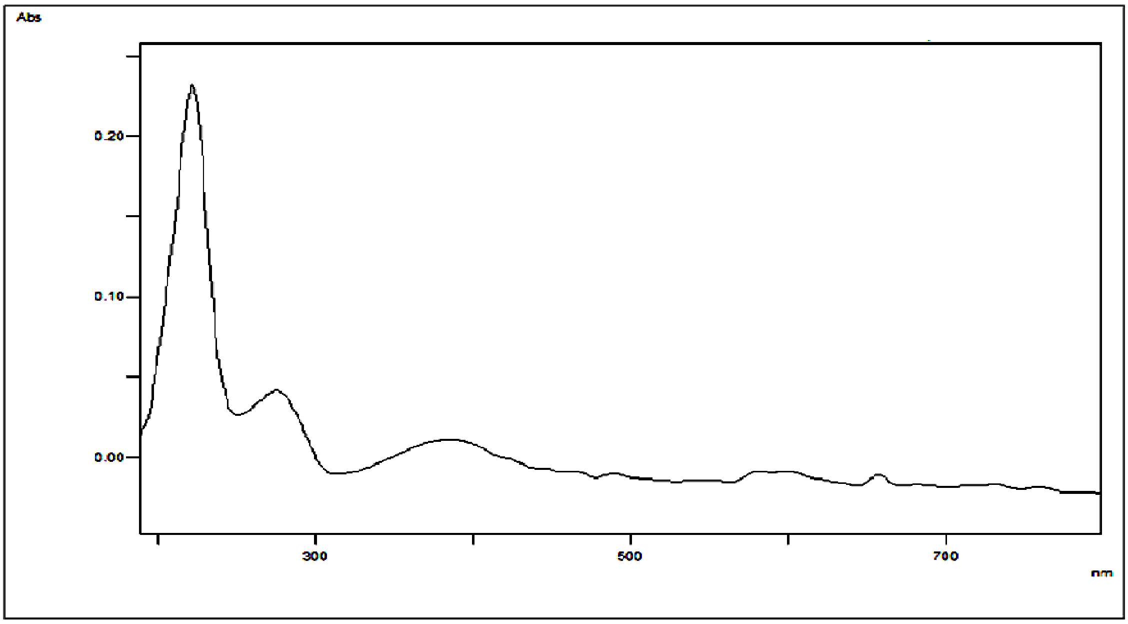

Figure 52 UV-Vis (CH_3OH) spectrum of compound **PNAP2O**

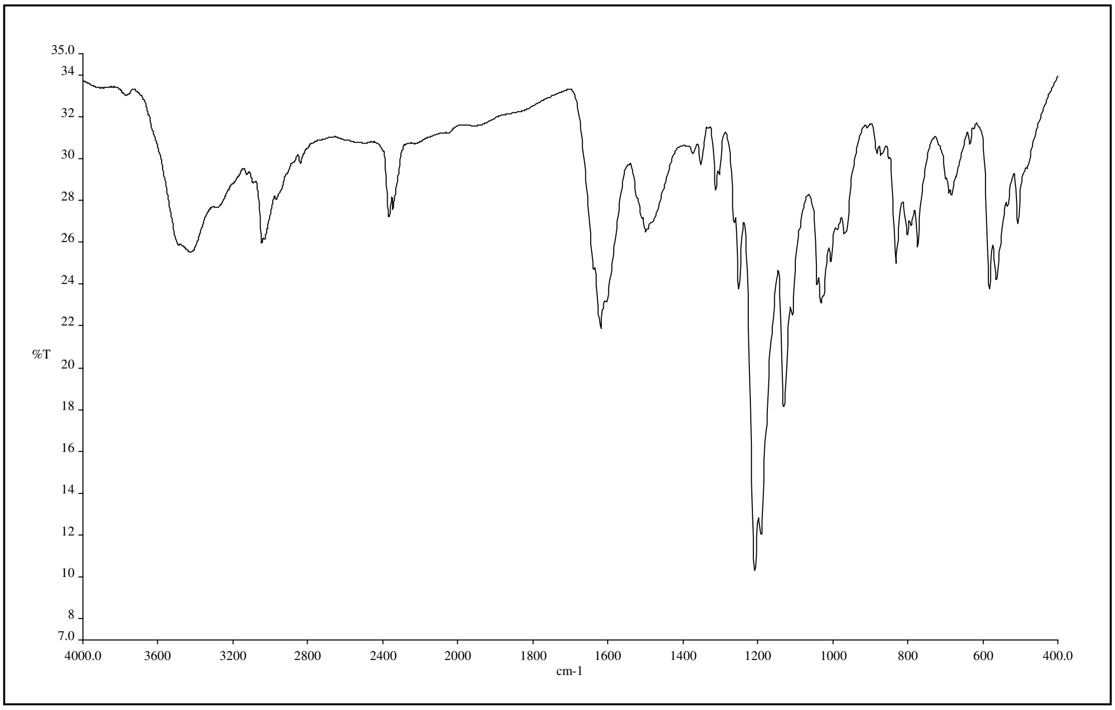

Figure 53 FT-IR (KBr) spectrum of compound **PNAP2O**

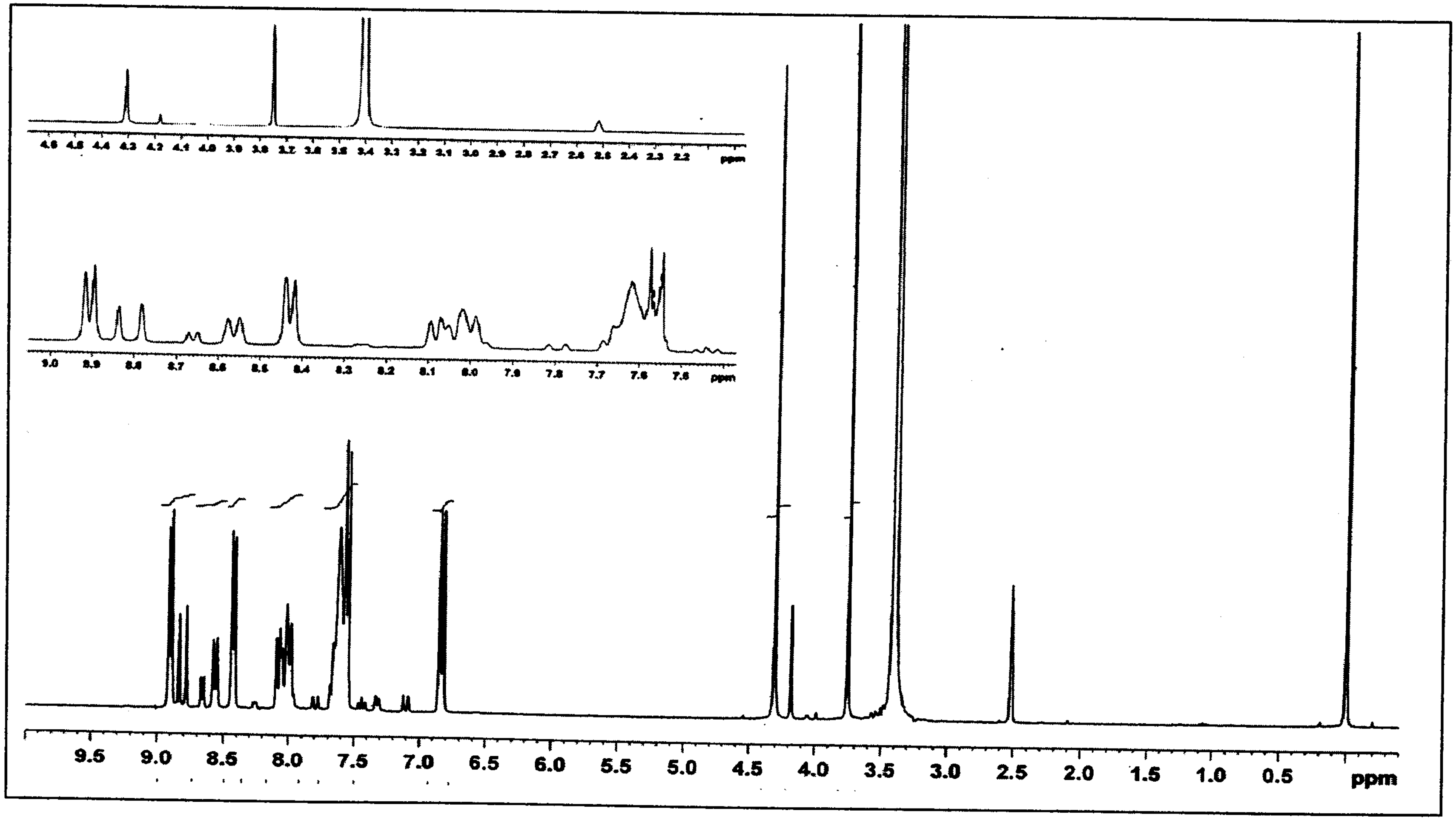

Figure 54 ^{1}H NMR (300 MHz, $CDCl_3$ + DMSO-d_6) spectrum of compound **PNAP2O**

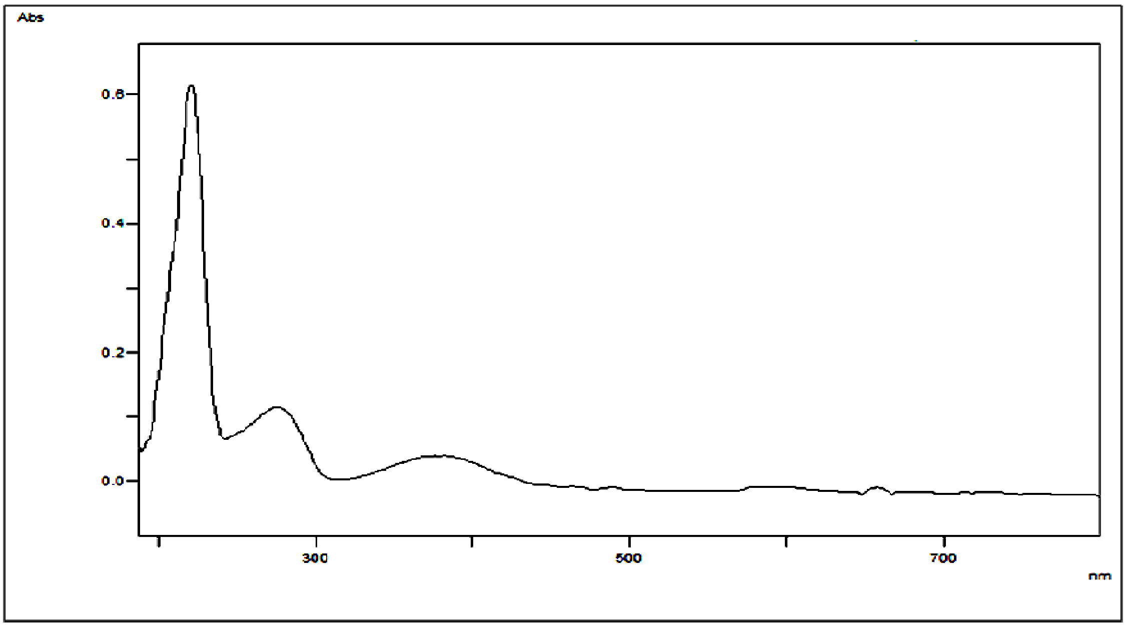

Figure 55 UV-Vis (CH_3OH) spectrum of compound **PNAP2C**

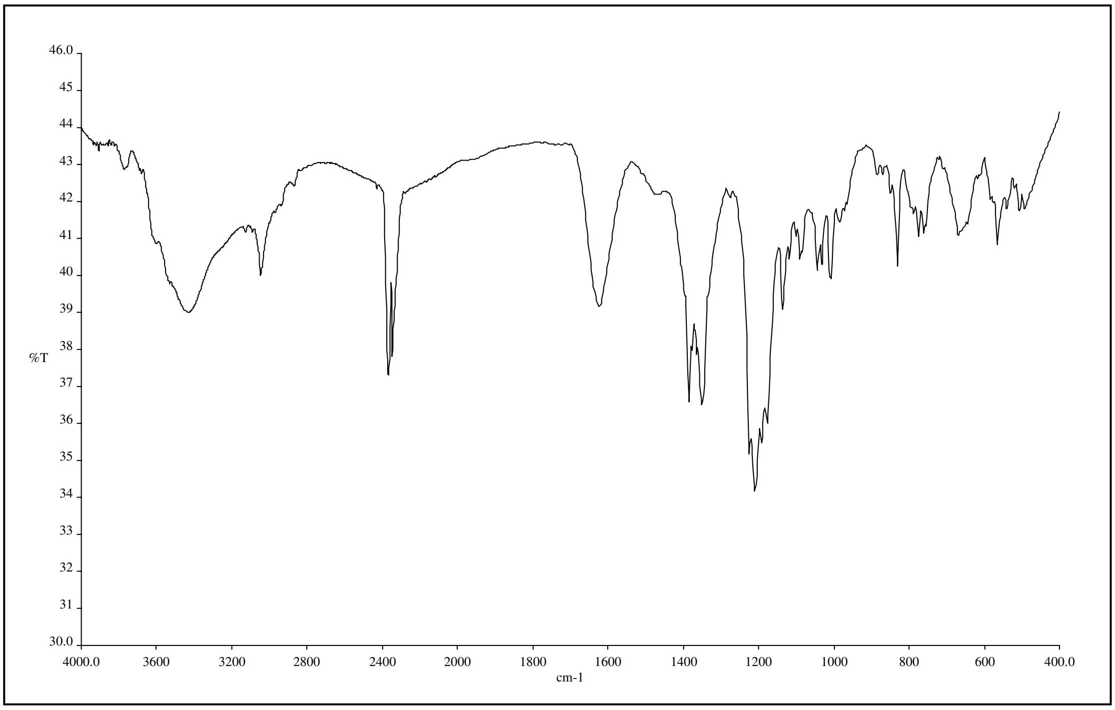

Figure 56 FT-IR (KBr) spectrum of compound **PNAP2C**

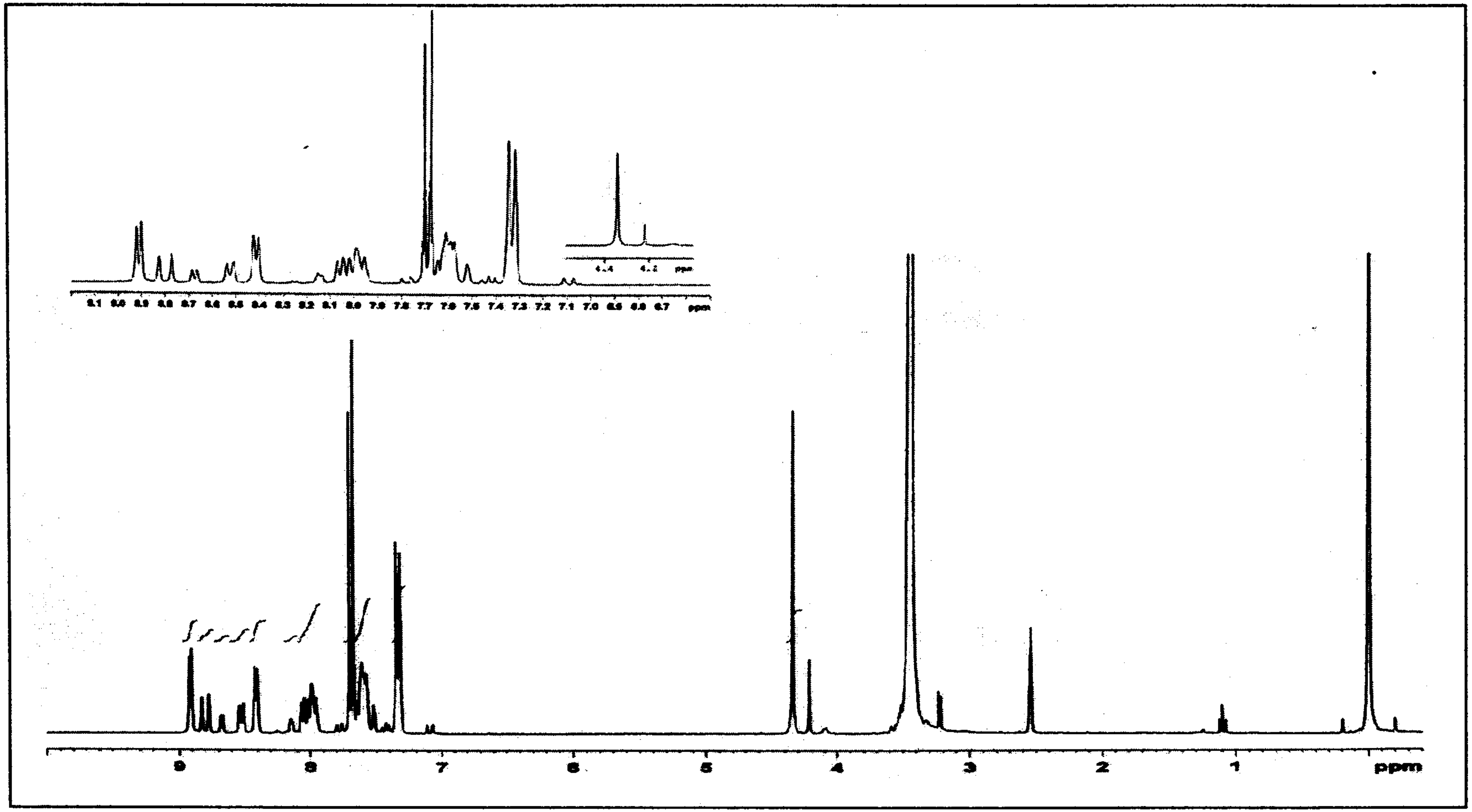

Figure 57 ^{1}H NMR (300 MHz, $CDCl_3$ + DMSO-d_6) spectrum of compound **PNAP2C**

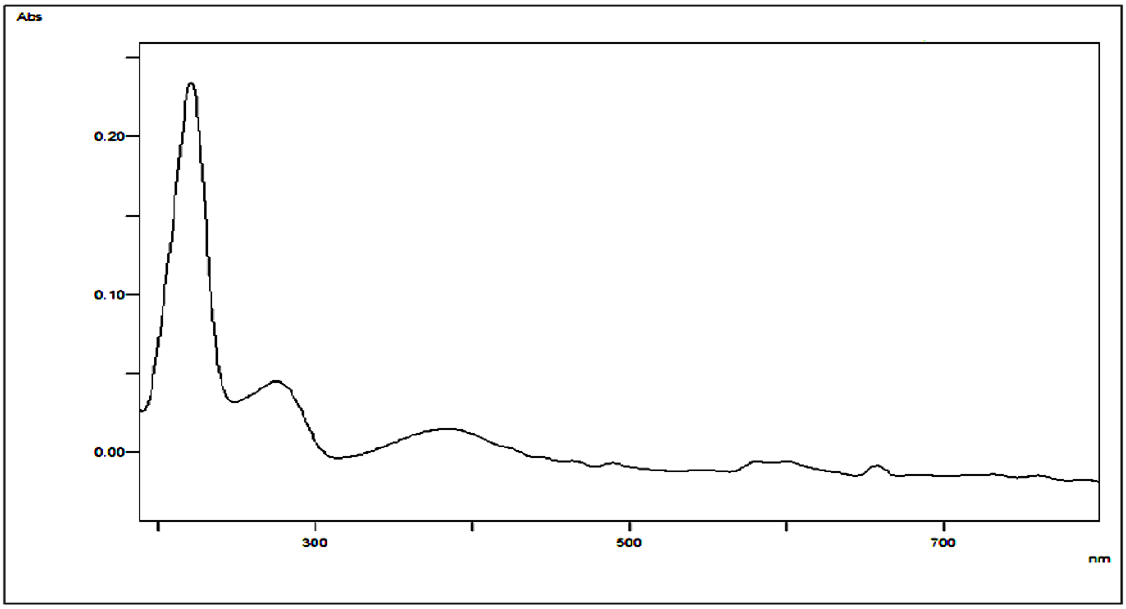

Figure 58 UV-Vis (CH_3OH) spectrum of compound **PNAP2B**

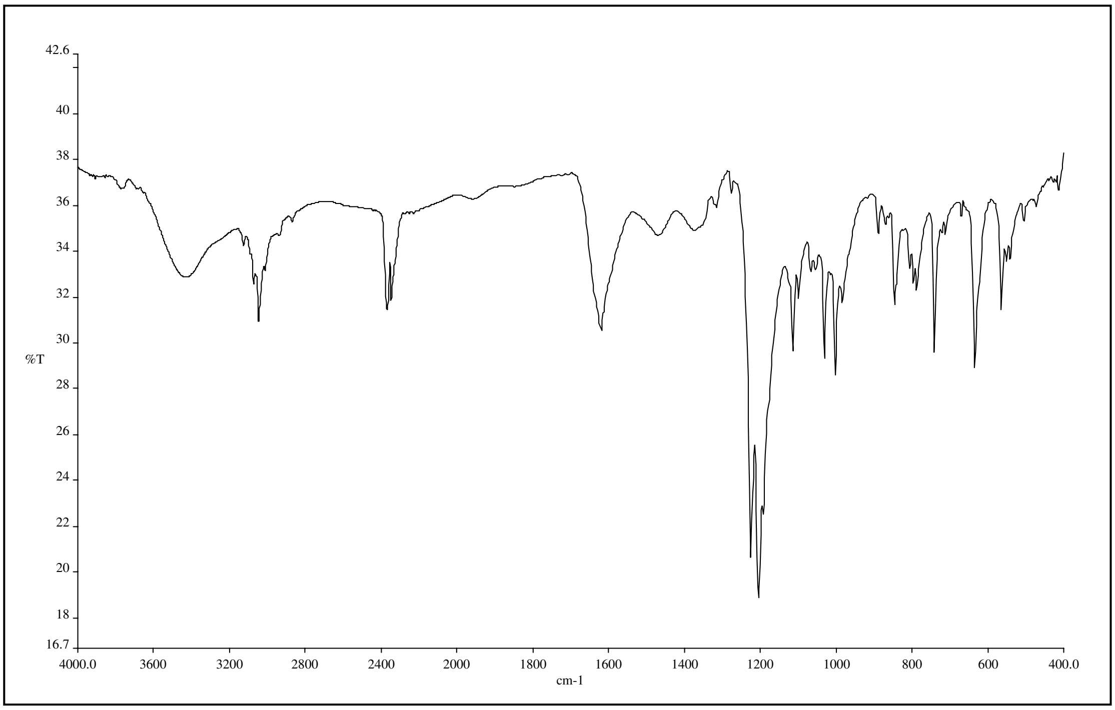

Figure 59 FT-IR (KBr) spectrum of compound **PNAP2B**

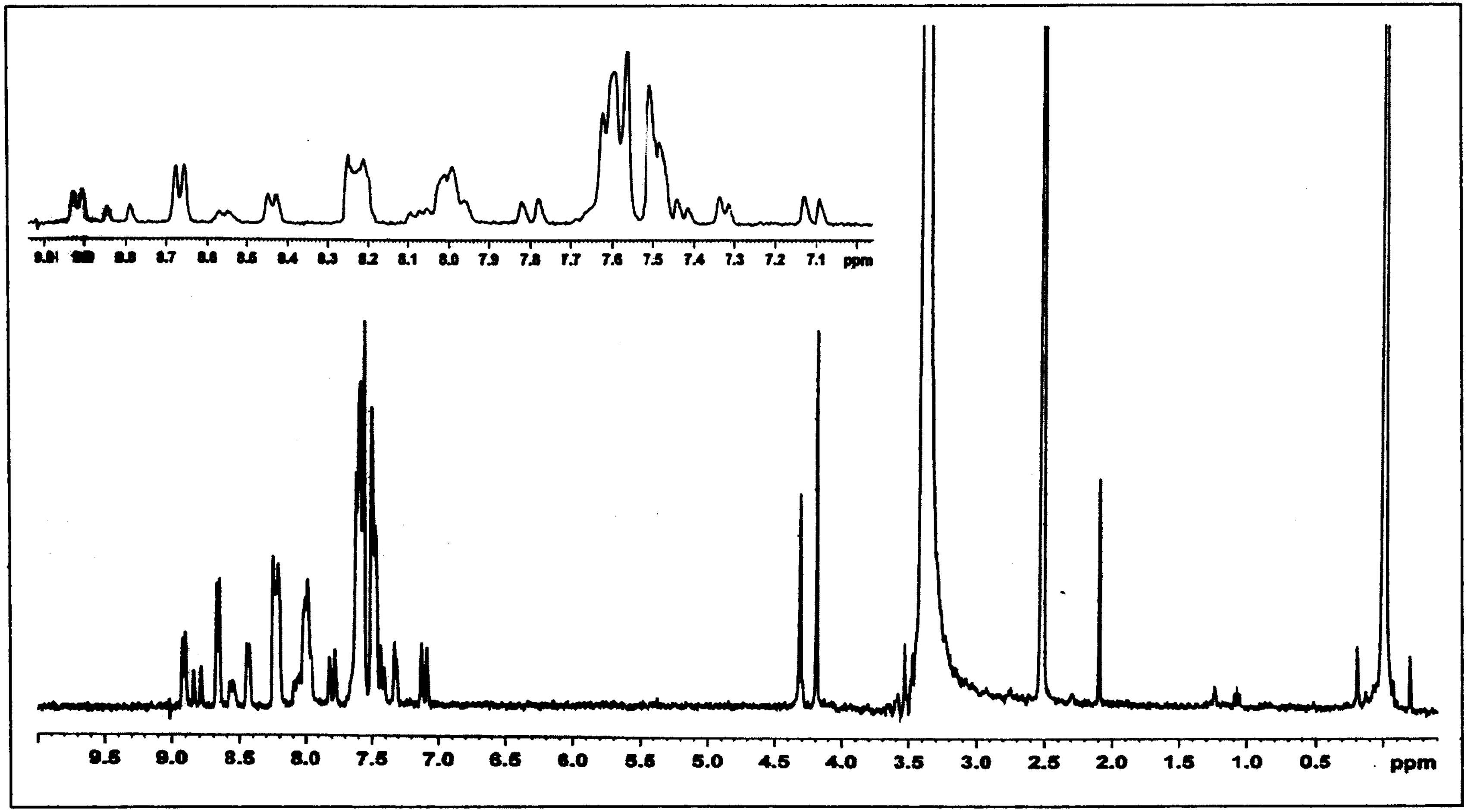

Figure 60 ^{1}H NMR (300 MHz, $CDCl_3$ + DMSO-d_6) spectrum of compound **PNAP2B**

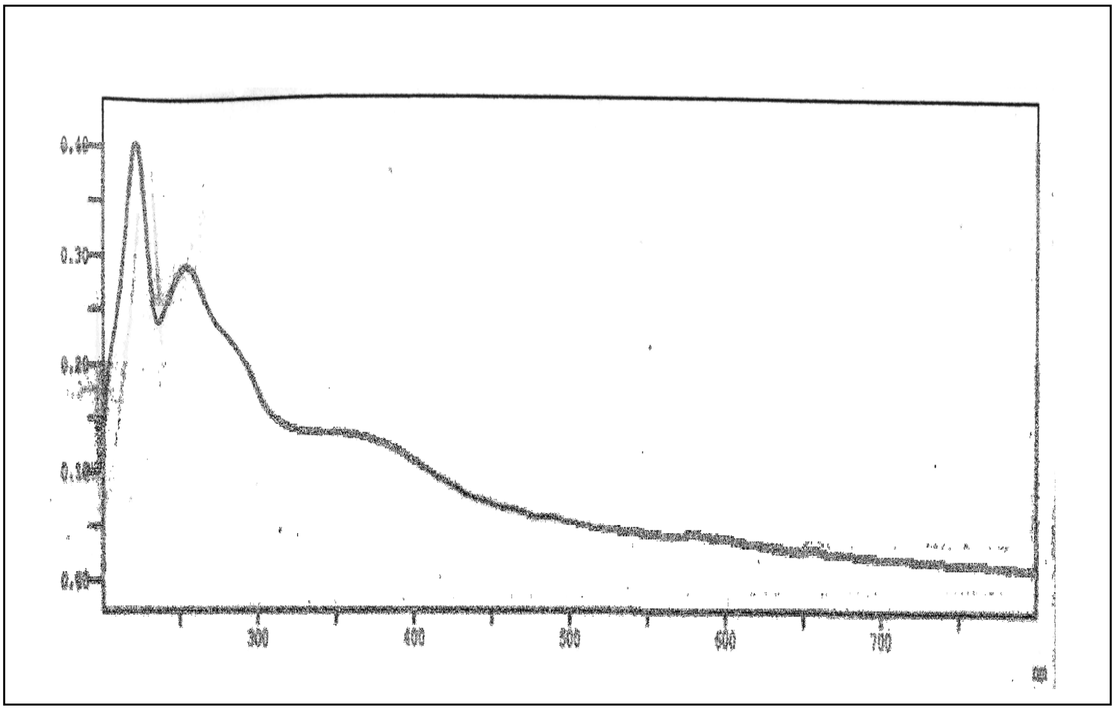

Figure 61 UV-Vis (CH_3OH) spectrum of compound **PNAP2N**

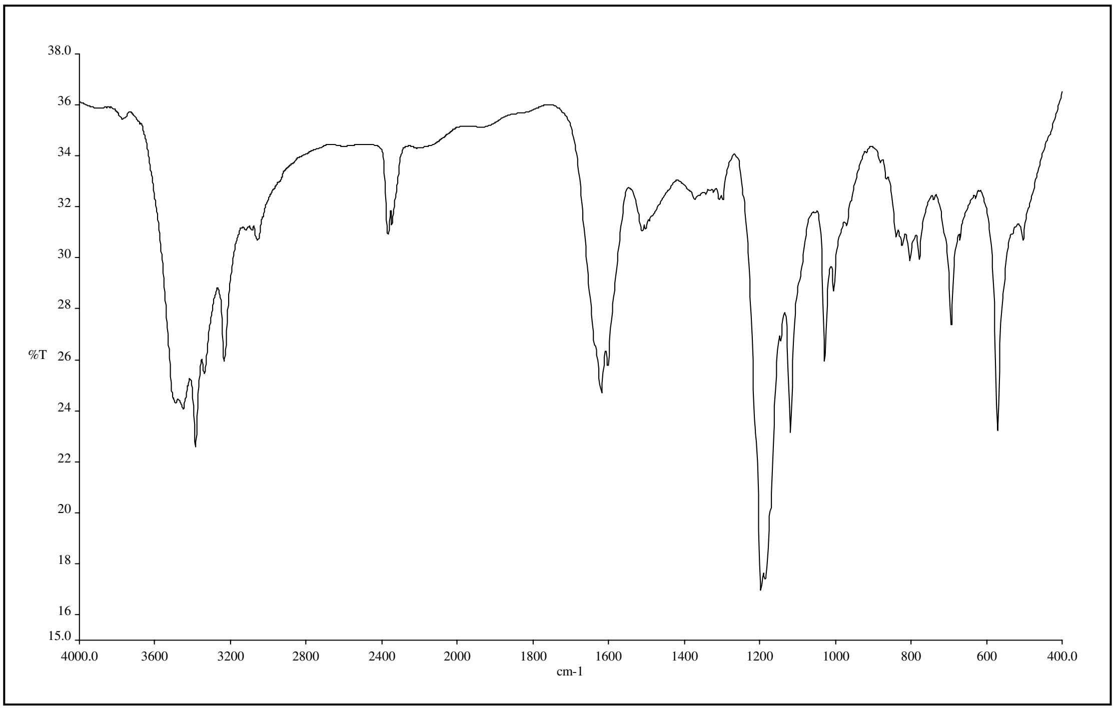

Figure 62 FT-IR (KBr) spectrum of compound **PNAP2N**

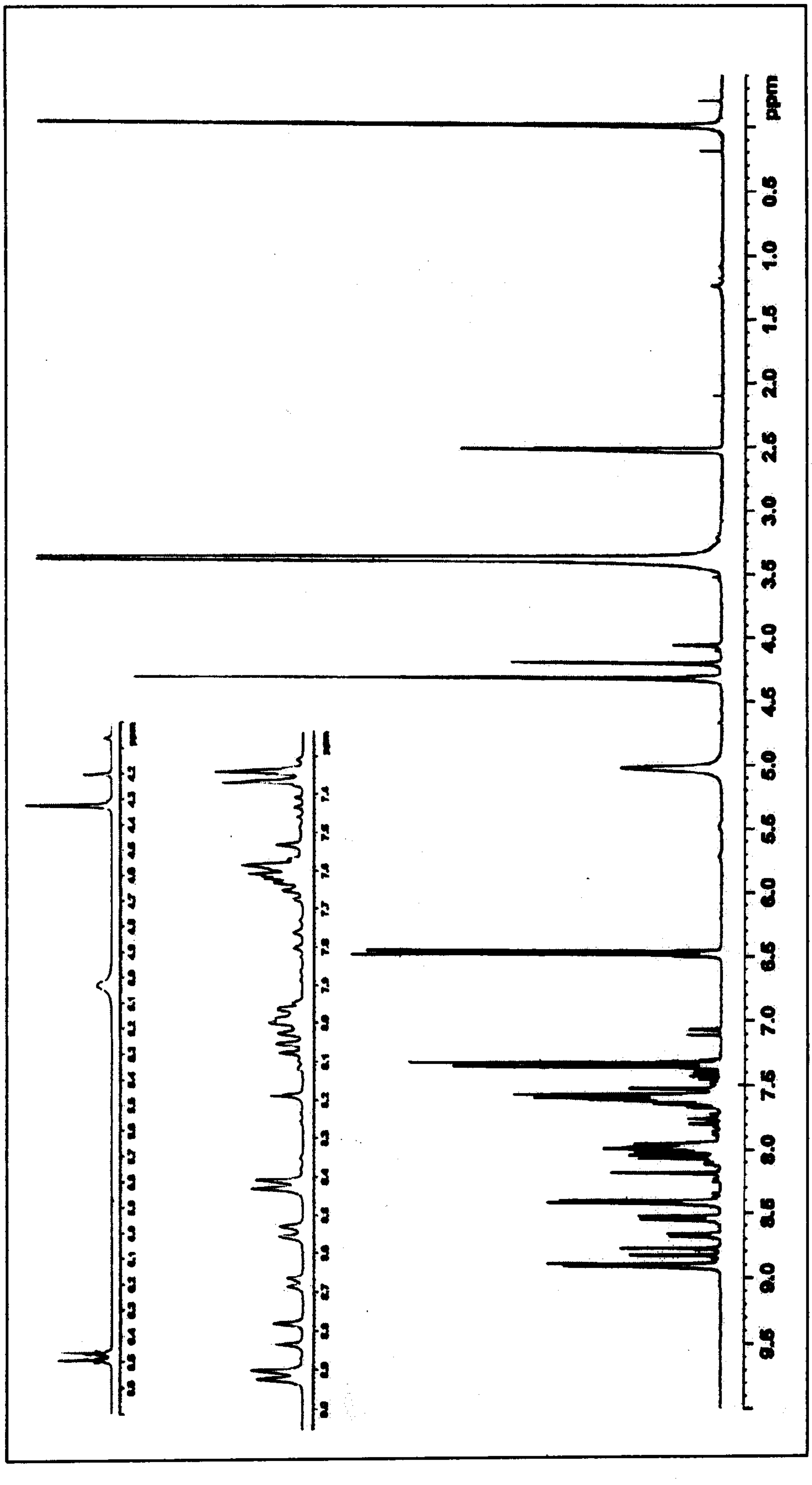

Figure 63 ¹H NMR (300 MHz, $CDCl_3$ + DMSO-d_6) spectrum of compound PNAP2N

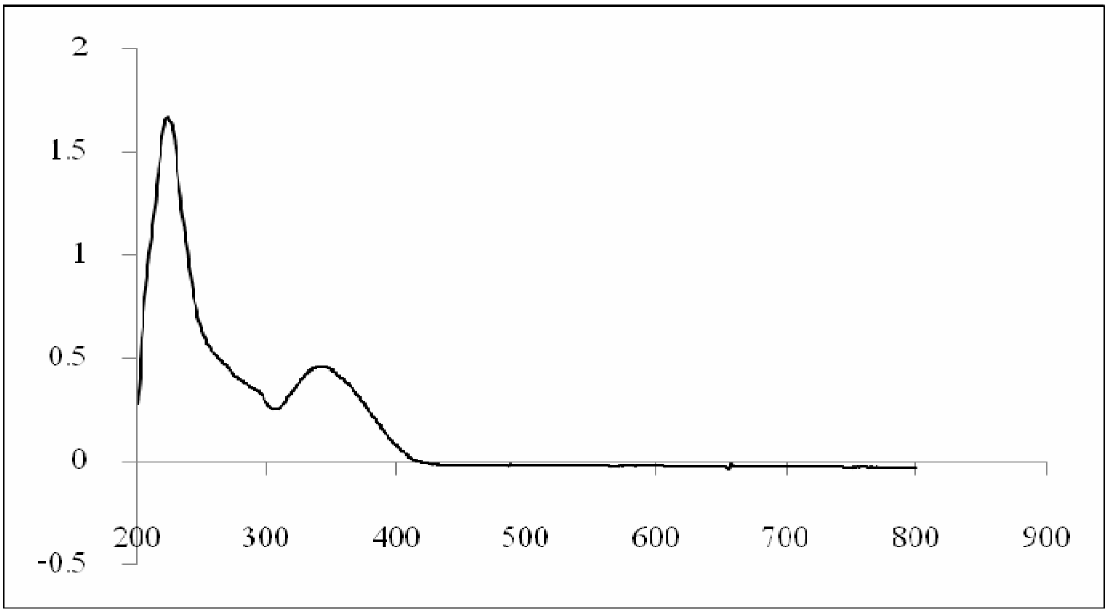

Figure 64 UV-Vis (CH_3OH) spectrum of compound **PNAP3M**

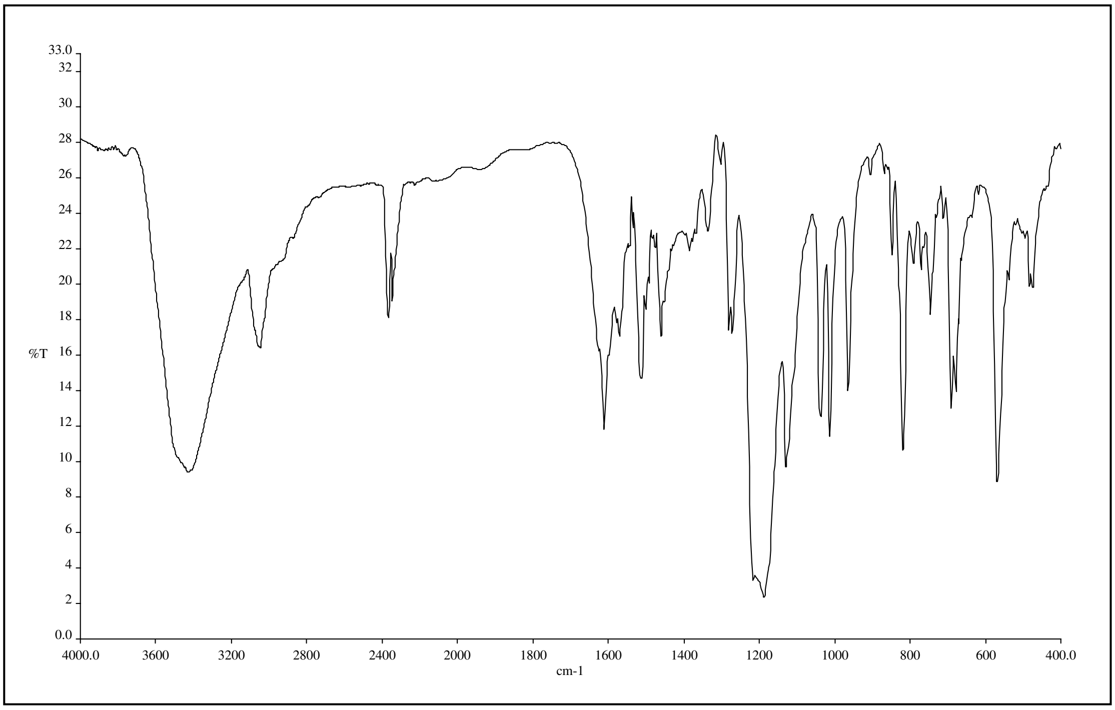

Figure 65 FT-IR (KBr) spectrum of compound **PNAP3M**

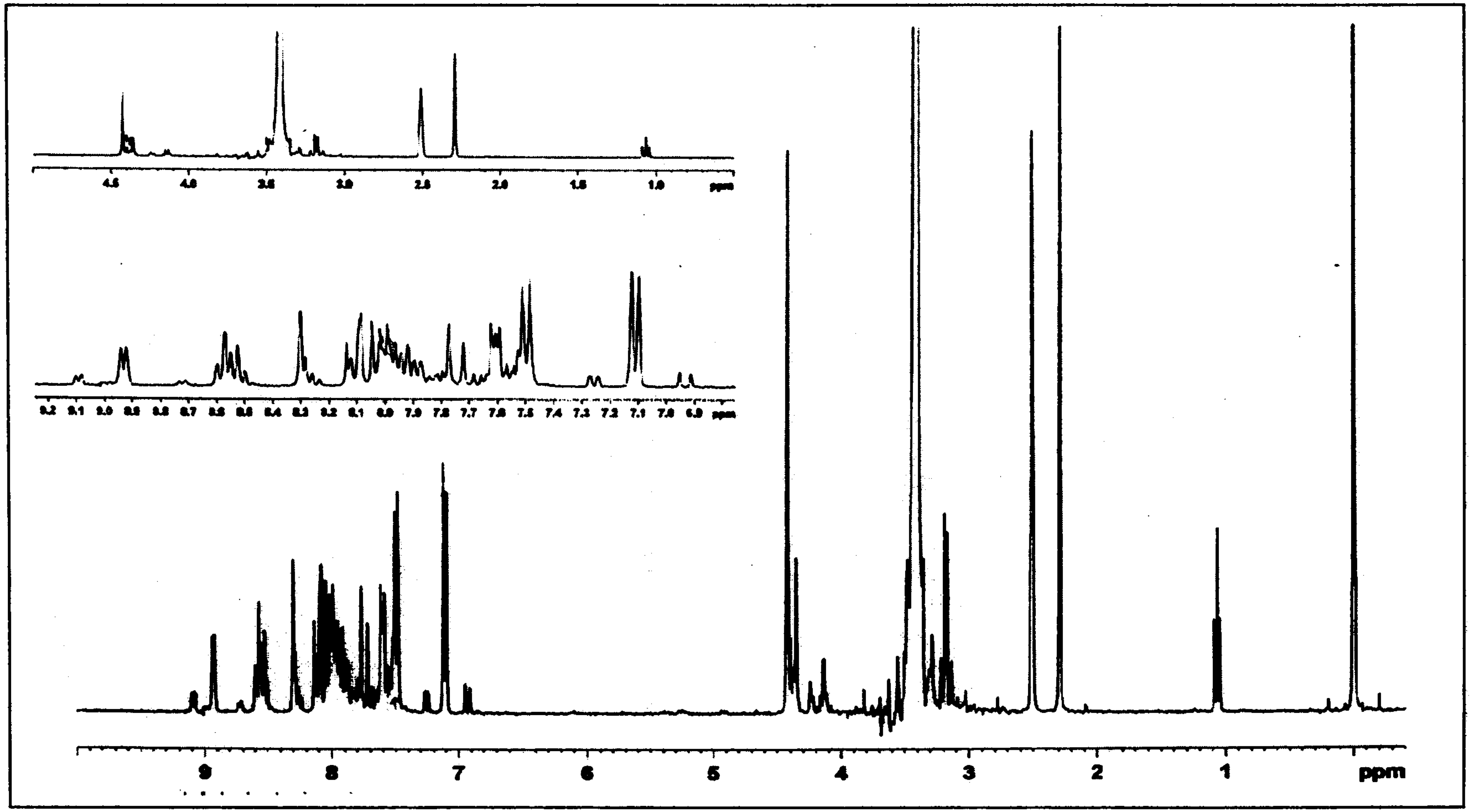

Figure 66 ^{1}H NMR (300 MHz, $CDCl_3$ + DMSO-d_6) spectrum of compound **PNAP3M**

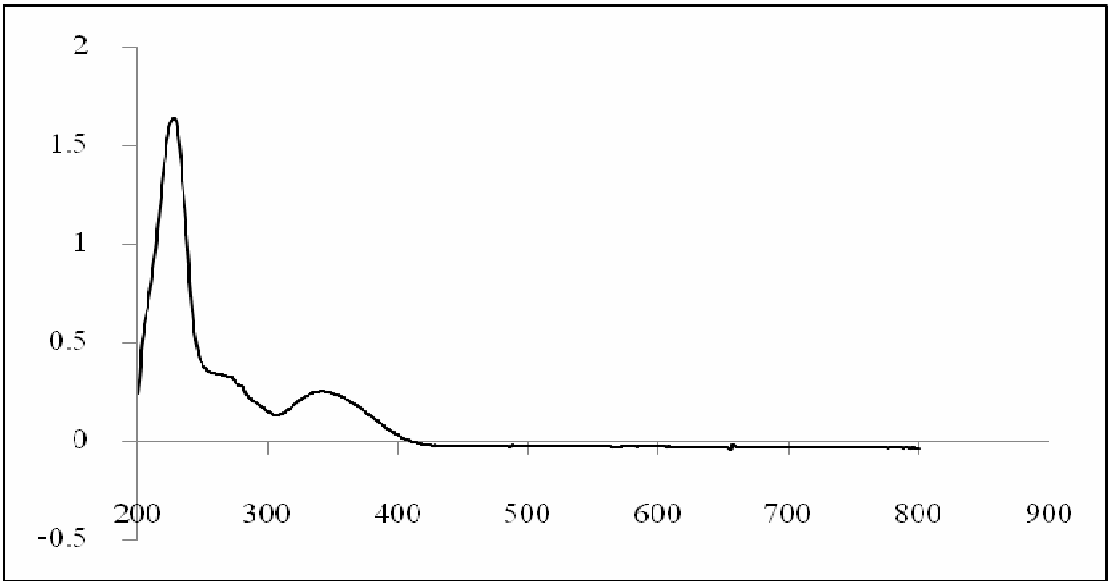

Figure 67 UV-Vis (CH_3OH) spectrum of compound **PNAP3O**

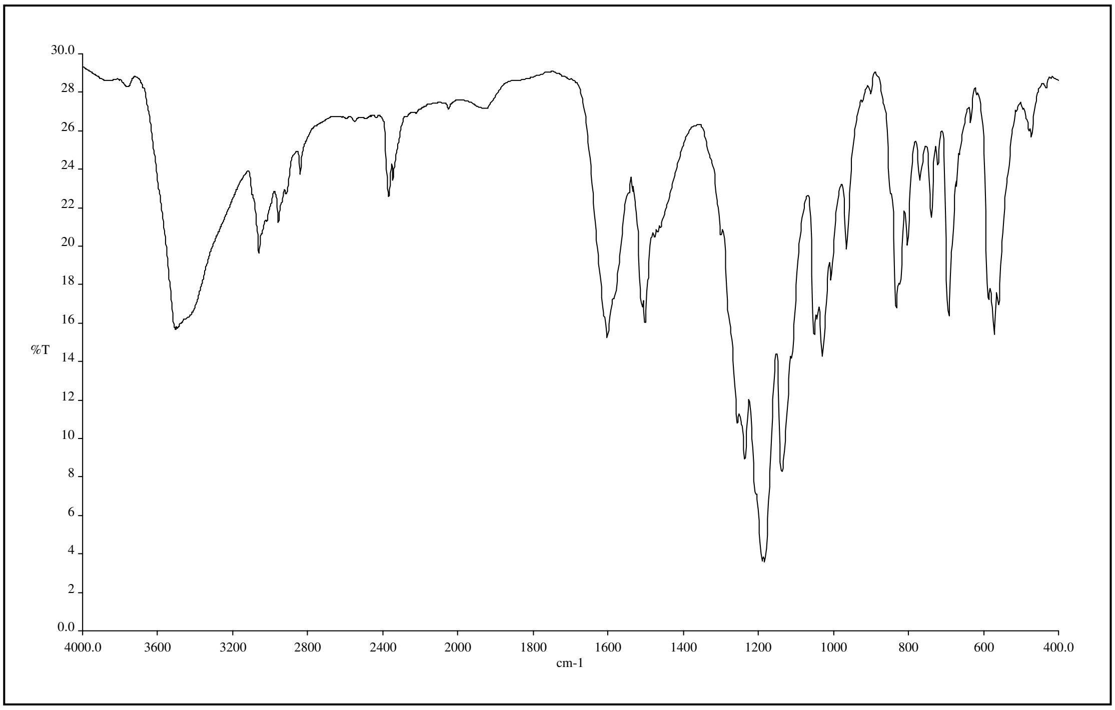

Figure 68 FT-IR (KBr) spectrum of compound **PNAP3O**

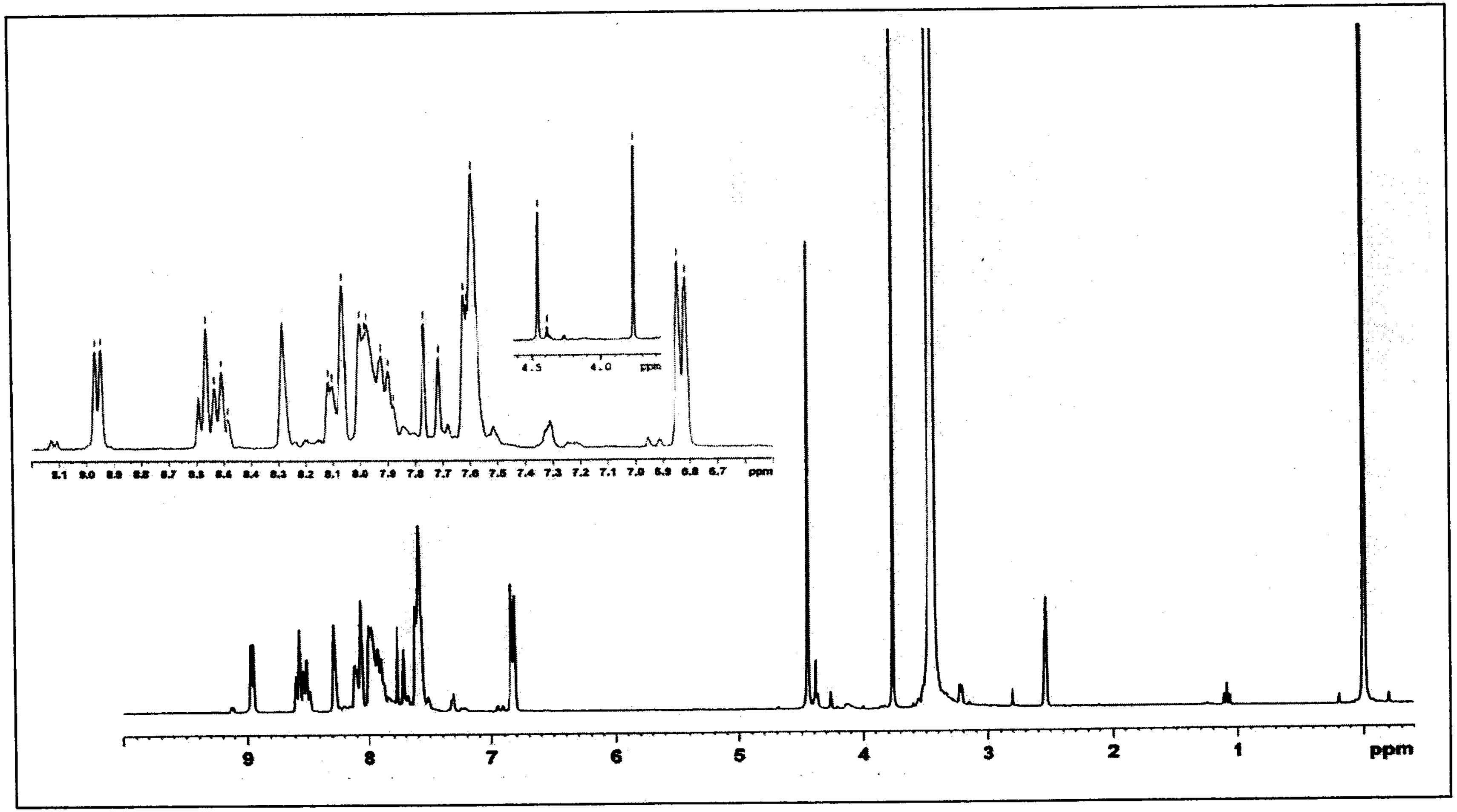

Figure 69 ^{1}H NMR (300 MHz, $CDCl_3$ + DMSO-d_6) spectrum of compound **PNAP3O**

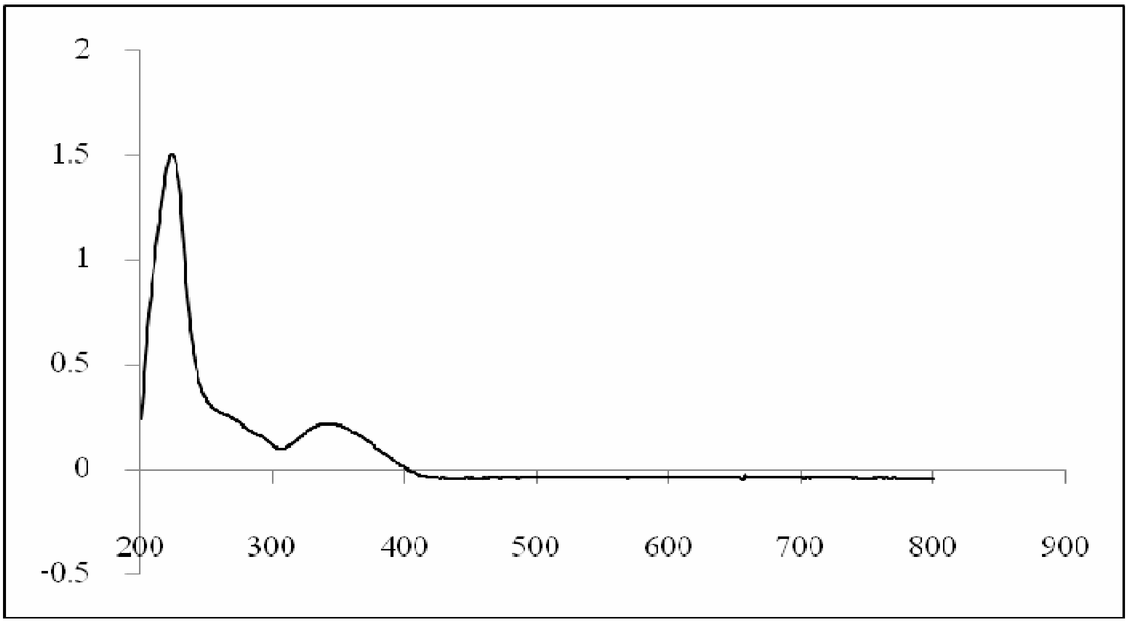

Figure 70 UV-Vis (CH_3OH) spectrum of compound **PNAP3C**

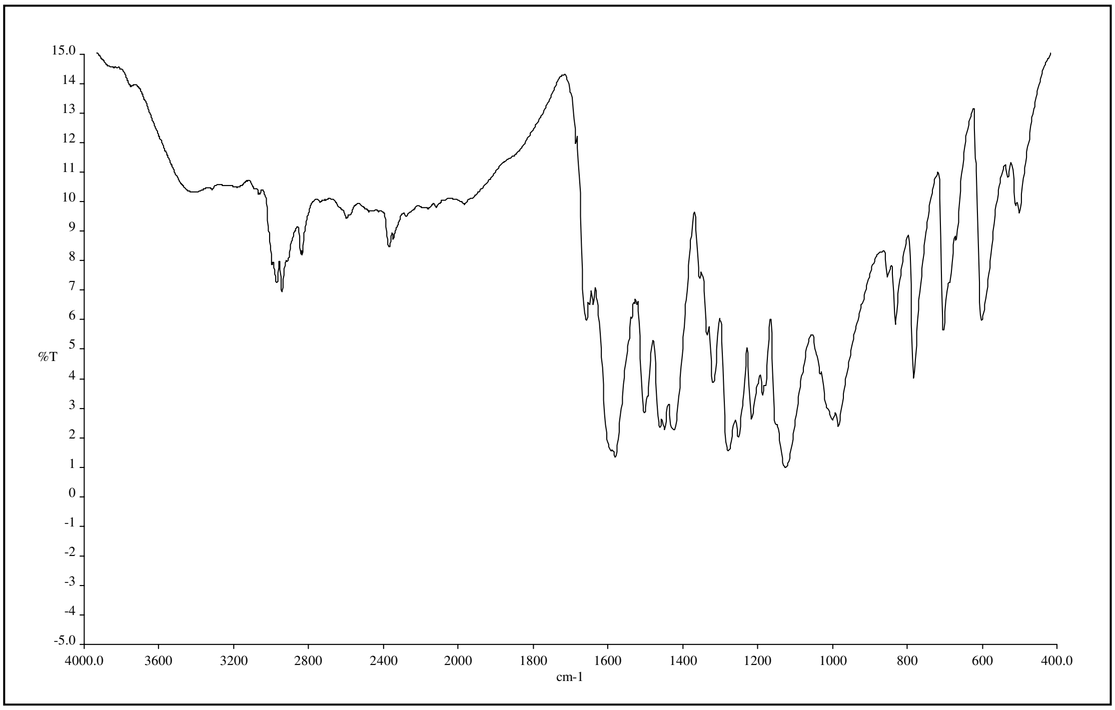

Figure 71 FT-IR (KBr) spectrum of compound **PNAP3C**

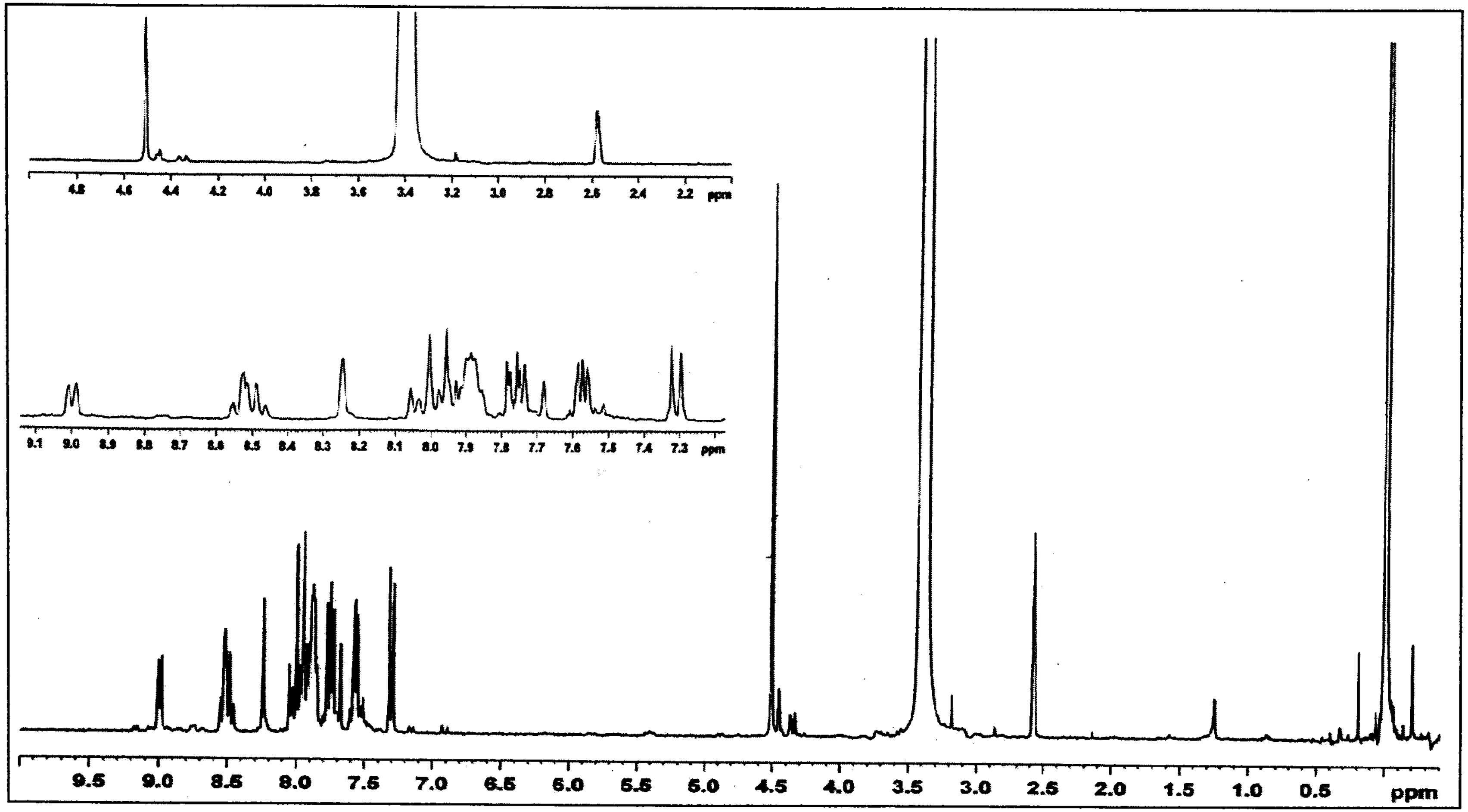

Figure 72 ^{1}H NMR (300 MHz, $CDCl_3$ + DMSO-d_6) spectrum of compound **PNAP3C**

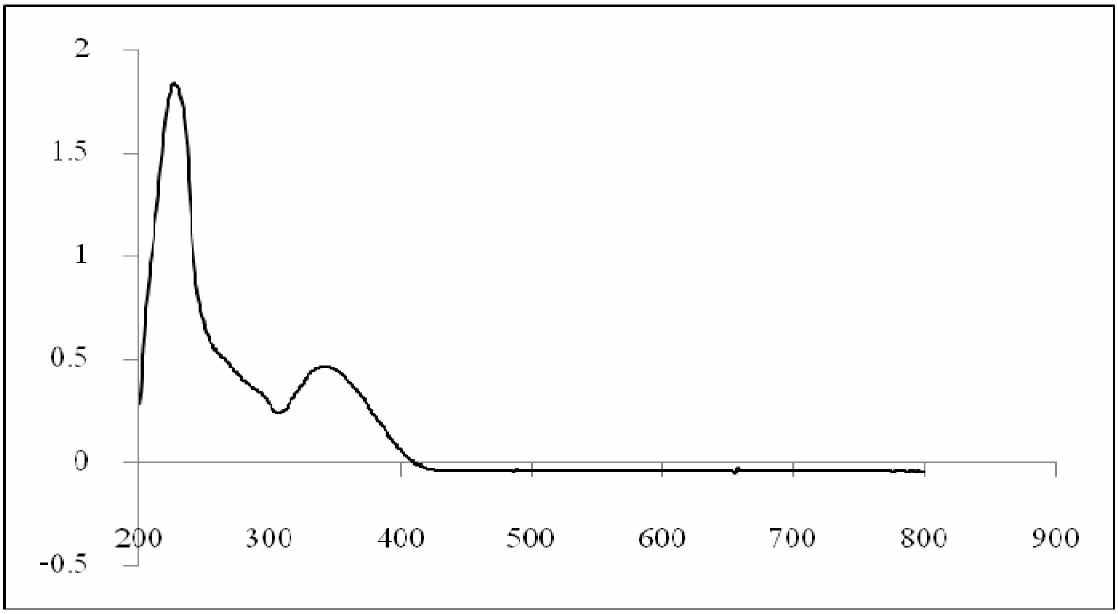

Figure 73 UV-Vis (CH_3OH) spectrum of compound **PNAP3B**

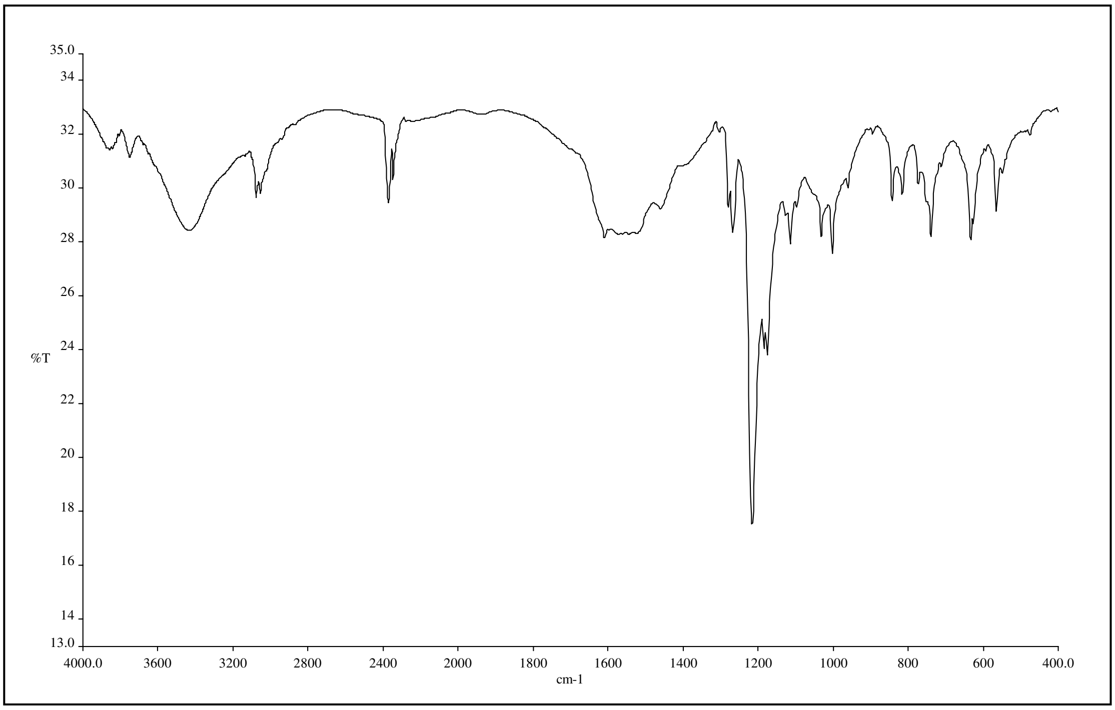

Figure 74 FT-IR (KBr) spectrum of compound **PNAP3B**

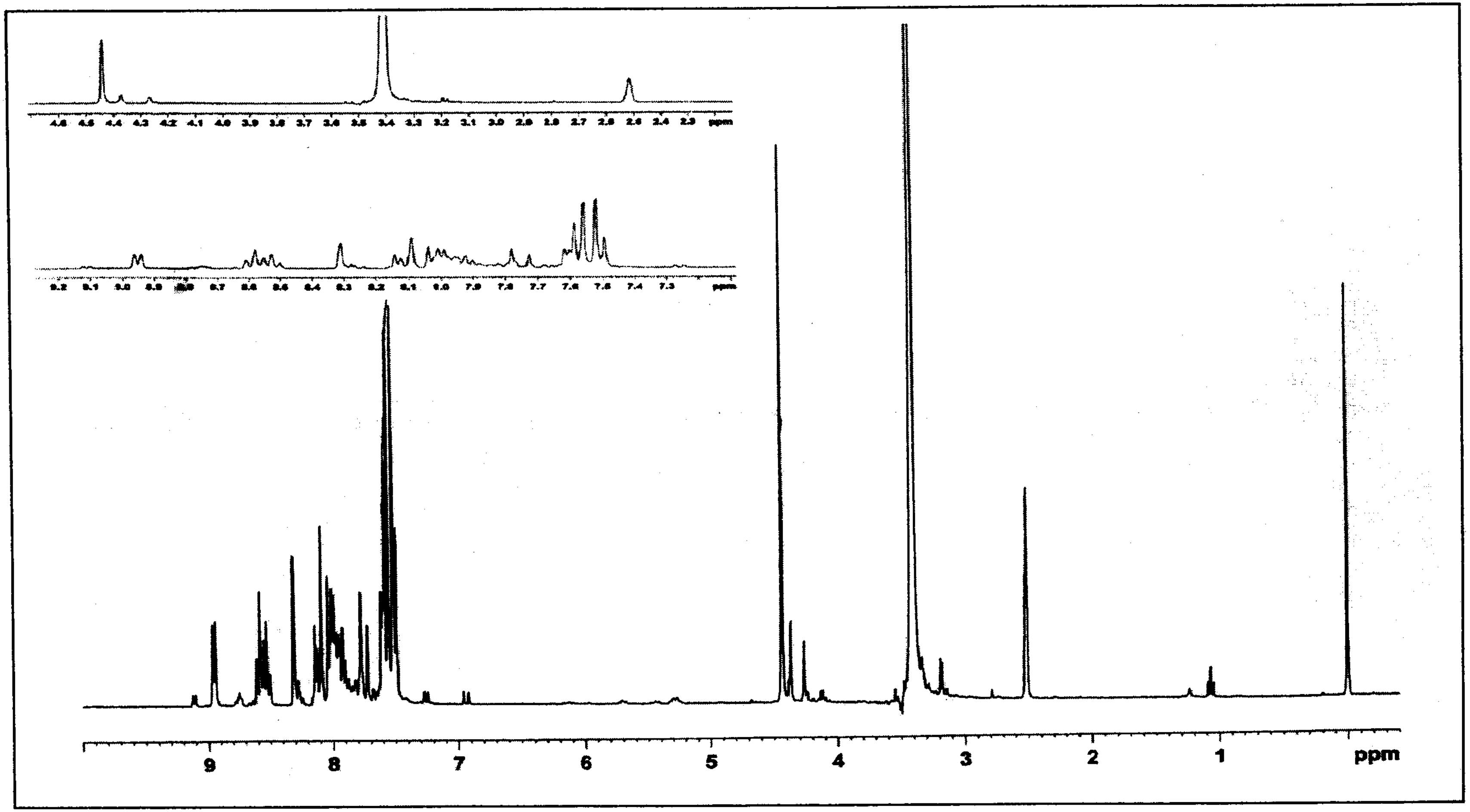

Figure 75 ^{1}H NMR (300 MHz, $CDCl_3$ + DMSO-d_6) spectrum of compound **PNAP3B**

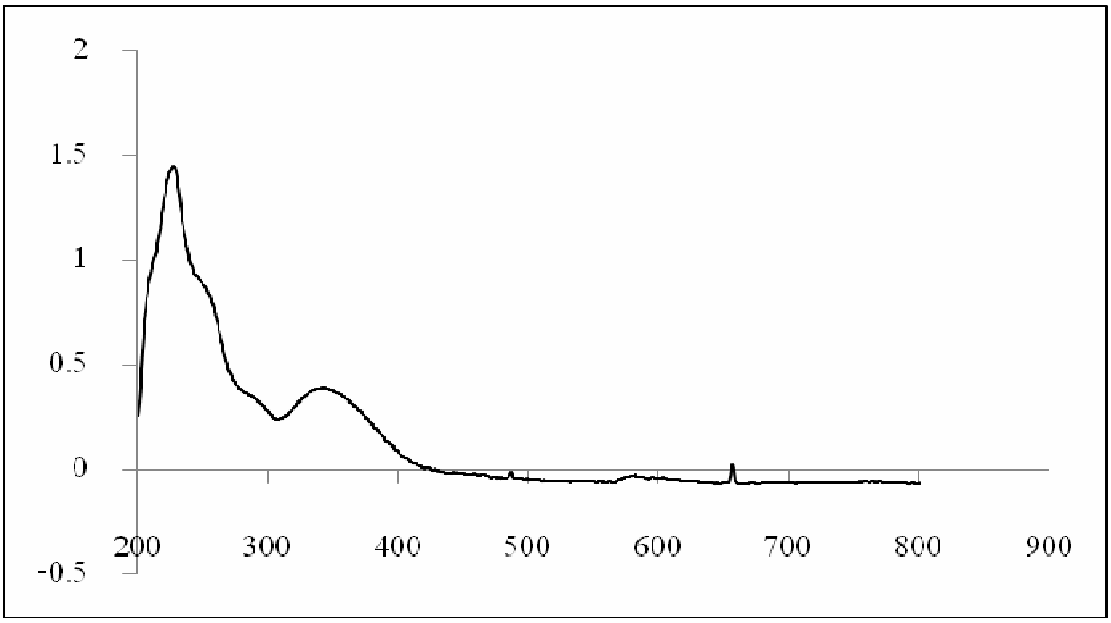

Figure 76 UV-Vis (CH_3OH) spectrum of compound **PNAP3N**

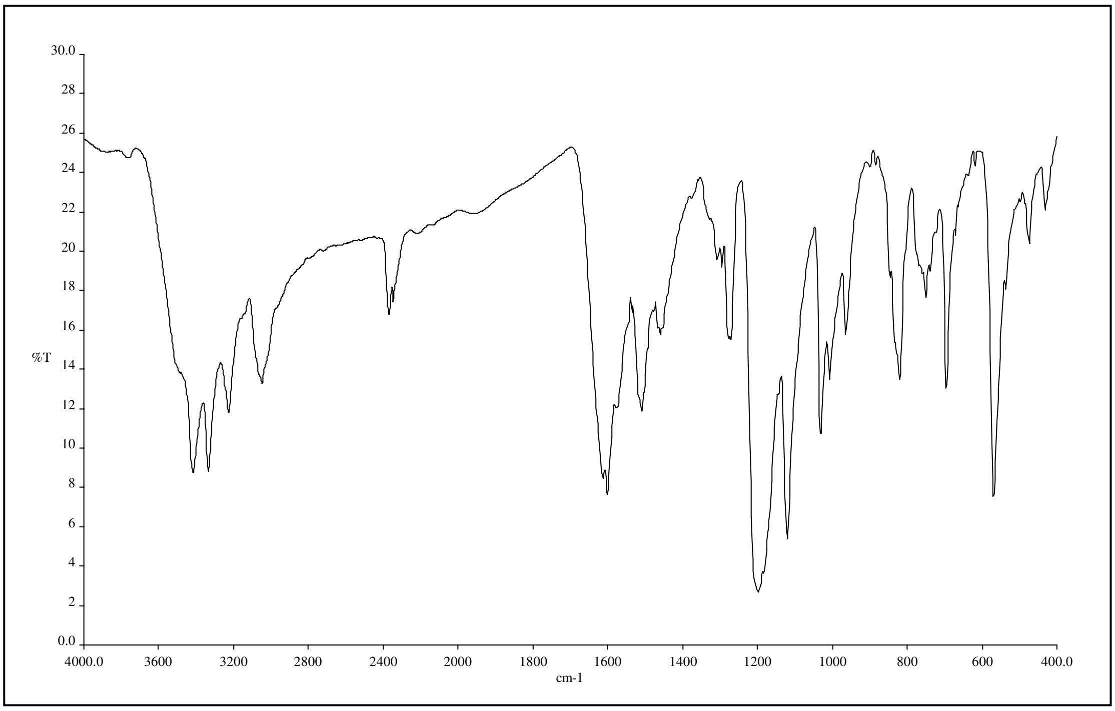

Figure 77 FT-IR (KBr) spectrum of compound **PNAP3N**

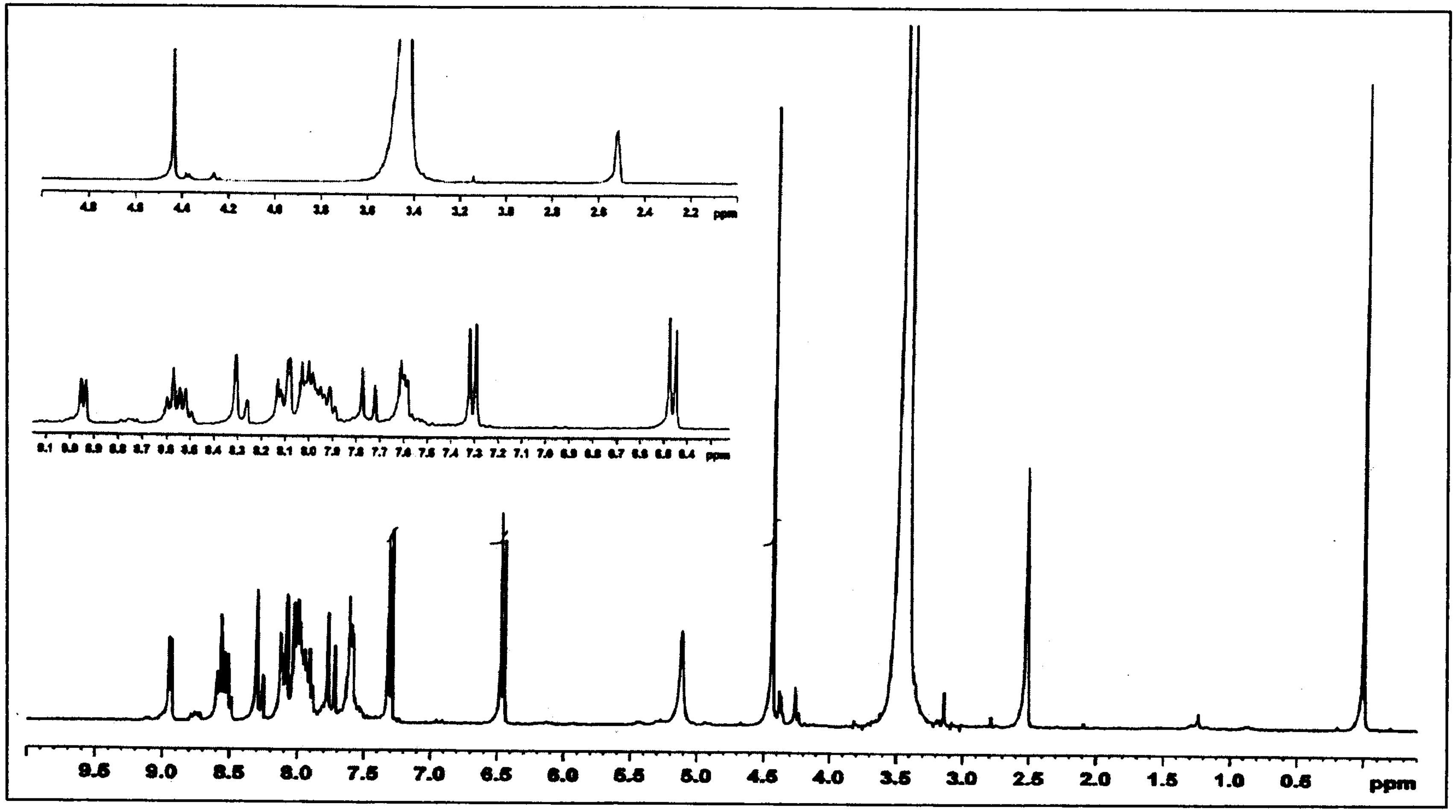

Figure 78 ^{1}H NMR (300 MHz, $CDCl_3$ + DMSO-d_6) spectrum of compound PNAP3N

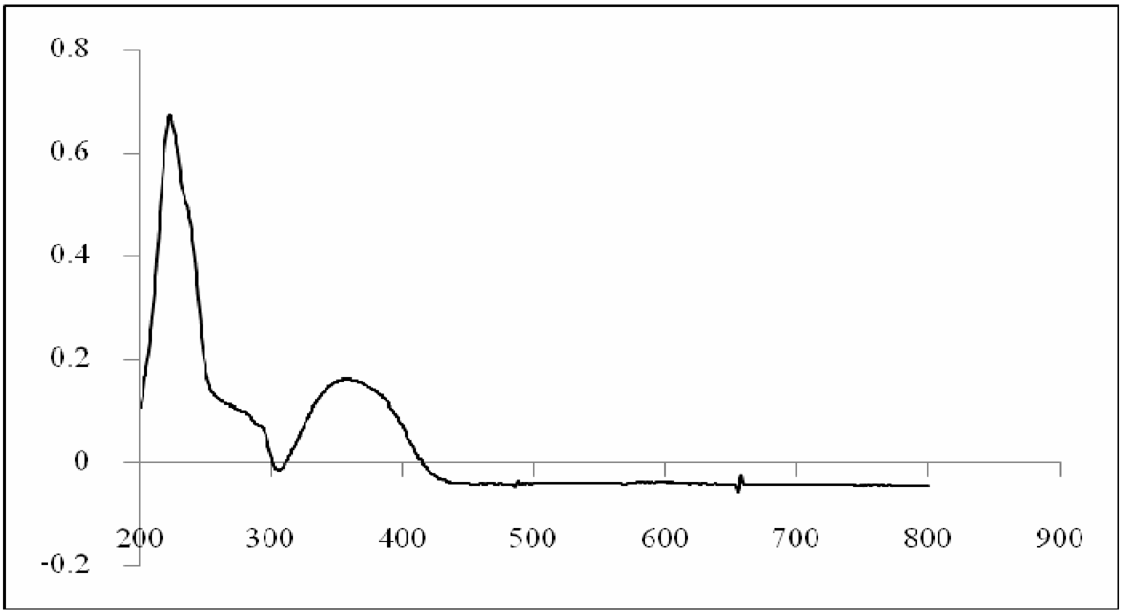

Figure 79 UV-Vis (CH_3OH) spectrum of compound **PNAP4M**

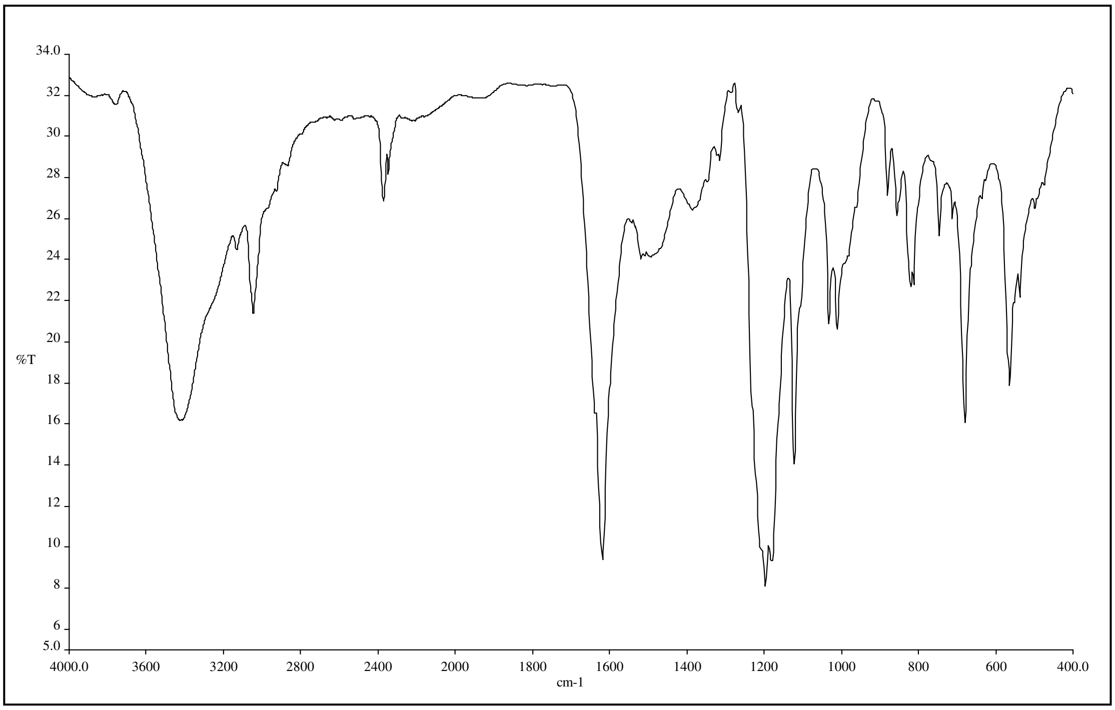

Figure 80 FT-IR (KBr) spectrum of compound **PNAP4M**

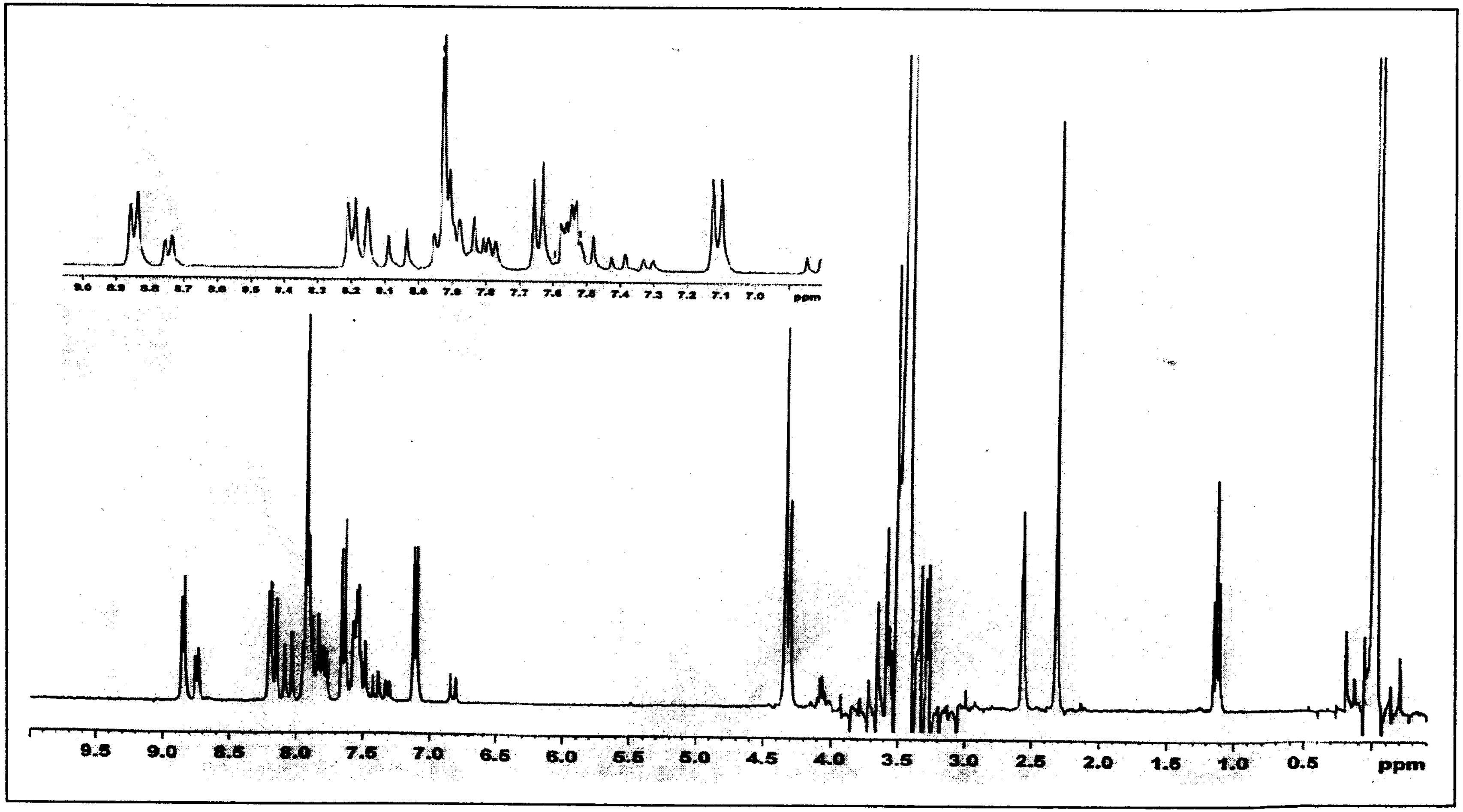

Figure 81 ^{1}H NMR (300 MHz, $CDCl_3$ + DMSO-d_6) spectrum of compound **PNAP4M**

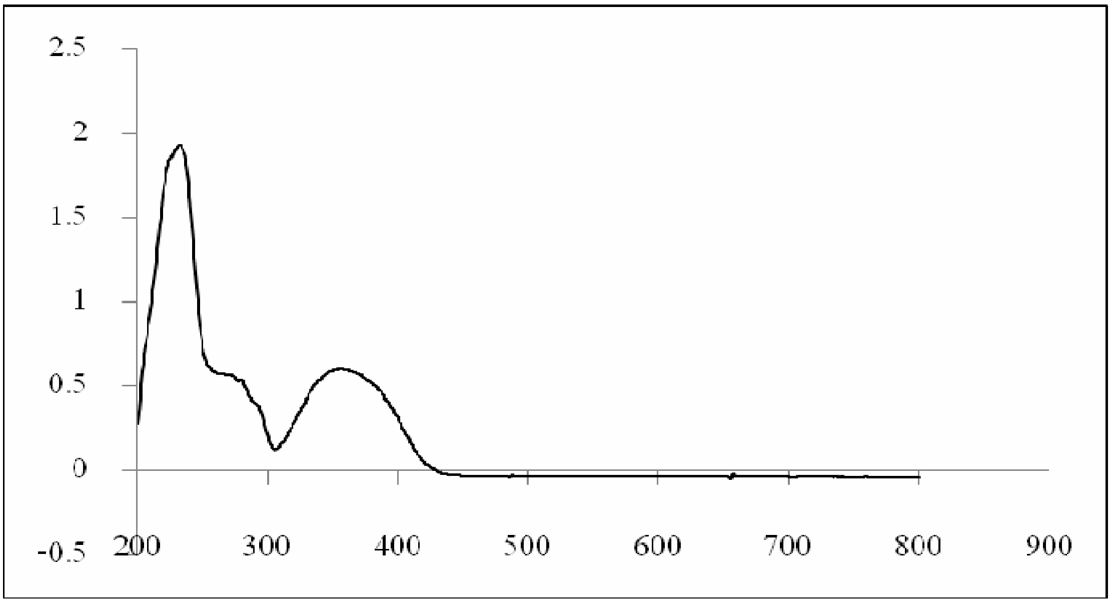

Figure 82 UV-Vis (CH_3OH) spectrum of compound **PNAP4O**

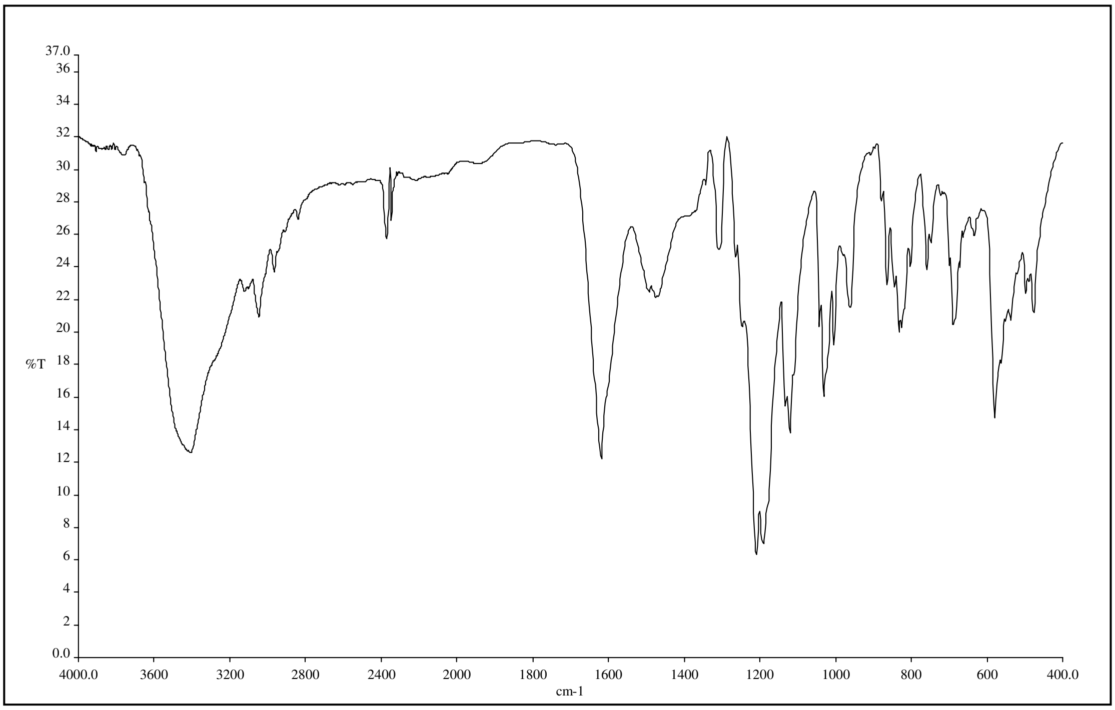

Figure 83 FT-IR (KBr) spectrum of compound **PNAP4O**

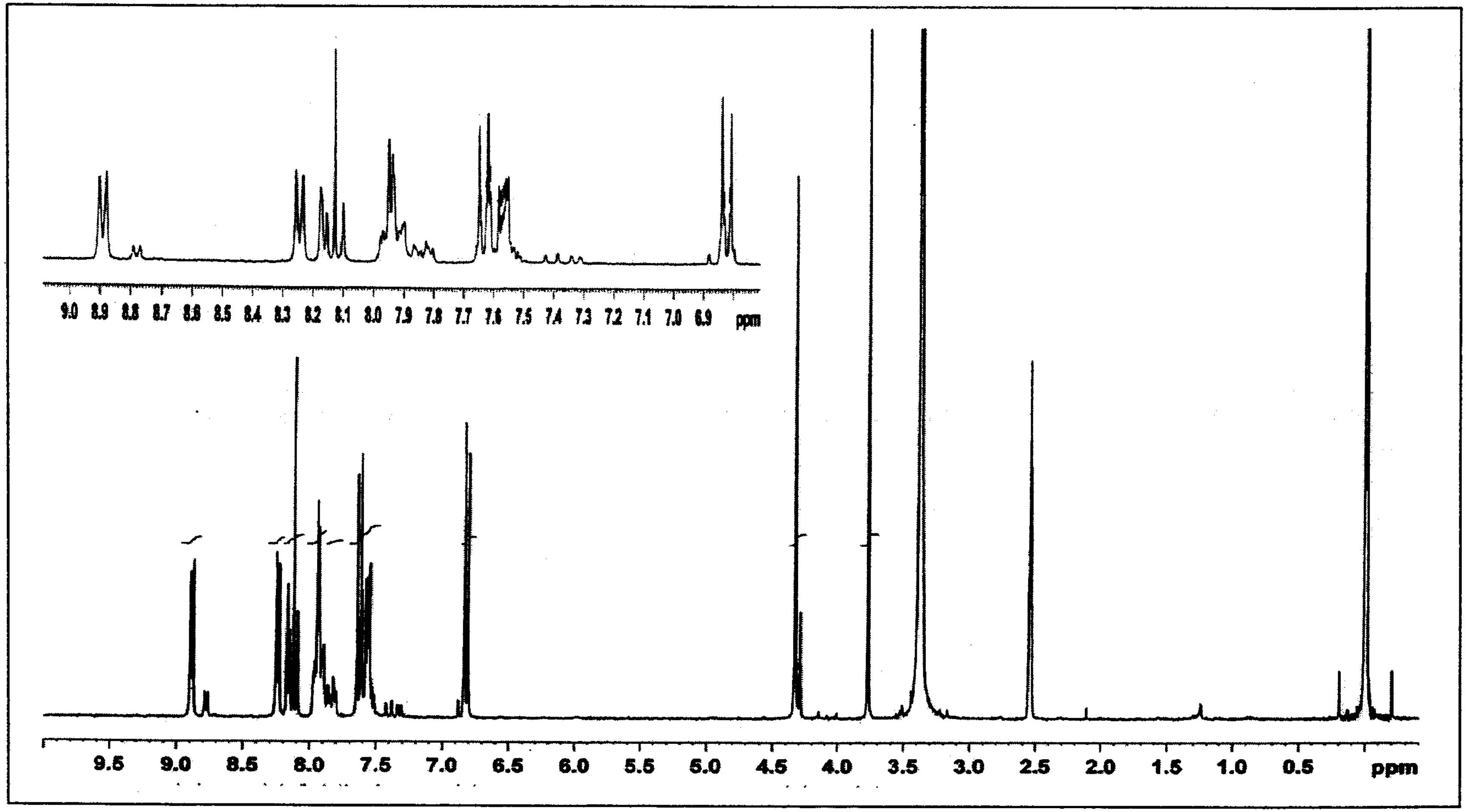

Figure 84 ^{1}H NMR (300 MHz, $CDCl_3$ + DMSO-d_6) spectrum of compound **PNAP4O**

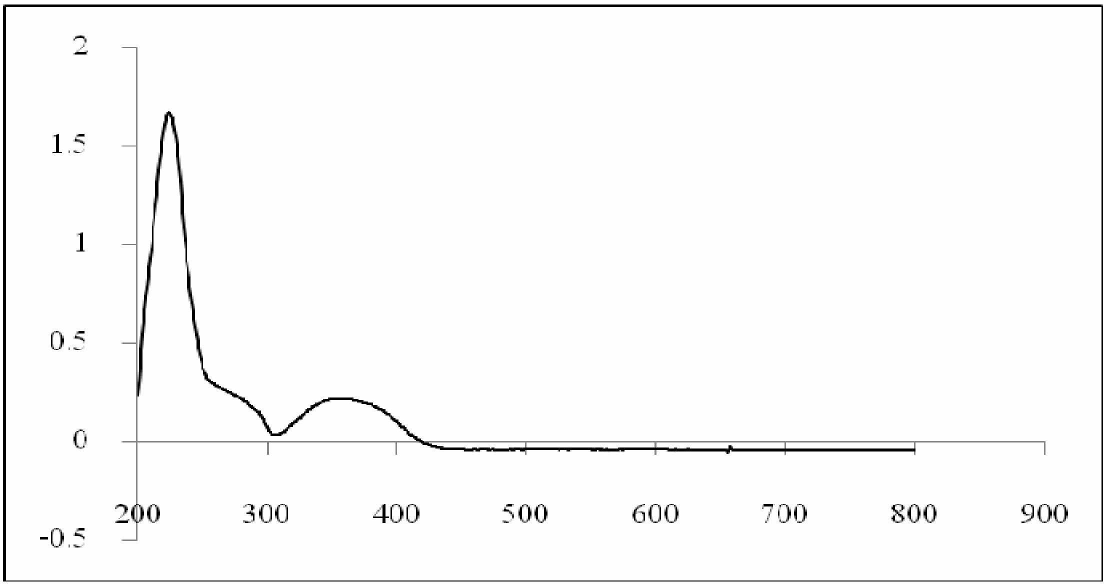

Figure 85 UV-Vis (CH_3OH) spectrum of compound **PNAP4C**

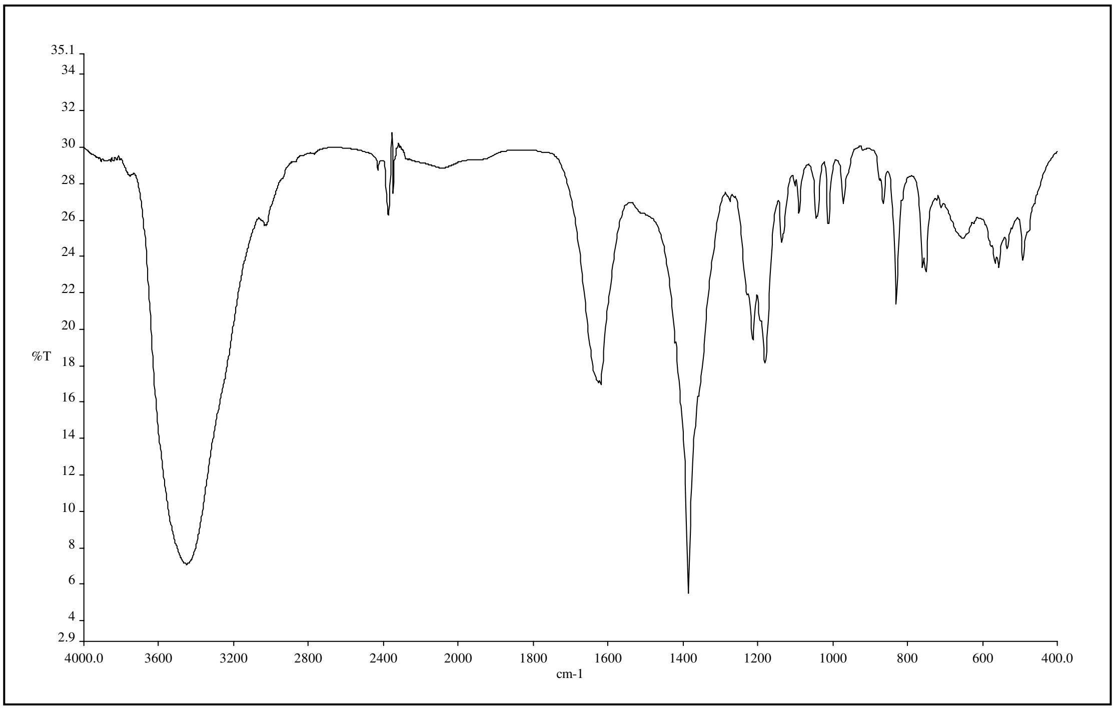

Figure 86 FT-IR (KBr) spectrum of compound **PNAP4C**

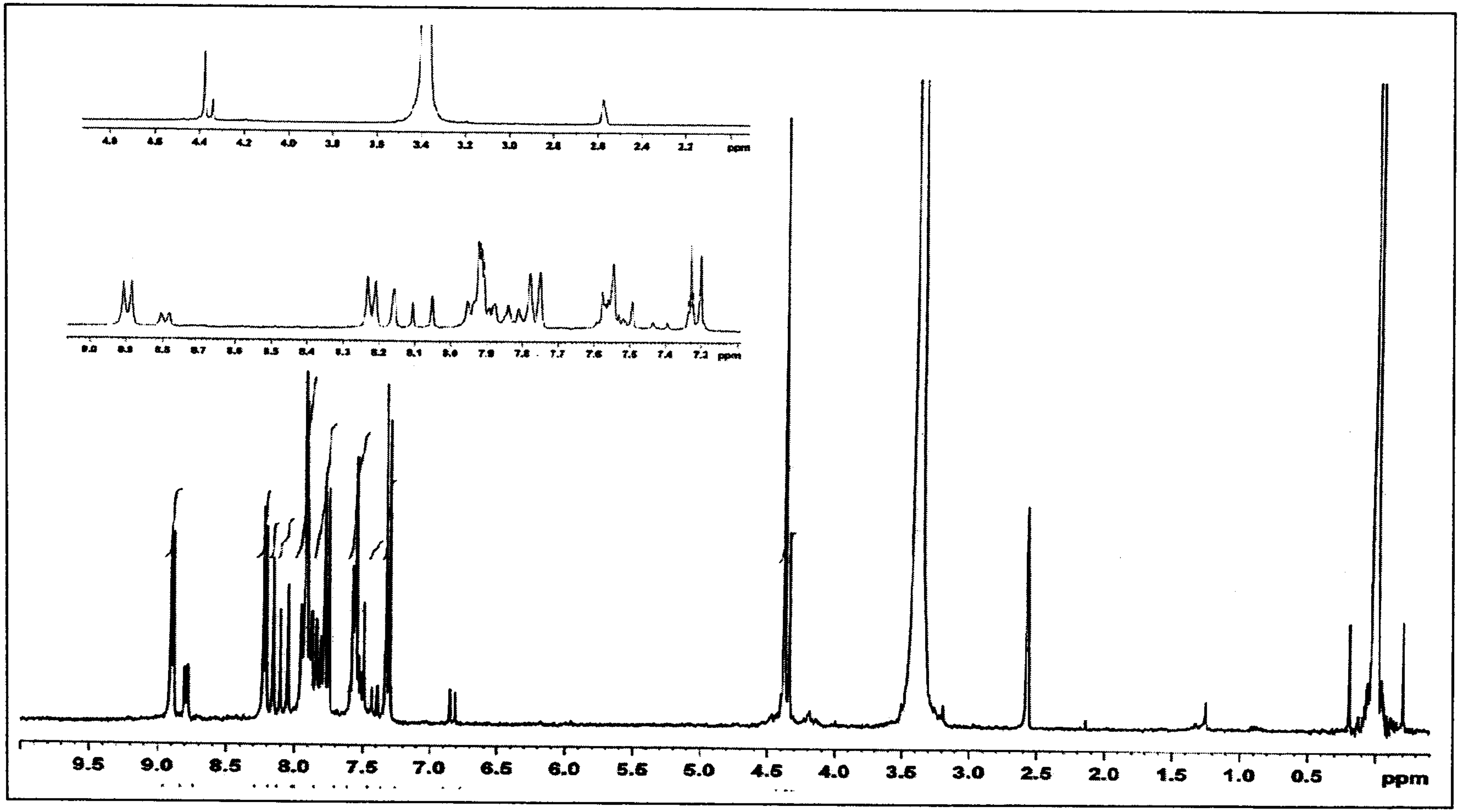

Figure 87 ^{1}H NMR (300 MHz, $CDCl_3$ + DMSO-d_6) spectrum of compound **PNAP4C**

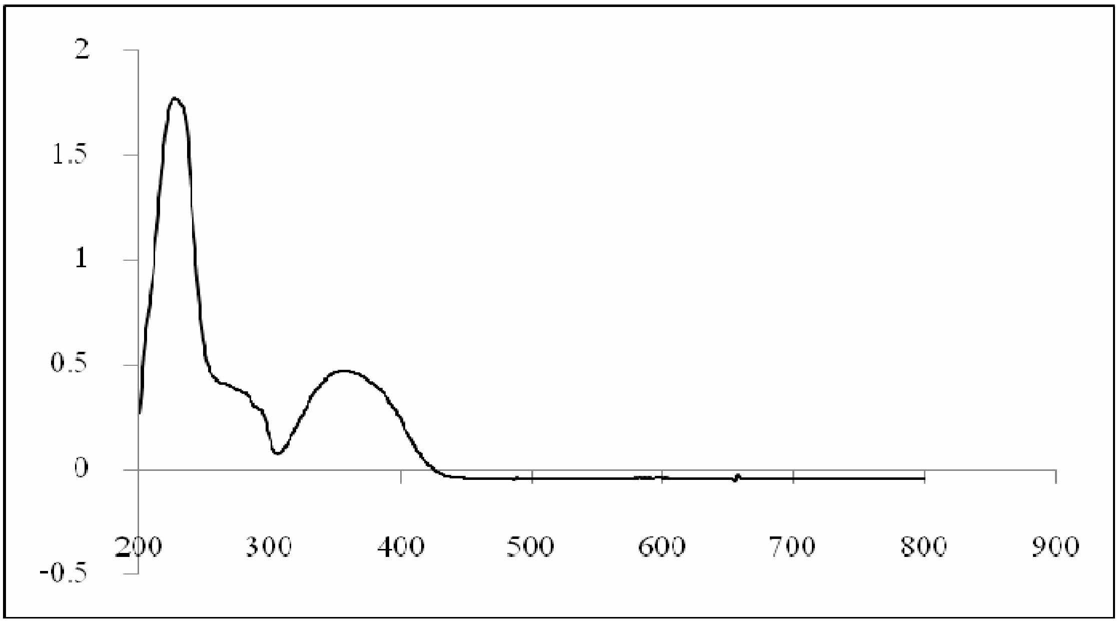

Figure 88 UV-Vis (CH_3OH) spectrum of compound **PNAP4B**

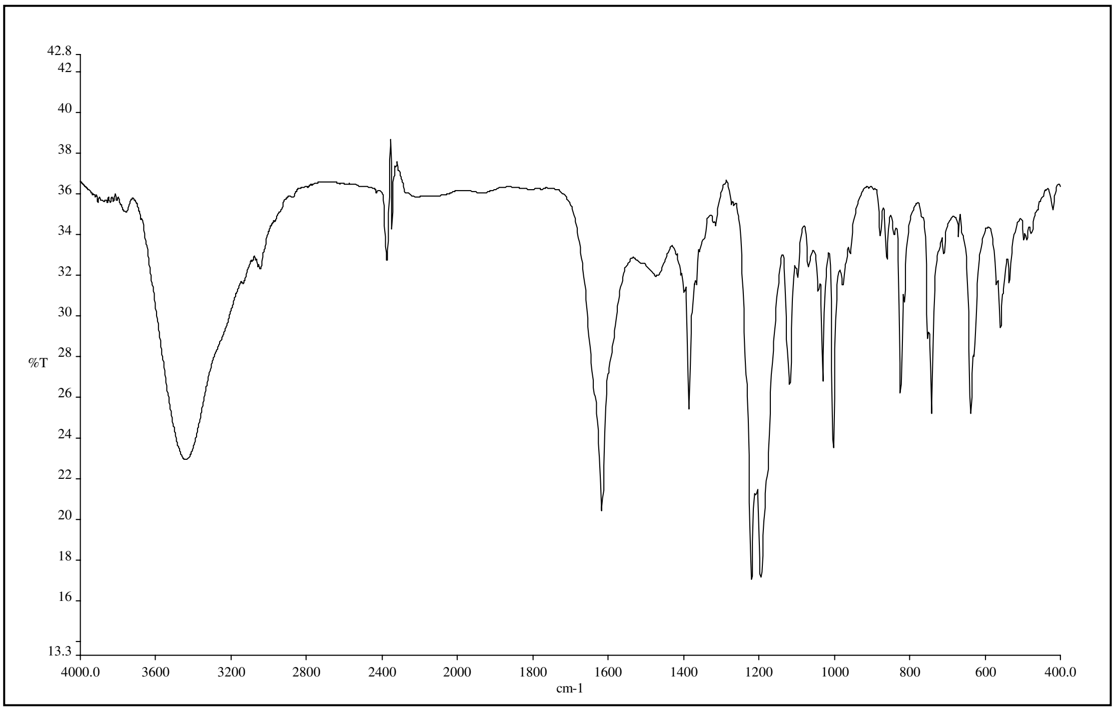

Figure 89 FT-IR (KBr) spectrum of compound **PNAP4B**

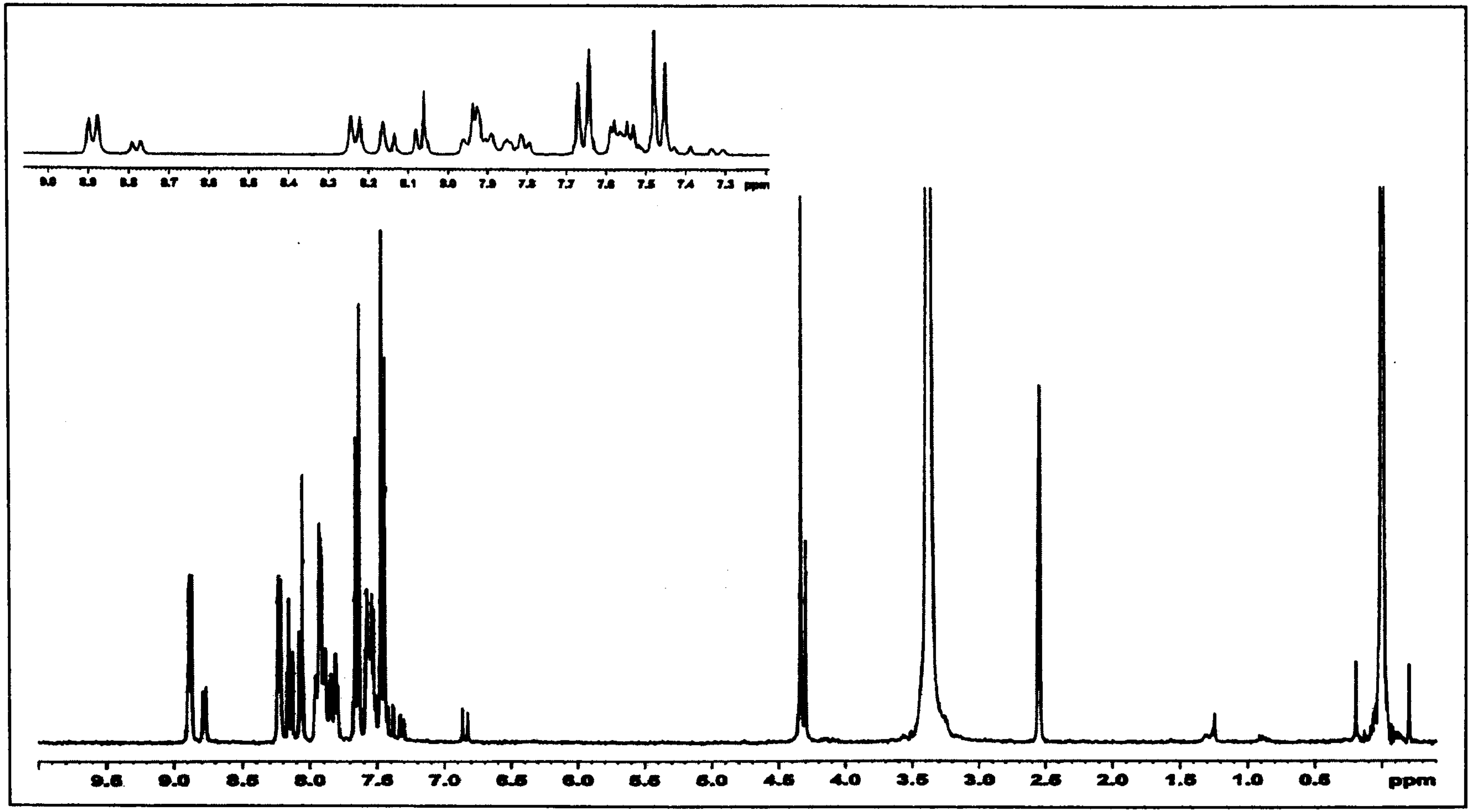

Figure 90 ^{1}H NMR (300 MHz, $CDCl_3$ + DMSO-d_6) spectrum of compound **PNAP4B**

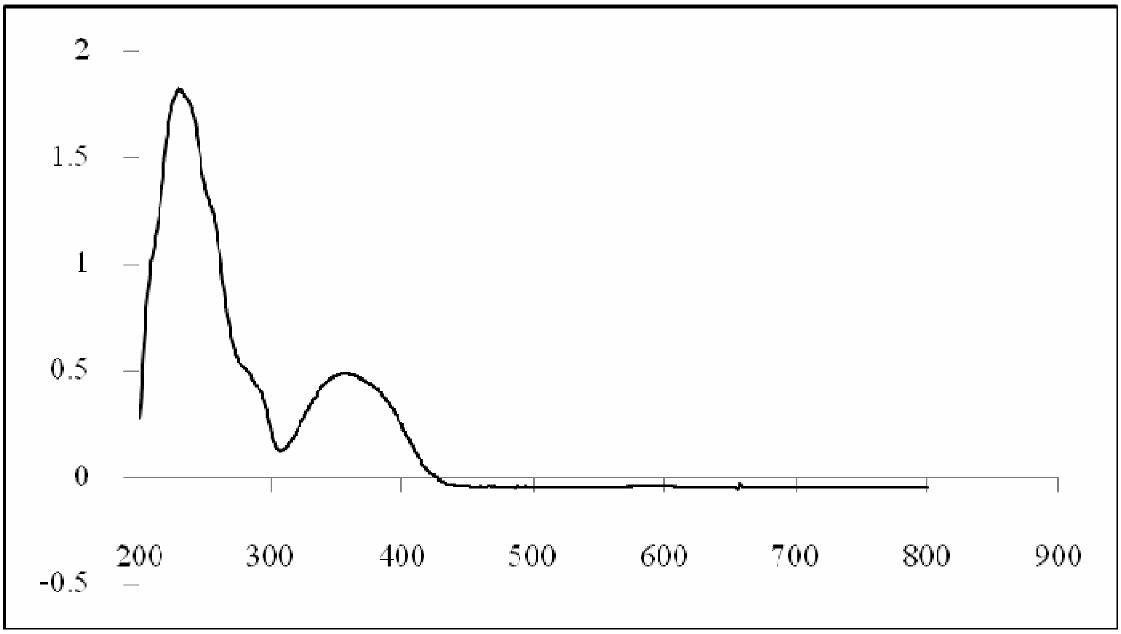

Figure 91 UV-Vis (CH_3OH) spectrum of compound **PNAP4N**

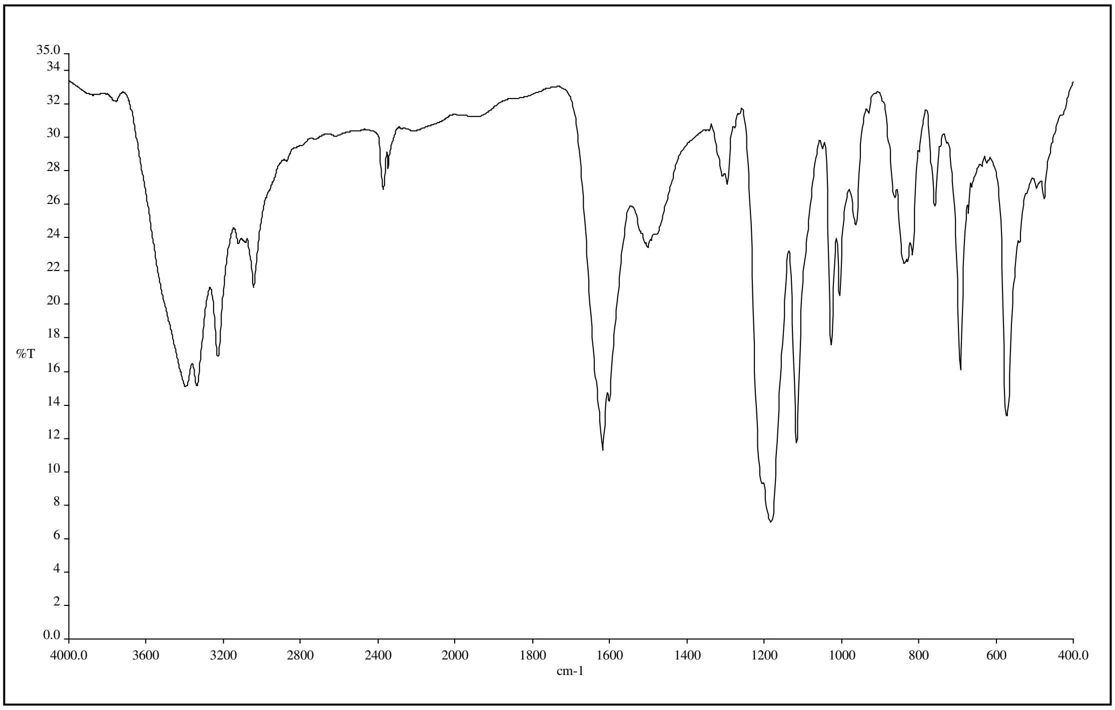

Figure 92 FT-IR (KBr) spectrum of compound **PNAP4N**

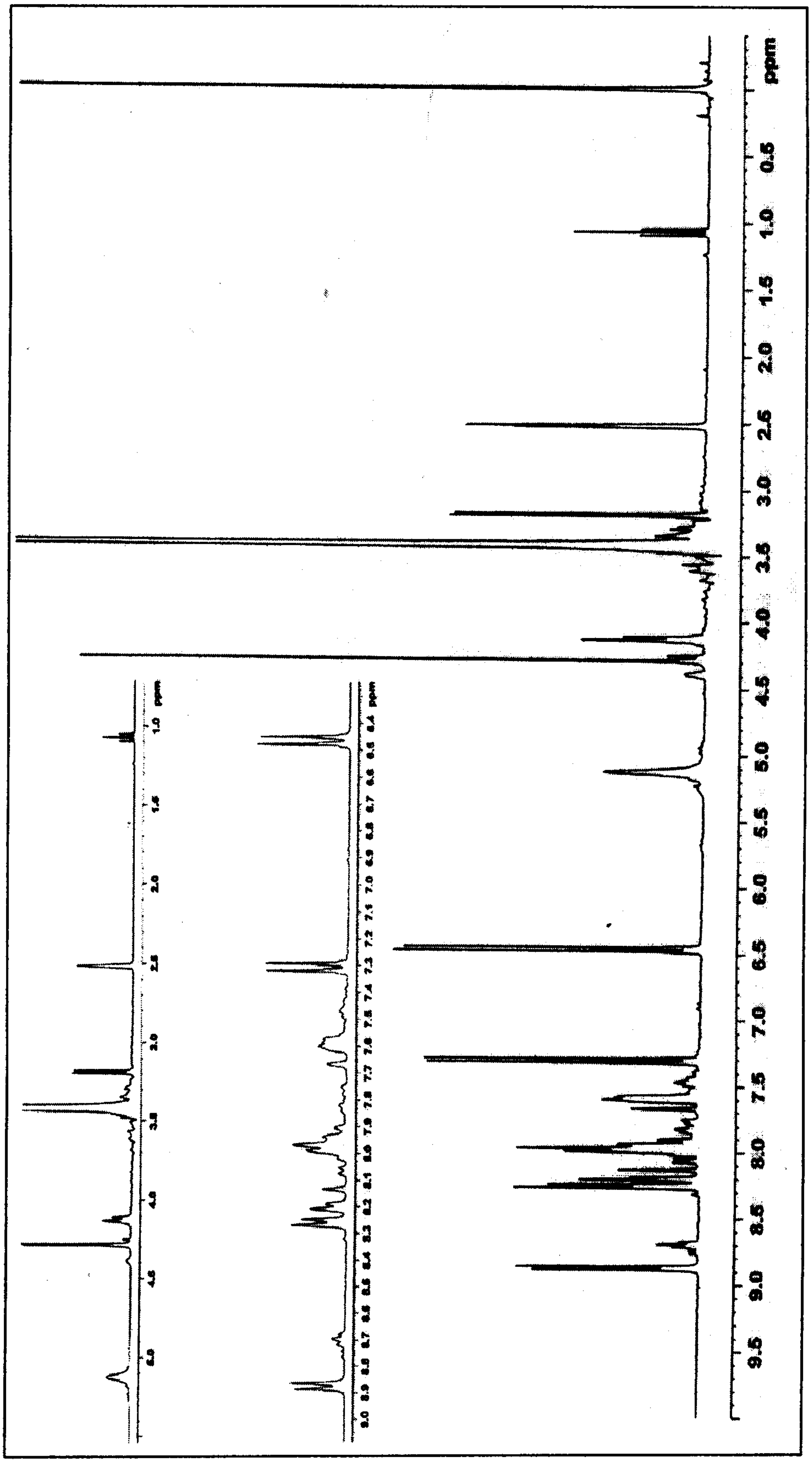

Figure 93 ^{1}H NMR (300 MHz, $CDCl_3$ + DMSO-d_6) spectrum of compound **PNAP4N**

VITAE

Name Miss Kullapa Chanawanno

Student ID 5010220012

Educational Attainment

Degree	Name of Institution	Year of Graduation
B.Sc. (Chemistry)	Prince of Songkla University	2006

Scholarship Awards during Enrolment

Scholarship was awarded by

- The Development and Promotion of Science and Technology Talents Project (DPST)
- The Center of Excellence for Innovation in Chemistry (PERCH-CIC), Commission on Higher Education, Ministry of Education, the Crystal Materials Research Unit (CMRU) and the Prince of Songkla University.

List of Publications and proceedings

Publications

1. Chantrapromma, S.; Chanawanno, K.; Fun, H.-K. 2007. "Bis[4-(4-hydroxystyryl)-1-methylpyridinium] triiodide iodide", *Acta Cryst.*, **E63**, o1554-o1556.
2. Chantrapromma, S.; Fun, H.-K.; Chanawanno, K.; Ruanwas, P. 2008. "Bis[(*E*)-2-(3-hydroxy-4-methoxyphenyl)ethenyl]-1-methylquinolinium tetraiodidozincate(II) methanol solvate", *Acta Cryst.*, **E64**, m126-m127.
3. Chantrapromma, S.; Kobkeatthawin, T.; Chanawanno, K.; Karalai, C.; Fun, H.-K. 2008. "(*E*)-2-[4-(Dimethylamino)styryl]-1-methylquinolinium iodide sesquihydrate", *Acta Cryst.*, **E64**, o876-o877.
4. Chanawanno, K.; Chantrapromma, S.; Fun, H.-K. 2008. "2-[(*E*)-2-(4-Chlorophenyl)ethenyl]-1-methylpyridinium iodide monohydrate", *Acta Cryst.*, **E64**, o1882- o1883.

5. Chantrapromma, S.; Chanawanno, K.; Fun, H.-K. 2009. "(*E*)-1-Methyl-4-[2-(1-naphthyl)vinyl]pyridinium 4-bromobenzenesulfonate", *Acta Cryst.*, **E65**, o1144-o1145.

6. Fun, H.-K.; Chanawanno, K.; Chantrapromma, S. 2009. "(*E*)-1-Methyl-4-[2-(2-naphthyl)vinyl]pyridinium iodide", *Acta Cryst.*, **E65**, o1406-o1407.

7. Fun, H.-K.; Chanawanno, K.; Chantrapromma, S. 2009. "2-[(*E*)-2-(4-Chlorophenyl)ethenyl]-1-methylpyridinium 4-chlorobenzenesulfonate", *Acta Cryst.*, **E65**, o1554-o1555.

8. Chanawanno, K.; Chantrapromma, S.; Fun, H.-K. 2009. "2-[(*E*)-2-(4-Chlorophenyl)ethenyl]-1-methylpyridinium 4- methoxybenzenesulfonate", *Acta Cryst.*, **E65**, o1549-o1550.

9. Chantrapromma, S.; Chanawanno, K.; Fun, H.-K. 2009. "2-[(*E*)-2-(4-Chlorophenyl)ethenyl]-1-methylpyridinium 4-bromobenzenesulfonate", *Acta Cryst.*, **E65**, o1884-o1885.

10. Fun, H.-K.; Chanawanno, K.; Chantrapromma, S. 2009. "(*E*)-1-Methyl-2-styrylpyridinium iodide", *Acta Cryst.*, **E65**, o1934-o1935.

11. Fun, H.-K.; Chanawanno, K.; Chantrapromma, S. 2009. "1,1′-Dimethyl-4,4′-(2,4-di-1-naphthyl-cyclobutane-1,3-diyl) dipyridinium-(*E*)-1-methyl-4-[2-(1-naphthyl)vinyl]pyridinium-4-aminobenzenesulfonate-water (0.25/1.50/2/2)", *Acta Cryst.*, **E65**, o2048-o2049.

12. Fun, H.-K.; Surasit, C.; Chanawanno, K.; Chantrapromma, S. 2009. "1,1′-Dimethyl-4,4′-[(2,4-diphenyl-cyclobutane-1,3-diyl) dipyridinium-(*E*)-1-methyl-4-styrylpyridinium benzenesulfonate (0.15/1.70/2)", *Acta Cryst.*, **E65**, o2346-o2347.

13. Fun, H.-K.; Chantrapromma, S.; Surasit, C.; Chanawanno, K. 2009. "(*E*)-1-Methyl-4-styrylpyridinium iodide monohydrate", *Acta Cryst.*, **E65**, o2676-o2677.

14. Fun, H.-K.; Surasit, C.; Chanawanno, K.; Chantrapromma, S. 2009. "Bis[(*E*)-1-methyl-4-styrylpyridinium] 4-chlorobenzenesulfonate iodide", *Acta Cryst.*, **E65**, o2633-o2634.
15. Chanawanno, K.; Chantrapromma, S.; Fun, H.-K. 2009. "Synthesis and crystal structure of 2-[(*E*)-2-(4-ethoxyphenyl)ethenyl]-1- methylpyridinium 4-methylbenzenesulfonate monohydrate", *X-Ray Struct. Anal. Online*, **25**, 127-128.
16. Chantrapromma, S.; Chanawanno, K.; Fun, H.-K. 2009. "(*E*)-1-Methyl-4-[2-(1-naphthyl)vinyl]pyridinium 4-chlorobenzenesulfonate", *Acta Cryst.*, **E65**, o3115-o3116.
17. Fun, H.-K.; Chanawanno, K.; Chantrapromma, S. 2010. "2-[(*E*)-2-(4-ethoxyphenyl)ethenyl]-1-methylpyridinium 4- bromobenzenesulfonate monohydrate", *Acta Cryst.*, **E66**, o305-o306.
18. Chanawanno, K.; Chantrapromma, S.; Anantapong, T.; Kanjana-Opas, A. 2009. "*In vitro* Antibacterial Activities of Silver (I) 4-substituted- benzenesulfonate Derivatives", *Lat. Am. J. Pharm.*, Accepted for Publication.
19. Chanawanno, K.; Chantrapromma, S.; Anantapong, T.; Kanjana-Opas, A.; Fun, H.-K. 2010. "Synthesis, Structure and *in vitro* Antibacterial Activities of New Hybrid Disinfectants Quaternary Ammonium Compounds: Pyridinium and quinolinium Stilbene Benzenesulfonates", *Eur. J. Med. Chem.*, Accepted for Publication.

Proceedings

1. Chanawanno, K.; Chantrapromma, S.; Fun, H.-K. Karalai, C. Syntheses and crystal structures of pyridinium and quinolinium derivatives.: Pure and Applied Chemistry International Conference (PACCON 2008), Sofitel Centara Grand Bangkok, Bangkok, Thailand. 30th January – 1st February 2008. (Poster)

2. Chanawanno, K.; Chantrapromma, S.; Karalai, C.; Fun, H.-K. Effect of 4-chlorobenzenesulfonate counter anion on nonlinear optical and absorption

properties of 2-[(*E*)-(4-chlorostyryl)]-1-methylpyridinium iodide monohydrate.: 34th Congress on Science and Technology of Thailand (STT 34), Queen Sirikit National Convention Center, Bangkok, Thailand. 31st October – 2nd November 2008. (Poster)

3. Chanawanno, K.; Chantrapromma, S.; Kanjana-Opas, A.; Fun, H.-K. Antibacterial and antifungi properties of the naphthalenyl-ethenylpyridinium benzenesulfonate salts.: The International Congress for Innovation in Chemistry (PERCH-CIC Congress VI), Jomtien Palm Beach Hotel & Resort Pattaya, Chonburi, Thailand. 3rd – 6th May 2009. (Poster)